# THE USE OF BILINEARLY WEIGHTED CROSS SECTIONS FOR FEW-GROUP TRANSIENT ANALYSIS

by

Myung Hyun Kim

B.S., Seoul National University, Korea
(1980)

S.M., Seoul National University, Korea
(1982)

SUBMITTED TO THE
DEPARTMENT OF NUCLEAR ENGINEERING
IN PARTIAL FULFILLMENT OF THE
REQUIREMENTS FOR THE
DEGREE OF

DOCTOR OF PHILOSOPHY

at the

MASSACHUSETTS INSTITUTE OF TECHNOLOGY

June 1988



Signature of Author _____
Department of Nuclear Engineering
April 21, 1988

Certified by _____
Allan F. Henry
Thesis Supervisor

Accepted by _____
Allan F. Henry
Chairman, Departmental Committee on Graduate Students

# THE USE OF BILINEARLY WEIGHTED CROSS SECTIONS

# FOR FEW GROUP TRANSIENT ANALYSIS

by

Myung Hyun Kim

Submitted to the Department of Nuclear Engineering
on April 21,1988 in partial fulfillment of the
requirements for the Degree of Doctor of Philosophy
in the field of Nuclear Engineering

## ABSTRACT

The validity of the few-group diffusion theory model for transient analysis is tested by comparison with the multi-group model. A bilinear weighting method of collapsing multi-group P-1 transport parameters into few-group parameters is introduced using a systematic derivation based on a variational principle. Two mutually consistent computer programs are developed. One is for energy spectra calculations and group collapsing, the other for simulation of reactor transient problems. A one-dimensional nodal method is implemented using the approximation that fluxes within a node should be quadratic functions determined by the node-average flux and two surface fluxes. Several tests are used to validate the two codes.

Two sets of weighted few-group parameters (flux-only-weighted conventional diffusion theory parameters and adjoint- and real-flux bilinearly weighted parameters) are tested by comparing their predictions of transient behavior with multi-group transient results. Results show that both methods are acceptably accurate for static cases, although the bilinearly weighted predictions are consistently more accurate. For transient cases, behavior is less consistent. In some instances, the regularly weighted cross sections provide more accurate results; in others, the bilinearly-weighted results are superior - significantly so for large step perturbations. At present there appears to be no compelling reason to use bilinearly weighted few-group cross sections for transient analysis. However study of certain second order effects that are outside the scope of the present thesis may change the conclusion.

Thesis Supervisor : Allan F. Henry

Title : Professor of Nuclear Engineering

ACKNOWLEDGEMENTS

I acknowledge with pleasure and gratitude the many contributions of my thesis advisor Prof. Allan F. Henry. He first suggested to me to work on this thesis topic and taught me how to think about adjoint weighting. In the course of dozens of meetings, he guided and encouraged me. He also made many important technical contributions. His expertise was and shall always be an inspiration for my work.

This work has also benefited from my discussions with members of reactor-control group: Prof. David D. Lanning who served as thesis reader, Prof. John E. Meyer, Dr. John A. Bernard, Pin-Wu Kao, Brian Avieles, Eduardo Cabrel, Mike Zerkle, Kwan Kwok and Eddy Lau.

The financial support was provided largely by a National Fellowship (the Department of Education, Korea) and partly by grant from the Department of Energy (Contract #DE-AC02-86NE37962.A000).

I am indebted to Ms. Rachel Morton for plentiful aid in using a VAX-computer and to Prof. Sow-Hsin Chen for his generous permission to use that machine. Special thanks are due to Dr. Kord Smith, of Studsvik of America, who kindly gave me valuable data.

For behind-the-scenes emotional support, I thank members of the Gate Bible Study at MIT, the Gartlands in Arlington and especially my parents in Korea. I sincerely thank these first two groups for all the friendship and prayers.

I don't know how to thank my wife, SeungEui, who has been just WONDERFUL. She encouraged me, supported me both emotionally and financially, and took care of me in many ways. Thanks, Love!

TABLE OF CONTENTS

## List of Figures

List of Tables

# Chapter 1

# INTRODUCTION

## 1.1 OVERVIEW AND MOTIVATION

Accurate information about the distribution of the neutron population in space and energy is the essential basis for the analysis of any nuclear reactor. The accurate prediction of neutron population during transient situations is also vital to reactor safety analysis. Consequently, there continues to be a strong incentive to develop efficient computational methods for accurate prediction of the neutronic distribution throughout the reactor under any condition of operation.

The multi-group transport theory model is capable of providing accurate analyses. Unfortunately, the geometrical heterogeneity of nuclear reactors results in computational problems (such as cost and running-time) for even the most advanced computers. Thus, the few-group approximation is commonly employed to obtain solutions with reasonable accuracy and computation time [H-1]. Another common approximation in use is to treat the angular dependence of the problem by the use of the diffusion theory model.

Diffusion theory assumes that the angular distribution of neutrons will be, at most, linearly anisotropic; the quantities of interest (such as flux distribution, control rod worths, etc.) can be predicted

accurately provided equivalent homogenized cross sections and diffusion coefficients can be determined [S-1]. A standard way of solving few-group diffusion theory equations is to use finite-difference methods. This computational technique has been the industry standard for years. However, the method has a drawback in that it requires very small computational grid sizes in order to give accurate results for power reactors having great complexity. As a result, accurate three-dimensional analysis by this method is too expensive to use in most cases.

In recent years, a class of modern nodal methods have been developed in order to achieve a faster speed of execution as well as more precise results [L-2]. The introduction of spatial homogenization theory provided a theoretical validity for the nodal methods which use relatively large node volumes (standard node size is about 20x20x20 $cm^3$). At MIT, the Analytic Nodal Method was developed and coded in a computer program known as QUANDRY [S-2]. Although modern nodal methods are less costly than the other methods, they are still quite slow for the routine, full three dimensional transient analyses (such as load following operation, startup operation, etc.). One way of circumventing this difficulty is the use of larger node size ( for example, 43x43x60 $cm^3$) along with a flux reconstrucion technique. Accordingly Supernodal methods have been implemented in the QUANDRY model and have provided reasonable accuracy and execution speed [G-1].

Thus, faster-running methods for full three-dimensional transient analyses are now available. However, all this is based on the presupposition that the few-group diffusion theory approximation in use is valid for transient analyses, a presupposition which is questionable,

especially for problems in which reactor power level and shapes change dramatically. It is, therefore, important to check the validity of current methodology before going into further development of fast running programs.

The accuracy of the conventional few-group diffusion approximation has been validated both theoretically and experimentally for static situations. However, this does not insure its accuracy when applied to transient situations. Moreover, experimental measurements have limitations if used as the reference values for comparisons. First of all, this experimental measurements themselves are subject to error when one tries to detect local power shapes within the complex geometry of real power reactors. Next, it is impossible to separate the effect of interest, namely neutron slowing down, from other effects (such as the effect of neutron diffusion near material interfaces, thermal feedback effects; noise effects, etc.). Futhermore, transient experiments and their analysis are very costly. Finally, safety considerations prohibit inducing severe transients in nuclear power reactors. All these difficulties are avoided if reference solutions are obtained numerically.

In this thesis, the accuracy of few-group approximation is measured by direct comparison of numerical solutions of few-group time-dependent equations with multi-group results. For this purpose, the multi-group P-1 approximation to the time-dependent transport equations is used as a standard. The same multi-group P-1 equations and their adjoints are used to generate multi-group flux- and current spectra. These spectra are used as weighting functions to calculate few-group parameters. Theory suggested that bilinearly weighted (with adjoint and real energy spectra)

few-group parameters should be superior to conventional flux-weighted parameters [P-1], [L-1]. However, this alternative weighting method has not been used in practice since it requires extra work for the calculation of the adjoint spectra and since current procedures appear to be adequate. The primary purpose of the present thesis is to test whether this adequacy holds for transient analysis.

## 1.2 THE FEW-GROUP APPROXIMATION

The standard multi-group P-1 equations can be written for N energy groups in matrix form as

$$\nabla\cdot[J(r)] + [A_0(r)][\Phi(r)] = [M(r)][\Phi(r)] \tag{1.1}$$

$$\frac{\partial}{\partial u}[\Phi(r)] + 3\,[A_{1_u}(r)][J_u(r)] = 0\,, \quad (u = x,y,z) \tag{1.2}$$

where $[\Phi(r)] = \text{col.}\ \{\phi_1(r),\phi_2(r),\cdots\phi_N(r)\}$

$[J_u(r)] = \text{col.}\ \{J_{1_u}(r),J_{2_u}(r),\cdots J_{N,u}(r)\}$

$[A_0(r)] = \{A_{0_{nn'}}(r)\}$, an $N \times N$ matrix (1.3)

$[A_{1_u}(r)] = \{A_{1_{u_{nn'}}}(r)\}$, an $N \times N$ matrix

$[M(r)] = \{M_{nn'}(r)\}$, an $N \times N$ matrix

Elements of matrices are defined as:

$$A_{0_{nn'}}(r) = \Sigma_{t_n}(r)\delta_{nn'} - \Sigma_{s_{0_{nn'}}}(r)$$

$$A_{1_{u_{nn'}}}(r) = -\Sigma_{t_n}(r)\delta_{nn'} - \Sigma_{s_{1_{u_{nn'}}}}(r) \qquad (1.4)$$

$$M_{nn'}(r) = \frac{1}{k_{eff}} \chi_n \nu\Sigma_{f_{n'}}(r)$$

where $\phi_n(r)$ = neutron flux of group n

$J_{n,u}(r)$ = net neutron current in direction u and group n

$\Sigma_{t_n}(r)$ = macroscopic total cross section for group n

$\Sigma_{s_{0_{nn'}}}(r)$ = macroscopic P-0 scattering transfer cross section from group n′ to group n

$\Sigma_{s_{1_{nn'}}}(r)$ = macroscopic P-1 scattering transfer cross section from group n′ to group n

$\chi_n$ = fission neutron yield fraction to group n

$\nu\Sigma_{f_n}(r)$ = macroscopic fission cross section for group n times the average number of neutrons emitted per fission

$k_{eff}$ = reactor eigenvalue

In principle to derive few-group equations, space-energy separability is assumed for the continuous energy P-1 equations:

$$\Phi(r,E) = \Phi_g(r)\ F_{0_g}^{k}(E)$$

$$J_u(r,E) = J_{g,u}(r)\ F_{1_g}^{k}(E) \qquad (u = x,y,z) \qquad (1.5)$$

for $r \subset$ region k

where g is an index for few-groups.

This assumption is made for each range of r inside a homogeneous (or homogenized) material consisting of composition k, and the flux energy spectra $F_{0_g}^{k}(E)$ and current energy spectra $F_{1_g}^{k}(E)$ are the P-0 and P-1 components of the asymptotic spectra associated with the material buckling for material k [H-1].

### 1.2.1 Conventional Few-Group Parameters

In practical reduction to few groups is made from the asymptotic multigroup P-1 equations for each homogenized material composition. Thus, the flux and current densities are approximated by

$$\begin{aligned} \Phi(\mathbf{r},E) &\simeq \phi_g(\mathbf{r})\ F_{0_n}^{k} \\ J_u(\mathbf{r},E) &\simeq J_{g,u}(\mathbf{r})\ F_{1_n}^{k} \qquad (u = x,y,z) \end{aligned} \tag{1.6}$$

$$\text{for } n \subset g \text{ and } \mathbf{r} \subset k$$

where the $F_{0_n}^{k}$ and $F_{1_n}^{k}$ are solutions to Eqs. (1.1) and (1.2) asymptotically for inside material k.

If Eqs. (1.6) are inserted into (1.1) and (1.2) and the result is required to be valid when summed over all n contained in each group g, reduced few-group P-1 equations result having the same form as (1.1) and (1.2) and with the fllowing conventional definitions of few group parameters:

$$\Sigma_{\alpha_g}^k(r) = \frac{\sum_{n \subset g} \Sigma_{\alpha_n}^k(r)\ F_{0_n}^k}{\sum_{n \subset g} F_{0_n}^k} \qquad (\alpha = f,t,a) \tag{1.7}$$

$$\chi_g = \sum_{n \subset g} \chi_n \tag{1.8}$$

$$\Sigma_{s_{0_{gg'}}}^k(r) = \frac{\sum_{n \subset g} \sum_{n' \subset g'} \Sigma_{s_{0_{nn'}}}^k(r)\ F_{0_{n'}}^k}{\sum_{n' \subset g'} F_{0_{n'}}^k} \tag{1.9}$$

$$D_g^k(r) = \frac{1}{3} \left[ \frac{\sum_{n \subset g} \sum_{n'} A_{1_{nn'}}^k(r)\ F_{1_{n'}}^k}{\sum_{n \subset g} F_{1_n}^k} \right]^{-1} \tag{1.10}$$

where it is assumed that $A_{1_{u_{nn'}}}$ is the same for all directions, u.

### 1.2.2 Bilinearly Weighted Few-Group Parameters

As will be shown in Chapter 2, theory suggests that more accurate few-group equations will result if the few-group parameters are weighted by both the real flux spectrum and the adjoint flux spectrum, (or, for some parameters, by the real current spectrum and the adjoint current spectrum). Bilinear weighting methods are not new. In the 1960's, a number of reactor physicists, Shaftman [S-3], Pitterle [P-1], Henry [H-2],

Little [L-1] and Buslik [B-1], proposed this alternative way of formulating the few group approximation. Henry and Buslik established the formulation of few group equations derived from a variational principle. Again the forms of the few-group P-1 equations are the same as the multi-group equations Eqs.(1.1) and (1.2). However, as will be shown in Chapter 2, new definitions of few-group parameters result. With certain simplifying assumptions these become:

$$\Sigma_{\alpha_g}^{k}(r) = \frac{N_g \sum_{n\subset g} \sum_{n'\subset g'} F_{0_n}^{*k}\ \Sigma_{\alpha_n}^{k}(r)\ F_{0_n}^{k}}{\sum_{n\subset g} F_{0_n}^{*k} \sum_{n\subset g} F_{0_n}^{k}} \qquad (\alpha = f,t) \qquad (1.11)$$

$$\chi_g = \frac{N_g \sum_{n\subset g} F_{0_n}^{*k}\ \chi_n}{\sum_{n\subset g} F_{0_n}^{*k}} \qquad (1.12)$$

$$\Sigma_{s_{0_{gg'}}}^{k}(r) = \frac{N_g \sum_{n\subset g} \sum_{n'\subset g'} F_{0_n}^{*k}\ \Sigma_{s_{0_{nn'}}}^{k}(r)\ F_{0_{n'}}^{k}}{\sum_{n\subset g} F_{0_n}^{*k} \sum_{n'\subset g'} F_{0_{n'}}^{k}} \qquad (1.13)$$

$$D_g^{-1\,k}(r) = \frac{3 \sum_{n\subset g} \sum_{n'} F_{1_n}^{*k}\ A_{1_{nn'}}(r)\ F_{1_{n'}}^{k}}{\sum_{n\subset g} F_{1_n}^{*k}\ F_{0_n}^{k} \sum_{n\subset g} F_{1_n}^{k}\ F_{0_n}^{*k}} \qquad (1.14)$$

$$\Sigma_{a_g}^{k}(r) = \Sigma_{t_g}^{k}(r) - \Sigma_{s_g}^{k}(r) = \Sigma_{t_g}^{k}(r) - \sum_{g'} \Sigma_{s_0 g' g}^{k}(r) \qquad (1.15)$$

where $N_g$ is the number of groups included in few-group g, $F_{0_n}^{*k}$ is the adjoint neutron flux spectrum and $F_{1_n}^{*k}$ is the adjoint neutron current spectrum for region k.

The conventional weighting method is thus seen to be a special case of the bilinear weighting method where all adjoint spectra are set to unity. Physically, the conventional approach assumes that all neutrons produced with different energies in a given group g produce the same effect asymptotically in the total neutron population. In other words the neutron importances are assumed to be constant throughout the slowing-down range from the fission energy to zero energy. Intuitively this assumption seems questionable.

## 1.3 OBJECTIVE AND SUMMARY

In this thesis, the accuracies of the two weighting schemes embodied in Eqs. (1.7 - 1.10) and Eqs. (1.11 - 1.15) are measured by direct comparison of predicted transient behavior compared with multi-group P-1 results. The main objective is to evaluate the error of the conventional two-group diffusion model in current use. All the comparisons are made for one-dimensional reactor models since computational costs are thereby reduced and since modelling the axial perturbations along a coolant channel during a transient is thought to be sufficient to test the accuracy of the two procedures for computing few-group parameters.

In chapter 2, the systematic derivation of few-group P-1 equations using a variational principle made stationary by the continuous energy, time-dependent P-1 equations and their adjoints is presented, and reduced function spaces which lead to the definition of few-group parameters are introduced.

The overall effort breaks down into two main tasks. First, a separate codes are needed for determining multi-group energy spectra (real and adjoint spectra for both flux and current) as well as for collapsing multi-group cross sections into 2-group parameters. An evaluation of temperature feedback coefficients is also incorporated in this codes. In chapter 3, calculational models underlying these codes are described and tests validating to codes themselves are presented.

The second task is to create a reliable one-dimensional, time-dependent nodal code which can be used for few-groups as well as for multi-groups. The underlying model and the numerical methods used to solve the resulting equations are presented in chapter 4. A validation that the code is solving the equations posed is presented for a few test problems.

In chapter 5, a number of transient problems, involving both simple and complex geometries, are investigated, and results predicted by the two weighting methods are discussed.

Chapter 6 presents conclusions along with some suggestions for future work.

Appendices provide detailed derivations of the theory presented, as well as descriptions of the test problems and the several transient problems analyzed.

# Chapter 2

## DERIVATION OF THE THEORY

### 2.1 INTRODUCTION

In this chapter the derivation of the few group transient equations and their few group parameters is given. Henry [H-2] derived time-dependent few-group P-1 equations from the Selengut-Wachspress variational principle; however, he obtained boundary conditions that impose discontinuities on the few-group fluxes and currents at interfaces. Buslik [B-1] proposed a Lagrange multiplier variational principle and obtained few-group P-1 equations with interface conditions consisting of continuity of few-group fluxes and currents. Since he applied his idea to the time independent P-1 equations, the derivation of time-dependent few-group equations is reviewed here. A systematic derivation produces the exact definitions of few-group P-1 parameters, called bilinearly weighted few-group parameters. Conventional few-group P-1 diffusion parameters can be derived from them as a special case.

### 2.2 CONTINUOUS ENERGY FORMS OF P-1 TRANSPORT EQUATIONS

Throughout this study, the P-1 approximation to the time-dependent transport equation serves as a basis for the derivation of the equations to be used. With the introduction of operator notation, they are represented as:

$$
\begin{aligned}
&V^{-1}\frac{\partial \Psi_0}{\partial t} = -\nabla\cdot\vec{\Psi}_1 - A\Psi_0 + k_{eff}^{-1}M\Psi_0 + \sum_{\iota}\chi_{d_\iota}\lambda_\iota C_\iota \\
&3\,V^{-1}\frac{\partial \vec{\Psi}_1}{\partial t} = -\nabla\Psi_0 - D^{-1}\vec{\Psi}_1 \qquad (2.1)\\
&\chi_{d_\iota}\frac{\partial C_\iota}{\partial t} = \chi_{d_\iota}M_{d_\iota}\Psi_0 - \chi_{d_\iota}\lambda_\iota C_\iota \quad ;\ \iota = 1,2,\cdots,I
\end{aligned}
$$

where

$$
\chi_{d_\iota}\lambda_\iota C_\iota = \chi_{d_\iota}(E)\lambda_\iota C_\iota(r,t)
$$

The linear integral operators, A, $D^{-1}$, M and $M_{d_\iota}$ are defined by the following operations on arbitrary functions u(r,E,t) and $\vec{v}(r,E,t)$.

$$
\begin{aligned}
Au &= \Sigma_t(r,E,t)u(r,E,t) - \int_0^\infty dE'\ \Sigma_{s_0}(r,E'\to E,t)u(r,E',t)\\
D^{-1}\vec{v} &= 3\Sigma_t(r,E,t)\vec{v}(r,E,t) - 3\int_0^\infty dE'\ \Sigma_{s_1}(r,E'\to E,t)\vec{v}(r,E',t)\\
Mu &= \sum_j (1-\beta_{eff}^j)\chi_p^j(E)\int_0^\infty dE'\nu\Sigma_f^j(r,E',t)u(r,E',t) \qquad (2.2)\\
M_{d_\iota}u &= \sum_j \beta_\iota^j \int_0^\infty dE'\ \nu\Sigma_f^j(r,E',t)u(r,E',t)
\end{aligned}
$$

The cross sections are taken to be piecewise continuous functions of position. The scalar function u(r,E,t) is assumed to vanish on the external boundary of the reactor. At any internal interface, the scalar function u(r,E,t) and the normal component of the vector function $\vec{v}(r,E,t)\cdot\vec{N}$ are continuous ($\vec{N}$ is a unit vector normal to an interface).

Detailed expressions for the elements of the operators cited above are given in references [H-2] and [B-1].

The equations adjoint to Equations (2.1) are obtained by applying the definition of adjoint operators. That is,

$$\int_R dV \int_o^\infty dE \int_{t_o}^{t_f} dt\ \Psi^* \Theta\ \Psi = \int_R dV \int_o^\infty dE \int_{t_o}^{t_f} dt\ \Psi\ \Theta^* \Psi^* \tag{2.3}$$

where $\Theta$ is the regular operator; $\Theta^*$ is its adjoint, and $\Psi$ and $\Psi^*$ are any two functions out of the spaces on which those operators operate. The resulting adjoint equations are:

$$\begin{aligned}
&- V^{-1}\frac{\partial \Psi_0^*}{\partial t} = \nabla\cdot\vec{\Psi}_1^* - A^*\Psi_0^* + \frac{1}{k_{eff}} M^*\Psi_0^* + \sum_\iota k_{eff}^{-1} M_{d_\iota}^* C_\iota^* \\
&-3\ V^{-1}\frac{\partial \vec{\Psi}_1^*}{\partial t} = \nabla\Psi_0^* - D^{*-1}\vec{\Psi}_1^* \\
&- \chi_{d_\iota}\frac{\partial C_\iota^*}{\partial t} = \lambda_\iota \chi_{d_\iota}\Psi_0^* - \lambda_\iota \chi_{d_\iota} C_\iota^* \quad ; \ \iota = 1,2,\cdots,I
\end{aligned} \tag{2.4}$$

where

$$\begin{aligned}
A^*u^* &= \Sigma_t(r,E,t)u^*(r,E,t) - \int_o^\infty dE'\ \Sigma_{s_0}(r,E\to E',t)u^*(r,E',t) \\
D^{*-1}\vec{v}^* &= 3\Sigma_t(r,E,t)\vec{v}^*(r,E,t) - 3\int_o^\infty dE'\ \Sigma_{s_1}(r,E\to E',t)\vec{v}^*(r,E',t) \\
M^*u^* &= \sum_j (1-\beta_{eff}^j)\nu\Sigma_f^j(r,E,t)\int_o^\infty dE'\chi_p^j(E')u^*(r,E',t) \\
M_{d_\iota}^* C_\iota^* &= \sum_j \beta_\iota^j\ \nu\Sigma_f^j(r,E,t)C_\iota^*(r,t)
\end{aligned} \tag{2.5}$$

## 2.3 APPLICATION OF THE VARIATIONAL PRINCIPLE

The functional used in this derivation was proposed by Buslik [B-1] for the time-independent P-1 equations. A first order Lagrange multiplier functional for these equations is:

$$
\begin{aligned}
&F\left[u,\vec{v},C_1,C_2,\cdots,C_I,u^*,\vec{v}^*,C_1^*,C_2^*,\cdots,C_I^*\right] \\
&= -\sum_k \int_{t_o}^{t_f} dt \int_{R_k} dV \int_o^\infty dE \left\{ u^*[\mathbf{A} - k_{eff}^{-1}\mathbf{M}]u - \nabla u^* \cdot \vec{v} + \vec{v}^* \cdot \nabla u + \vec{v}^* \cdot \mathbf{D}^{-1}\vec{v} \right. \\
&\qquad - \sum_\iota u^* \lambda_\iota \chi_{d_\iota} C_\iota + u^* v^{-1} \frac{\partial u}{\partial t} + 3\vec{v}^* v^{-1} \frac{\partial \vec{v}}{\partial t} \\
&\qquad \left. - C_\iota^* \chi_{d_\iota} k_{eff}^{-1} \mathbf{M}_{d_\iota} u + C_\iota^* \lambda_\iota \chi_{d_\iota} C_\iota + C_\iota^* \frac{\partial}{\partial t} \chi_{d_\iota} C_\iota \right\} \\
&+ \int_{t_o}^{t_f} dt \int_S dS \int_o^\infty dE \left\{ \alpha(r,E)[u(+,E,t) - u(-,E,t)] \right. \\
&\qquad \left. + \beta(r,E)[u^*(+,E,t) - u^*(-,E,t)] \right\} \qquad (2.6)
\end{aligned}
$$

The reactor has been subdivided into non-ovelapping regions $R_k$ such that the functions $u, u^*, \vec{v}, \vec{v}^*$ are all continuous in the interior of every $R_k$, and u and $u^*$ vanish on the external surface of the reactor. The surface S is the union of all the internal boundary surfaces of the $R_k$. Over the interior surface S, at least one of the functions $u, u^*, \vec{v}, \vec{v}^*$ is discontinuous. The unit vector $\vec{N}$ is set to be normal to any interior surface and (+) or (-) notation is set to the side of the surface corresponding to the head (+) or tail (-) of the vector $\vec{N}$. The following figure illustrates this convention for two-dimensional geometry.

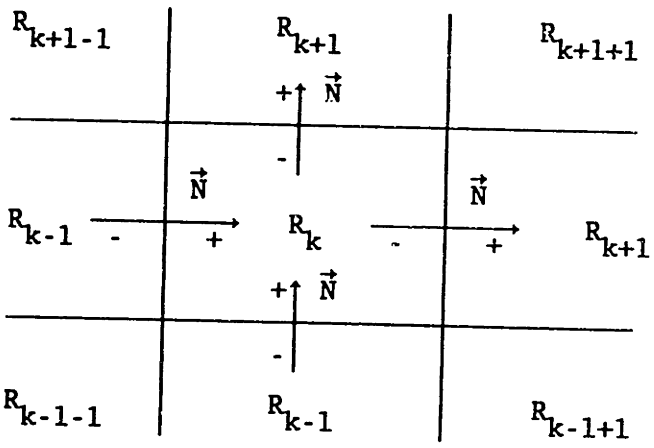


Figure 2.1 Sign convention of the functions on the interfaces

The constraint conditions of continuity of flux on S are included by the Lagrange multipliers, $\alpha$ and $\beta$.

The first-order variation of the functional, with respect to arbitrary and independent variations in $u, u^*, \vec{v}, \vec{v}^*, C_\iota$ and $C_\iota^*$ ($\iota=1,2,\cdots,I$), can be obtained when all the second terms were neglected. Using the definition of adjoint operators given by Eq. (2.3) and applying the conditions of zero ($u^*, \vec{v}^*$ and $C_\iota^* = 0.$ at $t_0$; $u, \vec{v}$ and $C_\iota = 0.$ at $t_f$) we obtain, after a considerable amount of algebra involving partial integration over the $R_k$ [H-1]:

$$\delta F = F\left( u+\delta u, \vec{v}+\delta\vec{v}, C_\iota+\delta C_\iota, u^*+\delta u^*, \vec{v}^*+\vec{v}^*, C_\iota^*+\delta C_\iota^* \right)$$

$$- F\left( u, \vec{v}, C_\iota, u^*, \vec{v}^*, C_\iota^* \right)$$

$$
\begin{aligned}
-\sum_k \int_{t_o}^{t_f} dt \int_{R_k} dV \int_o^\infty dE \Bigg\{ & \delta u^* \Big[ (A - k_{eff}^{-1} M) u + \nabla\cdot\vec{v} - \sum_\iota \lambda_\iota \chi_{d_\iota} C_\iota + V^{-1}\frac{\partial u}{\partial t} \Big] \\
& + \delta\vec{v}^*\cdot\Big[ \nabla u + D^{-1}\vec{v} + 3V^{-1}\frac{\partial\vec{v}}{\partial t} \Big] \\
& - \sum_\iota \delta C_\iota^* \Big[ k_{eff}^{-1}\chi_{d_\iota} M_{d_\iota} u - \lambda_\iota \chi_{d_\iota} C_\iota - \frac{\partial}{\partial t}\chi_{d_\iota} C_\iota \Big] \Bigg\} \\
+ \int_{t_o}^{t_f} dt \int_S dS \int_o^\infty dE \Bigg\{ & \delta\alpha(r,E)[u(+,E,t) - u(-,E,t)] \\
& + \delta u^*(+,E,t)\,[\beta(r,E) + \vec{v}(+,E,t)\cdot\vec{N}] \\
& - \delta u^*(-,E,t)\,[\beta(r,E) + \vec{v}(-,E,t)\cdot\vec{N}] \Bigg\} \\
+ \sum_k \int_{t_o}^{t_f} dt \int_{R_k} dV \int_o^\infty dE \Bigg\{ & \delta u \Big[ (A^* - k_{eff}^{-1} M^*) u^* + \nabla\cdot\vec{v}^* \\
& - \sum_d k_{eff}^{-1} \Big[\int_o^\infty dE\, \chi_{d_\iota}(E)\Big] M_{d_\iota}^* C_\iota^* - V^{-1}\frac{\partial u^*}{\partial t} \Big] \\
& + \delta\vec{v}\cdot\Big[ -\nabla u^* + D^{*-1}\vec{v}^* - 3V^{-1}\frac{\partial\vec{v}^*}{\partial t} \Big] \\
& - \sum_\iota \delta C_\iota \Big[ \chi_{d_\iota}\lambda_\iota u^* - \lambda_\iota \chi_{d_\iota} C_\iota^* + \frac{\partial}{\partial t}\chi_{d_\iota} C_\iota^* \Big] \Bigg\} \\
+ \int_{t_o}^{t_f} dt \int_S dS \int_o^\infty dE \Bigg\{ & \delta\beta(r,E)[u^*(+,E,t) - u^*(-,E,t)] \\
& + \delta u(+,E,t)\,[\alpha(r,E) - \vec{v}^*(+,E,t)\cdot\vec{N}] \\
& - \delta u(-,E,t)\,[\alpha(r,E) - \vec{v}^*(-,E,t)\cdot\vec{N}] \Bigg\}
\end{aligned}
\tag{2.7}
$$

Setting this first order variation to zero for arbitrary variations in the argument functions yields the regular and adjoint equations (2.1) and (2.4) along with the continuity conditions of fluxes and normal currents across internal interface.

To obtain a few-group approximation, we shall assume that the material composition within each $R_k$ is homogeneous (or homogenized) and

that (possibly time-dependent) multi-group spectrum functions $F_{0_n}^{k}(t)$, $F_{0_n}^{*k}(t)$, $\tilde{F}_{1_n}^{k}(t)$, $\tilde{F}_{1_n}^{*k}(t)$ for each material and the energy dependences of $\alpha(r,E)$ and $\beta(r,E)$ on each material interface are known. Trial functions are then chosen as:

$$
\begin{aligned}
u(r,E,t) &= F_{0_n}^{k}(t)\ \phi_g(r,t)\ /\Delta E_n \\
u^*(r,E,t) &= F_{0_n}^{*k}(t)\ \phi_g^*(r,t) \\
\vec{v}(r,E,t) &= \tilde{F}_{1_n}^{k}(t)\cdot\vec{J}_g(r,t)\ /\Delta E_n \\
\vec{v}^*(r,E,t) &= \tilde{F}_{1_n}^{*k}(t)\cdot\vec{J}_g^*(r,t)
\end{aligned}
\qquad (2.8)
$$

for $r \subset k$, $E \subset \Delta E_n$ and $n \subset g$

and

$$
\begin{aligned}
\alpha(r,E,t) &= g_n(t)\ a_g(r) \\
\beta(r,E,t) &= h_n(t)\ b_g(r)
\end{aligned}
\qquad (2.9)
$$

for $r$ on S, $E \subset \Delta E_n$ and $n \subset g$

Thus the entire energy range has been broken up into N non-overlapping, multigroup energy ranges $\Delta E_n$. Multigroup spectra for fluxes and currents are taken as spatially constant (although possibly time-dependent) within a given region $R_k$. Although the $F_{0_n}^{k}$ and $F_{0_n}^{*k}$ spectra are chosen so that they may vary from region to region, the $g_n$ and $h_n$ do not vary with position on S. The trial functions for $\vec{v}$ and $\vec{v}^*$ involve dyadic current spectrum functions. However, in keeping with the fact that asymptotic

current spectra are the same for all three components of the current, the dyadics $\tilde{F}_{1_n}^{k}$ and $\tilde{F}_{1_n}^{*k}$ are defined as:

$$\tilde{F}_{1_n}^{k}(t) = \tilde{I}\, F_{1_n}^{k}(t) \qquad (2.10)$$

$$\tilde{F}_{1_n}^{*k}(t) = \tilde{I}\, F_{1_n}^{*k}(t)$$

where $\tilde{I}$ is the unit diagonal dyadic.

The time dependent spectrum functions are normalized in such a manner that the conventional flux-weighted few-group parameters can be obtained by taking $F_{0_n}^{*k} = F_{1_n}^{*k} = 1$. One way to do this is as follows:

$$\sum_{n\subset g} F_{0_n}^{k}(t)\, g_n(t) = 1\ , \qquad \sum_{n\subset g} F_{0_n}^{*k}(t)\, h_n(t) = N_g$$

$$\sum_{n\subset g} \tilde{F}_{1_n}^{*k}(t)\, F_{0_n}^{k}(t) = \tilde{I}, \qquad \sum_{n\subset g} \tilde{F}_{1_n}^{k}(t)\, F_{0_n}^{*k}(t) = \tilde{I} \qquad (2.11)$$

where $N_g$ is the number of groups included in few-group g. As a result Eq. (2.8) leads to:

$$\phi_g(\mathbf{r},t) = \sum_{n\subset g} \int_{\Delta E_n} dE\ g_n(t) u(\mathbf{r},E,t)$$

$$\phi_g^{*}(\mathbf{r},t) = \frac{1}{N_g} \sum_{n\subset g} \int_{\Delta E_n} dE\ h_n(t) u^{*}(\mathbf{r},E,t)/\Delta E_n \qquad (2.12)$$

$$\vec{J}_g(\mathbf{r},t) = \sum_{n\subset g} \int_{\Delta E_n} dE\ F_{0_n}^{*k}(t)\vec{v}(\mathbf{r},E,t)$$

$$\vec{J}_g^{\,*}(r,t) = \sum_{n \subset g} \int_{\Delta E_n} dE\; F_{0_n}^{k}(t)\vec{v}^{\,*}(r,E,t)/\Delta E_n$$

Methods for generating the spectrum functions will be described in Chapter 3. The regular and adjoint interface spectra, $g_n$ and $h_n$, may be chosen arbitrarily, and to preserve the usual meanings of $\phi_g$ and $\phi_g^*$ they have been taken as unity ($g_n = h_n = 1.$; all n) for the numerical examples in this thesis. As will be described in Chapter 6, this choice may be a source of error.

## 2.4 FEW-GROUP P-1 TRANSPORT EQUATIONS

If the trial functions of Eqs.(2.8) and (2.9) are substituted into F and the resulting reduced functional made stationary with respect to independent and arbitrary variations of the adjoint components, $\phi_g^*$, $\vec{J}_g^*$, $C_\iota^*$ and $a_g$, we obtain the following equations:

$$\sum_{n \subset g} F_{0_n}^{*k} \left\{ \sum_{g' n' \subset g'} \left( A_{nn'}^{k} + V_n^{-1}\, \omega_{0_n}^{k} \delta_{nn'} - k_{eff}^{-1}\, M_{nn'}^{k} \right) F_{0_{n'}}^{k} \phi_{g'}(r,t) + \nabla\cdot\left( \tilde{F}_{1_n}^{k} \cdot \vec{J}_g(r,t) \right) - \sum_\iota \lambda_\iota \chi_{d_{\iota,n}} C_\iota(r,t) + V_n^{-1}\, F_{0_n}^{k} \frac{\partial}{\partial t} \phi_g(r,t) \right\} = 0. \tag{2.13}$$

$$\sum_{n \subset g} \tilde{F}_{1_n}^{*k} \cdot \left\{ F_{0_n}^{k}\, \nabla\phi_g(r,t) + 3\, V_n^{-1}\, \tilde{F}_{1_n}^{k} \cdot \frac{\partial}{\partial t} \vec{J}_g(r,t) + \sum_{g' n' \subset g'} \left( [D_{nn'}^{-1}]^{k} + 3 V_n^{-1}\, \omega_{1_n}^{k} \right) \tilde{F}_{1_{n'}}^{k} \cdot \vec{J}_{g'}(r,t) \right\} = 0. \tag{2.14}$$

$$k_{eff}^{-1} \sum_{g'} \sum_{n' \subset g'} \mathbf{M}_{d_{\iota,n'}}^{k} F_{0_{n'}}^{k} \phi_{g'}(r,t) - \lambda_{\iota} C_{\iota}(r,t) = \frac{\partial}{\partial t} C_{\iota}(r,t) \qquad (2.15)$$

$$\sum_{n \subset g} g_n F_{0_n}^{k+} \phi_g(r_s^+,t) = \sum_{n \subset g} g_n F_{0_n}^{k-} \phi_g(r_s^-,t) \qquad (2.16)$$

$$\sum_{n \subset g} F_{0_n}^{*k+} h_n b_g(r) = - \sum_{n \subset g} F_{0_n}^{*k+} F_{1_n}^{k+} \left[ \vec{J}_g(r_s^+,t) \cdot \vec{N} \right] \qquad (2.17)$$

$$\sum_{n \subset g} F_{0_n}^{*k-} h_n b_g(r) = - \sum_{n \subset g} F_{0_n}^{*k-} F_{1_n}^{k-} \left[ \vec{J}_g(r_s^-,t) \cdot \vec{N} \right] \qquad (2.18)$$

where

$$\mathbf{A}_{nn'}^{k} = \Sigma_{t_n}^{k}(t)\delta_{nn'} - \Sigma_{s_{0_{nn'}}}^{k}(t)$$
$$= \int_{\Delta E_n} dE\, \Sigma_t^k(E,t)/\Delta E_n - \int_{\Delta E_n} dE \int_{\Delta E_{n'}} dE'\, \Sigma_{s_0}^k(E' \to E,t)/\Delta E_{n'},$$

$$[\mathbf{D}_{nn'}^{-1},]^k = 3\, \Sigma_{t_n}^{k}(t)\delta_{nn'} - 3\, \Sigma_{s_{1_{nn'}}}^{k}(t)$$
$$= 3\int_{\Delta E_n} dE\, \Sigma_t^k(E,t)/\Delta E_n - 3\int_{\Delta E_n} dE \int_{\Delta E_{n'}} dE'\, \Sigma_{s_1}^k(E' \to E,t)/\Delta E_{n'},$$

$$\mathbf{M}_{nn'}^{k} = \sum_{j} (1-\beta_{eff}^{j}) \chi_{p_n}^{j,k}\, \nu\Sigma_{f_{n'}}^{j,k}(t)$$
$$= \sum_{j} (1-\beta_{eff}^{j}) \int_{\Delta E_n} dE\, \chi_{p_n}^{j,k}(E) \int_{\Delta E_{n'}} dE'\, \nu\Sigma_{f_{n'}}^{j,k}(E',t)/\Delta E_{n'}, \qquad (2.19)$$

$$\mathbf{M}_{d_{\iota,n'}}^{k} = \sum_{j} \beta_{\iota}^{j}\, \nu\Sigma_{f_{n'}}^{j,k}(t)$$
$$= \sum_{j} \beta_{\iota}^{j} \int_{\Delta E_{n'}} dE'\, \nu\Sigma_{f_{n'}}^{j,k}(E',t)/\Delta E_{n'},$$

$$V_n^{-1} = (1./\Delta E_n) \int_{\Delta E_n} dE\ V^{-1}(E)$$

$$\omega_{i_n}^k = \frac{1}{F_{i_n}^k(t)} \frac{\partial}{\partial t} F_{i_n}^k(t) \ ; \ i=0,1$$

If we define few-group parameters as the following:

$$\Sigma_{t_g}^k(t) = \sum_{n\subset g} \sum_{n'\subset g'} F_{0_n}^{*k}\, \Sigma_{t_n}^k(t)\, \delta_{nn'}\, F_{0_{n'}}^k$$

$$\Sigma_{s_{0_{gg'}}}^k(t) = \sum_{n\subset g} \sum_{n'\subset g'} F_{0_n}^{*k}\, \Sigma_{s_{0_{nn'}}}^k(t)\, F_{0_{n'}}^k$$

$$\Sigma_{a_g}^k(t) = \Sigma_{t_g}^k(t) - \sum_{g'} \Sigma_{s_{0_{g'g}}}^k(t)$$

$$D_{gg'}^{-1,k}(t) = \sum_{n\subset g} \sum_{n'\subset g'} F_{1_n}^{*k}\, D_{nn'}^{-1,k}(t)\, F_{1_{n'}}^k \qquad (2.20)$$

$$\chi_{p_g}^k(t) = \sum_{n\subset g} F_{0_n}^{*k}\, \chi_{p_n}^k$$

$$\chi_{d_{\iota,g}}^k(t) = \sum_{n\subset g} F_{0_n}^{*k}\, \chi_{d_{\iota,n}}^k \ ; \quad (\iota=1,2,\cdots,I)$$

$$\nu\Sigma_{f_{g'}}^k(t) = \sum_{n'\subset g'} \nu\Sigma_{f_{n'}}^k(t)\, F_{0_{n'}}^k$$

$$V_{i_g}^{-1,k}(t) = \sum_{n\subset g} F_{i_n}^{*k}\, V_{i_n}^{-1,k}\, F_{i_n}^k \ ; \quad (i=0,1)$$

$$\omega_{i_g}^k(t) = V_{i_g}^k(t) \sum_{n\subset g} F_{i_n}^{*k} \frac{1}{V_{i_n}} \frac{\partial}{\partial t} F_{i_n}^k(t) \ ; \quad (i=0,1)$$

Eqs. (2.13) through (2.18) become the few-group P-1 equations:

$$V_{0_g}^{-1,k} \frac{\partial}{\partial t}\phi_g(r,t) = -\nabla\cdot\vec{J}_g(r,t) - \sum_{g'}\left[A_{gg'}^{k}(t) + V_{0_g}^{-1,k}\omega_{0_g}^{k}\delta_{gg'} - k_{eff}^{-1}M_{gg'}^{k}(r)\right]\phi_{g'}(r,t) + \sum_{\iota}\chi_{d_{\iota,g}}^{k}\lambda_{\iota}C_{\iota}(r,t) \quad (2.21)$$

$$3\,V_{1_g}^{-1,k}\frac{\partial}{\partial t}\vec{J}_g(r,t) = -\nabla\phi_g(r,t) - \sum_{g'}\left[D_{gg'}^{-1,k}(r) + 3\,V_{1_g}^{-1,k}\omega_{1_g}^{k}\delta_{gg'}\right]\vec{J}_{g'}(r,t) \quad (2.22)$$

$$\frac{\partial}{\partial t}C_{\iota}(r,t) = k_{eff}^{-1}\sum_{g'}M_{d_{\iota,g'}}^{k}(r)\phi_{g'}(r,t) - \lambda_{\iota}C_{\iota}(r,t) \quad (2.23)$$

where

$$A_{gg'}^{k} = \Sigma_{t_g}^{k}(t)\delta_{gg'} - \Sigma_{s_{gg'}}^{k}(t)$$

$$M_{gg'}^{k} = \sum_{j}(1-\beta_{eff}^{j})\chi_{p_g}^{j,k}\,\nu\Sigma_{f_{g'}}^{j,k}(t) \quad (2.24)$$

$$M_{d_{\iota,g'}}^{k} = \sum_{j}\beta_{\iota}^{j}\,\nu\Sigma_{f_{g'}}^{j,k}(t)$$

with interface boundary conditions:

$$\phi_g(r_s^{+},t) = \phi_g(r_s^{-},t) \quad (2.25)$$

$$\vec{J}_g(r_s^{+},t)\cdot\vec{N} = \vec{J}_g(r_s^{-},t)\cdot\vec{N} \quad (2.26)$$

Equations (2.20) are the definitions of the bilinearly-weighted few-group P-1 parameters.

## 2.5 FEW-GROUP DIFFUSION THEORY CONSTANTS

The conventional diffusion theory model neglects adjoint spectra weighting. Thus from the viewpoint of bilinearly-weighted parameters, it assumes the adjoint weighting to be a unit weighting. However, detailed spectra shapes for real reactor compositions will be shown in Chapter 5 not to be at all flat. Thus, from the variational point of view, one would expect bilinearly weighted few-group parameters to yield more accurate predictions of reactor behavior.

If the $D^{k}_{nn'}$ are diagonal ($D^{k}_{nn'} = D^{k}_{n}\,\delta_{nn'}$), the P-0 and P-1 components of the infinite medium spectra are related by:

$$\begin{aligned} F_{1}{}^{k}_{n} &\propto B^{k}_{m} D^{k}_{n} F_{0}{}^{k}_{n} \\ F^{*k}_{1n} &\propto B^{k}_{m} D^{k}_{n} F^{*k}_{0n} \,/\, N_{g} \end{aligned} \tag{2.27}$$

where $(B^{k}_{m})^{2}$ is the material buckling of region k (See Chapter 3) and the devision by $N_{g}$ is because of the normalization, Eq.(2.11). The definition of the diffusion coefficient can then be simplified. Applying Eq. (2.27) to the the definition of $D^{-1,k}_{gg'}$ in (2.20), and using (2.11) yields

$$D_{gg'}^{-1,k} = \delta_{gg'} D_g^{-1,k} = \frac{\sum_{n\subset g} (B_m^k D_n^k F_{o_n}^{*k})(D_n^{-1})^k (B_m^k D_n^k F_{o_n}^k)}{\sum_{n\subset g} (B_m^k D_n^k F_{o_n}^{*k}) F_{o_n}^k \sum_{n\subset g} (B_m^k D_n^k F_{o_n}^k) F_{o_n}^{*k}}$$

$$= \frac{1}{\sum_{n\subset g} F_{o_n}^{*k} D_n^k F_{o_n}^k}$$

If now we reduce to the conventional flux-weighted form of diffusion coefficient by setting $F_{o_n}^{*k} = 1$, we obtain

$$D_g^k = \sum_{n\subset g} D_n^k F_{o_n}^k \tag{2.28}$$

The other conventional few-group constants reduce to:

$$\Sigma_{\alpha_g}^k(r) = \sum_{n\subset g} \Sigma_{\alpha_n}^k(r) F_{o_n}^k \qquad (\alpha = t, f)$$

$$\Sigma_{s_{o_{gg'}}}^k(r) = \sum_{n\subset g} \sum_{n'\subset g'} \Sigma_{s_{o_{nn'}}}^k(r) F_{o_{n'}}^k$$

$$\chi_{p_g}^k = \sum_{n\subset g} \chi_{p_n}^k \qquad \chi_{d_{\iota,g}}^k = \sum_{n\subset g} \chi_{d_{\iota,n}}^k \quad (\iota=1,2,\cdots,I)$$

$$V_{i_g}^{-1,k} = \sum_{n\subset g} V_n^{-1,k} F_{i_n}^k ; \quad (i=0,1) \tag{2.29}$$

$$\omega_{i_g} = V_{i_g} \sum_{n\subset g} \frac{1}{V_n} \frac{d}{dt} F_{i_n}^k(t) ; \quad (i=0,1)$$

# Chapter 3

## GENERATION OF FEW-GROUP PARAMETERS

### 3.1 INTRODUCTION

In Chapter 2, Equation (2.20) which defines the bilinearly weighted parameters and Equations (2.28) and (2.29) which define the conventional diffusion theory constants were derived. For consistency with the few-group equations, unstarred weighting functions (real flux spectra and current spectra) and starred weighting functions (adjoint flux spectra and current spectra) should also be obtained from the P-1 approximation to the transport equations, (2.1) and (2.4).

In this chapter, the energy spectrum calculation method will be presented and validated by comparison with analytic solutions. Collapsing procedures to obtain few-group parameters are also validated by comparison with results of a commercial computer program, CASMO-3 [S-4].

### 3.2 SPECTRUM CALCULATIONS

For consistency the P-1 equations (2.1) and (2.4) are taken as the starting point for the calculation of real and adjoint energy spectra.

### 3.2.1 Real Spectrum Calculation

Removing the time-dependency, we may rewrite Eq. (2.1) as:

$$\nabla\cdot\vec{\Psi}_1(r,E) + \Sigma_t(r,E)\Psi_0(r,E) = \int_0^\infty dE'\ \Sigma_{s_0}(r,E'\to E)\Psi_0(r,E') + k_{eff}^{-1}\sum_j \chi^j(E)\int_0^\infty dE'\nu\Sigma_f^j(r,E')\Psi_0(r,E') \tag{3.1}$$

$$\nabla\Psi_0(r,E) + 3\Sigma_t(r,E)\vec{\Psi}_1(r,E) = 3\int_0^\infty dE'\ \Sigma_{s_1}(r,E'\to E)\vec{\Psi}_1(r,E') \tag{3.2}$$

For the multi-group energy spectrum calculation, it is assumed that homogenized multi-group cross sections over the large, isotopically homogeneous regions of interest are known. Therefore, within a given homogeneous material composition, a particular solution for $\Psi_0(r,E)$ and $\Psi_1(r,E)$ may be written as separable functions of space and energy. A Fourier transform approach gives the following approximations [H-1]:

$$\Psi_0(r,E) = F_0(E)\ \exp\ (-iB_m\cdot r) \tag{3.3}$$

$$\vec{\Psi}_1(r,E) = F_1(E)\ \left[\exp\ (-iB_m\cdot r)\right]\ \vec{u} \tag{3.4}$$

where $\vec{u}$ is a unit vector of direction of the vector $\vec{B}$ and $B_m^2$ is the materials buckling. Substitution into the Eq. (3.1) (with homogeneous cross sections which are independent of r) yields the P-1 equations for the continuous energy spectra:

$$-iB_m F_1^k(E) + \Sigma_t^k(E) F_0^k(E) = \int_0^\infty dE' \left[ \Sigma_{s_0}^k(E' \to E) + k_{eff}^{-1} \sum_j \chi^j(E) \nu \Sigma_f^{jk}(E') \right] F_0^k(E') \tag{3.5}$$

$$-iB_m F_0^k(E) + 3\Sigma_t^k(E) F_1^k(E) = 3\int_0^\infty dE' \; \Sigma_{s_1}^k(E' \to E) F_1^k(E') \tag{3.6}$$

Now we express these equations in multi-group form with the functions $F_{0_n}^k(E)$ and $F_{1_n}^k(E)$ replaced by the energy spectra $F_{0_n}^k$ and $F_{1_n}^k$. Dropping superscripts k, we obtain:

$$-iB_m F_{1_n} + \Sigma_{t_n} F_{0_n} = \sum_{n'} \Sigma_{s_{0_{nn'}}} F_{0_{n'}} + k_{eff}^{-1} \chi_n \sum_{n'} \nu \Sigma_{f_{n'}} F_{0_{n'}} \tag{3.7}$$

$$-iB_m F_{0_n} + 3 \Sigma_{t_n} F_{1_n} = 3 \sum_{n'} \Sigma_{s_{1_{nn'}}} F_{1_{n'}} \tag{3.8}$$

Next it is convenient to write these equations in matrix form:

$$[A_0][F_0] = iB_m[F_1] + k_{eff}^{-1} [\chi][\nu\Sigma_f]^T[F_0] \tag{3.9}$$

$$3\,[A_1][F_1] = iB_m[F_0] \tag{3.10}$$

where
$$[F_0] = \text{column } \{F_{0_1}, F_{0_2}, \cdots, F_{0_N}\}$$
$$[F_1] = \text{column } \{F_{1_1}, F_{1_2}, \cdots, F_{1_N}\}$$
$$[A_0] = \{A_{0_{nn'}}\},\ N\times N \text{ matrix};\quad A_{0_{nn'}} = \Sigma_{t_n}\delta_{nn'} - \Sigma_{s_{0_{nn'}}} \tag{3.11}$$
$$[A_1] = \{A_{1_{nn'}}\},\ N\times N \text{ matrix};\quad A_{1_{nn'}} = \Sigma_{t_n}\delta_{nn'} - \Sigma_{s_{1_{nn'}}}$$
$$[\chi] = \text{column } \{\chi_1, \chi_2, \cdots, \chi_N\}$$
$$[\nu\Sigma_f] = \text{column } \{\nu\Sigma_{f_1}, \nu\Sigma_{f_2}, \cdots, \nu\Sigma_{f_N}\}$$

Taking the inverse matrix of $[A_1]$ permits Eq. (3.10) to be rewritten as:

$$[F_1] = i\, B_m\, [D]\, [F_0] \tag{3.12}$$

where $[D] = \frac{1}{3}\,[A_1]^{-1}$. Thus we obtain:

$$\left([A_0] - B_m^2\,[D]\right)\,[F_0] = k_{eff}^{-1}\,[\chi]\,[\nu\Sigma_f]^T\,[F_0] \tag{3.13}$$

This is the equation to be solved for the flux spectrum.

### 3.2.2 Adjoint Spectrum Calculation

Equations for the adjoint energy spectra are derived in an analogous way from Eq. (2.4). The Adjoint continuous P-1 equations are:

$$\begin{aligned} -\nabla\cdot\vec{\Psi}_1^*(r,E) + \Sigma_t(r,E)\Psi_0^*(r,E) &= \int_o^\infty dE'\ \Sigma_{s_0}(r,E\to E')\Psi_0^*(r,E') \\ &\quad + k_{eff}^{-1}\sum_j \nu\Sigma_f^j(r,E)\int_o^\infty dE'\chi^j(E')\Psi_0^*(r,E') \end{aligned} \tag{3.14}$$

$$-\nabla\Psi_0^*(r,E) + 3\Sigma_t(r,E)\vec{\Psi}_1^*(r,E) = 3\int_o^\infty dE'\ \Sigma_{s_1}(r,E\to E')\vec{\Psi}_1^*(r,E') \tag{3.15}$$

Applying the same procedure which was used for real spectra, we obtain:

$$iB_m F^*_{1n} + \Sigma_{t_n} F^*_{0n} = \sum_{n'} \Sigma_{s_{0n'n}} F^*_{0n'} + k^{-1}_{eff} \nu\Sigma_{f_n} \sum_{n'} \chi_{n'} F^*_{0n'} \qquad (3.16)$$

$$iB_m F^*_{0n} + 3\,\Sigma_{t_n} F^*_{1n} = 3 \sum_{n'} \Sigma_{s_{1n'n}} F^*_{1n'} \qquad (3.17)$$

In matrix form these become:

$$[A^*_0][F^*_0] = -\,iB_m[F^*_1] + k^{-1}_{eff}\,[\nu\Sigma_f{}^*][\chi^*]^T[F_0] \qquad (3.18)$$

$$3\,[A^*_1][F^*_1] = -\,iB_m[F^*_0] \qquad (3.19)$$

where
$$[F^*_0] = \text{column}\,(F^*_{0_1}, F^*_{0_2}, \cdots, F^*_{0_N})$$
$$[F^*_1] = \text{column}\,(F^*_{1_1}, F^*_{1_2}, \cdots, F^*_{1_N}) \qquad (3.20)$$
$$[A^*_0] = [A_0]^T = (A^*_{0nn'}),\ N\times N \text{ matrix};\quad A^*_{0nn'} = \Sigma_{t_n}\delta_{nn'} - \Sigma_{s_{0n'n}}$$
$$[A^*_1] = [A_1]^T = (A^*_{1nn'}),\ N\times N \text{ matrix};\quad A^*_{1nn'} = \Sigma_{t_n}\delta_{nn'} - \Sigma_{s_{1n'n}}$$
$$[\chi^*] = [\chi] = \text{column}\,(\chi_1, \chi_2, \cdots, \chi_N)$$
$$[\nu\Sigma_f{}^*] = [\nu\Sigma_f] = \text{column}\,(\nu\Sigma_{f_1}, \nu\Sigma_{f_2}, \cdots, \nu\Sigma_{f_N})$$

Eq. (3.19) may be rewritten as:

$$[F^*_1] = -\,i\,B_m\,[D^*]\,[F^*_0] \qquad (3.21)$$

where $[D^*] = \frac{1}{3}\,[A^*_1]^{-1}$.

Then we have:

$$\left([A_0^*] - B_m^2 [D^*]\right) [F_0^*] = k_{eff}^{-1} [\nu\Sigma_f] [\chi]^T [F_0^*] \qquad (3.22)$$

This is the equation to be solved for the adjoint flux spectrum.

## 3.3 NUMERICAL IMPLEMENTATION

Solving Equations (3.13) and (3.22) governing the energy spectra is an eigenvalue problem whose largest eigenvalue (always real, but either positive or negative) is the fundamental material buckling $(B_m^2)_1$. The solutions corresponding to $(B_m^2)_1$ are the asymptotic spectra which prevail at some distance from material discontinuities.

### 3.3.1 Real Flux Spectrum Calculation

The fundamental material buckling $(B_m^2)_1$ can be found easily by taking $k_{eff} = 1.0$ and normalizing the fission source to unity. The overall procedure for solving Eq. (3.13) is summarized in the following six steps:

1. Set both $k_{eff}$ and $[\nu\Sigma_f]^T[F_0]$ equal to 1.
2. Assume $B_m^2 = 0$. Solve $[A_0]\ [F_0] = [\chi]$ for $F_{0_n}$ (Iteration is needed for the upscattering energy groups). This step yields the infinite-medium spectra.
3. Find one-group diffusion parameters:

$$\Sigma_a^1 = \sum_n \Sigma_{a_n} F_{0_n} / \phi^1$$

$$\nu\Sigma_f^1 = \sum_n \Sigma_{f_n} F_{0_n} / \phi^1$$

$$D^1 = \sum_n D_n F_{0_n} / \phi^1$$

where $\phi^1 = \sum_n F_{0_n}$

4. Estimate $B_m^2$ from:

$$( D^1 B_m^2 + \Sigma_a^1 ) \phi^1 = \nu\Sigma_f^1 \phi^1$$

$$B_m^2 = \frac{\nu\Sigma_f^1 - \Sigma_a^1}{D^1}$$

5. Using this value of $B_m^2$, solve:

$$( [A_0] + B_m^2[D] ) [F_0] = [\chi]$$

6. Repeat step 3 through 5 until both $B_m^2$ and the spectrum converge.

The asymptotic current spectrum is obtained from Eq. (3.12). Here, the current spectrum $F_{1_n}$ can have either a positive or negative sign depending on the sign of $B_m^2$ and it may also contains imaginary unit i. However, only its energy shape is needed to obtain few-group parameters. Accordingly for use in (2.8) we renormalize results in accord with (2.27) and (2.11).

### 3.3.2 Adjoint Flux Spectrum Calculation

The adjoint spectrum equation (3.22) can be solved using the same solution algorithm as the real spectrum equation. The operators in Eq. (3.20) which are adjoint to the operators in Eq. (3.11) require a transformation of data in order to utilize the same algorithm [D-1]. The transformation consists of:

1. Reversing the order of the group structure of the cross section data (e.g. $\Sigma_{s_0 gg'} \rightarrow \Sigma_{s_0 G+1-g,G+1-g'}$)
2. Transposing the matrices $[A_0^*]$ and $[D^*]$ (e.g. $\Sigma_{s_0 gg'} \rightarrow \Sigma_{s_0 g'g}$)
3. Interchanging $\nu\Sigma_{f_g}$ and $\chi_g$ terms.

The same matrix structures as for the real spectrum equation result. Since a matrix and its transpose have the same eigenvalue, the calculated $B_m^2$ ought to be the same as for the real spectrum equation. Accordingly steps 2 through 4 can be omitted from the six steps described above. The resulting adjoint flux spectrum is obtained in reverse group order, $g = G,G-1,\cdots,1$.

### 3.3.3 Computer Code

The numerical methods outlined in (3.3.1) and (3.3.2) were incorporated into a computer code, hereafter referred to as MESADES (Multi-group Energy Spectra with Adjoint Energy Spectra). This computer

code solves the multi-group energy spectrum equations for both real spectra and adjoint spectra. It also collapses multi-group cross-sections into both conventional diffusion theory constants and bilinearly weighted transport parameters.

The program was written in the VAX FORTRAN language. Several versions of program were written for special purposes. A detailed listing of the code is not given in this thesis. However a list of the program and input/output description can be found in the code manual which is available on request to the MIT Department of Nuclear Engineering.

## 3.4 TEST PROBLEMS

As a first test for the computer code MESADES, it is useful to choose a simple problem for which solutions can be found by hand calculation. Hand calculations were performed for three energy groups in the reverse order to the calculational procedure programed in MESADES. That is, a 3-group adjoint spectra and all the 3-group diffusion parameters (except absorption cross sections) were assumed as known. Next absorption cross sections were chosen to satisfy the criticality. Then, the real flux spectrum was calculated for this critical reactor composition. This result was compared with the output of MESADES. MESADES produced the same material buckling and the same real and adjoint flux spectra as those from hand calculation. Collapsed 1-group parameters also matched each other. Details of the hand calculation can be found in Appendix 1.

As a second test for MESADES, its accuracy was tested by comparison with the industry computer code, CASMO-3 [S-4]. Twenty-three-group cross

sections for three different fuel-assembly compositions were collapsed into 2-group cross sections by MESADES. Homogenized 23-group cross sections for three fuel-assemblies (A00,C00, and CL0) are given in Appendix 2. Since bilinearly weighted 2-group parameters are not available from CASMO-3, collpased 2-group cross sections were compared only for the conventional weighting. MESADES produced the same 2-group parameters as the CASMO-3. Edited 2-group parameters from CASMO-3 and MESADES are given in Appendix 2 and 5 respectively.

# Chapter 4

## MULTI-GROUP NODAL TRANSIENT ANALYSIS

### 4.1 INTRODUCTION

The primary purpose of this thesis is to investigate the validity of procedures for collapsing few-group parameters from multi-group cross sections. Thus the energy behavior of the neutrons is the principal concern. Spatial behavior is of course coupled to energy behavior in multiregion cores. However, one would expect most of the physics of that coupling to be present in one-dimensional situations. Because of this, and because of the great expense of a three dimensional multi-group transient code, the basic multi-group nodal transient computer program used in this study was written for one-dimensional geometry.

In order to cover the range of transient analysis of general interest four kinds of transients were modeled : step reactivity changes, control rod bank movements, reactor coolant-inlet-temperatute changes and core coolant-flow-rate changes. Because highly accurate thermal-hydraulic feedback modelling was not a major concern, a simple thermal-hydraulic model was implemented, namely that used in the WIGL-code [V-1].

For meaningful numerical comparisons, consistency is the essential key in order to avoid differences due to essentially different models rather than to the approximations being investigated. Accordingly, the reference model was derived from the P-1 equations as was the spectrum

model in chapter 3. Also, one single program was written to be run for both multi-group transients and few-group transients. As a starting point for cross-section group-collapsing, it was assumed that equivalent homogenized multi-group transport parameters, which are spatially constant over large volumes, can be used.

In the present chapter, the derivation of the multi-group, time-dependent nodal equations is given. Numerical schemes used for solving the nodal equations and thermal hydraulic equations are also introduced. Finally the accuracy of the program developed is tested by comparisons with analytic solutions and with QUANDRY.

## 4.2 DERIVATION OF TIME-DEPENDENT NODAL EQUATIONS

To maintain consistency, the P-1 equations (2.1) are used as the basis of the time-dependent nodal balance equations. For one-dimensional slab geometry, we may rewrite Eq.(2.1) for energy group g as

$$
\begin{aligned}
V_{0_g}^{-1}(x)\frac{\partial}{\partial t}\phi_g(x,t) &= -\frac{\partial}{\partial x}J_g(x,t) - \sum_{g'}\left[\Sigma_{t_g}(x,t)\delta_{gg'} - \Sigma_{s_{0_{gg'}}}(x,t)\right]\phi_{g'}(x,t) \\
&\quad + k_{eff}^{-1}[1-\beta_{eff}(x)]\chi_{p_g}(x)\sum_{g'}\nu\Sigma_{f_{g'}}(x,t)\phi_{g'}(x,t) \\
&\quad + \sum_{\iota}\chi_{d_{\iota,g}}(x)\lambda_\iota C_\iota(x,t) \qquad (4.1)\\
\frac{\partial}{\partial x}\phi_g(x,t) &= -3\sum_{g'}\left[\Sigma_{t_g}(x,t)\delta_{gg'} - \Sigma_{s_{1_{gg'}}}(x,t)\right]J_{g'}(x,t) \\
\frac{\partial}{\partial t}C_\iota(x,t) &= k_{eff}^{-1}\beta_\iota(x)\sum_{g'}\nu\Sigma_{f_{g'}}(x,t)\phi_{g'}(x,t) - \lambda_\iota C_\iota(x,t) \\
&\qquad \iota = 1,2,\cdots,I
\end{aligned}
$$

where the time-derivative of the current has been neglected since it is expected to produce a negligible effect for problems of interest.

For convenience, Eq.(4.1) is cast in matrix form:

$$[V_0^{-1}(x)]\frac{\partial}{\partial t}[\phi(x,t)] = -\frac{\partial}{\partial x}[J(x,t)] - [A_0(x,t)][\phi(x,t)] + k_{eff}^{-1}[1-\beta_{eff}(x)][\chi_p(x)][\nu\Sigma_f(x,t)]^T[\phi(x,t)] + \sum_\iota [\chi_{d_\iota}(x)]\lambda_\iota C_\iota(x,t) \tag{4.2}$$

$$\frac{\partial}{\partial x}[\phi(x,t)] = -[D^{-1}(x,t)][J(x,t)] \tag{4.3}$$

$$\frac{\partial}{\partial t}C_\iota(x,t) = k_{eff}^{-1}\beta_\iota(x)[\nu\Sigma_f(x,t)]^T[\phi(x,t)] - \lambda_\iota C_\iota(x,t) \qquad \iota=1,2,\cdots,I \tag{4.4}$$

where

$$[\phi(x,t)] = \text{column}\{\phi_1(x,t),\phi_2(x,t),\cdots,\phi_G(x,t)\}$$

$$[J(x,t)] = \text{column}\{J_1(x,t),J_2(x,t),\cdots,J_G(x,t)\}$$

$$[A_0(x,t)] = \{A_{0_{gg'}}(x,t)\},\ G\times G \text{ matrix};\quad A_{0_{gg'}}(x,t) = \Sigma_{t_g}(x,t)\delta_{gg'} - \Sigma_{s_{0_{gg'}}}(x,t)$$

$$[A_1(x,t)] = \{A_{1_{gg'}}(x,t)\},\ G\times G \text{ matrix};\quad A_{1_{gg'}}(x,t) = \Sigma_{t_g}(x,t)\delta_{gg'} - \Sigma_{s_{1_{gg'}}}(x,t) \tag{4.5}$$

$$[D^{-1}(x,t)] = 3\,[A_1(x,t)]$$

$$[\chi_p(x)] = \text{column}\{\chi_{p_1}(x),\chi_{p_2}(x),\cdots,\chi_{p_G}(x)\}$$

$$[\chi_{d_\iota}(x)] = \text{column}\ \{\chi_{d_{\iota,1}}(x), \chi_{d_{\iota,2}}(x), \cdots, \chi_{d_{\iota,G}}(x)\}$$

$$[\nu\Sigma_f(x,t)] = \text{column}\ \{\nu\Sigma_{f_1}(x,t), \nu\Sigma_{f_2}(x,t), \cdots, \nu\Sigma_{f_G}(x,t)\}.$$

### 4.2.1 Time Differencing Method

Consider a time step $\Delta_n = t^{n+1} - t^n$. Equation (4.4) can be solved analytically within this time step as

$$C_\iota(x,t) = e^{-\lambda_\iota (t-t^n)} \left\{ C_\iota(x)^n + \int_{t^n}^{t} dt'\, e^{\lambda_\iota (t'-t^n)} k_{eff}^{-1} \beta_\iota(x) [\nu\Sigma_f(x,t')]^T [\phi(x,t')] \right\}. \tag{4.6}$$

We assume that $[\nu\Sigma_f(x,t')]^T[\phi(x,t')]$ varies linearly with time during time step $\Delta_n$:

$$[\nu\Sigma_f(x,t)]^T[\phi(x,t)] \simeq \left([\nu\Sigma_f(x)]^T[\phi(x)]\right)^n \frac{(t^{n+1} - t)}{\Delta_n} + \left([\nu\Sigma_f(x)]^T[\phi(x)]\right)^{n+1} \frac{(t-t^n)}{\Delta_n} \tag{4.7}$$

where superscript n or n+1 indicates whether the matrix is evaluated at time $t^n$ or $t^{n+1}$, respectively. (This representation is adopted throughout the text.)

Application of this assumption to Eq.(4.6) gives

$$C_\iota^{n+1}(x) = C_\iota^n(x)\theta_\iota^n + k_{eff}^{-1}\left[[\nu\Sigma_f(x)]^T[\phi(x)]\right]^{n+1}\frac{\beta_\iota(x)}{\lambda_\iota}\zeta_\iota^n$$

$$k_{eff}^{-1}\left[[\nu\Sigma_f(x)]^T[\phi(x)]\right]^{n}\frac{\beta_\iota(x)}{\lambda_\iota}\eta_\iota^n \qquad (4.8)$$

where

$$\zeta_\iota^n = 1 - \frac{1}{\lambda_\iota\,\Delta_n}\left(1 - e^{-\lambda_\iota\Delta_n}\right)$$

$$\eta_\iota^n = \frac{1}{\lambda_\iota\,\Delta_n}\left(1 - e^{-\lambda_\iota\Delta_n}\right) - e^{-\lambda_\iota\Delta_n} \qquad (4.9)$$

$$\theta_\iota^n = e^{-\lambda_\iota\Delta_n}.$$

Fully implicit time-difference of Eq.(4.2) for the time interval $\Delta_n$ gives

$$\frac{1}{\Delta_n}[V_0^{-1}(x)][\phi(x)]^{n+1} = \frac{1}{\Delta_n}[V_0^{-1}(x)][\phi(x)]^n - \frac{d}{dx}[J(x)]^{n+1}$$

$$- [A_0(x)]^{n+1}[\phi(x)]^{n+1} \qquad (4.10)$$

$$+ k_{eff}^{-1}[1-\beta_{eff}(x)][\chi_p(x)]^{n+1}\left[[\nu\Sigma_f(x)]^T[\phi(x)]\right]^{n+1}$$

$$+ \sum_\iota [\chi_{d_\iota}(x)]^{n+1}\lambda_\iota C_\iota^{n+1}(x).$$

Now we substitute $C_\iota^{n+1}(x)$ as given by Eq.(4.8) to obtain

$$\frac{d}{dx}[J(x)]^{n+1} + [A_0(x)]^{n+1}[\phi(x)]^{n+1} + \frac{1}{\Delta_n}[V_0^{-1}(x)][\phi(x)]^{n+1}$$

$$- k_{eff}^{-1}\left\{[1-\beta_{eff}(x)][\chi_p(x)]^{n+1} + \sum_i \beta_i(x)[\chi_{d_i}(x)]^{n+1}\zeta_i^n\right\}$$

$$\times\left\{[\nu\Sigma_f(x)]^T[\phi(x)]\right\}^{n+1}$$

$$= k_{eff}^{-1}\sum_i \beta_i(x)[\chi_{d_i}(x)]^{n+1}\eta_i^n\left\{[\nu\Sigma_f(x)]^T[\phi(x)]\right\}^n \qquad (4.11)$$

$$+ \frac{1}{\Delta_n}[V_0^{-1}(x)][\phi(x)]^n + \sum_i [\chi_{d_i}(x)]^{n+1}\lambda_i\,\theta_i^n\,C_i^n(x)$$

Equation (4.3), (4.8) and (4.11) constitute the starting point of our reference nodal model.

### 4.2.2 Derivation of Spatial Coupling Equations

Now assume that homogeneous group parameters, spatially constant over the large regions, called nodes, are available.

In order to solve the model equations, (4.8) and (4.11) are used to eliminate the current terms. Instead of solving the equations analytically as with QUANDRY (a very complex procedure in more than two-energy groups), a less rigorous approximation is used here. For a given node, the flux shape is approximated by a quadratic expansion determined by the node-average flux, $[\bar{\phi}_i]$ and node surface-average fluxes, $[\phi(x_i)]$ and $[\phi(x_{i+1})]$.

$$[\phi(x)]^n \simeq [\phi(x_i^+)]^n\, Q_i^-(x) + [\bar{\phi}_i]^n\, \tilde{Q}_i(x) + [\phi(x_{i+1}^-)]^n\, Q_i^+(x) \quad (4.12)$$

The quadratic functions $Q_i(x)$ satisfy the following conditions:

| | $Q_i^-(x)$ | $\tilde{Q}_i(x)$ | $Q_i^+(x)$ |
|---|---|---|---|
| $fn(x_i)$ | 1. | 0. | 0. |
| $\frac{1}{h_i}\int_{x_i}^{x_{i+1}} dx\ fn(x)$ | 0. | 1. | 0. |
| $fn(x_{i+1})$ | 0. | 0. | 1. |

(4.13)

The following functions satisfy these conditions for the slab geometry:

$$Q_i^-(x) = \frac{(x_{i+1}-x)}{h_i}\left[\,1 - \frac{3}{h_i}(x - x_i)\,\right]$$

$$\tilde{Q}_i(x) = \frac{6}{h_i^2}(x - x_i)(x_{i+1} - x) \quad (4.14)$$

$$Q_i^+(x) = \frac{(x-x_i)}{h_i}\left[\,1 - \frac{3}{h_i}(x_{i+1} - x)\right]$$

where $h_i = x_{i+1} - x_i$.

Substitution of these expansion forms into Eq.(4.3) and (4.11) leads to long, tedious algebra. A complete derivation of the current-flux

relation is given in Appendix 3. In summary the derivation procedure is as the follows:

1. With Eq.(4.12) substituted into Eq.(4.3), $[J_i(x_i^+)]$ and $[J_i(x_{i+1}^-)]$ become by functions of $[\bar{\phi}_i]$, $[\phi(x_i^+)]$ and $[\phi(x_{i+1}^-)]$.

2. Eliminating the $[\phi(x_{i+1}^-)]$ from these two equations, yields $[J_i(x_{i+1}^-)]$ as a function of $[J_i(x_i^+)]$, $[\phi(x_i^+)]$ and $[\bar{\phi}_i]$.

3. Integrating Eq.(4.11) over node i, leads to a nodal balance equation relating is given as a relation of $[J_i(x_i^+)]$, $[J_{i+1}(x_{i+1}^-)]$ and $[\bar{\phi}_i]$.

4. Substituting the $[J_i(x_{i+1}^-)]$ from step 2 into the equation resulting from step 3, yields $[J_i(x_i^+)]$ as a function of $[\bar{\phi}_i]$ and $[\phi(x_i^+)]$.

5. An analogous procedure is applied to node i-1 to give $[J_{i-1}(x_i^-)]$ as a function of $[\bar{\phi}_{i-1}]$ and $[\phi(x_i^-)]$.

6. The two separate expressions for $[J(x_i)]$ from steps 4 and 5 can be combined to eliminate the surface-average flux $[\phi(x_i)]$.

The final equation relating the net current at time $t_{n+1}$ to two, neighboring, node-average fluxes at time $t_n$ and $t_{n+1}$ is found to have the form

$$[K_i]\,[J(x_i)]^{n+1} = [f^R_{i-1}]\,[TA_{i-1}]\,[\bar{\phi}_{i-1}]^{n+1} - [f^L_i]\,[TA_i]\,[\bar{\phi}_i]^{n+1}$$
$$+ [f^R_{i-1}]\,[TM_{i-1}]\,[\bar{\phi}_{i-1}]^{n+1} - [f^L_i]\,[TM_i]\,[\bar{\phi}_i]^{n+1}$$
$$+ [f^R_{i-1}]\,[TD_{i-1}]\,[\bar{\phi}_{i-1}]^{n} - [f^L_i]\,[TD_i]\,[\bar{\phi}_i]^{n}$$
$$+ [f^R_{i-1}]\,[TC_{i-1}]\,[SD_{i-1}]^{n} - [f^L_i]\,[TC_i]\,[SD_i]^{n} \qquad (4.15)$$

The coefficient matrices are defined as:

$$[K_i]^{n+1} = \frac{1}{2}\left(h_{i-1}\,[f^R_{i-1}]\,[D^{-1}_{i-1}]^{n+1} + h_i\,[f^L_i]\,[D^{-1}_i]^{n+1}\right)$$

$$[TA_i]^{n+1} = [I] - \frac{1}{6}h_i^2\,[D^{-1}_i]^{n+1}[\bar{A}_{0i}]^{n+1} - \frac{1}{6}h_i^2\,[D^{-1}_i]^{n+1}\frac{1}{\Delta_n}[V_0]^{-1}$$

$$[TM_i]^{n+1} = \frac{1}{6}\,h_i^2\,[D^{-1}_i]^{n+1}[M_i]^{n+1} \qquad (4.16)$$

$$[TD_i]^{n+1} = \frac{1}{6}\,h_i^2\,[D^{-1}_i]^{n+1}[MD_i]^{n} + \frac{1}{6}\,h_i^2\,[D^{-1}_i]^{n+1}\frac{1}{\Delta_n}[V_0]^{-1}$$

$$[TC_i]^{n+1} = \frac{1}{6}\,h_i^2\,[D^{-1}_i]^{n+1}$$

$$[SD_i]^{n} = \sum_{\iota}\,[\chi_{d_{\iota,i}}]\,\lambda_{\iota_i}\,\theta^n_{\iota_i}\,\bar{C}^{\,n}_{\iota_i}$$

where $[D^{-1}]$ is a GxG matrix containing elements $D^{-1}_{gg'}$. When off-diagonal P-1 scattering is neglected (i.e., when $\bar{\Sigma}_{s_1 gg'} = 0.$ for $g \neq g'$), $[D^{-1}]$ is a diagonal GxG matrix containing $3(\bar{\Sigma}_{tr_g})_i$.

The other matrices shown above are defined as:

$[f_i^R]$ is a diagonal GxG matrix containing discontinuity factors at the right (positive x-direction) side of node i

$[f_i^L]$ is a diagonal GxG matrix containing discontinuity factors at the left (negative x-direction) side of node i

$[M_i]^n$ is the GxG matrix $k_{eff}^{-1}\left[(1-\beta_{eff_i})[\bar{\chi}_{p_i}] + \sum_\iota \beta_{\iota_i}[\bar{\chi}_{d_{\iota,i}}]\zeta_{\iota_i}^n\right][\nu\bar{\Sigma}_{f_i}]^{T,n}$

$[MD_i]^n$ is a GxG matrix containing $k_{eff}^{-1}\sum_\iota \beta_{\iota_i}[\bar{\chi}_{d_{\iota,i}}]\eta_{\iota_i}^n[\nu\bar{\Sigma}_{f_i}]^{T,n}$.

### 4.2.3 Derivation of Nodal Balance Equations

In the previous section, an expression for the net surface current is derived in terms of two neighboring node-average fluxes. Integration of Eq.(4.11) over node i yields

$$[J(x_{i+1})]^{n+1} - [J(x_i)]^{n+1} + h_i[\bar{A}_{0_i}]^{n+1}[\bar{\phi}_i]^{n+1} + h_i\frac{1}{\Delta_n}[V_0]^{-1}[\bar{\phi}_i]^{n+1} - h_i[M_i]^{n+1}[\bar{\phi}_i]^{n+1} - h_i\frac{1}{\Delta_n}[V_0]^{-1}[\bar{\phi}_i]^n + h_i[MD_i]^{n+1}[\bar{\phi}_i]^n + h_i[SD_i]^n. \quad (4.17)$$

Substituting Eq.(4.15) for both $[J(x_{i+1})]$ and $[J(x_i)]$, leads to a three-point formula relating three neighboring, node-average-fluxes. Complete derivation of the nodal balance equations is given in Appendix 4. The final equation is

$$
\begin{aligned}
&- [P^{i-1}]^{n+1} [\bar{\phi}_{i-1}]^{n+1} + [Q^{i}]^{n+1} [\bar{\phi}_{i}]^{n+1} - [R^{i+1}]^{n+1} [\bar{\phi}_{i+1}]^{n+1} \\
&= [U^{i-1}]^{n+1} [\bar{\phi}_{i-1}]^{n+1} + [V^{i}]^{n+1} [\bar{\phi}_{i}]^{n+1} + [W^{i+1}]^{n+1} [\bar{\phi}_{i+1}]^{n+1} \\
&\quad + [S_i]^{n+1} \qquad (4.18)
\end{aligned}
$$

where

$$
\begin{aligned}
[S_i]^{n+1} = {} & [UD^{i-1}]^{n+1}[\bar{\phi}_{i-1}]^{n} + [VD^{i}]^{n+1}[\bar{\phi}_{i}]^{n} + [WD^{i+1}]^{n+1}[\bar{\phi}_{i+1}]^{n} \\
& + [\alpha^{i-1}]^{n+1}[SD_{i-1}]^{n} + [\beta^{i}]^{n+1}[SD_{i}]^{n} + [\gamma^{i+1}]^{n+1}[SD_{i+1}]^{n}.
\end{aligned}
$$

Integration of equation (4.8) over node i gives a companion equations for the volume-averaged precursor concentrations.

$$
\begin{aligned}
\bar{C}_{\iota_i}^{n+1} = {} & \bar{C}_{\iota_i}^{n} \theta_{\iota_i}^{n} + k_{eff}^{-1} [\nu\bar{\Sigma}_{f_i}]^{T,n}[\bar{\phi}_i]^{n} \frac{\beta_{\iota_i}}{\lambda_{\iota_i}} \eta_{\iota_i}^{n} \qquad (4.19) \\
& + k_{eff}^{-1} [\nu\bar{\Sigma}_{f_i}]^{T,n+1}[\bar{\phi}_i]^{n+1} \frac{\beta_{\iota_i}}{\lambda_{\iota_i}} \zeta_{\iota_i}^{n}
\end{aligned}
$$

Definitions of the coefficient matrices are given in Appendix 4.

### 4.2.4 Boundary Conditions

External boundary conditions can be expressed in the following general form

$$[\phi(x_s)] = [\Gamma]\ [\vec{J}(x_s)]\cdot\vec{n} \qquad (4.20)$$

where $\vec{n}$ is an outgoing unit vector normal to the external boundary surface

$x_s$ is a external boundary position.

[Γ] matrix is a diagonal GxG matrix whose diagonal elements have the following values:

$\Gamma_g = 0.$ for zero flux boundary condition

$\Gamma_g = 2.$ for zero incoming current boundary condition

$\Gamma_g = \infty$ for zero current boundary condition

$\Gamma_g = 2 + 4/(\alpha_g^{-1}-1)$ for albedo boundary condition

where the albedo value $\alpha_g$ is defined as $(J_{in})_g/(J_{out})_g$.

The general boundary condition, Eq.(4.20) may be substituted into

Eq.(A3.20), for the net current on the external surface of node 1, to obtain:

$$
\begin{aligned}
[J(x_1)]^{n+1} = &- [K_1^{-1}]^{n+1} [f_1^L] [TA_1]^{n+1} [\bar{\phi}_1]^{n+1} \\
&- [K_1^{-1}]^{n+1} [f_1^L] [TM_1]^{n+1} [\bar{\phi}_1]^{n+1} \\
&- [K_1^{-1}]^{n+1} [f_1^L] [TD_1]^{n+1} [\bar{\phi}_1]^{n} \\
&- [K_1^{-1}]^{n+1} [f_1^L] [TC_1]^{n+1} [SD_1]^{n}
\end{aligned}
\tag{4.21}
$$

where $[K_1^{-1}]^{n+1} = [\Gamma] + \frac{1}{2} h_1 [f_1^L] [D_1^{-1}]^{n+1}$ (4.22)

The matrix structure of $[J(x_1)]$ is the same as that of $[J(x_i)]$ at internal nodes except for the zero current boundary condition, for which $[K_1^{-1}]$ become zero because of the infinite value of $[\Gamma]$, causing $[J(x_1)]$ to vanish from the nodal balance equation, (4.17).

Substituting Eq.(4.21) and (4.15) into Eq.(4.17) for node 1, yields the following two-point equation

$$
\begin{aligned}
&[Q^1]^{n+1} [\bar{\phi}_1]^{n+1} - [R^2]^{n+1} [\bar{\phi}_2]^{n+1} \\
&= [V^1]^{n+1} [\bar{\phi}_1]^{n+1} + [W^2]^{n+1} [\bar{\phi}_2]^{n+1} + [S_1]^{n+1}
\end{aligned}
\tag{4.23}
$$

where

$$
\begin{aligned}
[S_1]^{n+1} = &[VD^1]^{n+1}[\bar{\phi}_1]^{n} + [WD^2]^{n+1}[\bar{\phi}_2]^{n} \\
&+ [\beta^1]^{n+1}[SD_1]^{n} + [\gamma^2]^{n+1}[SD_2]^{n}.
\end{aligned}
$$

The matrices [Q],[R],[V],[W],[VD],[WD],[$\beta$] and [$\gamma$] are defined by

Eq.(A4.6) except for the zero current boundary codition, for which $[K_1^{-1}]$ is the null matrix.

An analogous procedure may be applied for the last node, I, at the other side of external boundary leading to

$$
\begin{aligned}
&- [P^{I-1}]^{n+1} [\bar{\phi}_{I-1}]^{n+1} + [Q^I]^{n+1} [\bar{\phi}_I]^{n+1} \\
&= [U^{I-1}]^{n+1} [\bar{\phi}_{I-1}]^{n+1} + [V^I]^{n+1} [\bar{\phi}_I]^{n+1} + [S_I]^{n+1}
\end{aligned} \tag{4.24}
$$

where

$$
\begin{aligned}
[S_I]^{n+1} = {} & [UD^{I-1}]^{n+1} [\bar{\phi}_{I-1}]^n + [VD^I]^{n+1} [\bar{\phi}_I]^n \\
& + [\alpha^{I-1}]^{n+1} [SD_{I-1}]^n + [\beta^I]^{n+1} [SD_I]^n
\end{aligned}
$$

### 4.2.5 Reduction to the Static Nodal Equations

For the initial steady state, a critical eigenvalue for the reactor must be evaluated. An axial profile of the neutron population, coolant temperature and average fuel temperature must also be evaluated.

At steady state, Eq.(4.2) may be reduced to:

$$
\begin{aligned}
&\frac{d}{dx} [J(x)] + [A_0(x)] [\phi(x)] = k_{eff}^{-1} [\chi(x)] [\nu\Sigma_f(x)]^T [\phi(x)] \\
&\frac{d}{dx} [\phi(x)] = - [D^{-1}(x)] [J(x)]
\end{aligned} \tag{4.25}
$$

where $[\chi(x)] = (1 - \beta_{eff}(x)) [\chi_p(x)] + \sum_\iota \beta_\iota(x) [\chi_{d_\iota}(x)]$.

The static spatial coupling equations and nodal balance equations may be derived as was done in Sections 4.2.3 and 4.2.4. However, elemination of time-dependent terms from the already derived dynamic equations leads to the static nodal equations.

Specifically, the steady state condition can be deduced by setting the time step $\Delta_n$ to infinity and making $[\phi(x)]^{n+1}$ and $[C_\iota(x)]^{n+1}$ the same as $[\phi(x)]^n$ and $[C_\iota(x)]^n$. Then, definitions of the parameters in Eq.(4.9) become:

$$\begin{aligned} \zeta_\iota &\simeq 1 \\ \eta_\iota &\simeq 0 \\ \theta_\iota &\simeq 0. \end{aligned} \tag{4.26}$$

and Eq.(4.19) becomes

$$C_\iota(x) = k_{eff}^{-1} \, [\nu\Sigma_f(x)]^T [\phi(x)] \, \frac{\beta_\iota(x)}{\lambda_\iota(x)}. \tag{4.27}$$

Also, the matrices in Eq. (4.16) become:

$$\begin{aligned} [K_i] &= \frac{1}{2} \left( h_{i-1} \, [f_{i-1}^R] \, [D_{i-1}^{-1}] + h_i \, [f_i^L] \, [D_i^{-1}] \right) \\ [TA_i] &= [I] - \frac{1}{6} h_i^2 \, [D_i^{-1}] \, [\bar{A}_{0i}] \\ [TM_i] &= \frac{1}{6} h_i^2 \, [D_i^{-1}] \, [M_i] \\ [TD_i] &= [\,0\,] \\ [TC_i] &= \frac{1}{6} h_i^2 \, [D_i^{-1}] \\ [SD_i] &= [\,0\,]. \end{aligned} \tag{4.28}$$

Therefore, the nodal balance equations are:

$$- [P^{i-1}]\ [\bar{\phi}_{i-1}] + [Q^{i}]\ [\bar{\phi}_{i}] - [R^{i+1}]\ [\bar{\phi}_{i+1}]$$
$$= k_{eff}^{-1} \left( [U^{i-1}]\ [\bar{\phi}_{i-1}] + [V^{i}]\ [\bar{\phi}_{i}] + [W^{i+1}]\ [\bar{\phi}_{i+1}] \right) \qquad (4.29)$$

$$\bar{C}_{\iota_i} = k_{eff}^{-1} \frac{\beta_{\iota_i}}{\lambda_{\iota_i}} [\nu\bar{\Sigma}_{f_i}]^{T}\ [\bar{\phi}_{i}]. \qquad (4.30)$$

The definitions of all matrices are the same as in Appendix 4 except for the simplifications implied by Eq.(4.28). Also $[M_i]$ is changed to a full G×G matrix containing $[\chi_i]\ [\nu\Sigma_{f_i}]^{T}$.

The nodal balance equations for the external boundary nodes are reduced in the same way to:

$$[Q^{1}]\ [\bar{\phi}_{1}] - [R^{2}]\ [\bar{\phi}_{2}] = k_{eff}^{-1} \left( [V^{1}]\ [\bar{\phi}_{1}] + [W^{2}]\ [\bar{\phi}_{2}] \right) \qquad (4.31)$$

$$- [P^{I-1}]\ [\bar{\phi}_{I-1}] + [Q^{I}]\ [\bar{\phi}_{I}]$$
$$= k_{eff}^{-1} \left( [U^{I-1}]\ [\bar{\phi}_{I-1}] + [V^{I}]\ [\bar{\phi}_{I}] \right) \qquad (4.32)$$

## 4.3 THERMAL-HYDRAULIC FEEDBACK MODEL AND TRANSIENT CONTROL MECHANISMS

As in the code QUANDRY, the thermal-hydraulic model used in WIGL [V-1] along with linear cross section feedback were used for simulationg the thermal-hydraulics of the reactor core and their attendant cross section variations. The detailed modelling is described in reference [S-1]. The only difference is that the models here are one-dimensional.

The thermal-hydraulic model in QUANDRY permits two mechanisms for initiating transients. Both the reactor coolant inlet temperature and the coolant flow rate may be varied as a function of time. These two mechanisms simulate a variety of transients (such as pump coastdown, a startup of inactive cold loop, etc.).

Another way of inducing a transient in a critical reactor is to alter the positions of the control rod banks. In the one-dimensional analysis, control rod motions were modeled as changes in macroscopic cross sections within individual nodes. The cross sections for a partially rodded node were assumed to be the volume-weighted average of the fully-rodded and fully-unrodded nodal cross sections. This approximation will be valid only when the neutron flux is spatially flat within the node. The "control rod cusping effect" due to non-flat flux shape within a partially rodded node was successfully overcomed by Joo [J-1]. However, his method was not implemented in the present code because of its complexity. Therefore, the node size for transient problems involving control rod movement is limited so as to be small enough to avoid a rod cusping problem.

## 4.4 NUMERICAL CONSIDERATIONS

### 4.4.1 The Sequence of Operations

In order to obtain the steady-state initial condition (power shape, temperature distribution, flux distribution, etc.), a static calculation should be performed as the first step. The sequence of step for a static calculation is outlined below:

1. Assuming a flat axial power shape, calculate thermal hydraulic variables ( $\bar{T}_f$, $\bar{T}_m$, $\bar{\rho}_m$ ).
2. Evaluate nodal cross-sections corresponding to the control rod position and thermal hydraulic feedback.
3. Calculate all coefficient matrices of Eq. (4.29) ( [P], [Q], [R], [U], [V] and [W] ).
4. Solve Eq. (4.29) iteratively for the eigenvalue, $k_{eff}^{-1}$ and the group flux shape, $[\bar{\phi}_i]$.
5. Calculate a new power shape and new thermal-hydraulic variables.
6. Repeat steps 2 through 5 until the eigenvalue and group flux shapes are converged.

Once the static calculation is terminated within a given error criteria, the $\bar{C}_{i}$ are calculated by Eq. (4.30). Transient calculations are carried out with the calculated $k_{eff}^{-1}$ used in the definitions of Equations (4.16). The steps are:

1. Calculate constants depending on the time step size $\Delta_n$ (such as $\zeta_{\iota,i}$, $\eta_{\iota,i}$, $\theta_{\iota,i}$ in Eq. (4.9) ).
2. Set the steady-state variables as references for the transient pertubations.
3. For the present time step, n, calculate matrices $[MD_i]$ and $[SD_i]$
4. For the next time step, n+1, evaluate the cross section changes due to control rod bank movement.
5. For time step n+1, evaluate the cross section changes due to the change of coolant-inlet-temperature and/or coolant-flow-rate.
6. Calculate the matrices of Eq. (4.16), $[M_i]$, $[D_i^{-1}]$, $[\bar{A}_{o_i}]$, $[K_i]$, $[TA_i]$, $[TM_i]$, $[TD_i]$ and $[TC_i]$.
7. Calculate all the coefficient matrices ( [P], [Q], [R], [U], [V] and [W] ) and the source matrix, [S] of Eq. (4.18).
8. Solve Eq. (4.18) iteratively for $[\bar{\phi}_i]^{n+1}$.
9. Solve Eq. (4.19) for $\bar{C}_{d_i}^{n+1}$.
10. Calculate the iteration accelation parameters.
11. Estimate the value of $[\bar{\phi}_i]^{n+2}$ for time step n+2.
12. Repeat steps 3 through 11 for each time step until one of the termination conditions is met.

### 4.4.2 Numerical Properties of the One-Dimensional Nodal Equations

The equations for which a solution is sought for the one-dimensional nodal method are given by Eqs. (4.18), (4.23) and (4.24) for internal nodes and the two external boundary nodes respectively. The equations for the static calculation, (4.29), (4.31) and (4.32), have the same numerical

properties as those for the transient calculation, except that they have much simpler forms. Therefore, all comments on numerical behaviors are hereafter given for the time-dependent equations.

All the matrices in Eq. (4.18) depend on the matrices, $[TA_i]$, $[TM_i]$, $[TD_i]$, $[TC_i]$, $[SD_i]$ and $[K_i^{-1}]$. These matrices are in turn determined by adding and multiplying the basic matrices: $[f_i^R]$, $[f_i^L]$, $[D_i^{-1}]$, $[\bar{A}_{0i}]$, $[M_i]$, $[MD_i]$ and $[V_0^{-1}]$. Among them, $[M_i]$ and $[MD_i]$ are full GxG matrices, whereas $[f_i^R]$, $[f_i^L]$ and $[V_0^{-1}]$ are diagonal matrices. the matrix $[D_i^{-1}]$ contains $\bar{\Sigma}_{s_1 gg',i}$ which makes it non-diagonal. Therefore, there is a matrix inversion problem involved with the evaluation of $[K_i^{-1}]$. The matrix $[\bar{A}_{0i}]$ obviously has non-diagonal components because it contains $P_0$-scattering terms, $\bar{\Sigma}_{s_0 gg'}$.

Appendix 2 provides multi-group cross section data for four different material compositions. Figure (4.1) shows the structure of the $[\bar{A}_{0i}]$ matrix specified by these data. Note that there is no upscattering for the first 12 energy groups (epithermal range , $\geq$ 6.091 eV). All the data given in Appendix 2 have no P-1 scattering cross sections, the diffusion coefficients being defined by transport cross sections. Therefore, the $[D_i^{-1}]$ matrix become a diagonal GxG matrix. Thus the definitions of Eq. (4.16), show that $[TA_i]$ has the structure shown by Fig. (4.1). $[TM_i]$ and $[TD_i]$ become full matrices, whereas $[TC_i]$, $[SD_i]$ and $[K_i^{-1}]$ become diagonal matrices. For this reason, the matrices $[P_i]$, $[Q_i]$ and $[R_i]$ have the form shown on Fig. (4.1), i.e. the structure of $[\bar{A}_{0i}]$, and $[U_i]$, $[V_i]$ and $[W_i]$ have a full GxG matrix form.

Equations (4.18), (4.23) and (4.24) can therefore be expressed in the supermatrix form:

$[\bar{A}_{0gg'}]$

| 2-group | 23-group g | g′ 1 | 2 | 3 | 4 | 5 | 6 | 7 | 8 | 9 | 10 | 11 | 12 | 13 | 14 | 15 | 16 | 17 | 18 | 19 | 20 | 21 | 22 | 23 |
|---|---|---|---|---|---|---|---|---|---|---|---|---|---|---|---|---|---|---|---|---|---|---|---|---|
| 1 | 1 | D | | | | | | | | | | | | | | | | | | | | | | |
| | 2 | L | D | | | | | | | | | | | | | | | | | | | | | |
| | 3 | L | L | D | | | | | | | | | | | | | | | | | | | | |
| | 4 | L | L | L | D | | | | | | | | | | | | | | | | | | | |
| | 5 | L | L | L | L | D | | | | | | | | | | | | | | | | | | |
| | 6 | L | L | L | L | L | D | | | | | | | | | | | | | | | | | |
| | 7 | L | L | L | L | L | L | D | | | | | | | | | | | | | | | | |
| | 8 | L | L | L | L | L | L | L | D | | | | | | | | | | | | | | | |
| | 9 | L | L | L | L | L | L | L | L | D | | | | | | | | | | | | | | |
| | 10 | L | L | L | L | L | L | L | L | L | D | | | | | | | | | | | | | |
| | 11 | L | L | L | L | L | L | L | L | L | L | D | | | | | | | | | | | | |
| | 12 | | L | L | L | L | L | L | L | L | L | L | D | | | | | | | | | | | |
| | 13 | | | L | L | L | L | L | L | L | L | L | L | D | U | | | | | | | | | |
| | 14 | | | L | | | L | L | L | L | L | L | L | L | D | U | U | U | | | | | | |
| | 15 | | | L | | | L | L | L | L | L | L | L | L | L | D | U | U | U | | | | | |
| | 16 | | | L | | | L | L | L | L | L | L | L | L | L | L | D | U | U | | | | | |
| | 17 | | | L | | | L | L | L | L | L | L | L | L | L | L | L | D | U | U | U | U | U | U |
| 2 | 18 | | | L | | | | L | L | L | L | L | L | L | L | L | L | L | D | U | U | U | U | U |
| | 19 | | | L | | | | L | L | L | L | L | L | L | L | L | L | L | L | D | U | U | U | U |
| | 20 | | | L | | | | L | L | L | L | L | L | L | L | L | L | L | L | L | D | U | U | U |
| | 21 | | | L | | | | L | L | L | L | L | L | L | L | L | L | L | L | L | L | D | U | U |
| | 22 | | | | | | | L | L | L | L | L | L | L | L | L | L | L | L | L | L | L | D | U |
| | 23 | | | | | | | | L | L | L | L | L | L | L | L | L | L | L | L | L | L | L | D |

U : up-scattering term
D : diagonal term
L : slowing-down term

Figure 4.1 Structure of the Matrix $[\bar{A}_0]$

$$\left( [H] - [\mathfrak{R}] \right) [\Psi] = [S] \tag{4.33}$$

Similarly Equations (4.29), (4.31) and (4.32) can be expressed as:

$$[H]\ [\Psi] = k_{eff}^{-1}\ [\mathfrak{R}]\ [\Psi] \tag{4.34}$$

where all the nodes for a given group are determined together so that

$$[\Psi] = \text{col.} \left( [\Psi_1], [\Psi_2], \cdots [\Psi_G] \right)$$

with $[\Psi_g] = \text{col.} \left( \phi_{g,1}, \phi_{g,2}, \cdots \phi_{g,I} \right)$ and

$$[H] = \begin{bmatrix} [H_{11}] & 0 & \cdots & 0 & 0 & \cdots & 0 \\ [H_{21}] & [H_{22}] & \cdots & 0 & 0 & \cdots & 0 \\ . & . & \cdots & 0 & 0 & \cdots & 0 \\ [\ ] & [\ ] & \cdots & [H_{m-1,m-1}] & 0 & \cdots & 0 \\ [H_{m1}] & [H_{m2}] & \cdots & [H_{m,m-1}] & [H_{m,m}] & \cdots & [H_{mG}] \\ . & . & \cdots & . & . & \cdots & . \\ [H_{G1}] & [H_{G2}] & \cdots & [H_{G,m-1}] & [H_{G,m}] & \cdots & [H_{GG}] \end{bmatrix}$$

$$[\mathfrak{R}] = \begin{bmatrix} [R_{11}] & [R_{12}] & \cdots & [R_{1G}] \\ [R_{21}] & [R_{22}] & \cdots & [R_{2G}] \\ . & . & \cdots & . \\ [R_{G1}] & [R_{G2}] & \cdots & [R_{GG}] \end{bmatrix} \tag{4.35}$$

$$[S] = \begin{bmatrix} [S_{11}] & 0 & \cdots & 0 \\ 0 & [S_{22}] & \cdots & 0 \\ . & . & \cdots & . \\ 0 & 0 & \cdots & [S_{GG}] \end{bmatrix}$$

The submatrices $[H_{gg'}]$ and $[R_{gg'}]$ making up $[\mathbf{H}]$ and $[\mathfrak{R}]$ have the form

$$[H_{gg'}] = \begin{bmatrix} Q^1_{gg'} & R^2_{gg'} & 0 & \cdots & 0 & 0 \\ P^1_{gg'} & Q^2_{gg'} & R^3_{gg'} & \cdots & 0 & 0 \\ 0 & P^2_{gg'} & Q^3_{gg'} & R^4_{gg'} \cdots & 0 & 0 \\ \cdot & \cdot & \cdot & \cdots & \cdot & \cdot \\ 0 & 0 & 0 & \cdots P^{I-2}_{gg'} & Q^{I-1}_{gg'} & R^I_{gg'} \\ 0 & 0 & 0 & \cdots & P^{I-1}_{gg'} & Q^I_{gg'} \end{bmatrix}$$

$$[R_{gg'}] = \begin{bmatrix} V^1_{gg'} & W^2_{gg'} & 0 & \cdots & 0 & 0 \\ U^1_{gg'} & V^2_{gg'} & W^3_{gg'} & \cdots & 0 & 0 \\ 0 & U^2_{gg'} & V^3_{gg'} & W^4_{gg'} \cdots & 0 & 0 \\ \cdot & \cdot & \cdot & \cdots & \cdot & \cdot \\ 0 & 0 & 0 & \cdots U^{I-2}_{gg'} & V^{I-1}_{gg'} & W^I_{gg'} \\ 0 & 0 & 0 & \cdots & U^{I-1}_{gg'} & V^I_{gg'} \end{bmatrix} \qquad (4.36)$$

where superscripts refer to mesh points.

### 4.4.3 Iteration Schemes

The static nodal equation, Eq. (4.34) is solved by a fission source iteration ( outer iteration ) scheme. Starting off with an initial spatially flat guess, for the fluxes, we update the fission rate and

eigenvalue, $k_{eff}^{-1}$ at each outer iteration using a power iteration scheme. The greatest concern with this eigenvalue iteration is its speed of convergence. The more powerful Wielandt method could be used. However, the simple power method avoids complexity, and computing time for eigenvalue iterations is far less than the time required for transient calculations.

The multi-group structure of matrices in Eq. (4.35) gives rise to two situations: an inner iteration without upscattering and one with upscattering. With the fission source given by the most recent outer iteration, the first group solution does not depend on other groups and can, therfore, be found by

$$[H_{11}]\ [\Psi_1] = k_{eff}^{-1} \sum_{g} [R_{1g}]\ [\Psi_g]. \tag{4.37}$$

The next group has a source whose scattering contribution depends only on the solution of the first group. Hence, its solution can also be found directly by solving the second group equation, and so forth. Here, the newest flux solutions are applied to the calculation of the scattering source. If p is used as the index for outer iterations, we have

$$[H_{gg}]\ [\Psi_g]^p = \frac{1}{(k_{eff})^{p-1}} \sum_{g'=1}^{G} [R_{gg'}]\ [\Psi_{g'}]^{p-1} - \sum_{g'=1}^{g-1} [H_{gg'}]\ [\Psi_{g'}]^p. \tag{4.38}$$

Next, we have situation with upscattering. We can no longer solve for group fluxes group-by-group as described above. However, upscattering

contributions are generally much less than the in-group-scattering contributions. We can, therefore, treat upscattering contributions by an upscattering iteration [D-1]. If u is used as the index for upscattering iterations and p as the one for outer iterations, we have

$$[H_{gg}]\ [\Psi_g]^{p,u} = \frac{1}{(k_{eff})^{p-1}} \sum_{g'=1}^{G} [R_{gg'}]\ [\Psi_{g'}]^{p-1} - \sum_{g'=1}^{g-1} [H_{gg'}]\ [\Psi_{g'}]^{p,u} - \sum_{g'=g+1}^{G} [H_{gg'}]\ [\Psi_{g'}]^{p,u-1} \qquad (4.39)$$

where $[\Psi_g]^{p,0} = [\Psi_g]^{p-1,U}$.

The cost of performing U upscattering iterations is approximately equivalent to solving a problem with $(U-1)\times(G-\bar{G}+1)$ additional groups, where $\bar{G}$ denotes the index of the first group that has a nonzero upscattering source [S-6]. Experience with several problems shows that U values may be fixed between 5 and 10.

In most cases, because of the size of matrix $[H_{gg}]$, the solution of Eq.(4.37), (4.38) and (4.39) should not be sought by direct matrix inversion. However, for one-dimensional problems, the matrix $[H_{gg}]$ is tridiagonal as shown in Eq. (4.36). Thus Eqs. (4.37) through (4.39) can be solved by the forward elimination, backward substitution method.

The transient nodal equation, Eq. (4.33) should also be solved by

iteration schemes. Because the [$\mathfrak{R}$] matrix is full, it should be moved to the right hand side for the outer iteration procedure. However, for faster convergence of fluxes, it is desirable to move only part of [$\mathfrak{R}$]. Experience with several tests suggests that the upper-diagonal part of [$\mathfrak{R}$], i.e. the [$R_{gg'}$] submatrices for g'>g, should be moved to the right hand side. Accordingly, we have the following modified equation:

$$\left( [H] - [\mathfrak{R}_1] \right) [\Psi] = [S] + [\mathfrak{R}_2] [\Psi] \tag{4.40}$$

where

$$[\mathfrak{R}_1] = \begin{bmatrix} [R_{11}] & 0 & \cdots & 0 \\ [R_{21}] & [R_{22}] & \cdots & 0 \\ \cdot & \cdot & \cdots & \cdot \\ [R_{G1}] & [R_{G2}] & \cdots & [R_{GG}] \end{bmatrix}$$

$$[\mathfrak{R}_2] = \begin{bmatrix} 0 & [R_{12}] & \cdots & [R_{1G}] \\ 0 & 0 & \cdots & [R_{2G}] \\ \cdot & \cdot & \cdots & \cdot \\ 0 & 0 & \cdots & 0 \end{bmatrix}$$

To facilitate rapid convergence of the group fluxes at each time step, an initial estimate of the fluxes is made by extrapolation from the previous time step. That is, a first estimate of fluxes at time step n+1 is given by

$$[\phi_i]^{n+1} = [\phi_i]^n \left\{ \frac{[\phi_i]^n}{[\phi_i]^{n-1}} \right\} \quad \text{for all node.} \tag{4.41}$$

### 4.4.4 The Computer Code OMNI-T

The numerical methods described above were incorporated into a computer code, hereafter referred to as OMNI-T (One-dimensional Multi-group Nodal AnalysIs Code for Transient Calculations).

OMNI-T was written in the VAX FORTRAN language. A substantial number of variables are defined in double precision. Because of the large memory requirements, the total number of energy groups and the delayed neutron precursor groups is limited to 25 and 6 respectively. In order not to have a rod cusping problem, node mesh size should be small near the control rod tips. Therefore, OMNI-T was programmed to handle non-uniform mesh spacing and multi-regions. The generalized albedo boundary condition is incorporated into OMNI-T with zero flux boundary condition, zero current boundary condition and zero incoming-current boundary condition. However, albedo boundary condition can be imposed on only one side of the reactor.

A detailed listing of the code and input/output description can be found in the code manual which is available on request to the MIT Department of Nuclear Engineering.

## 4.5 TEST PROBLEMS

In this section, results from several benchmark problems are presented. All of the problems were constructed to test the accuracy of computer code, OMNI-T. All of the geometries and cross sections are fully specified so that modeling ambiguities do not exist.

### 4.5.1 Two-Group Static Calculations

In order to test the accuracy of static calculation schemes in OMNI-T, steady-state flux distruibutions were compared with the QUANDRY [S-2] results.

The QUANDRY code is based on the analytic nodal method in which an analytic solution is sought within each node for the two-group diffusion equations. The only approximation applied with this method is that transverse leakage terms for a node are fitted by quadratic polynomials determined by the transverse leakages of three adjacent nodes. Therefore, QUANDRY provides analytic solutions when one-dimensional problems are solved. On the other hand, OMNI-T approximates the neutron fluxes within a node by quadratic functions. For this reason, comparisons of OMNI-T results with QUANDRY results would show the inherent accuracy of the quadratic polynomial expansion methods as compared with the analytical solution.

Section A5.1 of Appendix 5 described the benchmark problem studied for this purpose. The reactor has a five-zone core containing three

different fuel materials, each having a width of 20 cm. The core has 20 cm wide water reflectors on both sides and is symmetric about the center plane.

Table (4.1) summarizes the results for eigenvalues and normalized flux shapes. For the small nodal mesh size, the errors in OMNI-T are so small as to be essentially negligible. As the size of node increase, the errors also grow. The largest errors in flux shapes occurred at material interfaces, whereas errors were very small within a homogeneous region. The large errors at interfaces occur because the quadratic polynomial functions are not good enough to fit the fluxes at these locations.

Although the maximum error in the group-1 flux is about 5 % for the 5 cm node size, average errors are far less than this amount. Futhermore, the accuracy of the nodal calculation is not the primary concern of this study, and previous studies have indicated that, provided the same mesh spacings are used for approximate and reference calculations, test of the accuracy of two-group solutions compared with multi-group solutions are meaningful even if the spatial mesh is not completely converged. For these reasons the node size was permitted to be 5 cm for the realistic test cases to be described in Chapter 5.

Table 4.1 Summary of Results for the 2-Group Static Benchmark Problem

| | QUANDRY | OMNI-T |
|---|---|---|
| Node Size = 1 cm | | |
| # of nodes | 70 | 70 |
| # of outer itersions | 376 | 51 |
| $k_{eff}$ | 1.021925 | 1.021892 |
| | | (-0.003 %) |
| group 1 flux | | |
| max. error | | -0.272 % |
| R.M.S. error* | | 0.085 % |
| group 2 flux | | |
| max. error | | -0.275 % |
| R.M.S. error* | | 0.076 % |
| Node Size = 5 cm | | |
| # of nodes | 14 | 14 |
| # of outer itersions | 52 | 49 |
| $k_{eff}$ | 1.021921 | 1.021402 |
| | | (-0.051 %) |
| group 1 flux | | |
| max. error | | -5.033 % |
| R.M.S. error* | | 1.431 % |
| group 2 flux | | |
| max. error | | -3.767 % |
| R.M.S. error* | | 1.205 % |

* R.M.S. error : Root Mean Square Error

### 4.5.2 Two-Group Transient Calculations

In this section, the accuracy of transient predictions made by OMNI-T is compared with the results of QUANDRY. Because OMNI-T utilized the same thermal-hydraulic feedback model as in QUANDRY, the only differences between the two codes are the neutronic calculation methods.

As a test for the OMNI-T model, it is extremely useful to choose a case for which analytical solutions can also be found. A description of the fictitious homogeneous reactor chosen and the transient applied to it can be found in Section A5.2 of Appendix 5. The analytical solution was given for a step-wise perturbation of the thermal absorption cross section and was derived by Dias [D-2]. Appendix 6 shows the derivation of this analytical solution for one-dimensional diffusion equations. The results are modifications of the Dias's 3-D solutions.

Table (4.2) shows the results obtained from two computer codes, QUANDRY and OMNI-T. Both calculations were done for a time-step size of 0.02 sec. and a small node size (1.0 cm for QUANDRY and 0.5 cm for OMNI-T). OMNI-T is seen to be accurate compared with either QUANDRY or the analytical solution.

Table 4.2 Predicted reactor power changes due to a step decrease in thermal absorption (without thermal-hydraulic feedback)

| | ANALYTIC SOLUTION | QUANDRY | OMNI-T | ERROR RELATIVE TO QUANDRY |
|---|---|---|---|---|
| Initial k-eff | 1.014450 | 1.014452 | 1.014385 (-0.006 %) | -0.007 % |
| Power (KWt.) | | | | |
| 0.0 sec. | 1.0 | 1.0 | 1.0 | 0.000 % |
| 1.0 sec. | 3.13889 | 3.13195 (-0.221 %) | 3.13406 (-0.154 %) | 0.067 % |
| 2.0 sec. | 3.60725 | 3.59822 (-0.250 %) | 3.60197 (-0.146 %) | 0.104 % |
| 3.0 sec. | 4.14550 | 4.13420 (-0.273 %) | 4.13964 (-0.141 %) | 0.132 % |
| 4.0 sec. | 4.76406 | 4.75071 (-0.280 %) | 4.75743 (-0.139 %) | 0.141 % |

Tables (4.3) and (4.4) show the sensitivity of OMNI-T to the time step sizes and node sizes. The errors observed as compared with the reference solution are very small. The time step size is more sensitive than the node size because test was done for a homogeneous reactor for which the OMNI-T model (quadratic polynomial fitting for fluxes within a node) is quite accurate.

Table 4.3 Predicted reactor power changes (KWt.) due to a step decrease in thermal absorption (without thermal-hydraulic feedback) for various temporal mesh sizes

| TIME (sec.) | OMNI-T h = 0.5 cm | | | |
|---|---|---|---|---|
| | Δ= 0.01 sec | Δ= 0.05 sec | Δ= 0.1 sec. | Δ= 0.5 sec. |
| 0.0 | 1.0 | 1.0 | 1.0 | 1.0 |
| 0.5 | 2.92562 | 2.91891 (-0.229 %) | 2.90876 (-0.576 %) | 2.77403 (-5.18 %) |
| 1.0 | 3.13669 | 3.12872 (-0.254 %) | 3.11849 (-0.580 %) | 3.03418 (-3.27 %) |
| 1.5 | 3.36266 | 3.35315 (-0.283 %) | 3.34289 (-0.588 %) | 3.25503 (-3.20 %) |
| 2.0 | 3.60482 | 3.59427 (-0.293 %) | 3.58323 (-0.599 %) | 3.48981 (-3.19 %) |
| 2.5 | 3.86439 | 3.85360 (-0.279 %) | 3.84079 (-0.611 %) | 3.74144 (-3.18 %) |
| 3.0 | 4.14267 | 4.13180 (-0.262 %) | 4.11696 (-0.621 %) | 4.01121 (-3.17 %) |
| 3.5 | 4.44099 | 4.42944 (-0.260 %) | 4.41322 (-0.625 %) | 4.30041 (-3.17 %) |
| 4.0 | 4.76080 | 4.74792 (-0.271 %) | 4.73106 (-0.625 %) | 4.61044 (-3.16 %) |

Table 4.4 Predicted reactor power changes due to a step decrease in thermal absorption (without thermal-hydraulic feedback) for various spatial mesh sizes

| | OMNI-T $\Delta$ = 0.01 sec. | | | |
|---|---|---|---|---|
| | h = 0.5 cm | h = 1 cm | h = 2 cm | h = 5 cm |
| Initial k-eff | 1.014434 | 1.014385 (-0.0048 %) | 1.014189 (-0.0242 %) | 1.012818 (-0.1593 %) |
| Power (KWt.) 0.0 sec | 1.0 | 1.0 | 1.0 | 1.0 |
| 0.5 sec | 2.92562 | 2.92558 (-0.001 %) | 2.92545 (-0.006 %) | 2.92447 (-0.039 %) |
| 1.0 sec | 3.13669 | 3.13665 (-0.001 %) | 3.13649 (-0.006 %) | 3.13533 (-0.043 %) |
| 1.5 sec | 3.36266 | 3.36261 (-0.001 %) | 3.36242 (-0.007 %) | 3.36108 (-0.047 %) |
| 2.0 sec | 3.60482 | 3.60476 (-0.002 %) | 3.60454 (-0.008 %) | 3.60298 (-0.051 %) |
| 2.5 sec | 3.86439 | 3.86433 (-0.002 %) | 3.86407 (-0.008 %) | 3.86227 (-0.055 %) |
| 3.0 sec | 4.14267 | 14260 (-0.002 %) | 4.14230 (-0.009 %) | 4.14023 (-0.059 %) |
| 3.5 sec | 4.44099 | 4.44091 (-0.002 %) | 4.44057 (-0.009 %) | 4.43821 (-0.063 %) |
| 4.0 sec | 4.76080 | 4.76070 (-0.002 %) | 4.76032 (-0.010 %) | 4.75763 (-0.067 %) |

Tables (4.5) through (4.7) show the results from the other transients: perturbed by coolant flow-rate change, coolant inlet temperature change and control rod saw-tooth type movements. All these transients are unrealistically severe. All transient calculations were done with the time step intervals (0.05 sec.) and a small node size (5 cm

for QUANDRY and 1 cm for OMNI-T). Thermal-hydraulic feedback calculations were applied at every time step in order to update all macroscopic cross sections. The detailed description of data can be found in Section A5.2 of Appendix 5. The very small magnitudes of errors observed in these tables show that OMNI-T has sufficient accuracy for transient analyses.

Table 4.5 Predicted reactor power changes due to a coolant-flow-rate increase

$$W_{channel} = 10 + 2.0 \times time \ (gm/sec)$$

| | QUANDRY | OMNI-T |
|---|---|---|
| Initial k-eff | 1.005628 | 1.005553 (-0.0075 %) |
| Power at (KWt.) | | |
| 0. sec. | 1.0 | 1.0 |
| 2. sec. | 1.28461 | 1.28555 ( 0.073 %) |
| 4. sec. | 1.50702 | 1.50766 ( 0.042 %) |
| 6. sec. | 1.69093 | 1.69142 ( 0.029 %) |
| 8. sec. | 1.86604 | 1.86561 (-0.023 %) |
| 10. sec. | 2.03683 | 2.03662 (-0.010 %) |
| 12. sec. | 2.20668 | 2.20556 (-0.051 %) |
| 14. sec. | 2.37339 | 2.37232 (-0.045 %) |

Table 4.6 Predicted reactor power changes due to an inlet coolant temperature drop

$T_{inlet} = 533 - 5.0 \times time\ (^{o}K)$

| | QUANDRY | OMNI-T |
|---|---|---|
| Initial k-eff | 0.9968741 | 0.9967884 (-0.0086 %) |
| Power at (KWt.) | | |
| 0. sec. | 1.0 | 1.0 |
| 1. sec. | 1.14489 | 1.14420 (-0.060 %) |
| 2. sec. | 1.74638 | 1.74320 (-0.182 %) |
| 3. sec. | 2.17693 | 2.17017 (-0.311 %) |
| 4. sec. | 2.29284 | 2.28861 (-0.184 %) |
| 5. sec. | 2.58372 | 2.57757 (-0.238 %) |
| 6. sec. | 2.79736 | 2.79287 (-0.161 %) |
| 7. sec. | 3.03193 | 3.01989 (-0.397 %) |
| 8. sec. | 3.24767 | 3.23755 (-0.312 %) |
| 9. sec. | 3.45919 | 3.45167 (-0.217 %) |
| 10. sec. | 3.67066 | 3.66225 (-0.229 %) |

Table 4.7 Predicted reactor power changes due to the control rod movements
(All Rod Out 0.0 sec. through 2.5 sec. ,
All Rod In 5.0 sec. through 7.5 sec. ,
All Rod Out 10.0 sec. through 12.5 sec. )

| | QUANDRY | OMNI-T |
|---|---|---|
| Initial k-eff | 1.005628 | 1.005553 (-0.0075 %) |
| Power at (KWt.) | | |
| 0. sec. | 1.0 | 1.0 |
| 1. sec. | 1.23918 | 1.23969 ( 0.041 %) |
| 2. sec. | 1.93417 | 1.93238 (-0.093 %) |
| 3. sec. | 1.56205 | 1.55922 (-0.181 %) |
| 4. sec. | 1.45327 | 1.45267 (-0.041 %) |
| 5. sec. | 1.42505 | 1.42471 (-0.024 %) |
| 6. sec. | 1.16810 | 1.16779 (-0.027 %) |
| 7. sec. | 0.86892 | 0.86888 (-0.005 %) |
| 8. sec. | 0.91307 | 0.91366 ( 0.065 %) |
| 9. sec. | 0.96211 | 0.96277 ( 0.069 %) |
| 10. sec. | 0.99314 | 0.99379 ( 0.065 %) |
| 11. sec. | 1.23067 | 1.23193 ( 0.102 %) |
| 12. sec. | 1.89130 | 1.89121 (-0.005 %) |
| 13. sec. | 1.58449 | 1.58241 (-0.131 %) |
| 14. sec. | 1.47905 | 1.47889 (-0.011 %) |
| 15. sec. | 1.44902 | 1.44926 ( 0.017 %) |

### 4.5.3 Multi-Group Problems

In the previous section, the accuracy of OMNI-T was shown to be excellent for two-group transient analyses. The remaining question is whether it is also accurate for multi-group transient analyses. Unfortunately, we do not have available any computer codes for multi-group transient analyses. Therefore, tests for the multi-group transient mode were divided into two tests. One is done to check the multi-group energy spectrum calculation, and the other is done to test calculational stability.

In Chapter 3, the energy spectrum code, MESADES was introduced and shown to be valid. The OMNI-T code also solves the same P-1 transport equation and utilizes the same upscattering iteration scheme. Therefore, the calculational schemes in the OMNI-T are basically the same as the schemes in the MESADES, except for spatial dependencies. In order to isolate the energy dependency from the spatial dependencies, an artificial test problem was invented. Figure (4.2) shows the calculational procedures for this test.

At first, MESADES solved the asymptotic energy spectrum for fluxes and currents with their fundamental eigenvalue, i.e. ctitical material buckling, $B_m^2$. The homogeneous material composition used for this calculation was the assembly of A00REF in Appendix 2. The geometrical buckling for a bare homogeneous reactor is the same as the material buckling when the reactor is in the critical condition. From this fact, calculated material buckling ($1.490665 \times 10^{-3}$ $cm^{-2}$) was converted to the critical size (L = 81.36916 cm) for a slab reactor. At the next step, the

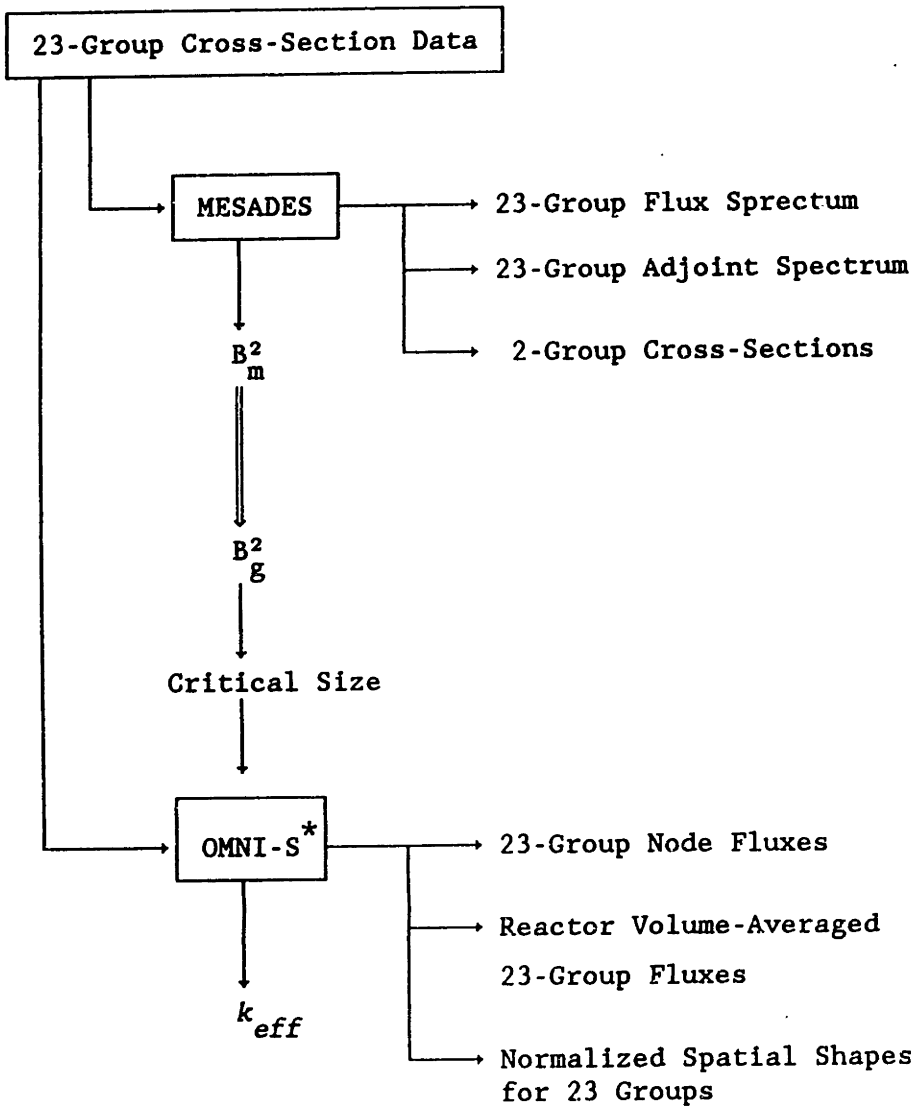


* OMNI-S : Static Calculation Part of OMNI-T

Figure 4.2 Test Procedure for the Spectrum Calculation Model in OMNI-T

OMNI-T calculated the static conditions for this critical slab reactor with the material properties used for the MESADES. If the slowing-down calculation schemes in the OMNI-T is correct and properly programmed, spatial fluxes should have a sine-shape which is identical for all energy groups and the groupwise volume-average fluxes ought to have the same group-to-group ratio as the asymptotic energy spectrum calculated by MESADES. Table (4.8) confirms that the OMNI-T is solving the multi-group static equations correctly.

Table 4.8 Calculated 23-Group Energy Spectrum for the A00REF Assembly

| group | MESADES | OMNI-T | % error |
|---|---|---|---|
| 1 | 0.007510 | 0.007510 | 0.0 |
| 2 | 0.030311 | 0.030311 | 0.0 |
| 3 | 0.063891 | 0.063891 | 0.0 |
| 4 | 0.066201 | 0.066201 | 0.0 |
| 5 | 0.062169 | 0.062170 | 0.0016 |
| 6 | 0.065762 | 0.065762 | 0.0 |
| 7 | 0.119874 | 0.119875 | 0.0008 |
| 8 | 0.103350 | 0.103350 | 0.0 |
| 9 | 0.016763 | 0.016763 | 0.0 |
| 10 | 0.111296 | 0.111296 | 0.0 |
| 11 | 0.059551 | 0.059550 | -0.0017 |
| 12 | 0.012257 | 0.012257 | 0.0 |
| 13 | 0.020117 | 0.020117 | 0.0 |
| 14 | 0.018623 | 0.018623 | 0.0 |
| 15 | 0.013941 | 0.013941 | 0.0 |
| 16 | 0.001867 | 0.001867 | 0.0 |
| 17 | 0.013282 | 0.013282 | 0.0 |
| 18 | 0.018812 | 0.018812 | 0.0 |
| 19 | 0.009811 | 0.009811 | 0.0 |
| 20 | 0.053350 | 0.053350 | 0.0 |
| 21 | 0.081322 | 0.081321 | -0.0012 |
| 22 | 0.032001 | 0.032001 | 0.0 |
| 23 | 0.017940 | 0.017940 | 0.0 |

The last test for the accuracy of OMNI-T concerns the calculational stability of the multi-group transient analysis. The two-group transient scheme was validated in the previous section. However there may be round-off errors in the multi-group case. These can be large for the iteration schemes involving large matrices. To evaluate this concern, a transient calculation using OMNI-T was performed with thermal-hydraulic feedback but without any perturbation. The same reactor problem as in Table (4.8) was simulated with the smallest time step interval (0.01 sec) in order to maximize the sources of round-off errors. Thermal-hydraulic feedback calculations were performed at every time step. The result shown in the following table shows that OMNI-T has excellent calculational stability even for problems involving many energy groups.

Table 4.9 Calculated reactor power changes from OMNI-T for the steady-state condition (with thermal-hydraulic feedback)

| Time (sec.) | The number of time step | Power (watt.) | Deviation |
|---|---|---|---|
| 0. | 0 | 1000. | |
| 0.01 | 1 | 999.9999 | |
| 0.02 | 2 | 999.9999 | |
| 0.10 | 10 | 999.9991 | |
| 0.20 | 20 | 999.9984 | |
| 0.23 | 23 | 999.9983 | $-1.7\times10^{-4}$ % |
| 0.50 | 50 | 999.9983 | $-1.7\times10^{-4}$ % |

# Chapter 5

## DISCUSSION OF RESULTS

### 5.1 INTRODUCTION

In this chapter, a number of transient problems are investigated using the one-dimensional nodal code described in the previous chapter. The accuracies of the two weighting schemes defined in Chapter 2 are measured by direct comparison of predicted transient behavior with multi-group P-1 results.

Even though the main objective of this thesis is to estimate the errors of two-group models compared with multi-group models, transient tests started first with the comparisons of one-group models versus two-group models. The bilinearly weighted one-group diffusion parameters collapsed from two-group diffusion parameters provide a simple set of numbers with which we can understand the characteristics of adjoint spectrum weighting more easily. The bilinearly weighted one-group cross sections are totally different from the conventionally weighted one-group cross sections. Therefore, tests of the two weighting methods for one-group models ought to uncover significant information and provide a good starting point for the study of bilinear weighting.

Accordingly, in the next section, the accuracy of one-group models for prediction of transient behavior are examined. A homogeneous bare reactor problem was chosen because its simple geometry avoids any computational errors involved with spatial discontinuities. Transients

were initiated either by a step pertubation or by control rod movements. This problem has already been studied by Dias [D-2]. His conclusion that adjoint weighting is superior to the unity weighting (here, the same as the conventional flux weighting) will be checked.

In order to provide a more realistic evaluation of the two weighting methods, twenty-three-group models were then applied to the various reactor problems (Section 5.3). For the estimation of few-group perturbations and temperature feedback coefficients, we need to determine weighted few-group parameters for a perturbed condition. Weighting with a perturbed (in most case, time-dependent) spectra is suggested by the variational principle, but is impractical. Accordingly several alternative combinations of weighting functions were tried to test accuracies.

## 5.2 APPLICATION TO TWO-GROUP TRANSIENT PROBLEMS

A homogeneous bare reactor was chosen for the two-group transient problem because it avoids any calculational errors due to spatial discontinuties, which are a major source of errors in nodal analysis if discontinuity factors are not used. This problem is also ideal as the first transient test problem since it has previously been studied using the weighting functions : unity, Galerkin, and adjoint [D-2]. Dias tested these three weighting methods for simplified transient models derived by reducing the number of dimensions in space and energy. He found that adjoint weighting (here, the same as the space-independent bilinear weighting) was significantly superior to unity weighting (here, the same

as the conventional space-independent flux weighting) and to Galerkin weighting when used to derive the point kinetics model. He also found that adjoint weighting gave consistently better transient results for the other models involving spatial dependence. We can check his conclusions by solving essentially the same reactor problems.

Unfortunately a problem identical with that solved by Dias could not be solved because the nodal code used in this thesis is one-dimensional, whereas Dias used a 3-D code. However, all data were kept the same except for geometrical boundary conditions. An initially critical core was perturbed by the uniform step change in thermal absorption cross section at time zero. A complete list of data can be found in Appendix A5.2. The transient calculation was performed by the nodal code OMNI-T with a node mesh size of 1.0 cm and a time step size of 0.01 sec.

### 5.2.1 One-Group Diffusion Parameters

From the data in Appendix A5.2, we can calculate real and adjoint spectra for the unperturbed composition and perturbed composition using the computer code MESADES. The following table shows the calculated spectra along with the collapsed one-group cross section data.

As shown in Table (5.1), the adjoint spectrum is not flat (the fast to thermal ratio for the unpertubed adjoint fluxes is 0.6544 whereas the ratio for the real fluxes is 3.9192). This suggests that the conventional (unity) weighting will not yield a good approximation and that the conventional weighted parameters should be very different from the bilinearly weighted parameters. This expectation is confirmed by

calculated parameters shown in Table (5.1) and by the predicted initial criticality shown in Table (5.4).

Table 5.1 Calculated two-group spectra and the one-group diffusion parameters for the homogeneous bare reactor problem

**Unperturbed Spectra**

| | Real | | Adjoint | |
|---|---|---|---|---|
| group | Flux | Current | Flux | Current |
| 1 | 0.7967159 | 0.9370309 | 0.7910980 | 0.7130271 |
| 2 | 0.2032841 | 0.0629691 | 1.2089020 | 0.2869729 |

**Perturbed Spectra**

| | Real | | Adjoint | |
|---|---|---|---|---|
| group | Flux | Current | Flux | Current |
| 1 | 0.7958739 | 0.9367239 | 0.7886168 | 0.7119636 |
| 2 | 0.2041261 | 0.0632761 | 1.2113832 | 0.2880364 |

**Conventionally Weighted One-Group Parameters** ($cm^{-1}$)

| $\Sigma_{tr}$ | $\Sigma_a$ | $\nu\Sigma_f$ | $\Sigma_f$ |
|---|---|---|---|
| 0.2765511 | 0.02036894 | 0.02547902 | 0.01048519 |
| $\Sigma_s$ | $\chi$ | $\chi_d$ | $\upsilon$ (cm/sec) |
| 0.6663418 | 1.0 | 1.0 | 1.140415E+06 |

**Bilinearly Weighted One-Group Parameters** ($cm^{-1}$)

| $\Sigma_{tr}$ | $\Sigma_a$ | $\nu\Sigma_f$ | $\Sigma_f$ |
|---|---|---|---|
| 0.3383274 | 0.01597938 | 0.02547902 | 0.01048519 |
| $\Sigma_s$ | $\chi$ | $\chi_d$ | $\upsilon$ (cm/sec) |
| 0.6391064 | 0.7910979 | 0.7910979 | 9.676566E+05 |

The few-group perturbations are obtained by subtracting the few-group parameters of the unperturbed composition from those of perturbed composition. Therefore, few-group parameters need to be calculated at perturbed conditions as well as unperturbed conditions.

During a transient the multi-group cross sections change resulting in a change of energy spectra. The variational principle introduces in addition an adjoint spectra. We expect that the best trial function space will involve both perturbed real and adjoint infinite media spectra. However, mathematically the adjoint equations express an inversion of the time behavior ($\frac{\partial}{\partial t}$ is replaced by $-\frac{\partial}{\partial t}$). As a result, perturbed (time-dependent) adjoint spectra depend on the (generally unknown) final state. For this reason, it is hard to get the ideal weighting spectra for few-group perturbations.

Therefore, several combinations of weighting spectra (unperturbed spectra and perturbed spectra) were tried to test accuracies empirically. Table (5.2) shows six methods for determining few-group parameters for a perturbed composition.

Table 5.2 Summary of six methods for determining few-group perturbations

| | unperturbed composition $\Sigma_{\alpha_n}$ | Method | perturbed composition $\hat{\Sigma}_{\alpha_n}$ |
|---|---|---|---|
| Conventional Weighting | $\Sigma_{\alpha_g} = \sum_{n \subset g} \Sigma_{\alpha_n} F_n$ | 1 | $\hat{\Sigma}_{\alpha_g} = \sum_{n \subset g} \hat{\Sigma}_{\alpha_n} \hat{F}_n$ |
| | | 2 | $\hat{\Sigma}_{\alpha_g} = \sum_{n \subset g} \hat{\Sigma}_{\alpha_n} F_n$ |
| Bilinear Weighting | $\Sigma_{\alpha_g} = \sum_{n \subset g} F_n^* \Sigma_{\alpha_n} F_n$ | 3 | $\hat{\Sigma}_{\alpha_g} = \sum_{n \subset g} F_n^* \hat{\Sigma}_{\alpha_n} \hat{F}_n$ |
| | | 4 | $\hat{\Sigma}_{\alpha_g} = \sum_{n \subset g} F_n^* \hat{\Sigma}_{\alpha_n} F_n$ |
| | | 5 | $\hat{\Sigma}_{\alpha_g} = \sum_{n \subset g} \hat{F}_n^* \hat{\Sigma}_{\alpha_n} F_n$ |
| | | 6 | $\hat{\Sigma}_{\alpha_g} = \sum_{n \subset g} \hat{F}_n^* \hat{\Sigma}_{\alpha_n} \hat{F}_n$ |
| Perturbation | $\Delta\Sigma_{\alpha_g} = \hat{\Sigma}_{\alpha_g} - \Sigma_{\alpha_g}$ | | |

$F_n$ : multi-group real spectra of unperturbed composition

$F_n^*$ : multi-group adjoint spectra of unperturbed composition

$\hat{F}_n$ : multi-group real spectra of perturbed composition

$\hat{F}_n^*$ : multi-group adjoint spectra of perturbed composition

The one-group perturbations calculated from these methods are summarized in Table (5.3).

Table 5.3 Estimated one-group perturbations for the homogeneous reactor problem

| Method* | $\Delta \Sigma_a$ | $\Delta \Sigma_{tr}$ | $\Delta \nu\Sigma_f$ | $\Delta \Sigma_f$ |
|---|---|---|---|---|
| 1 | -3.066E-05 | 2.019E-04 | 8.334E-05 | 3.430E-05 |
| 2 | -7.928E-05 | 0.0 | 0.0 | 0.0 |
| 3 | -2.791E-05 | 1.939E-04 | 8.334E-05 | 3.430E-05 |
| 4 | -9.480E-05 | 0.0 | 0.0 | 0.0 |
| 5 | -1.482E-04 | 8.998E-04 | 0.0 | 0.0 |
| 6 | -8.001E-05 | 1.094E-03 | 8.334E-05 | 3.430E-05 |

| Method* | $\Delta \Sigma_s$ | $\Delta \upsilon$ | $\Delta \chi$ | $\Delta \chi_d$ |
|---|---|---|---|---|
| 1 | 6.169E-04 | -4.277E+03 | 0.0 | 0.0 |
| 2 | 0.0 | 0.0 | 0.0 | 0.0 |
| 3 | 9.217E-04 | -3.748E+03 | 0.0 | 0.0 |
| 4 | 0.0 | 0.0 | 0.0 | 0.0 |
| 5 | -3.234E-04 | -1.738E+03 | -2.481E-03 | -2.481E-03 |
| 6 | 6.018E-04 | -5.481E+03 | -2.481E-03 | -2.481E-03 |

* Perturbation evaluation method

Method 1 : C.W. with perturbed real spectra
2 : C.W. with unperturbed real spectra
3 : B.W. with unperturbed adjoint spectra and perturbed real spectra
4 : B.W. with unperturbed adjoint spectra and unperturbed real spectra
5 : B.W. with perturbed adjoint spectra and unperturbed real spectra
6 : B.W. with perturbed adjoint spectra and perturbed real spectra

### 5.2.2 Transient Results

The six schemes for finding perturbed one-group diffusion parameters were tested for the step perturbation. Table (5.4) shows the one-group predictions of transient behavior vs. the two-group reference results. As shown in this table, methods 5 and 6 lead to immense errors. (The reactor actually becomes super prompt critical.) These two methods estimate perturbations by weighting with the perturbed adjoint spectra at time $0^+$, the unperturbed adjoint spectra being used for the initial critical condition. Even though the change of adjoint spectra from the unperturbed to the perturbed condition is very small (the fast to thermal ratio change from 0.6544 to 0.6510), the perturbation is very sensitive to this difference.

Comparisons of the other methods with the reference solution show that failure to weight with the adjoint spectra leads to significant errors (Method 1 and Method 2). This result is consistent with the conclusions of Dias.

Although the bilinear weighting is shown to be superior to the conventional flux weighting, it is not easy to understand why method 4 is better than method 3. Intuitively, one would expect better results from method 3, which uses perturbed regular spectra. This expectation was slighted supported by the extreme case in which the delayed neutrons are neglected ($\beta_{eff} = 0.0$). Table (5.5) shows these results. Perhaps the safest conclusion is that there is little difference in accuracy between methods 3 and 4.

Table 5.4 Predicted reactor power changes due to a **stepwise rod bank ejection** for a homogeneous bare reactor **(without thermal feedback)**

| | 2-group | C.W.* 1 1-group | C.W.* 2 1-group |
|---|---|---|---|
| Initial k-eff | 1.014385 | 1.013932 (-0.045 %) | 1.013932 (-0.045 %) |
| Power at 0.0 sec | 1.0 | 1.0 | 1.0 |
| 1.0 sec | 3.136954 | 2.941624 (-6.227 %) | 1.826976 (-41.76 %) |
| 2.0 sec | 3.604735 | 3.341940 (-7.290 %) | 1.936119 (-46.29 %) |
| 3.0 sec | 4.142636 | 3.796733 (-8.350 %) | 2.051782 (-50.47 %) |
| 4.0 sec | 4.760755 | 4.313416 (-9.396 %) | 2.174354 (-54.33 %) |

| | B.W.** 3 1-group | B.W.** 4 1-group | B.W.** 5 1-group | B.W.** 6 1-group |
|---|---|---|---|---|
| Initial k-eff | 1.014402 ( 0.002 %) | 1.014402 ( 0.002 %) | 1.014402 ( 0.002 %) | 1.014402 ( 0.002 %) |
| Power at 0.0 sec | 1.0 | 1.0 | 1.0 | 1.0 |
| 1.0 sec | 3.141673 ( 0.150 %) | 3.140045 ( 0.099 %) | $6.719\times10^{5}$ ( ∞ %) | $1.818\times10^{5}$ ( ∞ %) |
| 2.0 sec | 3.611490 ( 0.187 %) | 3.609289 ( 0.126 %) | $3.343\times10^{10}$ ( ∞ %) | $2.221\times10^{9}$ ( ∞ %) |
| 3.0 sec | 4.151564 ( 0.216 %) | 4.148657 ( 0.145 %) | $1.663\times10^{15}$ ( ∞ ) | $2.714\times10^{13}$ ( ∞ %) |
| 4.0 sec | 4.772404 ( 0.245 %) | 4.768627 ( 0.165 %) | $8.276\times10^{19}$ ( ∞ ) | $3.316\times10^{17}$ ( ∞ %) |

* C.W. : (Flux only) Conventionally Weighted
** B.W. : (Flux and Adjoint-Flux) Bilinearly Weighted

Table 5.5 Predicted reactor power changes due to a stepwise rod bank ejection for a homogeneous bare reactor [without thermal feedback, no delayed neutrons ($\beta_{eff}$ = 0.0)]

| | 2-group | C.W.* 1 1-group | B.W.** 3 1-group | B.W.** 4 1-group |
|---|---|---|---|---|
| Initial k-eff | 1.014385 | 1.013932 (-0.045 %) | 1.014402 ( 0.002 %) | 1.014402 ( 0.002 %) |
| Power at 0.0 sec | 1.0 | 1.0 | 1.0 | 1.0 |
| 0.005 sec | 1.626321 | 2.043968 ( 25.68 %) | 1.626000 (-0.020 %) | 1.617831 (-0.522 %) |
| 0.05 sec | 1.2950E+2 | 1.2359E+3 ( 854.4 %) | 1.2544E+2 (-3.135 %) | 1.2284E+2 (-5.143 %) |
| 0.10 sec | 1.6772E+4 | 1.5224E+6 ( 8977. %) | 1.5684E+4 (-6.487 %) | 1.5089E+4 (-10.03 %) |
| 0.15 sec | 2.1722E+6 | 1.8754E+9 ( ∞ %) | 1.9610E+6 (-9.723 %) | 1.8535E+6 (-14.67 %) |
| 0.20 sec | 2.8133E+8 | 2.3102E+12 ( ∞ %) | 2.4519E+8 (-12.85 %) | 2.2768E+8 (-19.07 %) |

* C.W. : (Flux only) Conventionally Weighted
** B.W. : (Flux and Adjoint-Flux) Bilinearly Weighted

### 5.2.3 Alternative Method of Bilinear Weighting

In the previous section, we found that bilinearly weighted cross sections are better than conventionally weighted cross sections only if perturbations are estimated with fixed adjoint spectra weighting (weighted only by unperturbed spectra). The ideal weighting functions would be time-dependent adjoint and regular weighting functions. For practical

applications, however, the calculation of time-dependent adjoint spectra at every time step is virtually impossible since such spectra depend on the final condition of the reactor, which is not known a priori when feedback is present [L-3].

However for these test problems involving a uniform step perturbation of a homogeneous reactor, with no feedback, we do know the final condition a priori. The regular spectra changes are completed within a very short time period (in this problem about 0.3 sec.) and theory tells us that the perturbed adjoint should be used throughout the entire transient. Table (5.6) summarizes methods of computing few-group parameters based on this perturbed adjoint weighting scheme, and Table (5.7) shows the one-group perturbations obtained from these weighting procedures.

Table 5.6 Summary of alternative methods for determining few-group perturbations

| | unperturbed composition $\Sigma_{\alpha_n}$ | Method | perturbed composition $\hat{\Sigma}_{\alpha_n}$ |
|---|---|---|---|
| Bilinear Weighting | $\tilde{\Sigma}_{\alpha_g} = \sum_{n \subset g} \hat{F}^*_n \Sigma_{\alpha_n} F_n$ | 7 | $\hat{\Sigma}_{\alpha_g} = \sum_{n \subset g} \hat{F}^*_n \hat{\Sigma}_{\alpha_n} \hat{F}_n$ |
| | | 8 | $\hat{\Sigma}_{\alpha_g} = \sum_{n \subset g} \hat{F}^*_n \hat{\Sigma}_{\alpha_n} F_n$ |
| Perturbation | $\Delta\Sigma_{\alpha_g} = \hat{\Sigma}_{\alpha_g} - \tilde{\Sigma}_{\alpha_g}$ | | |

$F_n$ : multi-group real spectra of unperturbed composition

$F^*_n$ : multi-group adjoint spectra of unperturbed composition

$\hat{F}_n$ : multi-group real spectra of perturbed composition

$\hat{F}^*_n$ : multi-group adjoint spectra of perturbed composition

Table 5.7 One-group perturbations
for the homogeneous reactor problem

| Method* | $\Delta \Sigma_a$ | $\Delta \Sigma_{tr}$ | $\Delta \nu\Sigma_f$ | $\Delta \Sigma_f$ |
|---|---|---|---|---|
| 7 | -2.892E-05 | 1.936E-04 | 8.334E-05 | 3.430E-05 |
| 8 | -9.604E-05 | 0.0 | 0.0 | 0.0 |

| Method* | $\Delta \Sigma_s$ | $\Delta \upsilon$ | $\Delta \chi$ | $\Delta \chi_d$ |
|---|---|---|---|---|
| 7 | 9.252E-04 | -3.743E+03 | 0.0 | 0.0 |
| 8 | 0.0 | 0.0 | 0.0 | 0.0 |

* Perturbation evaluation method

Method 7 : B.W. with perturbed adjoint spectra and perturbed real spectra

8 : B.W. with perturbed adjoint spectra and unperturbed real spectra

Table (5.8) shows the resultant one-group prediction of transient behavior vs. the two-group results. The extreme case ($\beta_{eff}$= 0.0) is also tested, and results are shown in Table (5.9). These last two results do not show a strong advantage from using the alternative methods. For this reason and because of the difficulties estimating the perturbed adjoint spectra for non-step perturbations, this alternative method was not adopted, and only unperturbed adjoint spectra have been used for the test cases which follow.

Table 5.8 Predicted reactor power changes due to a **stepwise rod bank ejection** for a homogeneous bare reactor **(without thermal feedback)**

| | 2-group | B.W. 3 * 1-group | B.W. 4 * 1-group | B.W. 7 * 1-group | B.W. 8 * 1-group |
|---|---|---|---|---|---|
| Initial k-eff | 1.014385 | 1.014402 ( 0.002 %) | 1.014402 ( 0.002 %) | 1.014402 ( 0.002 %) | 1.014402 ( 0.002 %) |
| Power at 0.0 sec | 1.0 | 1.0 | 1.0 | 1.0 | 1.0 |
| 1.0 sec | 3.136954 | 3.141673 ( 0.150 %) | 3.140045 ( 0.099 %) | 3.212679 ( 2.414 %) | 3.228849 ( 2.929 %) |
| 2.0 sec | 3.604735 | 3.611490 ( 0.187 %) | 3.609289 ( 0.126 %) | 3.708206 ( 2.870 %) | 3.730328 ( 3.484 %) |
| 3.0 sec | 4.142636 | 4.151564 ( 0 216 %) | 4.148657 ( 0.145 %) | 4.280163 ( 3.320 %) | 4.309693 ( 4.033 %) |
| 4.0 sec | 4.760755 | 4.772404 ( 0.245 %) | 4.768627 ( 0.165 %) | 4.940339 ( 3.772 %) | 4.979040 ( 4.585 %) |

* Control rod perturbation evaluation method
  - 3 : B.W. with unperturbed adjoint spectra and perturbed real spectra
  - 4 : B.W. with unperturbed adjoint spectra and unperturbed real spectra
  - 7 : B.W. with perturbed adjoint spectra and perturbed real spectra
  - 8 : B.W. with perturbed adjoint spectra and unperturbed real spectra

B.W. : Bilinearly Weighted

Table 5.9 Predicted reactor power changes due to a **stepwise rod bank ejection** for a homogeneous bare reactor (**without thermal feedback,** **no delayed neutrons** ($\beta_{eff}$ = 0.0))

| | 2-group | B.W.** 3 1-group | B.W.** 4 1-group | B.W.*** 7 1-group | B.W.*** 8 1-group |
|---|---|---|---|---|---|
| Initial k-eff | 1.014385 | 1.014402 ( 0.002 %) | 1.014402 ( 0.002 %) | 1.014402 ( 0.002 %) | 1.014402 ( 0.002 %) |
| Power at 0.0 sec | 1.0 | 1.0 | 1.0 | 1.0 | 1.0 |
| 0.05 sec | 1.2950E+2 | 1.2544E+2 (-3.135 %) | 1.2284E+2 (-5.143 %) | 1.3231E+2 ( 2.170 %) | 1.3123E+2 ( 1.336 %) |
| 0.10 sec | 1.6772E+4 | 1.5684E+4 (-6.487 %) | 1.5089E+4 (-10.03 %) | 1.7448E+4 ( 4.031 %) | 1.7222E+4 ( 2.683 %) |
| 0.15 sec | 2.1722E+6 | 1.9610E+6 (-9.723 %) | 1.8535E+6 (-14.67 %) | 2.3009E+6 ( 5.925 %) | 2.2601E+6 ( 4.047 %) |
| 0.20 sec | 2.8133E+8 | 2.4519E+8 (-12.85 %) | 2.2768E+8 (-19.07 %) | 3.0343E+8 ( 7.856 %) | 2.9661E+8 ( 5.431 %) |

Control rod perturbation evaluation method

3 : B.W. with unperturbed adjoint spectra and perturbed real spectra

4 : B.W. with unperturbed adjoint spectra and unperturbed real spectra

7 : B.W. with perturbed adjoint spectra and perturbed real spectra

8 : B.W. with perturbed adjoint spectra and unperturbed real spectra

### 5.2.4 Frequency Term for Time-Dependent Spectra

In Chapter 2, definitions of few-group parameters (Equation 2.20) were derived using time-dependent energy spectra. Systematic derivation produced new parameters, $\omega_{i_g}$ (i=0 for flux spectra, i=1 for current spectra) which should be added to the few-group total cross sections. These additional terms act as correction terms to the absorption cross section (for i=0) or to the transport cross section (for i=1) [as shown in Eqs. (2.21) and (2.22)]. Previous results shown in this chapter were obtained without these correction terms. Since the changes in energy spectra were small, it was assumed that the $\omega_{i_g}$ are negligible. However in order to justify assumption, the $\omega_{i_g}$ should be estimated quantitatively.

For all the nodal calculations in this thesis, time derivatives of neutron currents have been neglected because of their negligible sizes. Therefore, the time derivatives of the current spectra were also neglected. Thus $\omega_{1_n}(t)$ (or $\omega_{1_g}(t)$ ) should be zero. Accordingly, only $\omega_{0_g}(t)$ needs to be estimated.

Calculation of time derivative of energy spectra is not feasible during a one-group model calculation; and it is not easy even for a two-group model calculation. However, we have analytical solutions for the step perturbation problem, and we can estimate $\omega_0$ term from analytical solutions. Appendix 6 gives the analytical solutions for this problem. Unnormalized energy spectra can be obtained as:

$$F_{o_1}(t) = F_{o_1}^{u} \left[ f_1 e^{\omega_1 t} + f_2 e^{\omega_2 t} + f_3 e^{\omega_3 t} \right]$$

$$F_{o_2}(t) = F_{o_2}^{u} \left[ f_1 r_1/r_0 e^{\omega_1 t} + f_2 r_2/r_0 e^{\omega_2 t} + f_3 r_3/r_0 e^{\omega_3 t} \right]$$

$$F_{o_1}^{*}(t) = F_{o_1}^{*u} \left[ f_1^{*} e^{\omega_1^{*} t} + f_2^{*} e^{\omega_2^{*} t} + f_3^{*} e^{\omega_3^{*} t} \right]$$

$$F_{o_2}^{*}(t) = F_{o_2}^{*u} \left[ f_1^{*} R_1/R_0 e^{\omega_1^{*} t} + f_2^{*} R_2/R_0 e^{\omega_2^{*} t} + f_3^{*} R_3/R_0 e^{\omega_3^{*} t} \right]$$

where $F_{o_n}^{u}$ = group-n unperturbed real flux spectrum and

$F_{o_n}^{*u}$ = group-n unperturbed adjoint flux spectrum.

Now, we can substitute these expressions into the definitions of $\omega_{o_g}$ in Eq. (2.20). Table (5.10) shows the values of $V_{o_g}^{-1}\omega_{o_g}(t)$ at each time step and the transient results having this correction term compared with the result without correction. Even though the correction term $\omega_{o_g}$ to the absorption cross section is relatively large ($V_o^{-1}\omega_o = 7.5361\times10^{-5}$ cm$^{-1}$) compared with the one-group perturbation to the absorption cross section ($\Delta\Sigma_a = -9.480\times10^{-5}$ cm$^{-1}$) at time zero, the correction term dies out very quickly ($4.9011\times10^{-7}$ cm$^{-1}$ at 0.001 sec and $4.0027\times10^{-10}$ cm$^{-1}$ at 0.1 sec). Therefore, it is valid to neglect it.

Table 5.10 Predicted reactor power changes due to a stepwise rod bank ejection for a homogeneous bare reactor (without thermal feedback) (time step size = 0.001 sec.)

| | 2-group | B.W.* 4 1-group without correction | B.W.* 4 1-group with correction | $V_0^{-1}\omega_0(t)$ ($cm^{-1}$) |
|---|---|---|---|---|
| Initial k-eff | 1.014385 | 1.014402 | 1.014402 | |
| Power at 0.0 sec | 1.0 | 1.0 | 1.0 | 7.536E-05 |
| 0.001 | 1.087889 | 1.087160 | 1.086671 | 4.901E-07 |
| 0.002 | 1.171416 | 1.169976 | 1.169081 | 4.000E-07 |
| 0.003 | 1.250738 | 1.248666 | 1.247434 | 3.322E-07 |
| 0.01 sec | 1.704845 | 1.700058 | 1.697673 | 1.228E-07 |
| 0.02 sec | 2.125944 | 2.120479 | 2.118048 | 4.655E-08 |
| 0.03 sec | 2.378125 | 2.373578 | 2.371612 | 2.196E-08 |
| 0.1 sec | 2.760474 | 2.761641 | 2.761484 | 4.003E-10 |
| 0.2 sec | 2.808167 | 2.810654 | 2.810626 | 1.907E-12 |
| 0.3 sec | 2.847494 | 2.850133 | 2.850106 | 9.143E-15 |
| 1.0 sec | 3.138651 | 3.141993 | 3.141963 | 1.094E-25 |
| 1.5 sec | | 3.368589 | 3.368557 | 0.0 |
| 2.0 sec | | 3.611526 | 3.611493 | 0.0 |

* B.W. ; (Flux and Adjoint-Flux) Bilinearly Weighted

### 5.2.5 The Control Rod Bank Withdrawal Problem

A transient resulting from control rod bank movement was simulated for the homogeneous bare reactor. The perturbations were simulated by changing the homogenized node cross sections when the control rods were withdrawn from a given node volume.

The cross section data and geometry were identical that of the step perturbation problem investigated previously. An unperturbed composition was regarded as a rodded composition and a perturbed composition was regarded as an unrodded composition. Withdrawal of a control rod was then represented by simply replacing the rodded composition with the unrodded composition, and partly rodded nodes were taken to have the volume averaged material properties of the rodded and unrodded compositions. Thus, $\hat{F}_n$ and $\hat{F}_n^*$ in Table (5.2) are the real and adjoint spectra of the unrodded composition. As a result we can use the cross section data given in Table (5.3) for the nodal perturbations due to control rod withdrawal.

Control rods were fully inserted into a reactor in its initial steady state. Then, they were withdrawn from the bottom of the core at a speed of 5 cm/sec. After 10 sec., the control rods were fully withdrawn. All feedback was again neglected. By using a small node mesh size (1 cm), a rod cusping problem was avoided.

Table (5.11) shows the results which are consistent with the step perturbation problem shown in Table (5.4).

Table 5.11 Predicted reactor power changes due to a control rod bank removal for a homogeneous bare reactor (without thermal feedback)

| | 2-group | C.W.* 1 1-group | C.W.* 2 1-group | B.W.** 3 1-group | B.W.** 4 1-group |
|---|---|---|---|---|---|
| Initial k-eff | 1.014385 | 1.013932 (-0.045 %) | 1.013932 (-0.045 %) | 1.014402 ( 0.002 %) | 1.014402 ( 0.002 %) |
| Power at 0.0 sec | 1.0 | 1.0 | 1.0 | 1.0 | 1.0 |
| 2.0 sec | 1.033280 | 1.038862 ( 0.540 %) | 1.021686 (-1.122 %) | 1.038643 ( 0.519 %) | 1.033058 (-0.021 %) |
| 4.0 sec | 1.266896 | 1.264381 (-0.199 %) | 1.162306 (-8.256 %) | 1.273479 ( 0.520 %) | 1.266400 (-0.039 %) |
| 6.0 sec | 1.967241 | 1.904448 (-3.192 %) | 1.492108 (-24.15 %) | 1.961977 (-0.268 %) | 1.967104 (-0.007 %) |
| 8.0 sec | 3.347095 | 3.093949 (-7.563 %) | 1.923649 (-42.53 %) | 3.308521 (-1.152 %) | 3.349538 ( 0.073 %) |
| 10. sec | 4.757850 | 4.314422 (-9.320 %) | 2.231740 (-53.09 %) | 4.743981 (-0.291 %) | 4.762973 ( 0.108 %) |

* C.W. : (Flux only) Conventionally Weighted
** B.W. : (Flux and Adjoint-Flux) Bilinearly Weighted

## 5.3 APPLICATION TO MULTI-GROUP TRANSIENT PROBLEMS

Here we deal with more realistic problems of energy spectra weighting. Twenty-three-group P-1 parameters are reduced to two-group P-1 parameters by two weighting methods, and transient behavior of the two-group models are compared with multi-group results. Test problems start with the homogeneous reactor problem and end with a more complex reactor problem having four different material regions.

### 5.3.1 Two-Group P-1 Parameters

All test problems have one or more material compositions which were described in Appendix 2. By running the computer code MESADES (described in Chapter 3), we can evaluate two kinds of two-group P-1 parameters.

Figures (5.1) through (5.4) show the calculated flux- and current spectra of material C00REF and A00REF. As shown, adjoint flux spectra are not completely flat, a situation which implies the need for adjoint weighting. (Conventional flux weighting assumes that adjoint spectra are flat throughout the twenty-three groups.) Adjoint current spectra ($F^*_{1_n}$) are not alwalys flat since they are defined as $D_n B_m F^*_{0_n}$ (Eq. 3.21). (Even if adjoint flux spectra are flat, adjoint current spectra are proportional to the diffusion coefficients.) Therefore, bilinearly weighted two-group parameters are quite different from conventionally weighted two-group parameters. Calculated two-group parameters can be found in Appendix 7, where two-group cross sections are evaluated for the reference temperature condition ($T_f$ = 900 $^0$K, $T_m$ = 585 $^0$K).

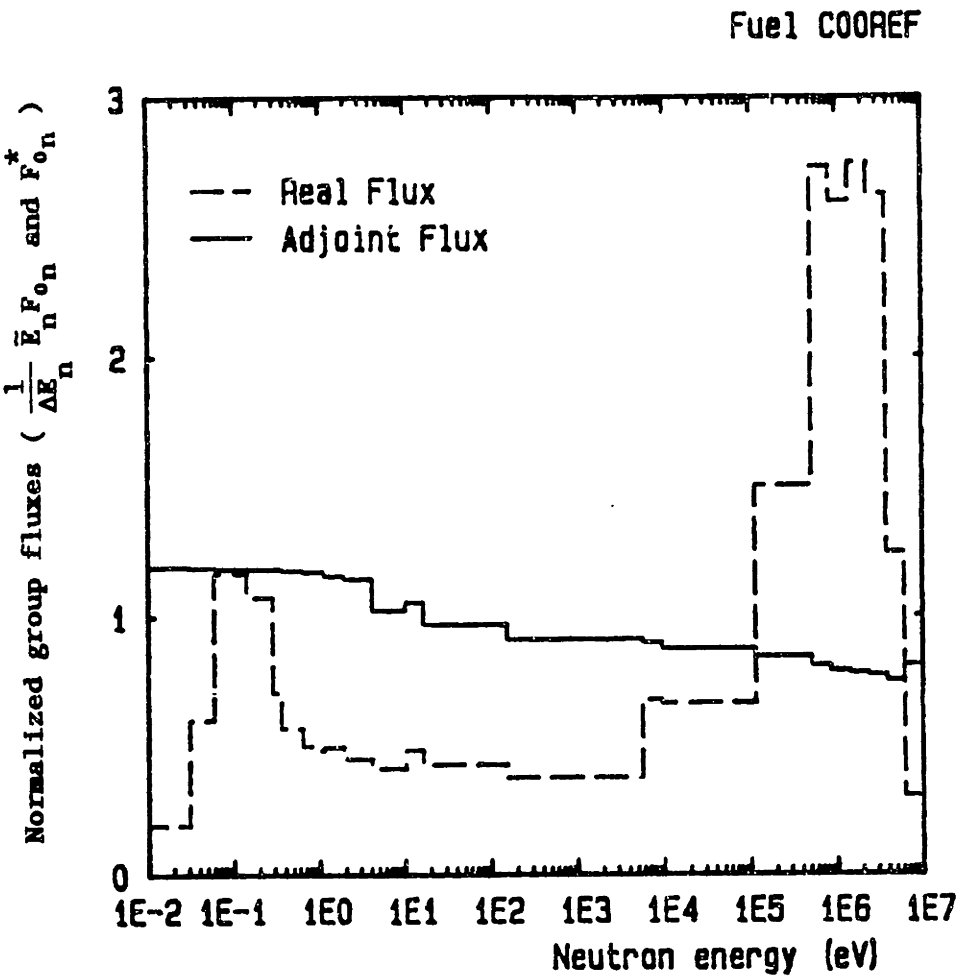


$F_{o_n}$ = real group-flux $= \int_{\Delta E_n} \phi(E)\, dE$

$F^*_{o_n}$ = adjoint group-flux $= \frac{1}{\Delta E_n} \int_{\Delta E_n} \phi^*(E)\, dE$

$\tilde{E}_n = \sqrt{E_{n-1} \cdot E_n}$

Figure 5.1 Twenty-three-group flux spectra for fuel assembly composition COOREF

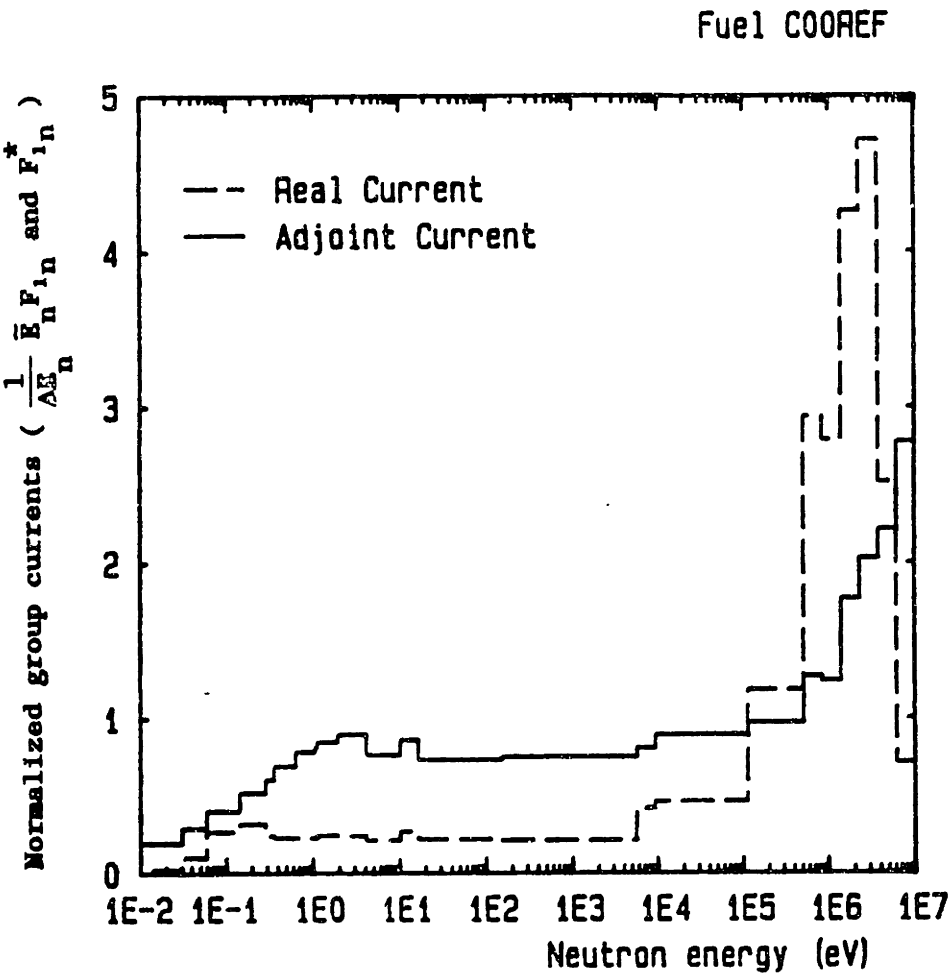


$F_{1_n}$ = real group-current = $D_n B_m F_{o_n}$

$F^*_{1_n}$ = adjoint group-current = $D_n B_m F^*_{o_n}$

Figure 5.2 Twenty-three-group current spectra for fuel assembly composition COOREF

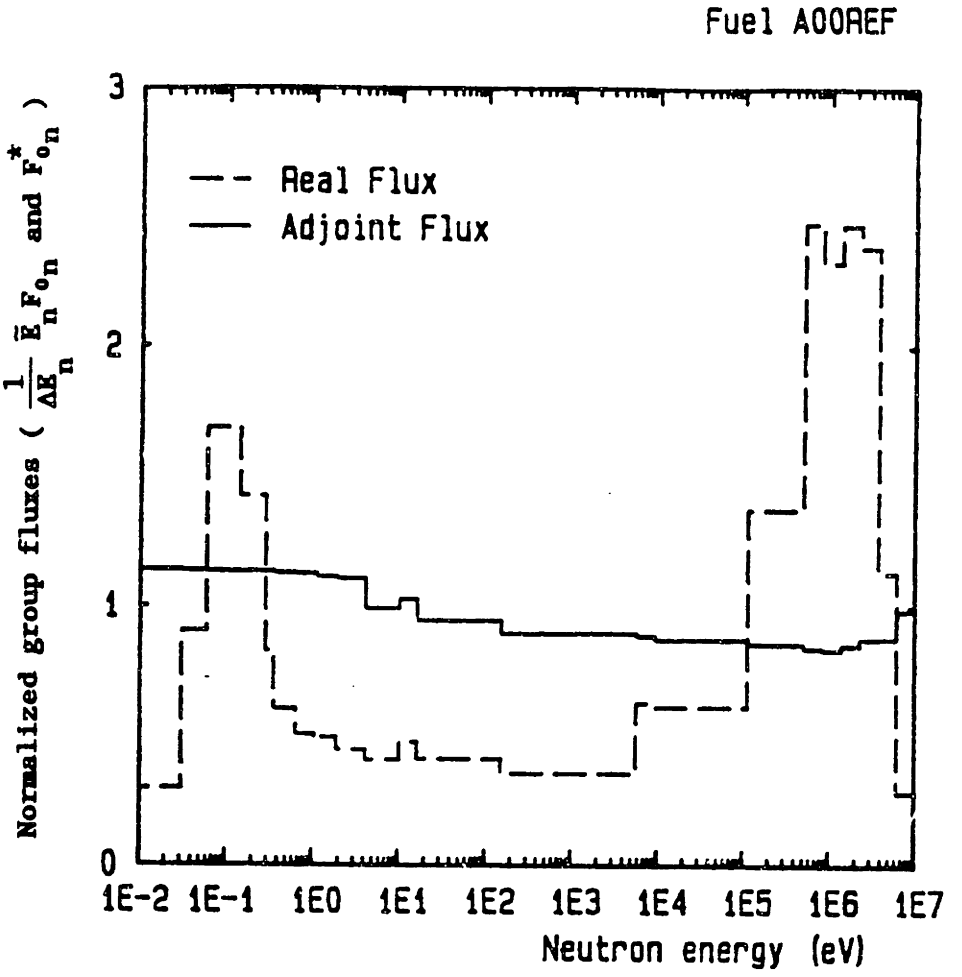


$F_{o_n}$ = real group-flux $= \int_{\Delta E_n} \phi(E)\, dE$

$F^*_{o_n}$ = adjoint group-flux $= \frac{1}{\Delta E_n} \int_{\Delta E_n} \phi^*(E)\, dE$

$\tilde{E}_n = \sqrt{E_{n-1} \cdot E_n}$

Figure 5.3 Twenty-three-group flux spectra for fuel assembly composition A00REF

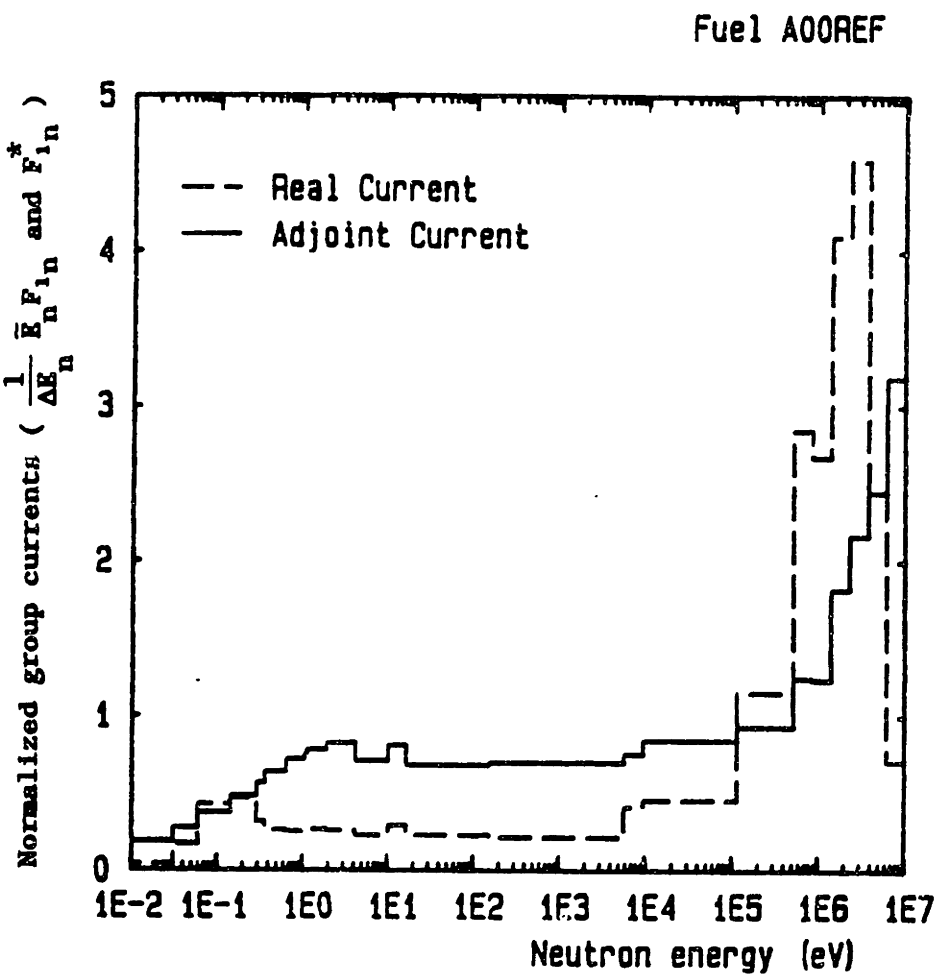


$F_{i_n}$ = real group-current $= D_n B_m F_{o_n}$

$F^*_{i_n}$ = adjoint group-current $= D_n B_m F^*_{o_n}$

Figure 5.4 Twenty-three-group current spectra for fuel assembly composition A00REF

The two-group parameters shown in Appendix 7 indicate that bilinearly weighted two-group parameters are almost the same as conventionally weighted parameters except for the absorption cross sections ($\Sigma_{a_g}$), fission spectrum ($\chi_g$) and delayed neutron fission spectrum ($\chi_{d_g}$). Fission cross sections ($\Sigma_{f_g}$ or $\nu\Sigma_{f_g}$) are identical for both weightings. As compared with conventionally weighted cross sections, bilinearly weighted $\chi_1$ and $\chi_{d_1}$ (both less than unity) make the reactor produce fewer fission neutrons, on the other hand the small values of the absorption cross sections compensate by reducing the capture of neutrons ($\Sigma_c = \Sigma_a - \Sigma_f$). In addition, with bilinear weighting, if more than one delayed neutron precursor group is represented, $\chi_{p_g}$ is found to be different from the $\chi_{d_{\iota,g}}$ ($\iota=1,\cdots,I$), and even for a one-group model, the bilinearly weighted total fission spectrum $\chi_1$ is different from $\chi_{p_1}$ and the $\chi_{d_{1,i}}$, since, in general, the total neutron fission spectrum ($\chi_g$) is calculated as

$$\chi_g = (1 - \beta_{eff})\, \chi_{p_g} + \sum_{\iota=1}^{I} \beta_\iota\, \chi_{d_{\iota,g}} \qquad (5.1)$$

where $\beta_{eff} = \sum_{\iota=1}^{I} \beta_\iota$

With conventional weighting, if all prompt and delayed fission neutrons appear in group-1, $\chi_{p_1} = \chi_{d_{\iota,1}} = \chi_1$.

### 5.3.2 Two-Group Temperature Feedback Coefficients

For transient problems involving with temperature feedback, the small differences in few-group feedback coefficients can lead to substantial differences in transient behavior. As with the perturbations themselves, values of temperature feedback coefficients depend on the choice of real and adjoint spectra. The following table shows several possible choices. The calculated temperature feedback coefficients themselves can be found in Appendix 7.

There is an additional term to be concerned with when estimating temperature coefficients. That is the few-group frequency $\omega_{i_g}^k(t)$ defined in Eq. (2.20). Both $\omega_{0_g}^k(t)$ and $\omega_{1_g}^k(t)$ were neglected in computing perturbations because their contributions to the transient results proved to be negligible. (See Section 5.2.4.) However, the contribution of $\omega_{0_g}(t)$ to the calculation of temperature feedback coefficients may not be negligible.

As shown in Eq. (2.21), the term $V_{0_g}^{-1}\omega_{0_g}\delta_{gg'}$, should be added to $A_{0_{gg'}}(t)$ (defined in Eq. 2.24), that is, to the definition of total cross sections in Eq. (2.20). Therefore, corrected few-group total cross section can be written as:

$$\Sigma_{t_g}^k(t) = \sum_{n\subset g} F_{0_n}^{*k}\,\Sigma_{t_n}^k(t)\,F_{0_n}^k(t) + \sum_{n\subset g} F_{0_n}^{*k}\,\frac{1}{V_{0_n}}\left[\frac{\partial}{\partial t}\,F_{0_n}^k(t)\right] \tag{5.2}$$

Table 5.12 Summary of four methods for computing few-group temperature feedback coefficients

| | 23-group data for reference temp. $T_0$ ( $\Sigma_{\alpha_n}$ ) | Method | 23-group data for elevated temp. $T_1$ ( $\hat{\Sigma}_{\alpha_n}$ ) |
|---|---|---|---|
| Conventional Weighting for group-g | $\Sigma_{\alpha_g} = \sum_{n \subset g} \Sigma_{\alpha_n} F_n$ | 1 | $\hat{\Sigma}_{\alpha_g} = \sum_{n \subset g} \hat{\Sigma}_{\alpha_n} \hat{F}_n$ |
| | | 2 | $\hat{\Sigma}_{\alpha_g} = \sum_{n \subset g} \hat{\Sigma}_{\alpha_n} F_n$ |
| Bilinear Weighting for group-g | $\Sigma_{\alpha_g} = \sum_{n \subset g} F_n^* \Sigma_{\alpha_n} F_n$ | 3 | $\hat{\Sigma}_{\alpha_g} = \sum_{n \subset g} F_n^* \hat{\Sigma}_{\alpha_n} \hat{F}_n$ |
| | | 4 | $\hat{\Sigma}_{\alpha_g} = \sum_{n \subset g} F_n^* \hat{\Sigma}_{\alpha_n} F_n$ |
| Temperature Coefficient for $\Sigma_{\alpha_g}$, $\alpha$ | $\alpha(\Sigma_{\alpha_g}) = \dfrac{(\hat{\Sigma}_{\alpha_g} - \Sigma_{\alpha_g})}{(T_1 - T_0)}$ | | |

$F_n$ : multi-group real spectra at temperature $T_0$

$F_n^*$ : multi-group adjoint spectra at temperature $T_0$

$\hat{F}_n$ : multi-group real spectra at temperature $T_1$

$\hat{F}_n^*$ : multi-group adjoint spectra at temperature $T_1$

Because there is no change of spectra in the steady state, the definition for the unperturbed condition (at temperature $T_0$) is

$$\Sigma_{t_g}^{k}(T_0) = \sum_{n \subset g} F_{o_n}^{*k} \Sigma_{t_n}^{k}(T_0) \; F_{o_n}^{k}(T_0) \tag{5.3}$$

When the temperature has been changed, flux spectra were also changed. Now, we can define the few-group total cross section at temperature $T_1$ as

$$\begin{aligned} \tilde{\Sigma}_{t_g}^{k}(T_1) &= \hat{\Sigma}_{t_g}^{k}(T_1) + \Omega_g \\ &= \sum_{n \subset g} F_{o_n}^{*k} \Sigma_{t_n}^{k}(T_1) \; F_{o_n}^{k}(T_1) \\ &\quad + \sum_{n \subset g} F_{o_n}^{*k} \frac{1}{V_{o_n}} \left[ \frac{\partial}{\partial t} F_{o_n}^{k}(T_1) \right] \end{aligned} \tag{5.4}$$

Using the definition in Table (5.12), we may write the corrected temperature coefficients as

$$\begin{aligned} \tilde{\alpha}^{k}(\Sigma_{t_g}) &= \frac{\hat{\Sigma}_{t_g}^{k}(T_1) - \Sigma_{t_g}^{k}(T_0)}{(T_1 - T_0)} + \frac{1}{\Delta T} \Omega_g \\ &= \alpha^{k}(\Sigma_{t_g}) + \frac{1}{\Delta T} \Omega_g \end{aligned} \tag{5.5}$$

Here, the time derivative of flux spectrum can be expressed as the derivative with respect to the temperature times the derivative of temperature with respect to time.

$$\left[\frac{\partial}{\partial t} F_{0_n}^{k}(T_1)\right] = \lim_{\Delta t \to 0} \left(\frac{\Delta F_{0_n}^{k}(T_1)}{\Delta t}\right) \simeq \lim_{\Delta t \to 0} \left(\frac{\Delta T}{\Delta t}\right)\left(\frac{\Delta F_{0_n}^{k}(T_1)}{\Delta T}\right) \qquad (5.6)$$

Therefore, we may write the correction term $\Omega_g$ as

$$\Omega_g = \left(\lim_{\Delta t \to 0} \frac{\Delta T}{\Delta t}\right) \left\{ \sum_{n \subset g} F_{0_n}^{*k} \frac{1}{V_{0_n}} \left[\frac{F_{0_n}^{k}(T_1) - F_{0_n}^{k}(T_0)}{(T_1 - T_0)}\right] \right\} \qquad (5.7)$$

This correction term has been shown to be very small as compared with the temperature coefficient $\alpha^{k}(\Sigma_{t_g})$. Therefore, we may omit it from the estimation of temperature coefficients.

### 5.3.3 The Homogeneous Bare Reactor Problems

Again, a homogeneous reactor was used for the first tests of the accuracy of a two-group model as compared with a 23-group model. The description of the test problems is given in Appendix A5.3. These problems were solved with a time step size of 0.02 sec. and a node mesh size of 4.06826 cm. The size of reactor was determined by the critical materials bucking.

Table (5.14) shows the predicted behavior of a few-group model vs. a multi-group model for a transient initiated by the drop (in one second) of a rod bank. Artificially, to simulate the rod drop, multi-group absorption cross sections were set to 1.0 $cm^{-1}$ for all twenty three groups. Table (5.13) provides the calculated two-group perturbations obtained by the four estimation procedures. Methods 1 through 4 are the same as those described in Table (5.2). As expected, only method 2 reproduced the same absorption cross sections for few groups.

Table 5.13 Estimated two-group perturbations for the homogeneous reactor problem

| Method* | group | $\Delta \Sigma_a$ | $\Delta \Sigma_{tr}$ | $\Delta \nu\Sigma_f$ | $\Delta \Sigma_f$ |
|---|---|---|---|---|---|
| C.W. 1 | 1 | 0.9937 | -0.001858 | -0.004296 | -0.001651 |
| | 2 | 0.9825 | -0.1707 | -0.02356 | -0.009741 |
| C.W. 2 | 1 | 1.0 | 0.0 | 0.0 | 0.0 |
| | 2 | 1.0 | 0.0 | 0.0 | 0.0 |
| B.W. 3 | 1 | 0.8844 | 0.007641 | -0.004296 | -0.001651 |
| | 2 | 0.9793 | -0.1702 | -0.02356 | -0.009741 |
| B.W. 4 | 1 | 0.9368 | 0.0 | 0.0 | 0.0 |
| | 2 | 0.9993 | 0.0 | 0.0 | 0.0 |

* Perturbation evaluation method

Method 1 : C.W. with perturbed real spectra
2 : C.W. with unperturbed real spectra
3 : B.W. with unperturbed adjoint spectra and perturbed real spectra
4 : B.W. with unperturbed adjoint spectra and unperturbed real spectra

Table 5.14 Predicted reactor power changes due to a control rod bank insertion for a homogeneous bare reactor (without thermal feedback)

| | 23 -group | C.W.* 1 2 - group | C.W.* 2 2 - group | B.W.** 3 2 - group | B.W.** 4 2 - group |
|---|---|---|---|---|---|
| Initial k-eff | 0.9998174 | 0.9998220 (0.00046%) | 0.9998220 (0.00046%) | 0.9998176 (0.00002%) | 0.9998176 (0.00002%) |
| Transient Power (Wt) | | | | | |
| 0.00 sec | 1000.000 | 1000.000 | 1000.000 | 1000.000 | 1000.000 |
| 0.02 sec | 660.0813 | 656.1016 (-0.603 %) | 658.0479 (-0.308 %) | 656.1896 (-0.590 %) | 651.6496 (-1.277 %) |
| 0.04 sec | 568.4490 | 564.6591 (-0.667 %) | 567.6227 (-0.145 %) | 563.5841 (-0.856 %) | 559.8849 (-1.507 %) |
| 0.1 sec | 280.4836 | 282.2112 ( 0.616 %) | 283.5767 ( 1.103 %) | 278.3099 (-0.775 %) | 277.3395 (-1.121 %) |
| 0.2 sec | 111.7631 | 112.9891 ( 1.097 %) | 113.4210 ( 1.483 %) | 110.6035 (-1.038 %) | 110.3697 (-1.247 %) |
| 0.3 sec | 52.27568 | 52.68035 ( 0.774 %) | 52.88340 ( 1.163 %) | 51.44155 (-1.596 %) | 51.36197 (-1.748 %) |
| 0.5 sec | 11.11057 | 10.99070 (-1.079 %) | 11.05838 (-0.470 %) | 10.72035 (-3.512 %) | 10.72173 (-3.500 %) |
| 1.0 sec | 3.0686E-03 | 8.1607E-03 ( 165.9 %) | 3.0690E-02 ( 900.1 %) | 8.1951E-03 ( 167.1 %) | 2.9284E-02 ( 854.3 %) |
| 1.5 sec | 2.7624E-03 | 7.3429E-03 ( 165.8 %) | 2.7615E-02 ( 899.7 %) | 7.3741E-03 ( 166.9 %) | 2.6351E-02 ( 853.9 %) |

* C.W. ; (Flux only) Conventionally Weighted
** B.W. ; (Flux and Adjoint-Flux) Bilinearly Weighted

As shown in Table (5.14), all of the few-group models predict the transient behavior almost as well as the multi-group model. Errors shown after 1.0 sec. had little meaning since the power level has dropped a factor of ~ $10^{-6}$ at that time. For the power changes before 1.0 sec., the conventionally weighted few-group models predict better than the bilinearly weighted models. However, there are no substantial differences among the four methods. Evidently two-group models can deal better with multi-group energy spectrum effects than can a one-group model with two-group effects.

Similar results were found for a second transient case which was very slow and initiated by a different perturbation. Table (5.15) shows results of an inlet-coolant-temperature drop transient. A resultant drop in average coolant temperature ( 2.9 $^{0}$K in 5.0 sec.) provided the reactor with positive reactivity insertion resulting an increase in power (37 % increase in 5.0 sec.) and average fuel temperature (4.4 $^{0}$K in 5.0 sec.). Bilinearly weighted two-group cross sections predicted initial criticality more precisely than conventionally weighted cross sections, and Method 4 gave the best prediction of transient behavior. However, here, Method 1 is more accurate than Method 3 although both showed acceptable accuracy. Thus, we no longer have a situation in which the bilinear weighting is consistently superior. Method 2 is consistently poor for both this and the previous test problem.

Table 5.15 Predicted reactor power changes due to an inlet coolant temperature drop for a homogeneous bare reactor

$$T_{inlet} = 533 - 1.0 \times time\ (^{o}K)$$

| | 23-group | C.W.* 1 2-group | C.W.* 2 2-group | B.W.** 3 2-group | B.W.** 4 2-group |
|---|---|---|---|---|---|
| Initial k-eff | 0.9992971 | 0.9993274 (0.0030 %) | 0.9993886 (0.0092 %) | 0.9993106 (0.0014 %) | 0.9993162 (0.0019 %) |
| Power at (watt) | | | | | |
| 0.0 sec | 1000.000 | 1000.000 | 1000.000 | 1000.000 | 1000.000 |
| 1.0 sec | 1026.899 | 1027.589 ( 0.067 %) | 1018.701 (-0.798 %) | 1028.429 ( 0.149 %) | 1027.213 ( 0.031 %) |
| 2.0 sec | 1100.758 | 1103.652 ( 0.263 %) | 1067.015 (-3.065 %) | 1106.700 ( 0.540 %) | 1101.323 ( 0.051 %) |
| 3.0 sec | 1186.935 | 1192.359 ( 0.457 %) | 1125.771 (-5.153 %) | 1197.603 ( 0.899 %) | 1188.061 ( 0.095 %) |
| 4.0 sec | 1277.297 | 1285.384 ( 0.633 %) | 1190.183 (-6.820 %) | 1292.285 ( 1.173 %) | 1279.112 ( 0.142 %) |
| 5.0 sec | 1368.737 | 1379.450 ( 0.783 %) | 1258.859 (-8.028 %) | 1387.361 ( 1.361 %) | 1371.357 ( 0.191 %) |

* C.W. : (Flux only) Conventionally Weighted
** B.W. : (Flux and Adjoint-Flux) Bilinearly Weighted

### 5.3.4 A Two-Region Unreflected Reactor Problem

With this problem (completely described in Appendix A5.4), we deal with a reactor geometry which has a material discontinuity as well as complex temperature feedback effects. The problem was solved with a time step size of 0.02 sec. and a node mesh size of 5 cm. Four different methods for the estimation of feedback coefficients were again tested. (Calculated values can be found in Appendix 7.)

Table (5.16) shows the predicted transient behavior for this test problem. The inlet-coolant-temperature was dropped in a parabolic fashion for 1.6 seconds. Because of the slow heat transfer rate in the fuel, fuel temperatures increased monotonically and the fuel temperature feedback and moderator temperature feedback worked in opposite directions during the 1.6 second time period. The most accurate method for this test was the conventional weighting model employing the perturbed regular flux spectrum (method 1). However, the bilinear weighting model (method 3) showed almost the same results. Method 2 was again the worst case with much larger errors than the others.

Table 5.16 Predicted reactor power changes due to an inlet coolant temperature variation for a 2-region bare reactor

$$T_{inlet} = 533 - 16 \times time + 10 \times (time)^2 \quad (^{o}K)$$

| | 23-group | C.W.* 1 2-group | C.W.* 2 2-group | B.W.** 3 2-group | B.W.** 4 2-group |
|---|---|---|---|---|---|
| Initial k-eff | 1.115511 | 1.113042 (-0.221 %) | 1.113062 (-0.220 %) | 1.117620 ( 0.189 %) | 1.117463 ( 0.175 %) |
| Power at (MWt.) | | | | | |
| 0.0 sec | 100.0000 | 100.0000 | 100.0000 | 100.0000 | 100.0000 |
| 0.2 sec | 119.4067 | 119.7447 ( 0.283 %) | 113.7756 (-4.716 %) | 120.1353 ( 0.610 %) | 121.7032 ( 1.923 %) |
| 0.4 sec | 156.7846 | 158.5741 ( 1.141 %) | 136.6556 (-12.84 %) | 159.8090 ( 1.929 %) | 166.2058 ( 6.009 %) |
| 0.6 sec | 190.9679 | 194.6001 ( 1.902 %) | 155.7966 (-18.42 %) | 196.6414 ( 2.971 %) | 208.0675 ( 8.954 %) |
| 0.8 sec | 204.1706 | 208.7107 ( 2.224 %) | 164.7073 (-19.33 %) | 210.6937 ( 3.195 %) | 221.9410 ( 8.704 %) |
| 1.0 sec | 191.9919 | 195.7262 ( 1.945 %) | 160.8408 (-16.23 %) | 196.9248 ( 2.569 %) | 203.7094 ( 6.103 %) |
| 1.2 sec | 164.7855 | 167.0611 ( 1.381 %) | 146.7455 (-10.95 %) | 167.4711 ( 1.630 %) | 169.9427 ( 3.130 %) |
| 1.4 sec | 133.7129 | 134.7861 ( 0.803 %) | 127.1730 (-4.891 %) | 134.6850 ( 0.727 %) | 134.5013 ( 0.590 %) |
| 1.6 sec | 104.9536 | 105.3146 ( 0.344 %) | 106.2381 ( 1.224 %) | 104.9584 ( 0.005 %) | 103.5086 (-1.377 %) |

* C.W. : (Flux only) Conventionally Weighted
** B.W. : (Flux and Adjoint-Flux) Bilinearly Weighted

### 5.3.5 Four-Region Reactor Problems

With this problem we deal with a more realistic reactor geometry with reflectors at the bottom and top of the core. The reactor core consists of two homogenized fuel regions one of which contains burnable poison rods. A complete description of this problem can be found in Appendix A5.5. For this reactor, two transient problems were examined.

Table (5.17) shows the results of a control rod bank withdrawal. Withdrawal of control rods (at a speed of 1 cm/sec. from the center of the core) was simulated by the same method used in Section 5.2.5. Perturbations were effected by replacing the fuel composition CLOREF with the fuel composition COOREF (CLOREF has lower reactivity than COOREF because of the presence of burnable poisons). The reference 23-group calculation was performed by moving the material interface upwards. However, the weighted two-group calculation can not be simulated in this manner. Withdrawal of a control rod bank was simulated as a perturbed fuel composition (fuel COOREF at a lower half region of the core) being introduced into an unperturbed fuel region (a upper half region of fuel CLOREF). Therefore, we have a choice of using any of the methods described in Table (5.2). There, an "unperturbed composition" was regarded as the fuel composition CLOREF and a "perturbed composition" was regarded as the fuel composition COOREF. A simple replacement of the initial two-group cross sections for the rodded composition by those of the unrodded composition was not accurate for the bilinear weighting. (This replacement corresponds to Method 1 for the conventional weighting scheme and to Method 5 for the bilinear weighting scheme.) As we found

earlier (Table 5.4), a simple replacement of bilinearly weighted two-group cross sections (Method 5) led to an large error in prediction of transient behavior. The error in predicted power (not shown in any tables) was -22.4 % at 3.0 sec.

Table (5.18) shows the perturbations which result from the weighting methods listed in Table (5.2). These were used for the transient results of Table (5.17). As shown in Table (5.17), the bilinearly weighted parameters produce more accurate results than the conventionally weighted parameters. Method 2 remains the worst case. However, Method 4 is here better than 3.

Table 5.17 Predicted reactor power changes due to a control rod bank removal for a 4-region reactor with reflectors (without thermal feedback)

rod removal speed = 1 cm/sec

| | 23 -group | C.W.* 1 2 - group | C.W.* 2 2 - group | B.W.** 3 2 - group | B.W.** 4 2 - group |
|---|---|---|---|---|---|
| Initial k-eff | 1.157756 | 1.154939 (-0.243 %) | 1.154939 (-0.243 %) | 1.160787 ( 0.262 %) | 1.160787 ( 0.262 %) |
| Transient Power (MWt) | | | | | |
| 0.0 sec | 100.0000 | 100.0000 | 100.0000 | 100.0000 | 100.0000 |
| 0.5 sec | 110.0039 | 109.9081 (-0.087 %) | 109.7485 (-2.232 %) | 110.2119 ( 0.189 %) | 109.9887 (-0.014 %) |
| 1.0 sec | 124.3440 | 124.0278 (-0.254 %) | 123.6315 (-0.573 %) | 124.8540 ( 0.410 %) | 124.2823 (-0.050 %) |
| 1.5 sec | 144.8936 | 144.1440 (-0.517 %) | 143.3868 (-1.040 %) | 145.8893 ( 0.687 %) | 144.7555 (-0.095 %) |
| 2.0 sec | 175.4051 | 173.7786 (-0.927 %) | 172.4400 (-1.690 %) | 177.2325 ( 1.042 %) | 175.1340 (-0.155 %) |
| 2.5 sec | 223.4070 | 219.8914 (-1.574 %) | 217.5416 (-2.625 %) | 226.7882 ( 1.513 %) | 222.8852 (-0.234 %) |
| 3.0 sec | 305.7446 | 297.7067 (-2.629 %) | 293.4070 (-4.035 %) | 312.3971 ( 2.176 %) | 304.6900 (-0.345 %) |

* C.W. ; (Flux only) Conventionally Weighted
** B.W. ; (Flux and Adjoint-Flux) Bilinearly Weighted

Table 5.18 Estimated two-group perturbations for the control rod bank removal in the four-region reactor problem

| Method* | group | $\Delta \Sigma_a$ | $\Delta \Sigma_{tr}$ | $\Delta \nu\Sigma_f$ | $\Delta \Sigma_f$ |
|---|---|---|---|---|---|
| C.W. 1 | 1 | -8.2904E-05 | -5.1567E-04 | 3.6596E-04 | 1.4216E-04 |
| | 2 | -6.6082E-03 | -3.1748E-03 | 8.3318E-03 | 3.4446E-03 |
| C.W. 2 | 1 | 7.6500E-05 | 4.3660E-04 | 4.3878E-04 | 1.7285E-04 |
| | 2 | -7.1658E-03 | -7.8469E-03 | 7.4897E-03 | 3.0965E-03 |
| B.W. 3 | 1 | -1.0831E-04 | -3.8610E-04 | 3.6596E-04 | 1.4216E-04 |
| | 2 | -6.5550E-03 | -3.2661E-03 | 8.3318E-03 | 3.4446E-03 |
| B.W. 4 | 1 | 2.5128E-05 | 4.9220E-04 | 4.3878E-04 | 1.7285E-04 |
| | 2 | -7.1571E-03 | -7.8727E-03 | 7.4897E-03 | 3.0965E-03 |

| Method* | group | $\Delta \Sigma_{s_{g,1}}$ | $\Delta \Sigma_{s_{g,2}}$ | $\Delta \nu_g$ |
|---|---|---|---|---|
| C.W. 1 | 1 | -1.8835E-03 | -6.8235E-05 | 3.7088E+05 |
| | 2 | -3.6995E-04 | 9.6200E-04 | -2.6534E+03 |
| C.W. 2 | 1 | 8.5710E-04 | 5.7490E-06 | -10.0 |
| | 2 | -2.9890E-05 | -3.5980E-03 | -0.3 |
| B.W. 3 | 1 | -2.2135E-03 | -8.0157E-05 | 3.3838E+05 |
| | 2 | -3.6750E-04 | 1.0230E-03 | -2.6800E+03 |
| B.W. 4 | 1 | 8.6330E-04 | 6.7540E-06 | -10.0 |
| | 2 | -2.9670E-05 | -3.6140E-03 | -0.3 |

* Perturbation evaluation method

Method 1 : C.W. with perturbed real spectra
2 : C.W. with unperturbed real spectra
3 : B.W. with unperturbed adjoint spectra and perturbed real spectra
4 : B.W. with unperturbed adjoint spectra and unperturbed real spectra

The final test problem involved a temperature feedback transient in this four region reactor. Table (5.19) shows the results of an inlet-coolant-temperature drop transient. Here, Method 1 gives the best prediction although it is almost same as Method 3. As for the best, there were another inconsistent results between methods 3 and 4 as well as between conventional weighting and bilinear weighting.

The most consistent finding in this chapter is that Method 2, based on a flat adjoint energy shape and unperturbed weighting spectra, yields unacceptably large errors. The other important finding for these multi-group transient tests is that conventionally weighted two-group parameters (based on perturbed spectra) do not produce large errors in the prediction of reactor power (always less than 3 %) even for severe transients.

Table 5.19 Predicted reactor power changes due to an inlet coolant temperature drop for a 4-region reactor with reflectors

$$T_{inlet} = 533 - 1.0 \times time \quad (^0K)$$

| | 23-group | C.W.* 1 2-group | C.W.* 2 2-group | B.W.** 3 2-group | B.W.** 4 2-group |
|---|---|---|---|---|---|
| Initial k-eff | 1.154104 | 1.151535 (-0.223 %) | 1.151347 (-0.239 %) | 1.157057 ( 0.257 %) | 1.156787 ( 0.232 %) |
| Power at (MWt.) | | | | | |
| 0.0 sec | 100.0000 | 100.0000 | 100.0000 | 100.0000 | 100.0000 |
| 2.0 sec | 113.7658 | 114.4816 ( 0.629 %) | 109.4544 (-3.790 %) | 114.7917 ( 0.902 %) | 116.4168 ( 2.330 %) |
| 4.0 sec | 124.8574 | 126.3873 ( 1.225 %) | 117.5138 (-5.882 %) | 126.7844 ( 1.543 %) | 128.9911 ( 3.311 %) |
| 6.0 sec | 133.3730 | 135.6143 ( 1.680 %) | 124.0137 (-7.017 %) | 136.0237 ( 1.987 %) | 138.4235 ( 3.787 %) |
| 8.0 sec | 140.8884 | 143.7804 ( 2.053 %) | 129.7400 (-7.913 %) | 144.2311 ( 2.373 %) | 146.8824 ( 4.254 %) |
| 10. sec | 148.1061 | 151.6585 ( 2.399 %) | 135.1444 (-8.752 %) | 152.1685 ( 2.743 %) | 155.1485 ( 4.755 %) |

* C.W. ; (Flux only) Conventionally Weighted
** B.W. ; (Flux and Adjoint-Flux) Bilinearly Weighted

### 5.3.6 Comments on the Predicted Power Shapes

Since the bilinearly weighted cross sections are very different from conventionally weighted cross sections, all the various reaction rates for a node (absorption reaction rate, fission neutron production rate, etc.) are predicted differently by the two weighting schemes. (See Section 5.3.1.) For this reason, spatial power distributions should also be predicted differently.

Tables (5.20) through (5.23) show the errors in predicted axial power shapes for four different transient problems. (The same transient problems as in Tables (5.15), (5.16), (5.17) and (5.19) respectively.) From all tables, it is hard to find a consistency of superiority among the four methods. However, Method 2 is always inferior to all others in predicting axial power shape. Generally, bilinear weighting schemes (Method 3 and Method 4) produced smaller errors in high power regions, whereas conventional weighting schemes (Method 1) produced smaller errors in low power regions and at reflector boundaries.

Table 5.20 Predicted axial power shape changes due to an inlet coolant temperature drop for a homogeneous bare reactor

$T_{inlet} = 533 - 1.0 \times time\ (^{o}K)$

| | 23-group | C.W.* 1 2-group | C.W.* 2 2-group | B.W.** 3 2-group | B.W.** 4 2-group |
|---|---|---|---|---|---|
| Initial k-eff | 0.9992971 | 0.9993274 (0.0030 %) | 0.9993886 (0.0092 %) | 0.9993106 (0.0014 %) | 0.9993162 (0.0019 %) |
| Normalized Power shape node # | | | | | |
| Top 20 | 0.116299 | -0.120 % | 1.06 % | -0.125 % | 0.471 % |
| 18 | 0.569359 | -0.115 % | 0.994 % | -0.119 % | 0.447 % |
| 13 | 1.41635 | -0.058 % | 0.447 % | -0.059 % | 0.206 % |
| 8 | 1.48094 | 0.045 % | -0.383 % | 0.046 % | -0.172 % |
| 3 | 0.634169 | 0.133 % | -1.012 % | 0.136 % | -0.468 % |
| Bottom 1 | 0.130654 | 0.148 % | -1.108 % | 0.152 % | -0.518 % |
| Power at 2.0 sec (watts) | 1100.758 | 1103.652 ( 0.263 %) | 1067.015 (-3.065 %) | 1106.700 ( 0.540 %) | 1101.323 ( 0.051 %) |
| Normalized Power shape at 2.0 sec node # | | | | | |
| Top 20 | 0.115849 | -0.134 % | 1.133 % | -0.139 % | 0.502 % |
| 18 | 0.567409 | -0.129 % | 1.062 % | -0.134 % | 0.471 % |
| 13 | 1.41423 | -0.066 % | 0.481 % | -0.069 % | 0.216 % |
| 8 | 1.48260 | 0.050 % | -0.404 % | 0.052 % | -0.178 % |
| 3 | 0.636674 | 0.150 % | -1.093 % | 0.155 % | -0.496 % |
| Bottom 1 | 0.131287 | 0.166 % | -1.208 % | 0.172 % | -0.559 % |

* C.W. : (Flux only) Conventionally Weighted
** B.W. : (Flux and Adjoint-Flux) Bilinearly Weighted

Table 5.21 Predicted axial power shapes for a 2-region bare reactor with thermal-hydraulic feedback

| | 23-group | C.W.* 1 2-group | C.W.* 2 2-group | B.W.** 3 2-group | B.W.** 4 2-group |
|---|---|---|---|---|---|
| Initial k-eff | 1.115511 | 1.113042 (-0.221 %) | 1.113062 (-0.220 %) | 1.117620 ( 0.189 %) | 1.117463 ( 0.175 %) |
| Normalized Power shape node # | | | | | |
| Top 20 | 0.0624343 | 1.302 % | 2.167 % | -0.312 % | -0.189 % |
| 18 | 0.314205 | 1.216 % | 2.066 % | -0.339 % | -0.188 % |
| 13 | 1.00463 | 0.562 % | 1.087 % | -0.533 % | -0.385 % |
| 8 | 1.83607 | -0.242 % | -0.274 % | 0.114 % | 0.162 % |
| 3 | 0.960000 | -0.580 % | -1.434 % | 0.612 % | 0.269 % |
| Bottom 1 | 0.202722 | -0.598 % | -1.688 % | 0.682 % | 0.179 % |

* C.W. : (Flux only) Conventionally Weighted
** B.W. : (Flux and Adjoint-Flux) Bilinearly Weighted

Table 5.22 Predicted axial power shape changes due to a control rod bank removal for a 4-region reactor with reflectors (without thermal feedback)

rod removal speed = 1 cm/sec

| | 23 -group | C.W.* 1 2 - group | C.W.* 2 2 - group | B.W.** 3 2 - group | B.W.** 4 2 - group |
|---|---|---|---|---|---|
| Initial k-eff | 1.157756 | 1.154939 (-0.243 %) | 1.154939 (-0.243 %) | 1.160787 ( 0.262 %) | 1.160787 ( 0.262 %) |
| Normalized Power shape node # | | | | | |
| Top 26 | 0.152204 | 0.850 % | 0.850 % | -5.608 % | -5.608 % |
| 21 | 0.483451 | 2.783 % | 2.783 % | 1.450 % | 1.450 % |
| 16 | 1.13333 | 1.183 % | 1.183 % | 1.102 % | 1.102 % |
| 13 | 1.89212 | -0.198 % | -0.198 % | 0.838 % | 0.838 % |
| 8 | 1.98748 | -0.839 % | -0.839 % | 0.198 % | 0.198 % |
| Bottom 3 | 0.931842 | -3.532 % | -3.532 % | -10.266 % | -10.266 % |
| Power at 2.0 sec ( MWt) | 175.4047 | 173.7783 (-0.927 %) | 172.4397 (-1.690 %) | 177.2325 ( 1.042 %) | 175.1341 (-0.154 %) |
| Normalized Power shape at 2.0 sec node # | | | | | |
| Top 26 | 0.153971 | 0.695 % | 0.627 % | -5.687 % | -5.754 % |
| 21 | 0.492260 | 2.636 % | 2.559 % | 1.359 % | 1.276 % |
| 16 | 1.16909 | 1.166 % | 1.231 % | 1.119 % | 1.175 % |
| 13 | 1.90475 | -0.173 % | -0.209 % | 0.852 % | 0.808 % |
| 8 | 1.95038 | -0.807 % | -0.815 % | 0.206 % | 0.204 % |
| Bottom 3 | 0.906872 | -3.487 % | -3.486 % | -10.235 % | -10.224 % |

* C.W. ; (Flux only) Conventionally Weighted
** B.W. ; (Flux and Adjoint-Flux) Bilinearly Weighted

Table 5.23 Predicted axial power shapes
for a 4-region reactor with reflectors
with thermal-hydraulic feedback

| | 23-group | C.W.* 1 2-group | C.W.* 2 2-group | B.W.** 3 2-group | B.W.** 4 2-group |
|---|---|---|---|---|---|
| Initial k-eff | **1.154104** | **1.151535** (-0.223 %) | **1.151347** (-0.239 %) | **1.157057** ( 0.256 %) | **1.156787** ( 0.232 %) |
| Normalized Power shape node # | | | | | |
| Top 26 | 0.1580193 | -0.090 % | 1.068 % | -6.321 % | -6.254 % |
| 21 | 0.488992 | 2.235 % | 3.188 % | 1.046 % | 1.129 % |
| 16 | 1.11818 | 0.994 % | 1.501 % | 0.967 % | 1.025 % |
| 13 | 1.85639 | -0.198 % | 0.086 % | 0.828 % | 0.927 % |
| 8 | 1.99663 | -0.669 % | -1.060 % | 0.367 % | 0.322 % |
| Bottom 3 | 0.960283 | -3.136 % | -4.098 % | -9.887 % | -10.073 % |

* C.W. ; (Flux only) Conventionally Weighted
** B.W. ; (Flux and Adjoint-Flux) Bilinearly Weighted

# Chapter 6

## CONCLUSIONS AND RECOMMENDATIONS

### 6.1 OVERVIEW OF THE INVESTIGATION

The objective of this investigation was to determine by direct comparison of predicted transient behavior compared with multi-group P-1 results the accuracy of two weighting schemes for few-group parameters: conventionally weighted and bilinearly weighted. From the viewpoint of the variational principle from which the few group model were derived in this thesis, the bilinear weighting method has more theoretical justification.

In Chapter 2, definitions of bilinearly weighted few-group cross sections were derived systematically using a variational principle. This derivation was carried out by applying Buslik's functional [B-1] which is made statinary by the time-dependent P-1 equations and their adjoint. Conventional definitions of diffusion parameters were found as a special case of bilinearly weighted cross sections.

The differences of these two weighting schemes as applied to transient analysis were determined using a consistent nodal calculation. First, twenty-three-group cross sections were collapsed into two-group cross sections by the spectrum code, MESADES. Next, both sets of cross sections (multi-group, conventionally weighted two-group and bilinearly weighted two-group) were employed to predict transient behavior using the nodal code, OMNI-T.

In Chapter 3, a method for computing real and adjoint spectra was introduced. The numerical schemes used for the code MESADES were described in detail. Test problems showed that MESADES is valid for spectrum calculations and the subsequent calculation of few-group parameters.

In Chapter 4, one-dimensional nodal transient equations were derived using the assumption that spatial flux shapes within a node are quadratic functions fitted to the node-average flux and two surface fluxes. Detailed numerical schemes were also introduced. Validation of the nodal code OMNI-T was established by comparisons of two-group results with analytical solutions and with the results of QUANDRY. OMNI-T was shown to produce accurate prediction of reactor criticality and group fluxes at steady state (with maximum errors in node average fluxes of approximately 0.3 % for a 1 cm mesh spacing). It also predicts accurate power levels for transients involving temperature feedback and control rod movements (with maximum errors in power level of 0.18 %).

Finally, Chapter 5 was devoted to the comparisons of transient behavior predicted by the two different weighted few-group models. Errors in predicted power levels compared with multi-group results were measured for various test cases. Various methods for generating few-group perturbations and temperature coefficients based on the different choices of adjoint flux spectrum and real flux spectrum were examined.

Results of the entire investigation and conclusions derived from these results are summarized in Section 6.2. Finally, recommendations for future study are made in Section 6.3.

## 6.2 SUMMARY OF RESULTS, CONCLUSIONS

A variational principle made stationary by the multi-group P-1 equations provided a systematic derivation of few-group P-1 equations as well as the definitions of their parameters. This application resulted in additional group-parameters, $V_g^{-1}\omega_{0g}(t)$, defined for both bilinearly weighted cross sections and conventionally weighted cross sections (See Eq. 2.20 and 2.29). The importance of these additional terms, which have the effect of altering the total macroscopic cross section was examined for transient solutions. By comparison of predicted power levels, it was proved that the correction, $V_g^{-1}\omega_{0g}(t)$, has a negligible effect on transient solutions. Therefore, we can neglect the additional parameter, $\omega_{0g}(t)$.

Of the six methods studied for generating few-group cross sections and temperature coefficients, only those using time-constant adjoint spectra weighting gave reasonable results. This implies that, for the estimation of few-group cross sections, if a perturbed adjoint spectra is being used as weight function, the same weight function should be used for the initial steady state reference condition. Of these constant adjoint spectra weighting methods, unperturbed adjoint spectra weighting usually gave better results than perturbed adjoint weighting.

Of the two methods examined for the conventionally weighted few-group perturbations, the use of unperturbed real spectra led to consistently inferior results.

Comparisons of one-group transient solutions with two-group reference solutions showed that failure to weight with the adjoint spectra caused unacceptable errors in the prediction of reactor power. Table (6.1) presents a summary of maximum errors in predicted powers.

Table 6.1 Comparison of maximum errors in one-group predictions of total power relative to two-group results

| | C.W. 1 | 2 | B.W. 3 | 4 |
|---|---|---|---|---|
| Step perturbation | -9.4 % | -54. % | 0.25 % | 0.17 % |
| Control rods removal | -9.3 % | -53. % | -0.29 % | 0.11 % |

C.W. : conventionally weighted one-group
B.W. : bilinearly weighted one-group

Perturbation estimation method
Method 1 : C.W. with perturbed real spectra
2 : C.W. with unperturbed real spectra
3 : B.W. with unperturbed adjoint spectra and perturbed real spectra
4 : B.W. with unperturbed adjoint spectra and unperturbed real spectra

For more realistic reactor transient problems, two-group solutions were compared with twenty-three-group solutions. All test problems were severe transients. In every test problem, the conventionally weighted cross sections predicted very accurate results; however the bilinearly weighted cross sections did not yield consistently better results than the

conventionally weighted cross sections. We conclude that these result indicate no pressing need to use bilinearly weighted cross sections for transient analysis. Table (6.2) summarizes the maximum errors in power predicted by two-group models relative to twenty-three-group results.

Table 6.2 Comparison of maximum errors in two-group predictions of total power relative to twenty-three-group results

| | C.W. 1 | 2 | B.W. 3 | 4 |
|---|---|---|---|---|
| Reactor shutdown in homogeneous reactor | -1.079 % | -0.470 % | -3.512 % | -3.500 % |
| $T_{inlet}$ drop in homogeneous reactor | 0.783 % | -8.028 % | 1.361 % | 0.191 % |
| $T_{inlet}$ change in two-region reactor | 2.224 % | -19.33 % | 3.195 % | 8.704 % |
| $T_{inlet}$ drop in four-region reactor | 2.399 % | -8.752 % | 2.743 % | 4.755 % |
| Control rods removal in four-region reactor | -2.629 % | -4.035 % | 2.176 % | -0.345 % |

C.W. : conventionally weighted one-group
B.W. : bilinearly weighted one-group

Perturbation estimation method
Method 1 : C.W. with perturbed real spectra
2 : C.W. with unperturbed real spectra
3 : B.W. with unperturbed adjoint spectra and perturbed real spectra
4 : B.W. with unperturbed adjoint spectra and unperturbed real spectra

## 6.3 RECOMMENDATIONS FOR FUTURE RESEARCH

### 6.3.1 Refinements in Derivation of Few-Group Cross Sections

For this thesis, the Buslik's variational principle was used [B-1]. His trial functions for the fluxes and currents, although discontinuous in a multi-group sense from one material composition to the next, yield continuity of few-group fluxes and currents at internal interfaces. In this regard, the resultant few-group equations having bilinearly weighted cross sections are similar to the regular few-group equations. Although this characteristics is convenient, there may be a loss in accracy. Buslik's scheme requires that the energy shape for group g ($F_{0_n}$; nCg) on an interface between two compositions be the same for all interfaces throughout the reactor. Moreover, in order to preserve the usual meaning of the few-group flux $\phi_g$, that shape has been taken as $F_{0_n}$ = constant; nCg. Yet, on either side of an interface the $F_{0_n}$ have the asymptotic shapes for the compositions on those sides. Thus the Buslik's scheme, while it retain the desired few-group continuity conditions, may do violence to the physics of the problem. This point has not been examined in the present thesis.

In Henry's paper [H-2], an alternative derivation based on a different variational expression yields a few-group theory in which few-group fluxes and currents are discontinuous across material interfaces. Such discontinuous interface boundary conditions complicate

the analysis. However, discontinuity factors have already been implemented in the nodal code OMNI-T. Therefore, it should be possible to examine the alternative bilinear weighting scheme. This should be done.

### 6.3.2 Application to the Other Reactors

The superiority of the bilinearly weighted cross sections to the conventionally weighted cross sections was unambiguous when one-group equations were derived from two-group equations. However, bilinearly weighted two-group parameters were not always superior to conventionally weighted parameters when derived from twenty-three-group parameters. This inconsistency may be due to the fact that the adjoint spectra shapes for the twenty-three-group cases are fairly flat in energy. (See Figures 5.1 and 5.2.) If so, adjoint weighting will not change the ultimate two-group results.

However, all the reactor models investigated in this thesis were for PWR's. Different reactor designs (such as FBR's, HTGR's, etc.) using different materials will have different adjoint and real spectra, and the characteristics of bilinear weighting may be different for each type of reactor. Thus, bilinear weighting should be tested for other types of reactors.

Also, since bilinear weighting seems to help if the number of groups in the reference model is small, the possibility of using fewer groups for multi-group spectrum codes but collapsing by bilinear weighting should be examined.

### 6.3.3 Application to the Safety Analysis

In this thesis, bilinearly weighted cross sections consistently predicted criticality more accurately. (although errors using the standard procedure were found to be quite acceptable.) However, conventional weighting was found to be generally superior for analyzing the operational transients in PWRs. This situation could be different for super-prompt-critical transient problems which are the major concern in design accident analysis. In those transients, the neglected term $\omega_{0_g}(t)$ would be important. Therefore, the investigation of few-group cross sections should be extended to the problems of safety analyses.

### 6.3.4 Test on the Linearity of Few-Group Cross Sections to the Variance of Temperature

In this thesis, all temperature feedbacks were calculated by the linear feedback model which should be valid for small temperature changes. In estimating temperature coefficients, we also assumed linearity of cross sections. Since the twenty-three-group solutions are the reference solutions, for the purposes of numerical testing of few-group schemes, the twenty-three-group cross sections can be assumed to vary in any convenient way (here, as linear). Sinse, calculated real and adjoint spectra did not vary much with change in temperature, we also assumed that the two-group cross sections would be linear with change in temperature.

However, it would be prudent to investigate whether this linear assumption for the few-group parameters is valid. The small variance of

adjoint spectra may lead few-group cross sections to be slightly nonlinear in temperature. If this point was resolved, it would then be possible to ascribe differences in predicted behavior as due entirely to the bilinear vs. standard model and not to some neglected effect which may be of different importance for the two models.

## REFERENCES


B-1 A.J. Buslik, "Interface Conditions for Few-Group Neutron Diffusion Equations with Flux-Adjoint Weighted Constants," Nucl. Sci. Eng., 32, 233-240, (1968).

D-1 K.L. Derstine, "DIF3D: A Code to Solve One-, Two-, and Three-Dimensional Finite-Difference Diffusion Theory Problems," ANL-82-64, (April 1984).

D-2 A.F.V. Dias, "Systematic Derivation, from 3-D Nodal Equations, of Simpler Models for Describing Reactor Transients," Ph.D. Thesis, Department of Nuclear Engineering, M.I.T., Cambridge, Mass., (May 1987).

G-1 R.G. Gamino, "The Development and Application of Supernodal Methods to PWR Analysis," Ph.D. Thesis, Department of Nuclear Engineering, M.I.T., Cambridge, Mass., (May 1986).

H-1 A.F. Henry, Nuclear-Reactor Analysis, M.I.T. Press, Cambridge, Mass., (1975).

H-2 A.F. Henry, "Few-Group Approximations Based on a Variational Principle," Nucl. Sci. Eng., 27, 493-510, (1967).

J-1 H.S. Joo, "Resolution of the Control Rod Cusping Problem for Nodal Methods," Ph.D. Thesis, Department of Nuclear Engineering, M.I.T., Cambridge, Mass., (February 1984).

L-1 W.W. Little and R.W. Hardie, "Methods for Collapsing Fast-Reactor Neutron Cross Sections," Nucl. Sci. Eng., 29, 402-407, (1967).

L-2 R.D. Lawrence, "Progress in Nodal Methods for the Solution of the Neutron Diffusion and Transport Equations," Prog. Nucl. Energy, 17, 3, Pergamon Press, Oxford, England, (1986).

L-3 J. Lewins, "Variational Representations in Reactor Physics Derived from a Physical Principle," Nucl. Sci. Eng., 8, 95-104, (1960).

P-1 T.A. Pitterle and C.W. Maynard, "Bilinear-Averaging for Diffusion-Theory Parameters," Trans. Am. Nucl. Soc., 8, 205, (1965).

S-1 K.S. Smith, "Spatial Homogenization Methods for Light Water Reactor Analysis," Ph.D. Thesis, Department of Nuclear Engineering, M.I.T., Cambridge, Mass., (June 1980).

S-2 K.S. Smith, "An Analytic Nodal Method for Solving the Two-Group, Multidimensional, Static and Transient Neutron Diffusion Equations," SM Thesis, Department of Nuclear Engineering, M.I.T., Cambridge, Mass., (March 1979).

S-3 D.H. Shaftman and H. Greenspan, "An Importance-Weighting Procedure for Averaging Group Parameters in Multigroup Diffusion Theory," Reactor Physics Division Annual Report, ANL-7010, (1964).

S-4 K.S. Smith and K.R. Rempe, personal communications, Studsvik of America, Newton, Mass., (1987).

S-5 T.M. Sutton, "Wielandt Iteration as Applied to the Nodal Expansion Method," Proc. of Topical Meeting on Reactor Physics and Safety, Vol. 1, 215-222, Saratoga Springs, 17-19 September, (1986).

S-6 R.J.J. Stamm'ler and M.J. Abbate, Methods of Steady-State Reactor Physics in Nuclear Design, Academic Press, New York, N.Y., (1983).

V-1 A.V. Vota, N.J. Curlee and A.F. Henry, "WIGL3 - A Problem for the Steady State and Transient Solution of the One-Dimensional, Two-Group, Space-Time Diffusion Equations Accounting for Temperature, Xenon, and Control Feedback," WAPD-TM-788 (February 1969).

## Appendix 1

### TEST PROBLEM FOR THE SPECTRUM CODE MESADES

This test is designed to validate the accuracy of the spectrum code, MESADES which produces real and adjoint spectra from the cross section data. A 3-group problem is created artificially in order to check the accuracy of the spectrum code. An adjoint flux spectrum for a critical reactor composition is selected arbitrarily and the $\Sigma_{t,g}$ values for a 3-group cross section set are chosen to force criticality. The real flux spectrum is calculated from them. One-group cross sections are then found by both the conventional weighting and the bilinear weighting in accord with the definitions in Chapter 2, and these cross sections are inserted into the one-group criticality formula to ensure that they preserve criticality..

The 3-group diffusion theory parameters (except for the $\Sigma_{t,g}$) are taken to be

| group g | $D_g$ | $\nu\Sigma_{f_g}$ | $\chi_g$ | $\Sigma_{s_g}$ |
|---|---|---|---|---|
| 1 | 2.0 | 0.03 | 0.7 | 0.007 |
| 2 | 1.0 | 0.02 | 0.3 | 0.005 |
| 3 | 0.5 | 0.04 | 0.0 | 0.006 |

| $\Sigma_{s_{gg'}}$ g g' | 1 | 2 | 3 |
|---|---|---|---|
| 1 | 0.004 | 0. | 0. |
| 2 | 0.002 | 0.003 | 0.001 |
| 3 | 0.001 | 0.002 | 0.005 |

Using the data given above, values of total cross-sections are found from the critical condition (Eq. (3.22)):

$$( D_n B_m^2 + \Sigma_{t_n} ) \phi_n^* = k_{eff}^{-1} \nu\Sigma_{f_n} \sum_{n'} \chi_{n'} \phi_{n'}^* + \sum_{n'} \Sigma_{s_{n'n}} \phi_{n'}^* \qquad \text{(A1.1)}$$

where subscript n represent an energy group. In this equation the adjoint spectrum and material buckling are arbitrarily taken as:

$$\phi_1^* = 0.2$$
$$\phi_2^* = 0.4 \qquad B_m^2 = 0.001 \ (1/cm^2)$$
$$\phi_3^* = 0.4$$

The total cross-sections required for (A1.1) to be valid are then:

$$\Sigma_{t_1} = 0.0470 \ cm^{-1}$$
$$\Sigma_{t_2} = 0.0170 \ cm^{-1}$$
$$\Sigma_{t_3} = 0.0315 \ cm^{-1}$$

Now, Eq. (3.13) for real flux spectrum is solved:

$$( D_n B_m^2 + \Sigma_{t_n} ) \phi_n = k_{eff}^{-1} \chi_n \sum_{n'} \nu\Sigma_{f_{n'}} \phi_{n'} + \sum_{n'} \Sigma_{s_{nn'}} \phi_{n'} \qquad \text{(A1.2)}$$

The resultant normalized real flux spectrum is:

$\phi_1 = 0.388890$

$\phi_2 = 0.555555$

$\phi_3 = 0.055555$

According to the definitions of Eqs. (2.20) and (2.29), conventionally weighted 1-group diffusion parameters take on the values

$\bar{D} = 1.36111$ $\quad$ $\bar{\Sigma}_t = 0.0294722$

$\bar{\chi} = 1.0$ $\quad$ $\bar{\Sigma}_s = 0.00583333$

$\nu\bar{\Sigma}_f = 0.025$ $\quad$ $\bar{\Sigma}_a = 0.0236389$

and bilinearly weighted 1-group diffusion parameters are:

$\bar{D} = 1.16667$ $\quad$ $\bar{\Sigma}_t = 0.0244$

$\bar{\chi} = 0.78$ $\quad$ $\bar{\Sigma}_s = 0.00606667$

$\nu\bar{\Sigma}_f = 0.025$ $\quad$ $\bar{\Sigma}_a = 0.0183333$

When these two sets of parameters are substituted into the following, both of them reproduce the unity value of $k_{eff}$.

$$k_{eff} = \frac{\bar{\chi}\ \nu\bar{\Sigma}_f}{\bar{D}\ B_m^2 + \bar{\Sigma}_a} \quad \text{or} \quad \frac{\bar{\chi}\ \nu\bar{\Sigma}_f + \bar{\Sigma}_s}{\bar{D}\ B_m^2 + \bar{\Sigma}_t}$$

## Appendix 2

### CASMO-3 OUTPUT FOR THREE FUEL ASSEMBLIES AND WATER REFLECTOR

In this Appendix, twenty-three-group macroscopic cross-section data are given for three fuel assemblies and water. These data have been produced by the computer code CASMO-3 and have been provided to us by Studsvik of America. All macroscopic cross sections are assembly homogenized cross-sections at BOL. For the preparation of temperature feedback coefficients, two set of cross-sections at different temperature (one for fuel and the other for moderator) are also provided [S-4]. A description of four different material compositions are summarized as the following:

| Assembly Name | Branch Index | U-235 w/o | B.P.* | Fuel Temp. °K | Mod. Temp. °K |
|---|---|---|---|---|---|
| CLO | CLOREF | 3.272 | Yes | 900. | 585. |
| | CLOTF | 3.272 | Yes | 1500. | 585. |
| | CLOTM | 3.272 | Yes | 900. | 620. |
| COO | COOREF | 3.274 | No | 900. | 585. |
| | COOTF | 3.274 | No | 1500. | 585. |
| | COOTM | 3.274 | No | 900. | 620. |
| AOO | AOOREF | 1.920 | No | 900. | 585. |
| | AOOTF | 1.920 | No | 1500. | 585. |
| | AOOTM | 1.920 | No | 900. | 620. |
| Water | REFREF | 0.0 | No | 900. | 585. |
| | REFTF | 0.0 | No | 1500. | 585. |
| | REFTM | 0.0 | No | 900. | 620. |

* B.P. : Burnable Poison

Macroscopic cross sections are given in Tables (A2.1) through (A2.12) for $\Sigma_{a_g}$, $\Sigma_{f_g}$, $\nu\Sigma_{f_g}$, $\Sigma_{tr_g}$ and $(\Sigma_{s_0})_{gg'}$. The fission neutron yield ratio $\chi_g$ is given at the end of each table. Collapsed 2-group and 4-group cross sections are shown for only the reference temperature branches ($T_f$= 900 K, $T_m$= 585 K).

The following table shows the energy group structure used in CASMO-3. A unit used for energy is eV.

ENERGY GROUP STRUCTURES

| MICRO | MACRO | EDIT-A | EDIT-B | ENERGY BOUND | ENERGY WIDTH |
|---|---|---|---|---|---|
| 1- 1 | 1 | 1 | 1 | 1.00000e+07 | 3.93450e+06 |
| 2- 2 | 2 | 1 | 1 | 6.06550e+06 | 2.38650e+06 |
| 3- 3 | 3 | 1 | 1 | 3.67900e+06 | 1.44800e+06 |
| 4- 4 | 4 | 1 | 1 | 2.23100e+06 | 8.78000e+05 |
| 5- 5 | 5 | 1 | 1 | 1.35300e+06 | 5.32000e+05 |
| 6- 6 | 6 | 1 | 2 | 8.21000e+05 | 3.21000e+05 |
| 7- 7 | 7 | 1 | 2 | 5.00000e+05 | 3.89000e+05 |
| 8- 8 | 8 | 1 | 2 | 1.11000e+05 | 1.01882e+05 |
| 9- 9 | 9 | 1 | 2 | 9.11800e+03 | 3.58800e+03 |
| 10- 10 | 10 | 1 | 3 | 5.53000e+03 | 5.38127e+03 |
| 11- 13 | 11 | 1 | 3 | 1.48730e+02 | 1.32762e+02 |
| 14- 14 | 12 | 1 | 3 | 1.59680e+01 | 6.09100e+00 |
| 15- 15 | 13 | 1 | 3 | 9.87700e+00 | 5.87700e+00 |
| 16- 19 | 14 | 1 | 3 | 4.00000e+00 | 2.14500e+00 |
| 20- 23 | 15 | 1 | 3 | 1.85500e+00 | 7.58000e-01 |
| 24- 24 | 16 | 1 | 3 | 1.09700e+00 | 7.70000e-02 |
| 25- 28 | 17 | 1 | 3 | 1.02000e+00 | 3.95000e-01 |
| 29- 29 | 18 | 2 | 4 | 6.25000e-01 | 2.75000e-01 |
| 30- 30 | 19 | 2 | 4 | 3.50000e-01 | 7.00000e-02 |
| 31- 33 | 20 | 2 | 4 | 2.80000e-01 | 1.40000e-01 |
| 34- 36 | 21 | 2 | 4 | 1.40000e-01 | 8.20000e-02 |
| 37- 38 | 22 | 2 | 4 | 5.80000e-02 | 2.80000e-02 |
| 39- 40 | 23 | 2 | 4 | 3.00000e-02 | 3.00000e-02 |

Delayed neutron data are used commonly for all materials. The followings are the effective delayed neutron fractions ($\beta_{eff,d}$), the decay constants ($\lambda_d$) and the fission yield ratios of delayed neutrons ($\chi_d$) for six delayed neutron precursor groups.

| precursor group $\iota$ | $\beta_\iota$ | $\lambda_\iota$ ($sec^{-1}$) |
|---|---|---|
| 1 | 2.62362E-04 | 1.272E-02 |
| 2 | 1.47061E-03 | 3.174E-02 |
| 3 | 1.29800E-03 | 1.160E-01 |
| 4 | 2.81003E-03 | 3.110E-01 |
| 5 | 8.83744E-04 | 1.400E+00 |
| 6 | 1.79511E-04 | 3.870E+00 |

| $\chi_{d_\iota}$ | precursor group $\iota$ | | | |
|---|---|---|---|---|
| | 1 | 2 | 3 | 4, 5 and 6 |
| energy group 1 | 0.0 | 0.0 | 0.0 | 0.0 |
| 2 | 0.0 | 0.0 | 0.0 | 0.0 |
| 3 | 0.0 | 0.0 | 0.0 | 0.0 |
| 4 | 0.0 | 0.0 | 0.0 | 0.0 |
| 5 | 5.27205E-02 | 1.03281E-01 | 1.23382E-01 | 1.07014E-01 |
| 6 | 8.50905E-02 | 3.10030E-01 | 2.34052E-01 | 2.37556E-01 |
| 7 | 6.63895E-01 | 5.07628E-01 | 4.82623E-01 | 5.58933E-01 |
| 8 | 1.96885E-01 | 7.84885E-02 | 1.58822E-01 | 9.58041E-02 |
| 9 | 8.90128E-04 | 3.62131E-04 | 7.09065E-04 | 4.38009E-04 |
| 10 | 5.14544E-04 | 2.09332E-04 | 4.09880E-04 | 2.53194E-04 |
| 11 | 3.49049E-06 | 1.42004E-06 | 2.78048E-06 | 1.71758E-06 |
| 12 | 0.0 | 0.0 | 0.0 | 0.0 |
| 13 | 0.0 | 0.0 | 0.0 | 0.0 |
| 14 | 0.0 | 0.0 | 0.0 | 0.0 |
| 15 | 0.0 | 0.0 | 0.0 | 0.0 |
| 16 | 0.0 | 0.0 | 0.0 | 0.0 |
| 17 | 0.0 | 0.0 | 0.0 | 0.0 |
| 18 | 0.0 | 0.0 | 0.0 | 0.0 |
| 19 | 0.0 | 0.0 | 0.0 | 0.0 |
| 20 | 0.0 | 0.0 | 0.0 | 0.0 |
| 21 | 0.0 | 0.0 | 0.0 | 0.0 |
| 22 | 0.0 | 0.0 | 0.0 | 0.0 |
| 23 | 0.0 | 0.0 | 0.0 | 0.0 |

The following table shows the average neutron speed calculated for reference temperature branches of each material.

********** NEUTRON AVG. SPEED (cm/sec) **********

CLOREF (TF 900, TM 585)

| | | | | |
|---|---|---|---|---|
| 3.648551E+09 | 2.932388E+09 | 2.309097E+09 | 1.811623E+09 | 1.411800E+09 |
| 1.098117E+09 | 6.036171E+08 | 2.193185E+08 | 1.223034E+08 | 2.503212E+07 |
| 9.278253E+06 | 4.973232E+06 | 3.341497E+06 | 2.257391E+06 | 1.682454E+06 |
| 1.426042E+06 | 1.198684E+06 | 9.432396E+05 | 7.730894E+05 | 5.900688E+05 |
| 4.061547E+05 | 3.085472E+05 | 1.967787E+05 | | |

COOREF (TF 900, TM 585)

| | | | | |
|---|---|---|---|---|
| 3.643104E+09 | 2.932444E+09 | 2.309011E+09 | 1.811292E+09 | 1.411678E+09 |
| 1.098264E+09 | 6.036943E+08 | 2.196195E+08 | 1.223351E+08 | 2.504133E+07 |
| 9.291056E+06 | 4.973585E+06 | 3.341633E+06 | 2.256979E+06 | 1.682377E+06 |
| 1.426025E+06 | 1.198584E+06 | 9.429886E+05 | 7.728660E+05 | 5.899092E+05 |
| 4.060154E+05 | 3.083503E+05 | 1.972553E+05 | | |

AOOREF (TF 900, TM 585)

| | | | | |
|---|---|---|---|---|
| 3.648130E+09 | 2.932703E+09 | 2.309217E+09 | 1.811590E+09 | 1.411636E+09 |
| 1.098016E+09 | 6.035027E+08 | 2.193318E+08 | 1.222955E+08 | 2.502825E+07 |
| 9.263040E+06 | 4.970497E+06 | 3.341274E+06 | 2.256694E+06 | 1.682182E+06 |
| 1.425951E+06 | 1.198277E+06 | 9.417134E+05 | 7.716195E+05 | 5.890859E+05 |
| 4.052336E+05 | 3.065304E+05 | 2.047782E+05 | | |

REFREF (TF 900, TM 585)

| | | | | |
|---|---|---|---|---|
| 3.648551E+09 | 2.932388E+09 | 2.309097E+09 | 1.811623E+09 | 1.411800E+09 |
| 1.098117E+09 | 6.036171E+08 | 2.193185E+08 | 1.223034E+08 | 2.503212E+07 |
| 9.278253E+06 | 4.973232E+06 | 3.341497E+06 | 2.257391E+06 | 1.682454E+06 |
| 1.426042E+06 | 1.198684E+06 | 9.432396E+05 | 7.730894E+05 | 5.900688E+05 |
| 4.061547E+05 | 3.085472E+05 | 1.967787E+05 | | |

A2.1 Fuel Composition CLOREF

* C A S M O -3 3.4 87/07/07 STUDSVIK * EXECUTION 87/10/21 17:34:54

* BATCH CLO: TAVE
* BURNUP = 0.000 V= 0.0 TF= 900.0 TM= 585.0 BOR= 500.0

**********************************************************************
* K-INF = 1.09551 K-EFF = 1.09551 *
* B2G = 0.000e+00 B2M = 1.548e-03 H2 = 61.69 *
**********************************************************************

MACRO GROUPS

ASSM AVERAGED CROSS SECTIONS
******************************

| GROUP | ABSORPTION | FISSION | NU-FISSION | TRANSPORT |
|---|---|---|---|---|
| 1 | 5.08463e-03 | 5.83321e-03 | 2.01065e-02 | 9.20225e-02 |
| 2 | 5.47438e-03 | 3.76348e-03 | 1.13892e-02 | 1.07378e-01 |
| 3 | 4.18299e-03 | 3.79341e-03 | 1.04369e-02 | 1.20989e-01 |
| 4 | 3.43542e-03 | 2.88547e-03 | 7.50771e-03 | 1.40641e-01 |
| 5 | 1.29893e-03 | 4.18107e-04 | 1.05922e-03 | 2.03478e-01 |
| 6 | 1.12676e-03 | 2.51033e-04 | 6.27446e-04 | 2.03312e-01 |
| 7 | 1.23464e-03 | 2.74771e-04 | 6.74034e-04 | 2.79012e-01 |
| 8 | 3.13369e-03 | 4.17338e-04 | 1.01159e-03 | 3.12063e-01 |
| 9 | 5.33976e-03 | 7.29649e-04 | 1.76553e-03 | 3.52563e-01 |
| 10 | 1.24077e-02 | 2.13619e-03 | 5.16766e-03 | 3.84660e-01 |
| 11 | 3.30217e-02 | 6.84982e-03 | 1.65683e-02 | 4.20098e-01 |
| 12 | 2.17673e-02 | 8.53836e-03 | 2.06526e-02 | 3.88194e-01 |
| 13 | 6.25808e-02 | 6.90562e-03 | 1.67033e-02 | 4.25598e-01 |
| 14 | 1.39836e-02 | 3.77672e-03 | 9.13495e-03 | 4.07755e-01 |
| 15 | 1.88916e-02 | 6.37445e-03 | 1.54186e-02 | 4.38861e-01 |
| 16 | 3.15988e-02 | 1.71684e-02 | 4.15269e-02 | 4.65682e-01 |
| 17 | 2.56783e-02 | 1.18604e-02 | 2.86881e-02 | 4.82836e-01 |
| 18 | 3.76804e-02 | 1.87711e-02 | 4.54033e-02 | 5.50802e-01 |
| 19 | 6.09458e-02 | 3.41495e-02 | 8.25995e-02 | 6.32553e-01 |
| 20 | 6.63231e-02 | 3.54120e-02 | 8.56546e-02 | 7.36135e-01 |
| 21 | 9.24773e-02 | 4.92711e-02 | 1.19178e-01 | 9.63822e-01 |
| 22 | 1.32854e-01 | 7.46853e-02 | 1.80647e-01 | 1.33254e+00 |
| 23 | 2.03848e-01 | 1.18216e-01 | 2.85939e-01 | 1.98906e+00 |

P0-SCATTERING
FROM GROUP 1
2.90275e-02 2.15546e-02 9.14689e-03 8.69333e-03 8.16523e-03
6.41401e-03 7.72310e-03 1.09230e-03 1.73538e-05 2.60281e-05
3.54184e-07 0.00000e+00 0.00000e+00 0.00000e+00 0.00000e+00
0.00000e+00 0.00000e+00 0.00000e+00 0.00000e+00 0.00000e+00
0.00000e+00 0.00000e+00 0.00000e+00
FROM GROUP 2
0.00000e+00 5.48127e-02 3.13633e-02 1.25851e-02 1.06272e-02
8.20260e-03 1.01838e-02 1.68635e-03 3.86182e-05 5.75309e-05
1.07635e-06 0.00000e+00 0.00000e+00 0.00000e+00 0.00000e+00
0.00000e+00 0.00000e+00 0.00000e+00 0.00000e+00 0.00000e+00
0.00000e+00 0.00000e+00 7.11789e-10
FROM GROUP 3
0.00000e+00 0.00000e+00 6.86084e-02 2.83978e-02 1.63561e-02
1.29399e-02 1.68499e-02 3.19577e-03 8.35797e-05 1.25355e-04
3.09271e-06 0.00000e+00 0.00000e+00 0.00000e+00 0.00000e+00
0.00000e+00 0.00000e+00 0.00000e+00 0.00000e+00 0.00000e+00
0.00000e+00 0.00000e+00 0.00000e+00
FROM GROUP 4
0.00000e+00 0.00000e+00 0.00000e+00 8.40211e-02 4.39899e-02
2.06099e-02 2.81340e-02 6.86036e-03 1.90462e-04 2.69625e-04
6.65192e-06 3.05196e-07 2.94466e-07 0.00000e+00 0.00000e+00
0.00000e+00 0.00000e+00 0.00000e+00 0.00000e+00 0.00000e+00
0.00000e+00 0.00000e+00 0.00000e+00
FROM GROUP 5
0.00000e+00 0.00000e+00 0.00000e+00 0.00000e+00 1.53790e-01
6.66143e-02 4.75940e-02 1.15437e-02 3.84020e-04 5.75973e-04
1.42100e-05 6.51944e-07 6.29052e-07 0.00000e+00 0.00000e+00
0.00000e+00 0.00000e+00 0.00000e+00 0.00000e+00 0.00000e+00
0.00000e+00 0.00000e+00 0.00000e+00
FROM GROUP 6
0.00000e+00 0.00000e+00 0.00000e+00 0.00000e+00 0.00000e+00
1.63848e-01 1.08582e-01 2.35522e-02 8.16301e-04 1.22435e-03
3.02060e-05 1.38587e-06 1.33717e-06 0.00000e+00 0.00000e+00
0.00000e+00 0.00000e+00 0.00000e+00 0.00000e+00 0.00000e+00
0.00000e+00 0.00000e+00 0.00000e+00
FROM GROUP 7
0.00000e+00 0.00000e+00 0.00000e+00 0.00000e+00 0.00000e+00
0.00000e+00 3.25699e-01 1.20227e-01 3.97173e-03 5.95695e-03
1.46965e-04 6.74266e-06 6.50586e-06 2.14343e-06 5.20269e-07
0.00000e+00 8.69697e-08 0.00000e+00 0.00000e+00 0.00000e+00
0.00000e+00 0.00000e+00 0.00000e+00
FROM GROUP 8
0.00000e+00 0.00000e+00 0.00000e+00 0.00000e+00 0.00000e+00
0.00000e+00 0.00000e+00 4.89973e-01 6.84186e-02 9.58634e-02
2.36461e-03 1.08488e-04 1.04676e-04 3.82048e-05 1.33530e-05
1.15665e-06 6.73403e-06 4.84508e-06 1.05151e-06 2.24133e-06
1.19647e-06 1.72890e-07 0.00000e+00

FROM GROUP 9
0.00000e+00 0.00000e+00 0.00000e+00 0.00000e+00 0.00000e+00
0.00000e+00 0.00000e+00 0.00000e+00 3.04957e-01 4.38558e-01
1.01436e-02 4.65378e-04 4.49045e-04 1.63891e-04 5.79159e-05
5.88323e-06 3.01805e-05 2.10117e-05 5.34841e-06 1.06968e-05
6.26531e-06 2.13937e-06 2.29084e-06
FROM GROUP 10
0.00000e+00 0.00000e+00 0.00000e+00 0.00000e+00 0.00000e+00
0.00000e+00 0.00000e+00 0.00000e+00 0.00000e+00 6.25629e-01
1.34105e-01 5.99118e-03 5.78072e-03 2.10985e-03 7.45581e-04
7.57380e-05 3.88531e-04 2.70495e-04 6.88529e-05 1.37707e-04
8.06568e-05 2.75412e-05 2.95071e-05
FROM GROUP 11
0.00000e+00 0.00000e+00 0.00000e+00 0.00000e+00 0.00000e+00
0.00000e+00 0.00000e+00 0.00000e+00 0.00000e+00 0.00000e+00
5.54347e-01 8.97625e-02 8.14252e-02 2.97187e-02 1.05020e-02
1.06682e-03 5.47266e-03 3.81012e-03 9.69836e-04 1.93968e-03
1.13610e-03 3.87936e-04 4.15644e-04
FROM GROUP 12
0.00000e+00 0.00000e+00 0.00000e+00 0.00000e+00 0.00000e+00
0.00000e+00 0.00000e+00 0.00000e+00 0.00000e+00 0.00000e+00
0.00000e+00 2.72949e-01 2.96226e-01 9.80068e-02 3.46327e-02
3.51812e-03 1.80474e-02 1.25647e-02 3.19828e-03 6.39656e-03
3.74654e-03 1.27930e-03 1.37069e-03
FROM GROUP 13
0.00000e+00 0.00000e+00 0.00000e+00 0.00000e+00 0.00000e+00
0.00000e+00 0.00000e+00 0.00000e+00 0.00000e+00 0.00000e+00
0.00000e+00 0.00000e+00 3.66282e-01 2.19340e-01 7.23326e-02
7.34788e-03 3.76939e-02 2.62428e-02 6.67987e-03 1.33595e-02
7.82490e-03 2.67199e-03 2.86285e-03
FROM GROUP 14
0.00000e+00 0.00000e+00 0.00000e+00 0.00000e+00 0.00000e+00
0.00000e+00 0.00000e+00 0.00000e+00 0.00000e+00 0.00000e+00
0.00000e+00 0.00000e+00 3.73852e-04 3.50890e-01 1.83481e-01
1.64660e-02 8.37633e-02 5.77519e-02 1.44417e-02 2.71102e-02
1.32250e-02 3.33543e-03 2.11300e-03
FROM GROUP 15
0.00000e+00 0.00000e+00 0.00000e+00 0.00000e+00 0.00000e+00
0.00000e+00 0.00000e+00 0.00000e+00 0.00000e+00 0.00000e+00
0.00000e+00 0.00000e+00 0.00000e+00 3.35716e-03 2.96166e-01
4.19484e-02 1.63605e-01 1.04850e-01 2.62204e-02 4.99832e-02
2.45344e-02 6.28305e-03 3.93876e-03
FROM GROUP 16
0.00000e+00 0.00000e+00 0.00000e+00 0.00000e+00 0.00000e+00
0.00000e+00 0.00000e+00 0.00000e+00 0.00000e+00 0.00000e+00
0.00000e+00 0.00000e+00 0.00000e+00 2.46771e-06 3.56071e-02
1.36676e-01 3.05922e-01 1.45086e-01 3.64204e-02 6.95583e-02
3.43537e-02 8.78541e-03 5.49080e-03

FROM GROUP 17
0.00000e+00 0.00000e+00 0.00000e+00 0.00000e+00 0.00000e+00
0.00000e+00 0.00000e+00 0.00000e+00 0.00000e+00 0.00000e+00
0.00000e+00 0.00000e+00 0.00000e+00 9.45398e-08 1.21125e-03
5.73877e-03 3.53926e-01 2.27775e-01 4.76653e-02 9.19925e-02
4.57379e-02 1.16653e-02 7.24500e-03
FROM GROUP 18
0.00000e+00 0.00000e+00 0.00000e+00 0.00000e+00 0.00000e+00
0.00000e+00 0.00000e+00 0.00000e+00 0.00000e+00 0.00000e+00
0.00000e+00 0.00000e+00 0.00000e+00 0.00000e+00 6.12347e-07
2.34543e-06 1.43518e-02 4.28567e-01 1.16157e-01 1.75652e-01
7.94223e-02 1.98177e-02 1.20991e-02
FROM GROUP 19
0.00000e+00 0.00000e+00 0.00000e+00 0.00000e+00 0.00000e+00
0.00000e+00 0.00000e+00 0.00000e+00 0.00000e+00 0.00000e+00
0.00000e+00 0.00000e+00 0.00000e+00 0.00000e+00 0.00000e+00
0.00000e+00 2.03312e-04 8.14302e-02 3.02089e-01 3.45257e-01
1.32348e-01 3.18809e-02 1.89237e-02
FROM GROUP 20
0.00000e+00 0.00000e+00 0.00000e+00 0.00000e+00 0.00000e+00
0.00000e+00 0.00000e+00 0.00000e+00 0.00000e+00 0.00000e+00
0.00000e+00 0.00000e+00 0.00000e+00 0.00000e+00 0.00000e+00
0.00000e+00 3.57742e-05 9.74521e-03 3.80040e-02 5.77870e-01
2.89627e-01 6.08074e-02 3.50647e-02
FROM GROUP 21
0.00000e+00 0.00000e+00 0.00000e+00 0.00000e+00 0.00000e+00
0.00000e+00 0.00000e+00 0.00000e+00 0.00000e+00 0.00000e+00
0.00000e+00 0.00000e+00 0.00000e+00 0.00000e+00 0.00000e+00
0.00000e+00 7.87082e-06 1.75795e-03 5.67996e-03 1.52946e-01
7.86130e-01 1.86708e-01 8.46900e-02
FROM GROUP 22
0.00000e+00 0.00000e+00 0.00000e+00 0.00000e+00 0.00000e+00
0.00000e+00 0.00000e+00 0.00000e+00 0.00000e+00 0.00000e+00
0.00000e+00 0.00000e+00 0.00000e+00 0.00000e+00 0.00000e+00
0.00000e+00 4.48522e-06 9.86004e-04 3.11638e-03 7.01485e-02
4.43521e-01 7.54249e-01 2.83737e-01
FROM GROUP 23
0.00000e+00 0.00000e+00 0.00000e+00 0.00000e+00 0.00000e+00
0.00000e+00 0.00000e+00 0.00000e+00 0.00000e+00 0.00000e+00
0.00000e+00 0.00000e+00 0.00000e+00 0.00000e+00 0.00000e+00
0.00000e+00 4.82100e-06 1.02988e-03 3.18830e-03 6.92022e-02
3.38084e-01 4.91940e-01 1.34569e+00

FISS SOURCE
2.57800e-02 1.13110e-01 2.12360e-01 2.28410e-01 1.76350e-01
1.11980e-01 1.15805e-01 1.58310e-02 2.02950e-04 1.80278e-04
5.06350e-07 0.00000e+00 0.00000e+00 0.00000e+00 0.00000e+00
0.00000e+00 0.00000e+00 0.00000e+00 0.00000e+00 0.00000e+00
0.00000e+00 0.00000e+00 0.00000e+00

EDIT-A GROUPS

ASSM AVERAGED CROSS SECTIONS
**********

| GROUP | ABSORPTION | FISSION | NU-FISSION | TRANSPORT |
|---|---|---|---|---|
| 1 | 9.02607e-03 | 2.46083e-03 | 6.25534e-03 | 2.79180e-01 |
| 2 | 9.11247e-02 | 4.97461e-02 | 1.20326e-01 | 9.62968e-01 |

PO-SCATTERING
FROM GROUP 1
4.78863e-01 1.64184e-02
FROM GROUP 2
1.73115e-03 1.22336e+00

FISS SOURCE
1.00001e+00 0.00000e+00

EDIT-B GROUPS

ASSM AVERAGED CROSS SECTIONS
**********

| GROUP | ABSORPTION | FISSION | NU-FISSION | TRANSPORT |
|---|---|---|---|---|
| 1 | 3.38814e-03 | 2.68341e-03 | 7.50104e-03 | 1.46179e-01 |
| 2 | 2.07776e-03 | 3.42724e-04 | 8.37794e-04 | 2.77875e-01 |
| 3 | 2.30075e-02 | 4.88675e-03 | 1.18204e-02 | 4.06604e-01 |
| 4 | 9.11247e-02 | 4.97461e-02 | 1.20326e-01 | 9.62968e-01 |

PO-SCATTERING
FROM GROUP 1
1.26779e-01 6.24458e-02 2.83671e-04 9.33438e-11
FROM GROUP 2
0.00000e+00 4.45591e-01 6.05795e-02 5.82671e-06
FROM GROUP 3
0.00000e+00 0.00000e+00 7.18565e-01 5.23771e-02
FROM GROUP
0.00000e+00 0.00000e+00 1.73115e-03 1.22336e+00

FISS SOURCE
7.56010e-01 2.43819e-01 1.80784e-04 0.00000e+00

A2.2 Fuel Composition CLOTF

* C A S M O -3 3.4 87/07/07 STUDSVIK * EXECUTION 87/10/21 17:34:54

* BATCH CLO: FUEL TEMP. BRANC
* BURNUP = 0.000 V= 0.0 TF=1500.0 TM= 585.0 BOR= 500.0

* K-INF = 1.08090 K-EFF = 1.08090 *
* B2G = 0.000e+00 B2M = 1.312e-03 M2 = 61.68 *

MACRO GROUPS

ASSM AVERAGED CROSS SECTIONS

| GROUP | ABSORPTION | FISSION | NU-FISSION | TRANSPORT |
|---|---|---|---|---|
| 1 | 5.05965e-03 | 5.79161e-03 | 1.99631e-02 | 9.17133e-02 |
| 2 | 5.44109e-03 | 3.73654e-03 | 1.13077e-02 | 1.07057e-01 |
| 3 | 4.15359e-03 | 3.76633e-03 | 1.03624e-02 | 1.20636e-01 |
| 4 | 3.41128e-03 | 2.86512e-03 | 7.45478e-03 | 1.40242e-01 |
| 5 | 1.28994e-03 | 4.15134e-04 | 1.05169e-03 | 2.02869e-01 |
| 6 | 1.11919e-03 | 2.49244e-04 | 6.22975e-04 | 2.02728e-01 |
| 7 | 1.22650e-03 | 2.72852e-04 | 6.69326e-04 | 2.78150e-01 |
| 8 | 3.11345e-03 | 4.14588e-04 | 1.00492e-03 | 3.11165e-01 |
| 9 | 5.37618e-03 | 7.24962e-04 | 1.75419e-03 | 3.51650e-01 |
| 10 | 1.30019e-02 | 2.11683e-03 | 5.12081e-03 | 3.84284e-01 |
| 11 | 3.46592e-02 | 6.85581e-03 | 1.65828e-02 | 4.20826e-01 |
| 12 | 2.20938e-02 | 8.66366e-03 | 2.09557e-02 | 3.87775e-01 |
| 13 | 6.57076e-02 | 6.95087e-03 | 1.68128e-02 | 4.28067e-01 |
| 14 | 1.39305e-02 | 3.75396e-03 | 9.07990e-03 | 4.06923e-01 |
| 15 | 1.88180e-02 | 6.33746e-03 | 1.53291e-02 | 4.37969e-01 |
| 16 | 3.14645e-02 | 1.70741e-02 | 4.12988e-02 | 4.64735e-01 |
| 17 | 2.55871e-02 | 1.18005e-02 | 2.85431e-02 | 4.81852e-01 |
| 18 | 3.75729e-02 | 1.87007e-02 | 4.52329e-02 | 5.49651e-01 |
| 19 | 6.09151e-02 | 3.41561e-02 | 8.26154e-02 | 6.31033e-01 |
| 20 | 6.62451e-02 | 3.53807e-02 | 8.55790e-02 | 7.34352e-01 |
| 21 | 9.19415e-02 | 4.88834e-02 | 1.18240e-01 | 9.62259e-01 |
| 22 | 1.31777e-01 | 7.38450e-02 | 1.78615e-01 | 1.33237e+00 |
| 23 | 2.02243e-01 | 1.16942e-01 | 2.82859e-01 | 1.98979e+00 |

P0-SCATTERING
FROM GROUP 1
2.89275e-02 2.15120e-02 9.13796e-03 8.67509e-03 8.13728e-03
6.38647e-03 7.68682e-03 1.08813e-03 1.73423e-05 2.60107e-05
3.53948e-07 0.00000e+00 0.00000e+00 0.00000e+00 0.00000e+00
0.00000e+00 0.00000e+00 0.00000e+00 0.00000e+00 0.00000e+00
0.00000e+00 0.00000e+00 0.00000e+00
FROM GROUP 2
0.00000e+00 5.46272e-02 3.12994e-02 1.25699e-02 1.06024e-02
8.17594e-03 1.01468e-02 1.68205e-03 3.85933e-05 5.74963e-05
1.07570e-06 0.00000e+00 0.00000e+00 0.00000e+00 0.00000e+00
0.00000e+00 0.00000e+00 0.00000e+00 0.00000e+00 0.00000e+00
0.00000e+00 0.00000e+00 7.11825e-10
FROM GROUP 3
0.00000e+00 0.00000e+00 6.83939e-02 2.83604e-02 1.63311e-02
1.29054e-02 1.67983e-02 3.18921e-03 8.35285e-05 1.25279e-04
3.09081e-06 0.00000e+00 0.00000e+00 0.00000e+00 0.00000e+00
0.00000e+00 0.00000e+00 0.00000e+00 0.00000e+00 0.00000e+00
0.00000e+00 0.00000e+00 0.00000e+00
FROM GROUP 4
0.00000e+00 0.00000e+00 0.00000e+00 8.37761e-02 4.39134e-02
2.05823e-02 2.80675e-02 6.84529e-03 1.90288e-04 2.69478e-04
6.64828e-06 3.05029e-07 2.94305e-07 0.00000e+00 0.00000e+00
0.00000e+00 0.00000e+00 0.00000e+00 0.00000e+00 0.00000e+00
0.00000e+00 0.00000e+00 0.00000e+00
FROM GROUP 5
0.00000e+00 0.00000e+00 0.00000e+00 0.00000e+00 1.53299e-01
6.64723e-02 4.75354e-02 1.15330e-02 3.83796e-04 5.75637e-04
1.42018e-05 6.51563e-07 6.28684e-07 0.00000e+00 0.00000e+00
0.00000e+00 0.00000e+00 0.00000e+00 0.00000e+00 0.00000e+00
0.00000e+00 0.00000e+00 0.00000e+00
FROM GROUP 6
0.00000e+00 0.00000e+00 0.00000e+00 0.00000e+00 0.00000e+00
1.63343e-01 1.08455e-01 2.35371e-02 8.15865e-04 1.22370e-03
3.01899e-05 1.38512e-06 1.33646e-06 0.00000e+00 0.00000e+00
0.00000e+00 0.00000e+00 0.00000e+00 0.00000e+00 0.00000e+00
0.00000e+00 0.00000e+00 0.00000e+00
FROM GROUP 7
0.00000e+00 0.00000e+00 0.00000e+00 0.00000e+00 0.00000e+00
0.00000e+00 3.24821e-01 1.20134e-01 3.96948e-03 5.95358e-03
1.46881e-04 6.73884e-06 6.50217e-06 2.14222e-06 5.19975e-07
0.00000e+00 8.69205e-08 0.00000e+00 0.00000e+00 0.00000e+00
0.00000e+00 0.00000e+00 0.00000e+00
FROM GROUP 8
0.00000e+00 0.00000e+00 0.00000e+00 0.00000e+00 0.00000e+00
0.00000e+00 0.00000e+00 4.88986e-01 6.83633e-02 9.58025e-02
2.36311e-03 1.08419e-04 1.04609e-04 3.81806e-05 1.33445e-05
1.15592e-06 6.72976e-06 4.84201e-06 1.05084e-06 2.23990e-06
1.19572e-06 1.72780e-07 0.00000e+00

FROM GROUP 9
0.00000e+00 0.00000e+00 0.00000e+00 0.00000e+00 0.00000e+00
0.00000e+00 0.00000e+00 0.00000e+00 3.04093e-01 4.38212e-01
1.01373e-02 4.65086e-04 4.48763e-04 1.63788e-04 5.78795e-05
5.87953e-06 3.01615e-05 2.09985e-05 5.34505e-06 1.06901e-05
6.26137e-06 2.13803e-06 2.28940e-06
FROM GROUP 10
0.00000e+00 0.00000e+00 0.00000e+00 0.00000e+00 0.00000e+00
0.00000e+00 0.00000e+00 0.00000e+00 0.00000e+00 6.24568e-01
1.34048e-01 5.98909e-03 5.77870e-03 2.10911e-03 7.45321e-04
7.57116e-05 3.88396e-04 2.70401e-04 6.88289e-05 1.37659e-04
8.06286e-05 2.75316e-05 2.94969e-05
FROM GROUP 11
0.00000e+00 0.00000e+00 0.00000e+00 0.00000e+00 0.00000e+00
0.00000e+00 0.00000e+00 0.00000e+00 0.00000e+00 0.00000e+00
5.53777e-01 8.96344e-02 8.13403e-02 2.96878e-02 1.04910e-02
1.06571e-03 5.46696e-03 3.80615e-03 9.68826e-04 1.93766e-03
1.13492e-03 3.87532e-04 4.15211e-04
FROM GROUP 12
0.00000e+00 0.00000e+00 0.00000e+00 0.00000e+00 0.00000e+00
0.00000e+00 0.00000e+00 0.00000e+00 0.00000e+00 0.00000e+00
0.00000e+00 2.72308e-01 2.96027e-01 9.79661e-02 3.46184e-02
3.51666e-03 1.80400e-02 1.25595e-02 3.19695e-03 6.39391e-03
3.74499e-03 1.27877e-03 1.37012e-03
FROM GROUP 13
0.00000e+00 0.00000e+00 0.00000e+00 0.00000e+00 0.00000e+00
0.00000e+00 0.00000e+00 0.00000e+00 0.00000e+00 0.00000e+00
0.00000e+00 0.00000e+00 3.65675e-01 2.19478e-01 7.23997e-02
7.35470e-03 3.77288e-02 2.62671e-02 6.68607e-03 1.33719e-02
7.83216e-03 2.67447e-03 2.86551e-03
FROM GROUP 14
0.00000e+00 0.00000e+00 0.00000e+00 0.00000e+00 0.00000e+00
0.00000e+00 0.00000e+00 0.00000e+00 0.00000e+00 0.00000e+00
0.00000e+00 0.00000e+00 5.17431e-04 3.50131e-01 1.83187e-01
1.65061e-02 8.37522e-02 5.77122e-02 1.44317e-02 2.70909e-02
1.32151e-02 3.33273e-03 2.11128e-03
FROM GROUP 15
0.00000e+00 0.00000e+00 0.00000e+00 0.00000e+00 0.00000e+00
0.00000e+00 0.00000e+00 0.00000e+00 0.00000e+00 0.00000e+00
0.00000e+00 0.00000e+00 0.00000e+00 4.01812e-03 2.95056e-01
4.11794e-02 1.64227e-01 1.04827e-01 2.62051e-02 4.99541e-02
2.45202e-02 6.27942e-03 3.93648e-03
FROM GROUP 16
0.00000e+00 0.00000e+00 0.00000e+00 0.00000e+00 0.00000e+00
0.00000e+00 0.00000e+00 0.00000e+00 0.00000e+00 0.00000e+00
0.00000e+00 0.00000e+00 0.00000e+00 2.81625e-06 4.07517e-02
1.35867e-01 3.00214e-01 1.45532e-01 3.63849e-02 6.94905e-02
3.43202e-02 8.77685e-03 5.48545e-03

FROM GROUP 17
0.00000e+00 0.00000e+00 0.00000e+00 0.00000e+00 0.00000e+00
0.00000e+00 0.00000e+00 0.00000e+00 0.00000e+00 0.00000e+00
0.00000e+00 0.00000e+00 0.00000e+00 1.00341e-07 1.53901e-03
6.58437e-03 3.51687e-01 2.27703e-01 4.77453e-02 9.18984e-02
4.56847e-02 1.16517e-02 7.23655e-03
FROM GROUP 18
0.00000e+00 0.00000e+00 0.00000e+00 0.00000e+00 0.00000e+00
0.00000e+00 0.00000e+00 0.00000e+00 0.00000e+00 0.00000e+00
0.00000e+00 0.00000e+00 0.00000e+00 0.00000e+00 6.16032e-07
2.39716e-06 1.61983e-02 4.25228e-01 1.15141e-01 1.76842e-01
7.93160e-02 1.97829e-02 1.20779e-02
FROM GROUP 19
0.00000e+00 0.00000e+00 0.00000e+00 0.00000e+00 0.00000e+00
0.00000e+00 0.00000e+00 0.00000e+00 0.00000e+00 0.00000e+00
0.00000e+00 0.00000e+00 0.00000e+00 0.00000e+00 0.00000e+00
0.00000e+00 2.05424e-04 8.77340e-02 2.96509e-01 3.42159e-01
1.32485e-01 3.17762e-02 1.88604e-02
FROM GROUP 20
0.00000e+00 0.00000e+00 0.00000e+00 0.00000e+00 0.00000e+00
0.00000e+00 0.00000e+00 0.00000e+00 0.00000e+00 0.00000e+00
0.00000e+00 0.00000e+00 0.00000e+00 0.00000e+00 0.00000e+00
0.00000e+00 3.57251e-05 1.03329e-02 4.03691e-02 5.72497e-01
2.89702e-01 6.09360e-02 3.49806e-02
FROM GROUP 21
0.00000e+00 0.00000e+00 0.00000e+00 0.00000e+00 0.00000e+00
0.00000e+00 0.00000e+00 0.00000e+00 0.00000e+00 0.00000e+00
0.00000e+00 0.00000e+00 0.00000e+00 0.00000e+00 0.00000e+00
0.00000e+00 7.87762e-06 1.76164e-03 5.73190e-03 1.58996e-01
7.79363e-01 1.86271e-01 8.53772e-02
FROM GROUP 22
0.00000e+00 0.00000e+00 0.00000e+00 0.00000e+00 0.00000e+00
0.00000e+00 0.00000e+00 0.00000e+00 0.00000e+00 0.00000e+00
0.00000e+00 0.00000e+00 0.00000e+00 0.00000e+00 0.00000e+00
0.00000e+00 4.49322e-06 9.87764e-04 3.12213e-03 7.08181e-02
4.52799e-01 7.46704e-01 2.84293e-01
FROM GROUP 23
0.00000e+00 0.00000e+00 0.00000e+00 0.00000e+00 0.00000e+00
0.00000e+00 0.00000e+00 0.00000e+00 0.00000e+00 0.00000e+00
0.00000e+00 0.00000e+00 0.00000e+00 0.00000e+00 0.00000e+00
0.00000e+00 4.83022e-06 1.03184e-03 3.19438e-03 6.93893e-02
3.43698e-01 4.98277e-01 1.34044e+00

A2.3 Fuel Composition CLOTM

```
* C A S M O -3  3.4 87/07/07 STUDSVIK * EXECUTION 87/10/21   17:34:54

*  BATCH CLO: MODERATOR BRANCH
*  BURNUP =      0.000 V= 0.0  TF=900.0  TM= 620.0 BOR= 500.0

**************************************************************************
* K-INF = 1.08119  K-EFF = 1.08119                                       *
*                  B2G =  0.000e+00  B2M =  1.056e-03  M2 =   76.89 *
**************************************************************************
```

MACRO GROUPS

ASSM AVERAGED CROSS SECTIONS

| GROUP | ABSORPTION | FISSION | NU-FISSION | TRANSPORT |
|---|---|---|---|---|
| 1 | 4.86888e-03 | 5.79733e-03 | 1.99828e-02 | 8.50657e-02 |
| 2 | 5.33236e-03 | 3.73644e-03 | 1.13074e-02 | 9.83868e-02 |
| 3 | 4.15123e-03 | 3.76572e-03 | 1.03608e-02 | 1.10723e-01 |
| 4 | 3.40819e-03 | 2.86264e-03 | 7.44833e-03 | 1.28685e-01 |
| 5 | 1.28864e-03 | 4.14736e-04 | 1.05068e-03 | 1.86586e-01 |
| 6 | 1.11935e-03 | 2.49337e-04 | 6.23206e-04 | 1.87307e-01 |
| 7 | 1.22849e-03 | 2.73428e-04 | 6.70739e-04 | 2.57140e-01 |
| 8 | 3.12753e-03 | 4.16667e-04 | 1.00996e-03 | 2.86704e-01 |
| 9 | 5.30023e-03 | 7.28989e-04 | 1.76393e-03 | 3.21466e-01 |
| 10 | 1.22404e-02 | 2.13371e-03 | 5.16166e-03 | 3.49084e-01 |
| 11 | 3.21167e-02 | 6.82444e-03 | 1.65070e-02 | 3.80221e-01 |
| 12 | 2.15351e-02 | 8.50143e-03 | 2.05633e-02 | 3.48039e-01 |
| 13 | 6.04994e-02 | 6.87647e-03 | 1.66328e-02 | 3.83873e-01 |
| 14 | 1.36843e-02 | 3.77648e-03 | 9.13436e-03 | 3.62927e-01 |
| 15 | 1.84641e-02 | 6.35302e-03 | 1.53667e-02 | 3.89946e-01 |
| 16 | 3.11226e-02 | 1.71647e-02 | 4.15180e-02 | 4.13267e-01 |
| 17 | 2.51306e-02 | 1.18578e-02 | 2.86819e-02 | 4.27280e-01 |
| 18 | 3.69769e-02 | 1.87663e-02 | 4.53915e-02 | 4.85690e-01 |
| 19 | 6.00850e-02 | 3.41465e-02 | 8.25922e-02 | 5.56823e-01 |
| 20 | 6.52872e-02 | 3.54248e-02 | 8.56856e-02 | 6.42754e-01 |
| 21 | 9.10866e-02 | 4.92205e-02 | 1.19055e-01 | 8.34358e-01 |
| 22 | 1.31196e-01 | 7.49045e-02 | 1.81178e-01 | 1.14693e+00 |
| 23 | 2.00794e-01 | 1.18699e-01 | 2.87107e-01 | 1.70028e+00 |

P0-SCATTERING

FROM GROUP 1

| | | | | |
|---|---|---|---|---|
| 2.68232e-02 | 1.89162e-02 | 7.97328e-03 | 7.92214e-03 | 7.66729e-03 |
| 6.10632e-03 | 7.36126e-03 | 1.00621e-03 | 1.44713e-05 | 2.17047e-05 |
| 2.95353e-07 | 0.00000e+00 | 0.00000e+00 | 0.00000e+00 | 0.00000e+00 |
| 0.00000e+00 | 0.00000e+00 | 0.00000e+00 | 0.00000e+00 | 0.00000e+00 |
| 0.00000e+00 | 0.00000e+00 | 0.00000e+00 | | |

FROM GROUP 2

| | | | | |
|---|---|---|---|---|
| 0.00000e+00 | 5.05248e-02 | 2.76478e-02 | 1.10392e-02 | 9.66989e-03 |
| 7.61151e-03 | 9.46137e-03 | 1.50241e-03 | 3.22670e-05 | 4.80081e-05 |
| 8.98183e-07 | 0.00000e+00 | 0.00000e+00 | 0.00000e+00 | 0.00000e+00 |
| 0.00000e+00 | 0.00000e+00 | 0.00000e+00 | 0.00000e+00 | 0.00000e+00 |
| 0.00000e+00 | 0.00000e+00 | 7.13619e-10 | | |

FROM GROUP 3

| | | | | |
|---|---|---|---|---|
| 0.00000e+00 | 0.00000e+00 | 6.32850e-02 | 2.45986e-02 | 1.43024e-02 |
| 1.16768e-02 | 1.53056e-02 | 2.79784e-03 | 6.97465e-05 | 1.04608e-04 |
| 2.58084e-06 | 0.00000e+00 | 0.00000e+00 | 0.00000e+00 | 0.00000e+00 |
| 0.00000e+00 | 0.00000e+00 | 0.00000e+00 | 0.00000e+00 | 0.00000e+00 |
| 0.00000e+00 | 0.00000e+00 | 0.00000e+00 | | |

FROM GROUP 4

| | | | | |
|---|---|---|---|---|
| 0.00000e+00 | 0.00000e+00 | 0.00000e+00 | 7.75568e-02 | 3.84659e-02 |
| 1.79447e-02 | 2.48592e-02 | 6.00373e-03 | 1.60682e-04 | 2.25087e-04 |
| 5.55311e-06 | 2.54782e-07 | 2.45824e-07 | 0.00000e+00 | 0.00000e+00 |
| 0.00000e+00 | 0.00000e+00 | 0.00000e+00 | 0.00000e+00 | 0.00000e+00 |
| 0.00000e+00 | 0.00000e+00 | 0.00000e+00 | | |

FROM GROUP 5

| | | | | |
|---|---|---|---|---|
| 0.00000e+00 | 0.00000e+00 | 0.00000e+00 | 0.00000e+00 | 1.42357e-01 |
| 5.86015e-02 | 4.06957e-02 | 9.73859e-03 | 3.20589e-04 | 4.80837e-04 |
| 1.18629e-05 | 5.44259e-07 | 5.25148e-07 | 0.00000e+00 | 0.00000e+00 |
| 0.00000e+00 | 0.00000e+00 | 0.00000e+00 | 0.00000e+00 | 0.00000e+00 |
| 0.00000e+00 | 0.00000e+00 | 0.00000e+00 | | |

FROM GROUP 6

| | | | | |
|---|---|---|---|---|
| 0.00000e+00 | 0.00000e+00 | 0.00000e+00 | 0.00000e+00 | 0.00000e+00 |
| 1.52632e-01 | 9.26298e-02 | 1.97136e-02 | 6.81142e-04 | 1.02163e-03 |
| 2.52047e-05 | 1.15640e-06 | 1.11577e-06 | 0.00000e+00 | 0.00000e+00 |
| 0.00000e+00 | 0.00000e+00 | 0.00000e+00 | 0.00000e+00 | 0.00000e+00 |
| 0.00000e+00 | 0.00000e+00 | 0.00000e+00 | | |

FROM GROUP 7

| | | | | |
|---|---|---|---|---|
| 0.00000e+00 | 0.00000e+00 | 0.00000e+00 | 0.00000e+00 | 0.00000e+00 |
| 0.00000e+00 | 2.95692e-01 | 1.00945e-01 | 3.31036e-03 | 4.96501e-03 |
| 1.22492e-04 | 5.61988e-06 | 5.42251e-06 | 1.78651e-06 | 4.33634e-07 |
| 0.00000e+00 | 7.24876e-08 | 0.00000e+00 | 0.00000e+00 | 0.00000e+00 |
| 0.00000e+00 | 0.00000e+00 | 0.00000e+00 | | |

FROM GROUP 8

| | | | | |
|---|---|---|---|---|
| 0.00000e+00 | 0.00000e+00 | 0.00000e+00 | 0.00000e+00 | 0.00000e+00 |
| 0.00000e+00 | 0.00000e+00 | 4.34000e-01 | 5.73459e-02 | 7.97695e-02 |
| 1.96756e-03 | 9.02716e-05 | 8.70996e-05 | 3.17898e-05 | 1.11109e-05 |
| 9.62434e-07 | 5.60331e-06 | 4.03154e-06 | 8.74946e-07 | 1.86498e-06 |
| 9.95573e-07 | 1.43859e-07 | 0.00000e+00 | | |

FROM GROUP 9
0.00000e+00 0.00000e+00 0.00000e+00 0.00000e+00 0.00000e+00
0.00000e+00 0.00000e+00 0.00000e+00 2.78843e-01 3.67317e-01
8.43760e-03 3.87107e-04 3.73521e-04 1.36327e-04 4.81751e-05
4.89373e-06 2.51045e-05 1.74778e-05 4.44887e-06 8.89773e-06
5.21156e-06 1.77956e-06 1.90555e-06
FROM GROUP 10
0.00000e+00 0.00000e+00 0.00000e+00 0.00000e+00 0.00000e+00
0.00000e+00 0.00000e+00 0.00000e+00 0.00000e+00 5.47615e-01
1.11858e-01 4.98311e-03 4.80808e-03 1.75485e-03 6.20132e-04
6.29945e-05 3.23158e-04 2.24983e-04 5.72678e-05 1.14537e-04
6.70857e-05 2.29072e-05 2.45424e-05
FROM GROUP 11
0.00000e+00 0.00000e+00 0.00000e+00 0.00000e+00 0.00000e+00
0.00000e+00 0.00000e+00 0.00000e+00 0.00000e+00 0.00000e+00
4.87971e-01 7.47087e-02 6.73770e-02 2.45914e-02 8.69007e-03
8.82762e-04 4.52847e-03 3.15277e-03 8.02511e-04 1.60503e-03
9.40090e-04 3.21006e-04 3.43933e-04
FROM GROUP 12
0.00000e+00 0.00000e+00 0.00000e+00 0.00000e+00 0.00000e+00
0.00000e+00 0.00000e+00 0.00000e+00 0.00000e+00 0.00000e+00
0.00000e+00 2.46637e-01 2.48802e-01 8.14979e-02 2.87990e-02
2.92551e-03 1.50074e-02 1.04482e-02 2.65954e-03 5.31909e-03
3.11545e-03 1.06381e-03 1.13980e-03
FROM GROUP 13
0.00000e+00 0.00000e+00 0.00000e+00 0.00000e+00 0.00000e+00
0.00000e+00 0.00000e+00 0.00000e+00 0.00000e+00 0.00000e+00
0.00000e+00 0.00000e+00 3.25121e-01 1.83531e-01 6.00961e-02
6.10483e-03 3.13172e-02 2.18033e-02 5.54984e-03 1.10995e-02
6.50117e-03 2.21997e-03 2.37854e-03
FROM GROUP 14
0.00000e+00 0.00000e+00 0.00000e+00 0.00000e+00 0.00000e+00
0.00000e+00 0.00000e+00 0.00000e+00 0.00000e+00 0.00000e+00
0.00000e+00 0.00000e+00 3.76623e-04 3.11563e-01 1.55281e-01
1.36929e-02 6.95865e-02 4.79664e-02 1.19926e-02 2.25065e-02
1.09763e-02 2.76797e-03 1.75353e-03
FROM GROUP 15
0.00000e+00 0.00000e+00 0.00000e+00 0.00000e+00 0.00000e+00
0.00000e+00 0.00000e+00 0.00000e+00 0.00000e+00 0.00000e+00
0.00000e+00 0.00000e+00 0.00000e+00 3.23963e-03 2.63587e-01
3.58285e-02 1.37069e-01 8.70941e-02 2.17665e-02 4.14536e-02
2.03171e-02 5.19894e-03 3.25830e-03
FROM GROUP 16
0.00000e+00 0.00000e+00 0.00000e+00 0.00000e+00 0.00000e+00
0.00000e+00 0.00000e+00 0.00000e+00 0.00000e+00 0.00000e+00
0.00000e+00 0.00000e+00 0.00000e+00 2.69690e-06 3.35464e-02
1.23786e-01 2.62308e-01 1.20759e-01 3.02551e-02 5.77235e-02
2.84647e-02 7.27574e-03 4.54720e-03

FROM GROUP 17
0.00000e+00 0.00000e+00 0.00000e+00 0.00000e+00 0.00000e+00
0.00000e+00 0.00000e+00 0.00000e+00 0.00000e+00 0.00000e+00
0.00000e+00 0.00000e+00 0.00000e+00 1.06867e-07 1.19908e-03
5.40209e-03 3.13895e-01 1.92046e-01 3.96660e-02 7.63872e-02
3.79138e-02 9.67022e-03 6.01034e-03
FROM GROUP 18
0.00000e+00 0.00000e+00 0.00000e+00 0.00000e+00 0.00000e+00
0.00000e+00 0.00000e+00 0.00000e+00 0.00000e+00 0.00000e+00
0.00000e+00 0.00000e+00 0.00000e+00 0.00000e+00 7.17783e-07
2.60362e-06 1.35250e-02 3.76186e-01 9.81404e-02 1.46404e-01
6.58313e-02 1.64466e-02 1.00660e-02
FROM GROUP 19
0.00000e+00 0.00000e+00 0.00000e+00 0.00000e+00 0.00000e+00
0.00000e+00 0.00000e+00 0.00000e+00 0.00000e+00 0.00000e+00
0.00000e+00 0.00000e+00 0.00000e+00 0.00000e+00 0.00000e+00
0.00000e+00 2.18258e-04 7.47873e-02 2.63511e-01 2.90774e-01
1.09541e-01 2.63648e-02 1.56988e-02
FROM GROUP 20
0.00000e+00 0.00000e+00 0.00000e+00 0.00000e+00 0.00000e+00
0.00000e+00 0.00000e+00 0.00000e+00 0.00000e+00 0.00000e+00
0.00000e+00 0.00000e+00 0.00000e+00 0.00000e+00 0.00000e+00
0.00000e+00 4.00975e-05 9.71717e-03 3.55422e-02 4.98750e-01
2.39690e-01 5.00627e-02 2.89549e-02
FROM GROUP 21
0.00000e+00 0.00000e+00 0.00000e+00 0.00000e+00 0.00000e+00
0.00000e+00 0.00000e+00 0.00000e+00 0.00000e+00 0.00000e+00
0.00000e+00 0.00000e+00 0.00000e+00 0.00000e+00 0.00000e+00
0.00000e+00 8.94228e-06 1.85464e-03 5.72217e-03 1.39959e-01
6.62944e-01 1.53301e-01 7.02230e-02
FROM GROUP 22
0.00000e+00 0.00000e+00 0.00000e+00 0.00000e+00 0.00000e+00
0.00000e+00 0.00000e+00 0.00000e+00 0.00000e+00 0.00000e+00
0.00000e+00 0.00000e+00 0.00000e+00 0.00000e+00 0.00000e+00
0.00000e+00 5.09405e-06 1.05706e-03 3.21690e-03 6.68023e-02
3.86435e-01 6.24849e-01 2.35487e-01
FROM GROUP 23
0.00000e+00 0.00000e+00 0.00000e+00 0.00000e+00 0.00000e+00
0.00000e+00 0.00000e+00 0.00000e+00 0.00000e+00 0.00000e+00
0.00000e+00 0.00000e+00 0.00000e+00 0.00000e+00 0.00000e+00
0.00000e+00 5.48496e-06 1.11308e-03 3.33086e-03 6.73127e-02
3.05434e-01 4.20241e-01 1.10948e+00

A2.4 Fuel Composition COOREF

```
* C A S M O -3  3.4 87/07/07 STUDSVIK * EXECUTION 87/10/21   17:34:54

*  BATCH C: TAVE
*  BURNUP =      0.000 V= 0.0  TF= 900.0  TM= 585.0  BOR= 500.0


*************************************************************************
* K-INF = 1.24079  K-EFF = 1.24079                                      *
                   B2G =  0.000e+00  B2M =  3.764e-03  M2 =   63.97 *
*************************************************************************
```

MACRO GROUPS

ASSM AVERAGED CROSS SECTIONS

| GROUP | ABSORPTION | FISSION | NU-FISSION | TRANSPORT |
|---|---|---|---|---|
| 1 | 5.15107e-03 | 6.22551e-03 | 2.14587e-02 | 9.27377e-02 |
| 2 | 5.71500e-03 | 4.01742e-03 | 1.21577e-02 | 1.07634e-01 |
| 3 | 4.46123e-03 | 4.05520e-03 | 1.11572e-02 | 1.21257e-01 |
| 4 | 3.66716e-03 | 3.08462e-03 | 8.02589e-03 | 1.40726e-01 |
| 5 | 1.38390e-03 | 4.47327e-04 | 1.13325e-03 | 2.03090e-01 |
| 6 | 1.19525e-03 | 2.68654e-04 | 6.71490e-04 | 2.02824e-01 |
| 7 | 1.30360e-03 | 2.94397e-04 | 7.22177e-04 | 2.78167e-01 |
| 8 | 3.31997e-03 | 4.47903e-04 | 1.08567e-03 | 3.13226e-01 |
| 9 | 5.61422e-03 | 7.83102e-04 | 1.89487e-03 | 3.56425e-01 |
| 10 | 1.29300e-02 | 2.29364e-03 | 5.54854e-03 | 3.89090e-01 |
| 11 | 3.41363e-02 | 7.34295e-03 | 1.77611e-02 | 4.24788e-01 |
| 12 | 2.14288e-02 | 9.12489e-03 | 2.20713e-02 | 3.89369e-01 |
| 13 | 6.36374e-02 | 7.38014e-03 | 1.78511e-02 | 4.28335e-01 |
| 14 | 1.11939e-02 | 4.04610e-03 | 9.78652e-03 | 4.06311e-01 |
| 15 | 1.51439e-02 | 6.81722e-03 | 1.64895e-02 | 4.36424e-01 |
| 16 | 2.80469e-02 | 1.83578e-02 | 4.44037e-02 | 4.63097e-01 |
| 17 | 2.10021e-02 | 1.26651e-02 | 3.06344e-02 | 4.79270e-01 |
| 18 | 3.17983e-02 | 2.01340e-02 | 4.86998e-02 | 5.45880e-01 |
| 19 | 5.55338e-02 | 3.65092e-02 | 8.83070e-02 | 6.27705e-01 |
| 20 | 5.99152e-02 | 3.76365e-02 | 9.10353e-02 | 7.29670e-01 |
| 21 | 8.47396e-02 | 5.23574e-02 | 1.26643e-01 | 9.54359e-01 |
| 22 | 1.24535e-01 | 7.91944e-02 | 1.91554e-01 | 1.31962e+00 |
| 23 | 1.95510e-01 | 1.25177e-01 | 3.02776e-01 | 1.97116e+00 |

P0-SCATTERING

```
FROM GROUP  1
 2.89963e-02  2.11982e-02  9.01510e-03  8.68983e-03  8.31202e-03
 6.60934e-03  8.00991e-03  1.12496e-03  1.73301e-05  2.59925e-05
 3.53699e-07  0.00000e+00  0.00000e+00  0.00000e+00  0.00000e+00
 0.00000e+00  0.00000e+00  0.00000e+00  0.00000e+00  0.00000e+00
 0.00000e+00  0.00000e+00  0.00000e+00
FROM GROUP  2
 0.00000e+00  5.46249e-02  3.09514e-02  1.25181e-02  1.07119e-02
 8.37724e-03  1.04782e-02  1.71784e-03  3.85819e-05  5.74508e-05
 1.07485e-06  0.00000e+00  0.00000e+00  0.00000e+00  0.00000e+00
 0.00000e+00  0.00000e+00  0.00000e+00  0.00000e+00  0.00000e+00
 0.00000e+00  0.00000e+00  0.00000e+00
FROM GROUP  3
 0.00000e+00  0.00000e+00  6.81740e-02  2.80661e-02  1.64227e-02
 1.31694e-02  1.72164e-02  3.23807e-03  8.34904e-05  1.25221e-04
 3.08940e-06  0.00000e+00  0.00000e+00  0.00000e+00  0.00000e+00
 0.00000e+00  0.00000e+00  0.00000e+00  0.00000e+00  0.00000e+00
 0.00000e+00  0.00000e+00  0.00000e+00
FROM GROUP  4
 0.00000e+00  0.00000e+00  0.00000e+00  8.34278e-02  4.36803e-02
 2.06847e-02  2.86108e-02  6.97495e-03  1.91004e-04  2.69332e-04
 6.64469e-06  3.04864e-07  2.94146e-07  0.00000e+00  0.00000e+00
 0.00000e+00  0.00000e+00  0.00000e+00  0.00000e+00  0.00000e+00
 0.00000e+00  0.00000e+00  0.00000e+00
FROM GROUP  5
 0.00000e+00  0.00000e+00  0.00000e+00  0.00000e+00  1.53249e-01
 6.62440e-02  4.78138e-02  1.15636e-02  3.83590e-04  5.75329e-04
 1.41942e-05  6.51215e-07  6.28348e-07  0.00000e+00  0.00000e+00
 0.00000e+00  0.00000e+00  0.00000e+00  0.00000e+00  0.00000e+00
 0.00000e+00  0.00000e+00  0.00000e+00
FROM GROUP  6
 0.00000e+00  0.00000e+00  0.00000e+00  0.00000e+00  0.00000e+00
 1.63512e-01  1.08235e-01  2.35590e-02  8.15596e-04  1.22329e-03
 3.01799e-05  1.38467e-06  1.33602e-06  0.00000e+00  0.00000e+00
 0.00000e+00  0.00000e+00  0.00000e+00  0.00000e+00  0.00000e+00
 0.00000e+00  0.00000e+00  0.00000e+00
FROM GROUP  7
 0.00000e+00  0.00000e+00  0.00000e+00  0.00000e+00  0.00000e+00
 0.00000e+00  3.24793e-01  1.20057e-01  3.96907e-03  5.95296e-03
 1.46866e-04  6.73813e-06  6.50149e-06  2.14199e-06  5.19920e-07
 0.00000e+00  8.69113e-08  0.00000e+00  0.00000e+00  0.00000e+00
 0.00000e+00  0.00000e+00  0.00000e+00
FROM GROUP  8
 0.00000e+00  0.00000e+00  0.00000e+00  0.00000e+00  0.00000e+00
 0.00000e+00  0.00000e+00  4.90967e-01  6.83611e-02  9.58620e-02
 2.36455e-03  1.08485e-04  1.04673e-04  3.82038e-05  1.33527e-05
 1.15662e-06  6.73385e-06  4.84496e-06  1.05148e-06  2.24127e-06
 1.19644e-06  1.72885e-07  0.00000e+00
```

FROM GROUP 9
0.00000e+00 0.00000e+00 0.00000e+00 0.00000e+00 0.00000e+00
0.00000e+00 0.00000e+00 0.00000e+00 3.09098e-01 4.37953e-01
1.01436e-02 4.65376e-04 4.49042e-04 1.63890e-04 5.79155e-05
5.88320e-06 3.01803e-05 2.10116e-05 5.34838e-06 1.06968e-05
6.26527e-06 2.13936e-06 2.29082e-06
FROM GROUP 10
0.00000e+00 0.00000e+00 0.00000e+00 0.00000e+00 0.00000e+00
0.00000e+00 0.00000e+00 0.00000e+00 0.00000e+00 6.29613e-01
1.34092e-01 5.99295e-03 5.78243e-03 2.11047e-03 7.45801e-04
7.57604e-05 3.88646e-04 2.70575e-04 6.88732e-05 1.37748e-04
8.06806e-05 2.75493e-05 2.95159e-05
FROM GROUP 11
0.00000e+00 0.00000e+00 0.00000e+00 0.00000e+00 0.00000e+00
0.00000e+00 0.00000e+00 0.00000e+00 0.00000e+00 0.00000e+00
5.57982e-01 8.97417e-02 8.14835e-02 2.97400e-02 1.05095e-02
1.06758e-03 5.47658e-03 3.81285e-03 9.70531e-04 1.94107e-03
1.13691e-03 3.88214e-04 4.15941e-04
FROM GROUP 12
0.00000e+00 0.00000e+00 0.00000e+00 0.00000e+00 0.00000e+00
0.00000e+00 0.00000e+00 0.00000e+00 0.00000e+00 0.00000e+00
0.00000e+00 2.74813e-01 2.95793e-01 9.79904e-02 3.46269e-02
3.51753e-03 1.80444e-02 1.25626e-02 3.19775e-03 6.39549e-03
3.74591e-03 1.27909e-03 1.37046e-03
FROM GROUP 13
0.00000e+00 0.00000e+00 0.00000e+00 0.00000e+00 0.00000e+00
0.00000e+00 0.00000e+00 0.00000e+00 0.00000e+00 0.00000e+00
0.00000e+00 0.00000e+00 3.68126e-01 2.19201e-01 7.23554e-02
7.35020e-03 3.77057e-02 2.62511e-02 6.68198e-03 1.33637e-02
7.82737e-03 2.67283e-03 2.86375e-03
FROM GROUP 14
0.00000e+00 0.00000e+00 0.00000e+00 0.00000e+00 0.00000e+00
0.00000e+00 0.00000e+00 0.00000e+00 0.00000e+00 0.00000e+00
0.00000e+00 0.00000e+00 3.82707e-04 3.52206e-01 1.83267e-01
1.64447e-02 8.36510e-02 5.76735e-02 1.44220e-02 2.70735e-02
1.32072e-02 3.33099e-03 2.11019e-03
FROM GROUP 15
0.00000e+00 0.00000e+00 0.00000e+00 0.00000e+00 0.00000e+00
0.00000e+00 0.00000e+00 0.00000e+00 0.00000e+00 0.00000e+00
0.00000e+00 0.00000e+00 0.00000e+00 3.39289e-03 2.97430e-01
4.17696e-02 1.63159e-01 1.04639e-01 2.61676e-02 4.98825e-02
2.44850e-02 6.27040e-03 3.93083e-03
FROM GROUP 16
0.00000e+00 0.00000e+00 0.00000e+00 0.00000e+00 0.00000e+00
0.00000e+00 0.00000e+00 0.00000e+00 0.00000e+00 0.00000e+00
0.00000e+00 0.00000e+00 0.00000e+00 2.47507e-06 3.58794e-02
1.38463e-01 3.04717e-01 1.44832e-01 3.63530e-02 6.94296e-02
3.42901e-02 8.76916e-03 5.48064e-03

FROM GROUP 17
0.00000e+00 0.00000e+00 0.00000e+00 0.00000e+00 0.00000e+00
0.00000e+00 0.00000e+00 0.00000e+00 0.00000e+00 0.00000e+00
0.00000e+00 0.00000e+00 0.00000e+00 9.44824e-08 1.21857e-03
5.77010e-03 3.55365e-01 2.27069e-01 4.75557e-02 9.17743e-02
4.56293e-02 1.16376e-02 7.22780e-03
FROM GROUP 18
0.00000e+00 0.00000e+00 0.00000e+00 0.00000e+00 0.00000e+00
0.00000e+00 0.00000e+00 0.00000e+00 0.00000e+00 0.00000e+00
0.00000e+00 0.00000e+00 0.00000e+00 0.00000e+00 6.10417e-07
2.33948e-06 1.44010e-02 4.29796e-01 1.15655e-01 1.75066e-01
7.91490e-02 1.97493e-02 1.20573e-02
FROM GROUP 19
0.00000e+00 0.00000e+00 0.00000e+00 0.00000e+00 0.00000e+00
0.00000e+00 0.00000e+00 0.00000e+00 0.00000e+00 0.00000e+00
0.00000e+00 0.00000e+00 0.00000e+00 0.00000e+00 0.00000e+00
0.00000e+00 2.02709e-04 8.14741e-02 3.03437e-01 3.43867e-01
1.31908e-01 3.17705e-02 1.88581e-02
FROM GROUP 20
0.00000e+00 0.00000e+00 0.00000e+00 0.00000e+00 0.00000e+00
0.00000e+00 0.00000e+00 0.00000e+00 0.00000e+00 0.00000e+00
0.00000e+00 0.00000e+00 0.00000e+00 0.00000e+00 0.00000e+00
0.00000e+00 3.56171e-05 9.72285e-03 3.79400e-02 5.77982e-01
2.88519e-01 6.05715e-02 3.49230e-02
FROM GROUP 21
0.00000e+00 0.00000e+00 0.00000e+00 0.00000e+00 0.00000e+00
0.00000e+00 0.00000e+00 0.00000e+00 0.00000e+00 0.00000e+00
0.00000e+00 0.00000e+00 0.00000e+00 0.00000e+00 0.00000e+00
0.00000e+00 7.82621e-06 1.74806e-03 5.64953e-03 1.52362e-01
7.84510e-01 1.85771e-01 8.42571e-02
FROM GROUP 22
0.00000e+00 0.00000e+00 0.00000e+00 0.00000e+00 0.00000e+00
0.00000e+00 0.00000e+00 0.00000e+00 0.00000e+00 0.00000e+00
0.00000e+00 0.00000e+00 0.00000e+00 0.00000e+00 0.00000e+00
0.00000e+00 4.45565e-06 9.79503e-04 3.09584e-03 6.97081e-02
4.41194e-01 7.51853e-01 2.82074e-01
FROM GROUP 23
0.00000e+00 0.00000e+00 0.00000e+00 0.00000e+00 0.00000e+00
0.00000e+00 0.00000e+00 0.00000e+00 0.00000e+00 0.00000e+00
0.00000e+00 0.00000e+00 0.00000e+00 0.00000e+00 0.00000e+00
0.00000e+00 4.78590e-06 1.02238e-03 3.16508e-03 6.87003e-02
3.35852e-01 4.88934e-01 1.33875e+00

FISS SOURCE
2.57800e-02 1.13110e-01 2.12360e-01 2.28410e-01 1.76350e-01
1.11980e-01 1.15805e-01 1.58310e-02 2.02950e-04 1.80278e-04
5.06350e-07 0.00000e+00 0.00000e+00 0.00000e+00 0.00000e+00
0.00000e+00 0.00000e+00 0.00000e+00 0.00000e+00 0.00000e+00
0.00000e+00 0.00000e+00 0.00000e+00

EDIT-A GROUPS

ASSM AVERAGED CROSS SECTIONS
**********

| GROUP | ABSORPTION | FISSION | NU-FISSION | TRANSPORT |
|---|---|---|---|---|
| 1 | 8.94316e-03 | 2.60299e-03 | 6.62130e-03 | 2.78835e-01 |
| 2 | 8.45165e-02 | 5.31908e-02 | 1.28658e-01 | 9.58796e-01 |

P0-SCATTERING
FROM GROUP 1
4.76980e-01 1.60485e-02
FROM GROUP 2
1.66292e-03 1.22432e+00

FISS SOURCE
1.00001e+00 0.00000e+00

EDIT-B GROUPS

ASSM AVERAGED CROSS SECTIONS
**********

| GROUP | ABSORPTION | FISSION | NU-FISSION | TRANSPORT |
|---|---|---|---|---|
| 1 | 3.57888e-03 | 2.85541e-03 | 7.97840e-03 | 1.46500e-01 |
| 2 | 2.18925e-03 | 3.66710e-04 | 8.96480e-04 | 2.77789e-01 |
| 3 | 2.28427e-02 | 5.22283e-03 | 1.26333e-02 | 4.09500e-01 |
| 4 | 8.45165e-02 | 5.31908e-02 | 1.28658e-01 | 9.58796e-01 |

P0-SCATTERING
FROM GROUP 1
1.26236e-01 6.31561e-02 2.84842e-04 0.00000e+00
FROM GROUP 2
0.00000e+00 4.45132e-01 6.00115e-02 5.77120e-06
FROM GROUP 3
0.00000e+00 0.00000e+00 7.21645e-01 5.22958e-02
FROM GROUP 4
0.00000e+00 0.00000e+00 1.66292e-03 1.22432e+00

FISS SOURCE
7.56010e-01 2.43819e-01 1.80784e-04 0.00000e+00

A2.5 Fuel Composition C00TF

```
* C A S M O -3  3.4 87/07/07 STUDSVIK * EXECUTION 87/10/21   17:34:54

*  BATCH C  : FUEL TEMP. BRANC
*  BURNUP =      0.000 V= 0.0  TF=1500.0  TM= 585.0  BOR= 500.0


*************************************************************************
* K-INF = 1.22445  K-EFF = 1.22445                                      *
*                  B2G =  0.000e+00  B2M =  3.509e-03  M2 =   63.96 *
*************************************************************************
```

MACRO GROUPS

ASSM AVERACED CROSS SECTIONS

| GROUP | ABSORPTION | FISSION | NU-FISSION | TRANSPORT |
|---|---|---|---|---|
| 1 | 5.12490e-03 | 6.18167e-03 | 2.13076e-02 | 9.24167e-02 |
| 2 | 5.67913e-03 | 3.98844e-03 | 1.20700e-02 | 1.07285e-01 |
| 3 | 4.42992e-03 | 4.02637e-03 | 1.10779e-02 | 1.20883e-01 |
| 4 | 3.64113e-03 | 3.06267e-03 | 7.96878e-03 | 1.40291e-01 |
| 5 | 1.37429e-03 | 4.44148e-04 | 1.12520e-03 | 2.02439e-01 |
| 6 | 1.18710e-03 | 2.66730e-04 | 6.66681e-04 | 2.02190e-01 |
| 7 | 1.29489e-03 | 2.92343e-04 | 7.17138e-04 | 2.77244e-01 |
| 8 | 3.29827e-03 | 4.44952e-04 | 1.07852e-03 | 3.12264e-01 |
| 9 | 5.65482e-03 | 7.78074e-04 | 1.88270e-03 | 3.55447e-01 |
| 10 | 1.35674e-02 | 2.27301e-03 | 5.49865e-03 | 3.88687e-01 |
| 11 | 3.58606e-02 | 7.35129e-03 | 1.77813e-02 | 4.25538e-01 |
| 12 | 2.17859e-02 | 9.26118e-03 | 2.24009e-02 | 3.88931e-01 |
| 13 | 6.69110e-02 | 7.43052e-03 | 1.79730e-02 | 4.30896e-01 |
| 14 | 1.11382e-02 | 4.02173e-03 | 9.72757e-03 | 4.05418e-01 |
| 15 | 1.50660e-02 | 6.77765e-03 | 1.63938e-02 | 4.35469e-01 |
| 16 | 2.79052e-02 | 1.82563e-02 | 4.41584e-02 | 4.62083e-01 |
| 17 | 2.09079e-02 | 1.26004e-02 | 3.04779e-02 | 4.78221e-01 |
| 18 | 3.16869e-02 | 2.00578e-02 | 4.85154e-02 | 5.44647e-01 |
| 19 | 5.55141e-02 | 3.65080e-02 | 8.83041e-02 | 6.26102e-01 |
| 20 | 5.98434e-02 | 3.75986e-02 | 9.09436e-02 | 7.27796e-01 |
| 21 | 8.41669e-02 | 5.19479e-02 | 1.25653e-01 | 9.52703e-01 |
| 22 | 1.23374e-01 | 7.83192e-02 | 1.89437e-01 | 1.31941e+00 |
| 23 | 1.93790e-01 | 1.23854e-01 | 2.99576e-01 | 1.97188e+00 |

P0-SCATTERING

FROM GROUP 1

| | | | | |
|---|---|---|---|---|
| 2.88925e-02 | 2.11549e-02 | 9.00649e-03 | 8.67123e-03 | 8.28299e-03 |
| 6.58058e-03 | 7.97194e-03 | 1.12062e-03 | 1.73195e-05 | 2.59766e-05 |
| 3.53484e-07 | 0.00000e+00 | 0.00000e+00 | 0.00000e+00 | 0.00000e+00 |
| 0.00000e+00 | 0.00000e+00 | 0.00000e+00 | 0.00000e+00 | 0.00000e+00 |
| 0.00000e+00 | 0.00000e+00 | 0.00000e+00 | | |

FROM GROUP 2

| | | | | |
|---|---|---|---|---|
| 0.00000e+00 | 5.44233e-02 | 3.08811e-02 | 1.25010e-02 | 1.06847e-02 |
| 8.34825e-03 | 1.04381e-02 | 1.71314e-03 | 3.85527e-05 | 5.74099e-05 |
| 1.07408e-06 | 0.00000e+00 | 0.00000e+00 | 0.00000e+00 | 0.00000e+00 |
| 0.00000e+00 | 0.00000e+00 | 0.00000e+00 | 0.00000e+00 | 0.00000e+00 |
| 0.00000e+00 | 0.00000e+00 | 0.00000e+00 | | |

FROM GROUP 3

| | | | | |
|---|---|---|---|---|
| 0.00000e+00 | 0.00000e+00 | 6.79463e-02 | 2.80265e-02 | 1.63964e-02 |
| 1.31327e-02 | 1.71617e-02 | 3.23113e-03 | 8.34372e-05 | 1.25142e-04 |
| 3.08743e-06 | 0.00000e+00 | 0.00000e+00 | 0.00000e+00 | 0.00000e+00 |
| 0.00000e+00 | 0.00000e+00 | 0.00000e+00 | 0.00000e+00 | 0.00000e+00 |
| 0.00000e+00 | 0.00000e+00 | 0.00000e+00 | | |

FROM GROUP 4

| | | | | |
|---|---|---|---|---|
| 0.00000e+00 | 0.00000e+00 | 0.00000e+00 | 8.31605e-02 | 4.35958e-02 |
| 2.06540e-02 | 2.85379e-02 | 6.95840e-03 | 1.90807e-04 | 2.69158e-04 |
| 6.64039e-06 | 3.04667e-07 | 2.93955e-07 | 0.00000e+00 | 0.00000e+00 |
| 0.00000e+00 | 0.00000e+00 | 0.00000e+00 | 0.00000e+00 | 0.00000e+00 |
| 0.00000e+00 | 0.00000e+00 | 0.00000e+00 | | |

FROM GROUP 5

| | | | | |
|---|---|---|---|---|
| 0.00000e+00 | 0.00000e+00 | 0.00000e+00 | 0.00000e+00 | 1.52724e-01 |
| 6.60921e-02 | 4.77512e-02 | 1.15522e-02 | 3.83351e-04 | 5.74970e-04 |
| 1.41853e-05 | 6.50808e-07 | 6.27956e-07 | 0.00000e+00 | 0.00000e+00 |
| 0.00000e+00 | 0.00000e+00 | 0.00000e+00 | 0.00000e+00 | 0.00000e+00 |
| 0.00000e+00 | 0.00000e+00 | 0.00000e+00 | | |

FROM GROUP 6

| | | | | |
|---|---|---|---|---|
| 0.00000e+00 | 0.00000e+00 | 0.00000e+00 | 0.00000e+00 | 0.00000e+00 |
| 1.62964e-01 | 1.08095e-01 | 2.35417e-02 | 8.15091e-04 | 1.22254e-03 |
| 3.01613e-05 | 1.38381e-06 | 1.33519e-06 | 0.00000e+00 | 0.00000e+00 |
| 0.00000e+00 | 0.00000e+00 | 0.00000e+00 | 0.00000e+00 | 0.00000e+00 |
| 0.00000e+00 | 0.00000e+00 | 0.00000e+00 | | |

FROM GROUP 7

| | | | | |
|---|---|---|---|---|
| 0.00000e+00 | 0.00000e+00 | 0.00000e+00 | 0.00000e+00 | 0.00000e+00 |
| 0.00000e+00 | 3.23854e-01 | 1.19958e-01 | 3.96666e-03 | 5.94935e-03 |
| 1.46777e-04 | 6.73405e-06 | 6.49755e-06 | 2.14070e-06 | 5.19605e-07 |
| 0.00000e+00 | 8.68587e-08 | 0.00000e+00 | 0.00000e+00 | 0.00000e+00 |
| 0.00000e+00 | 0.00000e+00 | 0.00000e+00 | | |

FROM GROUP 8

| | | | | |
|---|---|---|---|---|
| 0.00000e+00 | 0.00000e+00 | 0.00000e+00 | 0.00000e+00 | 0.00000e+00 |
| 0.00000e+00 | 0.00000e+00 | 4.69910e-01 | 6.83018e-02 | 9.57968e-02 |
| 2.36294e-03 | 1.08411e-04 | 1.04602e-04 | 3.81779e-05 | 1.33436e-05 |
| 1.15583e-06 | 6.72928e-06 | 4.84167e-06 | 1.05076e-06 | 2.23974e-06 |
| 1.19563e-06 | 1.72767e-07 | 0.00000e+00 | | |

FROM GROUP 9
0.00000e+00 0.00000e+00 0.00000e+00 0.00000e+00 0.00000e+00
0.00000e+00 0.00000e+00 0.00000e+00 3.08171e-01 4.37582e-01
1.31367e-02 4.65063e-04 4.48740e-04 1.63780e-04 5.78766e-05
5.87924e-06 3.01600e-05 2.09975e-05 5.34478e-06 1.06896e-05
6.26106e-06 2.13792e-06 2.28928e-06
FROM GROUP 10
0.00000e+00 0.00000e+00 0.00000e+00 0.00000e+00 0.00000e+00
0.00000e+00 0.00000e+00 0.00000e+00 0.00000e+00 6.28475e-01
1.34031e-01 5.99071e-03 5.78027e-03 2.10968e-03 7.45523e-04
7.57321e-05 3.88501e-04 2.70474e-04 6.88475e-05 1.37697e-04
8.06505e-05 2.75391e-05 2.95048e-05
FROM GROUP 11
0.00000e+00 0.00000e+00 0.00000e+00 0.00000e+00 0.00000e+00
0.00000e+00 0.00000e+00 0.00000e+00 0.00000e+00 0.00000e+00
5.57342e-01 8.96134e-02 8.13991e-02 2.97092e-02 1.04986e-02
1.06648e-03 5.47091e-03 3.80890e-03 9.69526e-04 1.93906e-03
1.13574e-03 3.87812e-04 4.15511e-04
FROM GROUP 12
0.00000e+00 0.00000e+00 0.00000e+00 0.00000e+00 0.00000e+00
0.00000e+00 0.00000e+00 0.00000e+00 0.00000e+00 0.00000e+00
0.00000e+00 2.74128e-01 2.95583e-01 9.79477e-02 3.46118e-02
3.51600e-03 1.80366e-02 1.25571e-02 3.19635e-03 6.39271e-03
3.74428e-03 1.27853e-03 1.36987e-03
FROM GROUP 13
0.00000e+00 0.00000e+00 0.00000e+00 0.00000e+00 0.00000e+00
0.00000e+00 0.00000e+00 0.00000e+00 0.00000e+00 0.00000e+00
0.00000e+00 0.00000e+00 3.67466e-01 2.19333e-01 7.24217e-02
7.35693e-03 3.77403e-02 2.62751e-02 6.68810e-03 1.33760e-02
7.83454e-03 2.67528e-03 2.86638e-03
FROM GROUP 14
0.00000e+00 0.00000e+00 0.00000e+00 0.00000e+00 0.00000e+00
0.00000e+00 0.00000e+00 0.00000e+00 0.00000e+00 0.00000e+00
0.00000e+00 0.00000e+00 5.36467e-04 3.51393e-01 1.82949e-01
1.64872e-02 8.36375e-02 5.76299e-02 1.44111e-02 2.70524e-02
1.31964e-02 3.32807e-03 2.10833e-03
FROM GROUP 15
0.00000e+00 0.00000e+00 0.00000e+00 0.00000e+00 0.00000e+00
0.00000e+00 0.00000e+00 0.00000e+00 0.00000e+00 0.00000e+00
0.00000e+00 0.00000e+00 0.00000e+00 4.09957e-03 2.96243e-01
4.09468e-02 1.63821e-01 1.04614e-01 2.61508e-02 4.98506e-02
2.44694e-02 6.26641e-03 3.92833e-03
FROM GROUP 16
0.00000e+00 0.00000e+00 0.00000e+00 0.00000e+00 0.00000e+00
0.00000e+00 0.00000e+00 0.00000e+00 0.00000e+00 0.00000e+00
0.00000e+00 0.00000e+00 0.00000e+00 2.84754e-06 4.13773e-02
1.37597e-01 2.98614e-01 1.45306e-01 3.63147e-02 6.93564e-02
3.42540e-02 8.75992e-03 5.47486e-03

FROM GROUP 17
0.00000e+00 0.00000e+00 0.00000e+00 0.00000e+00 0.00000e+00
0.00000e+00 0.00000e+00 0.00000e+00 0.00000e+00 0.00000e+00
0.00000e+00 0.00000e+00 0.00000e+00 1.00682e-07 1.56850e-03
6.67305e-03 3.52977e-01 2.26991e-01 4.76409e-02 9.16736e-02
4.55724e-02 1.16230e-02 7.21876e-03
FROM GROUP 18
0.00000e+00 0.00000e+00 0.00000e+00 0.00000e+00 0.00000e+00
0.00000e+00 0.00000e+00 0.00000e+00 0.00000e+00 0.00000e+00
0.00000e+00 0.00000e+00 0.00000e+00 0.00000e+00 6.14363e-07
2.39494e-06 1.63809e-02 4.26214e-01 1.14565e-01 1.76341e-01
7.90346e-02 1.97118e-02 1.20345e-02
FROM GROUP 19
0.00000e+00 0.00000e+00 0.00000e+00 0.00000e+00 0.00000e+00
0.00000e+00 0.00000e+00 0.00000e+00 0.00000e+00 0.00000e+00
0.00000e+00 0.00000e+00 0.00000e+00 0.00000e+00 0.00000e+00
0.00000e+00 2.04974e-04 8.82115e-02 2.97475e-01 3.40571e-01
1.32059e-01 3.16599e-02 1.87912e-02
FROM GROUP 20
0.00000e+00 0.00000e+00 0.00000e+00 0.00000e+00 0.00000e+00
0.00000e+00 0.00000e+00 0.00000e+00 0.00000e+00 0.00000e+00
0.00000e+00 0.00000e+00 0.00000e+00 0.00000e+00 0.00000e+00
0.00000e+00 3.55643e-05 1.03478e-02 4.04535e-02 5.72271e-01
2.88613e-01 6.07101e-02 3.48349e-02
FROM GROUP 21
0.00000e+00 0.00000e+00 0.00000e+00 0.00000e+00 0.00000e+00
0.00000e+00 0.00000e+00 0.00000e+00 0.00000e+00 0.00000e+00
0.00000e+00 0.00000e+00 0.00000e+00 0.00000e+00 0.00000e+00
0.00000e+00 7.83289e-06 1.75187e-03 5.70434e-03 1.58779e-01
7.77318e-01 1.85322e-01 8.49908e-02
FROM GROUP 22
0.00000e+00 0.00000e+00 0.00000e+00 0.00000e+00 0.00000e+00
0.00000e+00 0.00000e+00 0.00000e+00 0.00000e+00 0.00000e+00
0.00000e+00 0.00000e+00 0.00000e+00 0.00000e+00 0.00000e+00
0.00000e+00 4.46405e-06 9.81349e-04 3.10187e-03 7.04168e-02
4.51024e-01 7.43848e-01 2.82661e-01
FROM GROUP 23
0.00000e+00 0.00000e+00 0.00000e+00 0.00000e+00 0.00000e+00
0.00000e+00 0.00000e+00 0.00000e+00 0.00000e+00 0.00000e+00
0.00000e+00 0.00000e+00 0.00000e+00 0.00000e+00 0.00000e+00
0.00000e+00 4.79555e-06 1.02443e-03 3.17144e-03 6.88969e-02
3.41790e-01 4.95638e-01 1.33317e+00

A2.6 Fuel Composition COOTM

```
* C A S M O -3  3.4 87/07/07 STUDSVIK * EXECUTION 87/10/21   17:34:54

*  BATCH C  : MODERATOR BRANCH
*  BURNUP =      0.000 V= 0.0  TF=900.0  TM= 620.0 BOR= 500.0


**************************************************************************
* K-INF = 1.22687  K-EFF = 1.22687                                       *
*                  B2G =  0.000e+00  B2M =  2.842e-03  M2 =   79.82 *
**************************************************************************
```

MACRO GROUPS

ASSM AVERAGED CROSS SECTIONS

| GROUP | ABSORPTION | FISSION | NU-FISSION | TRANSPORT |
|---|---|---|---|---|
| 1 | 4.93526e-03 | 6.18928e-03 | 2.13338e-02 | 8.57900e-02 |
| 2 | 5.57253e-03 | 3.98998e-03 | 1.20747e-02 | 9.86511e-02 |
| 3 | 4.42923e-03 | 4.02730e-03 | 1.10805e-02 | 1.11002e-01 |
| 4 | 3.63957e-03 | 3.06150e-03 | 7.96574e-03 | 1.28778e-01 |
| 5 | 1.37354e-03 | 4.43942e-04 | 1.12467e-03 | 1.86206e-01 |
| 6 | 1.18757e-03 | 2.66903e-04 | 6.67112e-04 | 1.86816e-01 |
| 7 | 1.29737e-03 | 2.93044e-04 | 7.18857e-04 | 2.56297e-01 |
| 8 | 3.31374e-03 | 4.47230e-04 | 1.08404e-03 | 2.87867e-01 |
| 9 | 5.57002e-03 | 7.82401e-04 | 1.89317e-03 | 3.25320e-01 |
| 10 | 1.27445e-02 | 2.29120e-03 | 5.54265e-03 | 3.53492e-01 |
| 11 | 3.31449e-02 | 7.31385e-03 | 1.76907e-02 | 3.84806e-01 |
| 12 | 2.11791e-02 | 9.07777e-03 | 2.19573e-02 | 3.49203e-01 |
| 13 | 6.13399e-02 | 7.34300e-03 | 1.77613e-02 | 3.86371e-01 |
| 14 | 1.08935e-02 | 4.04624e-03 | 9.78685e-03 | 3.61546e-01 |
| 15 | 1.47121e-02 | 6.79475e-03 | 1.64352e-02 | 3.87605e-01 |
| 16 | 2.75691e-02 | 1.83546e-02 | 4.43960e-02 | 4.10778e-01 |
| 17 | 2.04538e-02 | 1.26625e-02 | 3.06281e-02 | 4.23845e-01 |
| 18 | 3.10771e-02 | 2.01298e-02 | 4.86895e-02 | 4.80987e-01 |
| 19 | 5.46534e-02 | 3.65057e-02 | 8.82985e-02 | 5.52240e-01 |
| 20 | 5.88355e-02 | 3.76570e-02 | 9.10847e-02 | 6.36672e-01 |
| 21 | 8.32159e-02 | 5.23219e-02 | 1.26557e-01 | 8.25550e-01 |
| 22 | 1.22671e-01 | 7.94578e-02 | 1.92191e-01 | 1.13511e+00 |
| 23 | 1.92194e-01 | 1.25727e-01 | 3.04108e-01 | 1.68433e+00 |

P0-SCATTERING

FROM GROUP 1

| | | | | |
|---|---|---|---|---|
| 2.67942e-02 | 1.85640e-02 | 7.84374e-03 | 7.91999e-03 | 7.81480e-03 |
| 6.30200e-03 | 7.64845e-03 | 1.03901e-03 | 1.44537e-05 | 2.16783e-05 |
| 2.94994e-07 | 0.00000e+00 | 0.00000e+00 | 0.00000e+00 | 0.00000e+00 |
| 0.00000e+00 | 0.00000e+00 | 0.00000e+00 | 0.00000e+00 | 0.00000e+00 |
| 0.00000e+00 | 0.00000e+00 | 0.00000e+00 | | |

FROM GROUP 2

| | | | | |
|---|---|---|---|---|
| 0.00000e+00 | 5.03383e-02 | 2.72404e-02 | 1.09749e-02 | 9.75596e-03 |
| 7.78683e-03 | 9.75662e-03 | 1.53420e-03 | 3.22436e-05 | 4.79474e-05 |
| 8.97048e-07 | 0.00000e+00 | 0.00000e+00 | 0.00000e+00 | 0.00000e+00 |
| 0.00000e+00 | 0.00000e+00 | 0.00000e+00 | 0.00000e+00 | 0.00000e+00 |
| 0.00000e+00 | 0.00000e+00 | 0.00000e+00 | | |

FROM GROUP 3

| | | | | |
|---|---|---|---|---|
| 0.00000e+00 | 0.00000e+00 | 6.28536e-02 | 2.42727e-02 | 1.43727e-02 |
| 1.19084e-02 | 1.56745e-02 | 2.84087e-03 | 6.96843e-05 | 1.04515e-04 |
| 2.57853e-06 | 0.00000e+00 | 0.00000e+00 | 0.00000e+00 | 0.00000e+00 |
| 0.00000e+00 | 0.00000e+00 | 0.00000e+00 | 0.00000e+00 | 0.00000e+00 |
| 0.00000e+00 | 0.00000e+00 | 0.00000e+00 | | |

FROM GROUP 4

| | | | | |
|---|---|---|---|---|
| 0.00000e+00 | 0.00000e+00 | 0.00000e+00 | 7.69641e-02 | 3.81632e-02 |
| 1.80241e-02 | 2.53410e-02 | 6.11972e-03 | 1.61279e-04 | 2.24877e-04 |
| 5.54794e-06 | 2.54545e-07 | 2.45595e-07 | 0.00000e+00 | 0.00000e+00 |
| 0.00000e+00 | 0.00000e+00 | 0.00000e+00 | 0.00000e+00 | 0.00000e+00 |
| 0.00000e+00 | 0.00000e+00 | 0.00000e+00 | | |

FROM GROUP 5

| | | | | |
|---|---|---|---|---|
| 0.00000e+00 | 0.00000e+00 | 0.00000e+00 | 0.00000e+00 | 1.41817e-01 |
| 5.82403e-02 | 4.09280e-02 | 9.76179e-03 | 3.20279e-04 | 4.80372e-04 |
| 1.18514e-05 | 5.43733e-07 | 5.24640e-07 | 0.00000e+00 | 0.00000e+00 |
| 0.00000e+00 | 0.00000e+00 | 0.00000e+00 | 0.00000e+00 | 0.00000e+00 |
| 0.00000e+00 | 0.00000e+00 | 0.00000e+00 | | |

FROM GROUP 6

| | | | | |
|---|---|---|---|---|
| 0.00000e+00 | 0.00000e+00 | 0.00000e+00 | 0.00000e+00 | 0.00000e+00 |
| 1.52290e-01 | 9.23000e-02 | 1.97251e-02 | 6.80604e-04 | 1.02082e-03 |
| 2.51848e-05 | 1.15549e-06 | 1.11489e-06 | 0.00000e+00 | 0.00000e+00 |
| 0.00000e+00 | 0.00000e+00 | 0.00000e+00 | 0.00000e+00 | 0.00000e+00 |
| 0.00000e+00 | 0.00000e+00 | 0.00000e+00 | | |

FROM GROUP 7

| | | | | |
|---|---|---|---|---|
| 0.00000e+00 | 0.00000e+00 | 0.00000e+00 | 0.00000e+00 | 0.00000e+00 |
| 0.00000e+00 | 2.94796e-01 | 1.00796e-01 | 3.30842e-03 | 4.96209e-03 |
| 1.22420e-04 | 5.61657e-06 | 5.41932e-06 | 1.78546e-06 | 4.33379e-07 |
| 0.00000e+00 | 7.24449e-08 | 0.00000e+00 | 0.00000e+00 | 0.00000e+00 |
| 0.00000e+00 | 0.00000e+00 | 0.00000e+00 | | |

FROM GROUP 8

| | | | | |
|---|---|---|---|---|
| 0.00000e+00 | 0.00000e+00 | 0.00000e+00 | 0.00000e+00 | 0.00000e+00 |
| 0.00000e+00 | 0.00000e+00 | 4.34998e-01 | 5.72894e-02 | 7.97698e-02 |
| 1.96754e-03 | 9.02705e-05 | 8.70986e-05 | 3.17894e-05 | 1.11108e-05 |
| 9.62424e-07 | 5.60325e-06 | 4.03150e-06 | 8.74937e-07 | 1.86496e-06 |
| 9.95562e-07 | 1.43858e-07 | 0.00000e+00 | | |

FROM GROUP 9
0.00000e+00 0.00000e+00 0.00000e+00 0.00000e+00 0.00000e+00
0.00000e+00 0.00000e+00 0.00000e+00 2.82982e-01 3.66712e-01
8.43753e-03 3.87104e-04 3.73518e-04 1.36326e-04 4.81748e-05
4.89369e-06 2.51043e-05 1.74777e-05 4.44883e-06 8.89767e-06
5.21152e-06 1.77954e-06 1.90553e-06
FROM GROUP 10
0.00000e+00 0.00000e+00 0.00000e+00 0.00000e+00 0.00000e+00
0.00000e+00 0.00000e+00 0.00000e+00 0.00000e+00 5.51580e-01
1.11837e-01 4.98453e-03 4.80944e-03 1.75535e-03 6.20308e-04
6.30124e-05 3.23250e-04 2.25047e-04 5.72841e-05 1.14570e-04
6.71048e-05 2.29137e-05 2.45494e-05
FROM GROUP 11
0.00000e+00 0.00000e+00 0.00000e+00 0.00000e+00 0.00000e+00
0.00000e+00 0.00000e+00 0.00000e+00 0.00000e+00 0.00000e+00
4.91558e-01 7.46828e-02 6.74280e-02 2.46100e-02 8.69664e-03
8.83431e-04 4.53190e-03 3.15515e-03 8.03119e-04 1.60625e-03
9.40802e-04 3.21249e-04 3.44194e-04
FROM GROUP 12
0.00000e+00 0.00000e+00 0.00000e+00 0.00000e+00 0.00000e+00
0.00000e+00 0.00000e+00 0.00000e+00 0.00000e+00 0.00000e+00
0.00000e+00 2.48504e-01 2.48378e-01 8.14838e-02 2.87940e-02
2.92500e-03 1.50048e-02 1.04464e-02 2.65908e-03 5.31817e-03
3.11491e-03 1.06362e-03 1.13961e-03
FROM GROUP 13
0.00000e+00 0.00000e+00 0.00000e+00 0.00000e+00 0.00000e+00
0.00000e+00 0.00000e+00 0.00000e+00 0.00000e+00 0.00000e+00
0.00000e+00 0.00000e+00 3.26938e-01 1.83363e-01 6.01079e-02
6.10603e-03 3.13234e-02 2.18076e-02 5.55093e-03 1.11017e-02
6.50245e-03 2.22041e-03 2.37901e-03
FROM GROUP 14
0.00000e+00 0.00000e+00 0.00000e+00 0.00000e+00 0.00000e+00
0.00000e+00 0.00000e+00 0.00000e+00 0.00000e+00 0.00000e+00
0.00000e+00 0.00000e+00 3.84786e-04 3.12944e-01 1.55103e-01
1.36751e-02 6.94932e-02 4.79013e-02 1.19763e-02 2.24760e-02
1.09616e-02 2.76428e-03 1.75120e-03
FROM GROUP 15
0.00000e+00 0.00000e+00 0.00000e+00 0.00000e+00 0.00000e+00
0.00000e+00 0.00000e+00 0.00000e+00 0.00000e+00 0.00000e+00
0.00000e+00 0.00000e+00 0.00000e+00 3.27251e-03 2.64918e-01
3.56656e-02 1.36674e-01 8.69200e-02 2.17228e-02 4.13705e-02
2.02763e-02 5.18851e-03 3.25176e-03
FROM GROUP 16
0.00000e+00 0.00000e+00 0.00000e+00 0.00000e+00 0.00000e+00
0.00000e+00 0.00000e+00 0.00000e+00 0.00000e+00 0.00000e+00
0.00000e+00 0.00000e+00 0.00000e+00 2.70219e-06 3.37964e-02
1.25602e-01 2.61209e-01 1.20548e-01 3.01995e-02 5.76173e-02
2.84124e-02 7.26236e-03 4.53884e-03

FROM GROUP 17
0.00000e+00 0.00000e+00 0.00000e+00 0.00000e+00 0.00000e+00
0.00000e+00 0.00000e+00 0.00000e+00 0.00000e+00 0.00000e+00
0.00000e+00 0.00000e+00 0.00000e+00 1.06748e-07 1.20503e-03
5.43014e-03 3.15440e-01 1.91425e-01 3.95774e-02 7.62071e-02
3.78244e-02 9.64741e-03 5.99616e-03
FROM GROUP 18
0.00000e+00 0.00000e+00 0.00000e+00 0.00000e+00 0.00000e+00
0.00000e+00 0.00000e+00 0.00000e+00 0.00000e+00 0.00000e+00
0.00000e+00 0.00000e+00 0.00000e+00 0.00000e+00 7.15525e-07
2.59672e-06 1.35686e-02 3.77620e-01 9.77094e-02 1.45924e-01
6.56103e-02 1.63911e-02 1.00321e-02
FROM GROUP 19
0.00000e+00 0.00000e+00 0.00000e+00 0.00000e+00 0.00000e+00
0.00000e+00 0.00000e+00 0.00000e+00 0.00000e+00 0.00000e+00
0.00000e+00 0.00000e+00 0.00000e+00 0.00000e+00 0.00000e+00
0.00000e+00 2.17615e-04 7.48296e-02 2.65028e-01 2.89604e-01
1.09189e-01 2.62763e-02 1.56461e-02
FROM GROUP 20
0.00000e+00 0.00000e+00 0.00000e+00 0.00000e+00 0.00000e+00
0.00000e+00 0.00000e+00 0.00000e+00 0.00000e+00 0.00000e+00
0.00000e+00 0.00000e+00 0.00000e+00 0.00000e+00 0.00000e+00
0.00000e+00 3.99274e-05 9.69454e-03 3.54866e-02 4.99251e-01
2.38803e-01 4.98753e-02 2.88417e-02
FROM GROUP 21
0.00000e+00 0.00000e+00 0.00000e+00 0.00000e+00 0.00000e+00
0.00000e+00 0.00000e+00 0.00000e+00 0.00000e+00 0.00000e+00
0.00000e+00 0.00000e+00 0.00000e+00 0.00000e+00 0.00000e+00
0.00000e+00 8.89291e-06 1.84447e-03 5.69222e-03 1.39451e-01
6.62102e-01 1.52562e-01 6.98763e-02
FROM GROUP 22
0.00000e+00 0.00000e+00 0.00000e+00 0.00000e+00 0.00000e+00
0.00000e+00 0.00000e+00 0.00000e+00 0.00000e+00 0.00000e+00
0.00000e+00 0.00000e+00 0.00000e+00 0.00000e+00 0.00000e+00
0.00000e+00 5.06111e-06 1.05022e-03 3.19610e-03 6.63908e-02
3.84501e-01 6.23398e-01 2.34158e-01
FROM GROUP 23
0.00000e+00 0.00000e+00 0.00000e+00 0.00000e+00 0.00000e+00
0.00000e+00 0.00000e+00 0.00000e+00 0.00000e+00 0.00000e+00
0.00000e+00 0.00000e+00 0.00000e+00 0.00000e+00 0.00000e+00
0.00000e+00 5.44553e-06 1.10508e-03 3.30691e-03 6.68307e-02
3.03457e-01 4.17780e-01 1.10436e+00

A2.7 Fuel Composition A00REF

```
* C A S M O -3  3.4 87/07/07 STUDSVIK * EXECUTION 87/10/21   17:34:54

*  BATCH A: TAVE
*  BURNUP =     0.000 V= 0.0  TF= 900.0  TM= 585.0  BOR= 500.0

*********************************************************************
* K-INF = 1.09500  K-EFF = 1.09500                                  *
*                  B2G =  0.000e+00  B2M =  1.491e-03  M2 =   63.72 *
*********************************************************************
```

MACRO GROUPS

ASSM AVERAGED CROSS SECTIONS

| GROUP | ABSORPTION | FISSION | NU-FISSION | TRANSPORT |
|---|---|---|---|---|
| 1 | 5.06194e-03 | 6.16485e-03 | 2.12438e-02 | 9.28545e-02 |
| 2 | 5.66426e-03 | 3.96507e-03 | 1.19977e-02 | 1.07618e-01 |
| 3 | 4.39937e-03 | 3.99221e-03 | 1.09818e-02 | 1.21252e-01 |
| 4 | 3.58956e-03 | 3.00508e-03 | 7.81465e-03 | 1.40716e-01 |
| 5 | 1.27302e-03 | 3.34368e-04 | 8.44465e-04 | 2.03088e-01 |
| 6 | 1.08512e-03 | 1.60830e-04 | 4.01761e-04 | 2.02821e-01 |
| 7 | 1.16944e-03 | 1.72685e-04 | 4.23609e-04 | 2.78199e-01 |
| 8 | 3.10937e-03 | 2.62741e-04 | 6.36859e-04 | 3.13109e-01 |
| 9 | 5.25595e-03 | 4.59431e-04 | 1.11169e-03 | 3.56242e-01 |
| 10 | 1.17164e-02 | 1.34872e-03 | 3.26269e-03 | 3.88044e-01 |
| 11 | 2.96822e-02 | 4.37623e-03 | 1.05852e-02 | 4.20430e-01 |
| 12 | 1.44068e-02 | 5.52303e-03 | 1.33591e-02 | 3.81745e-01 |
| 13 | 5.80364e-02 | 4.50337e-03 | 1.08927e-02 | 4.22313e-01 |
| 14 | 8.86819e-03 | 2.38187e-03 | 5.76115e-03 | 4.03458e-01 |
| 15 | 1.13440e-02 | 4.04334e-03 | 9.78005e-03 | 4.31939e-01 |
| 16 | 1.91888e-02 | 1.08675e-02 | 2.62862e-02 | 4.53171e-01 |
| 17 | 1.53100e-02 | 7.47716e-03 | 1.80858e-02 | 4.72710e-01 |
| 18 | 2.25107e-02 | 1.19372e-02 | 2.88736e-02 | 5.35083e-01 |
| 19 | 3.75682e-02 | 2.18736e-02 | 5.29071e-02 | 6.06828e-01 |
| 20 | 4.14382e-02 | 2.26308e-02 | 5.47394e-02 | 7.08204e-01 |
| 21 | 5.92713e-02 | 3.19293e-02 | 7.72312e-02 | 9.20792e-01 |
| 22 | 8.78220e-02 | 4.90784e-02 | 1.18710e-01 | 1.26312e+00 |
| 23 | 1.42299e-01 | 8.03659e-02 | 1.94388e-01 | 1.87175e+00 |

P0-SCATTERING

```
FROM GROUP  1
 2.86798e-02  2.11952e-02  9.01195e-03  8.69612e-03  8.33689e-03
 6.64031e-03  8.04740e-03  1.12659e-03  1.73292e-05  2.59912e-05
 3.53682e-07  0.00000e+00  0.00000e+00  0.00000e+00  0.00000e+00
 0.00000e+00  0.00000e+00  0.00000e+00  0.00000e+00  0.00000e+00
 0.00000e+00  0.00000e+00  0.00000e+00
FROM GROUP  2
 0.00000e+00  5.42631e-02  3.09350e-02  1.25123e-02  1.07162e-02
 8.39153e-03  1.05073e-02  1.72107e-03  3.84634e-05  5.74467e-05
 1.07477e-06  0.00000e+00  0.00000e+00  0.00000e+00  0.00000e+00
 0.00000e+00  0.00000e+00  0.00000e+00  0.00000e+00  0.00000e+00
 0.00000e+00  0.00000e+00  0.00000e+00
FROM GROUP  3
 0.00000e+00  0.00000e+00  6.78223e-02  2.80228e-02  1.64398e-02
 1.32106e-02  1.72826e-02  3.24566e-03  8.34919e-05  1.25224e-04
 3.08946e-06  0.00000e+00  0.00000e+00  0.00000e+00  0.00000e+00
 0.00000e+00  0.00000e+00  0.00000e+00  0.00000e+00  0.00000e+00
 0.00000e+00  0.00000e+00  0.00000e+00
FROM GROUP  4
 0.00000e+00  0.00000e+00  0.00000e+00  8.31751e-02  4.36341e-02
 2.07043e-02  2.87106e-02  6.99898e-03  1.91165e-04  2.69324e-04
 6.64449e-06  3.04856e-07  2.94137e-07  0.00000e+00  0.00000e+00
 0.00000e+00  0.00000e+00  0.00000e+00  0.00000e+00  0.00000e+00
 0.00000e+00  0.00000e+00  0.00000e+00
FROM GROUP  5
 0.00000e+00  0.00000e+00  0.00000e+00  0.00000e+00  1.53162e-01
 6.62263e-02  4.78409e-02  1.15721e-02  3.83579e-04  5.75313e-04
 1.41937e-05  6.51196e-07  6.28330e-07  0.00000e+00  0.00000e+00
 0.00000e+00  0.00000e+00  0.00000e+00  0.00000e+00  0.00000e+00
 0.00000e+00  0.00000e+00  0.00000e+00
FROM GROUP  6
 0.00000e+00  0.00000e+00  0.00000e+00  0.00000e+00  0.00000e+00
 1.63460e-01  1.08206e-01  2.35590e-02  8.15540e-04  1.22321e-03
 3.01778e-05  1.38457e-06  1.33592e-06  0.00000e+00  0.00000e+00
 0.00000e+00  0.00000e+00  0.00000e+00  0.00000e+00  0.00000e+00
 0.00000e+00  0.00000e+00  0.00000e+00
FROM GROUP  7
 0.00000e+00  0.00000e+00  0.00000e+00  0.00000e+00  0.00000e+00
 0.00000e+00  3.24797e-01  1.20046e-01  3.96872e-03  5.95243e-03
 1.46853e-04  6.73754e-06  6.50092e-06  2.14181e-06  5.19875e-07
 0.00000e+00  8.69037e-08  0.00000e+00  0.00000e+00  0.00000e+00
 0.00000e+00  0.00000e+00  0.00000e+00
FROM GROUP  8
 0.00000e+00  0.00000e+00  0.00000e+00  0.00000e+00  0.00000e+00
 0.00000e+00  0.00000e+00  4.91034e-01  6.83543e-02  9.58506e-02
 2.36426e-03  1.08472e-04  1.04660e-04  3.81992e-05  1.33510e-05
 1.15648e-06  6.73303e-06  4.84437e-06  1.05135e-06  2.24099e-06
 1.19630e-06  1.72864e-07  0.00000e+00
```

FROM GROUP 9
0.00000e+00 0.00000e+00 0.00000e+00 0.00000e+00 0.00000e+00
0.00000e+00 0.00000e+00 0.00000e+00 3.09268e-01 4.37879e-01
1.01416e-02 4.65286e-04 4.48956e-04 1.63859e-04 5.79043e-05
5.88206e-06 3.01745e-05 2.10075e-05 5.34735e-06 1.06947e-05
6.26406e-06 2.13895e-06 2.29038e-06
FROM GROUP 10
0.00000e+00 0.00000e+00 0.00000e+00 0.00000e+00 0.00000e+00
0.00000e+00 0.00000e+00 0.00000e+00 0.00000e+00 6.29614e-01
1.34009e-01 5.98910e-03 5.77872e-03 2.10912e-03 7.45323e-04
7.57118e-05 3.88397e-04 2.70402e-04 6.88291e-05 1.37660e-04
8.06289e-05 2.75317e-05 2.94969e-05
FROM GROUP 11
0.00000e+00 0.00000e+00 0.00000e+00 0.00000e+00 0.00000e+00
0.00000e+00 0.00000e+00 0.00000e+00 0.00000e+00 0.00000e+00
5.56924e-01 8.98573e-02 8.15455e-02 2.97627e-02 1.05175e-02
1.06840e-03 5.48075e-03 3.81575e-03 9.71270e-04 1.94255e-03
1.13778e-03 3.88510e-04 4.16258e-04
FROM GROUP 12
0.00000e+00 0.00000e+00 0.00000e+00 0.00000e+00 0.00000e+00
0.00000e+00 0.00000e+00 0.00000e+00 0.00000e+00 0.00000e+00
0.00000e+00 2.74434e-01 2.94833e-01 9.76238e-02 3.44974e-02
3.50437e-03 1.79769e-02 1.25156e-02 3.18578e-03 6.37156e-03
3.73190e-03 1.27430e-03 1.36534e-03
FROM GROUP 13
0.00000e+00 0.00000e+00 0.00000e+00 0.00000e+00 0.00000e+00
0.00000e+00 0.00000e+00 0.00000e+00 0.00000e+00 0.00000e+00
0.00000e+00 0.00000e+00 3.67644e-01 2.18580e-01 7.21284e-02
7.32713e-03 3.75874e-02 2.61687e-02 6.66101e-03 1.33218e-02
7.80281e-03 2.66444e-03 2.85477e-03
FROM GROUP 14
0.00000e+00 0.00000e+00 0.00000e+00 0.00000e+00 0.00000e+00
0.00000e+00 0.00000e+00 0.00000e+00 0.00000e+00 0.00000e+00
0.00000e+00 0.00000e+00 3.85228e-04 3.51787e-01 1.82984e-01
1.64192e-02 8.35198e-02 5.75839e-02 1.43997e-02 2.70311e-02
1.31861e-02 3.32553e-03 2.10672e-03
FROM GROUP 15
0.00000e+00 0.00000e+00 0.00000e+00 0.00000e+00 0.00000e+00
0.00000e+00 0.00000e+00 0.00000e+00 0.00000e+00 0.00000e+00
0.00000e+00 0.00000e+00 0.00000e+00 3.38043e-03 2.96620e-01
4.18298e-02 1.63069e-01 1.04500e-01 2.61327e-02 4.98166e-02
2.44530e-02 6.26224e-03 3.92570e-03
FROM GROUP 16
0.00000e+00 0.00000e+00 0.00000e+00 0.00000e+00 0.00000e+00
0.00000e+00 0.00000e+00 0.00000e+00 0.00000e+00 0.00000e+00
0.00000e+00 0.00000e+00 0.00000e+00 2.46812e-06 3.58438e-02
1.38153e-01 3.03813e-01 1.44179e-01 3.61867e-02 6.91120e-02
3.41333e-02 8.72905e-03 5.45557e-03

FROM GROUP 17
0.00000e+00 0.00000e+00 0.00000e+00 0.00000e+00 0.00000e+00
0.00000e+00 0.00000e+00 0.00000e+00 0.00000e+00 0.00000e+00
0.00000e+00 0.00000e+00 0.00000e+00 9.39164e-08 1.21424e-03
5.74757e-03 3.54551e-01 2.26568e-01 4.74133e-02 9.14979e-02
4.54924e-02 1.16026e-02 7.20603e-03
FROM GROUP 18
0.00000e+00 0.00000e+00 0.00000e+00 0.00000e+00 0.00000e+00
0.00000e+00 0.00000e+00 0.00000e+00 0.00000e+00 0.00000e+00
0.00000e+00 0.00000e+00 0.00000e+00 0.00000e+00 6.07186e-07
2.32766e-06 1.43722e-02 4.28537e-01 1.15164e-01 1.74177e-01
7.87215e-02 1.96425e-02 1.19921e-02
FROM GROUP 19
0.00000e+00 0.00000e+00 0.00000e+00 0.00000e+00 0.00000e+00
0.00000e+00 0.00000e+00 0.00000e+00 0.00000e+00 0.00000e+00
0.00000e+00 0.00000e+00 0.00000e+00 0.00000e+00 0.00000e+00
0.00000e+00 2.00736e-04 8.10494e-02 3.02178e-01 3.41102e-01
1.30593e-01 3.14489e-02 1.86672e-02
FROM GROUP 20
0.00000e+00 0.00000e+00 0.00000e+00 0.00000e+00 0.00000e+00
0.00000e+00 0.00000e+00 0.00000e+00 0.00000e+00 0.00000e+00
0.00000e+00 0.00000e+00 0.00000e+00 0.00000e+00 0.00000e+00
0.00000e+00 3.45043e-05 9.40785e-03 3.66642e-02 5.73026e-01
2.88630e-01 6.03521e-02 3.47656e-02
FROM GROUP 21
0.00000e+00 0.00000e+00 0.00000e+00 0.00000e+00 0.00000e+00
0.00000e+00 0.00000e+00 0.00000e+00 0.00000e+00 0.00000e+00
0.00000e+00 0.00000e+00 0.00000e+00 0.00000e+00 0.00000e+00
0.00000e+00 7.66976e-06 1.71307e-03 5.53782e-03 1.49586e-01
7.76347e-01 1.84312e-01 8.32718e-02
FROM GROUP 22
0.00000e+00 0.00000e+00 0.00000e+00 0.00000e+00 0.00000e+00
0.00000e+00 0.00000e+00 0.00000e+00 0.00000e+00 0.00000e+00
0.00000e+00 0.00000e+00 0.00000e+00 0.00000e+00 0.00000e+00
0.00000e+00 4.35294e-06 9.56906e-04 3.02438e-03 6.81361e-02
4.32529e-01 7.39776e-01 2.76866e-01
FROM GROUP 23
0.00000e+00 0.00000e+00 0.00000e+00 0.00000e+00 0.00000e+00
0.00000e+00 0.00000e+00 0.00000e+00 0.00000e+00 0.00000e+00
0.00000e+00 0.00000e+00 0.00000e+00 0.00000e+00 0.00000e+00
0.00000e+00 4.63208e-06 9.89520e-04 3.06336e-03 6.64979e-02
3.25711e-01 4.75510e-01 1.30440e+00

FISS SOURCE
2.57800e-02 1.13110e-01 2.12360e-01 2.28410e-01 1.76350e-01
1.11980e-01 1.15805e-01 1.58310e-02 2.02950e-04 1.80278e-04
5.06350e-07 0.00000e+00 0.00000e+00 0.00000e+00 0.00000e+00
0.00000e+00 0.00000e+00 0.00000e+00 0.00000e+00 0.00000e+00
0.00000e+00 0.00000e+00 0.00000e+00

EDIT-A GROUPS

ASSM AVERAGED CROSS SECTIONS
**********

| GROUP | ABSORPTION | FISSION | NU-FISSION | TRANSPORT |
|---|---|---|---|---|
| 1 | 8.14279e-03 | 1.90235e-03 | 4.91318e-03 | 2.80545e-01 |
| 2 | 6.18380e-02 | 3.40252e-02 | 8.23001e-02 | 9.50512e-01 |

P0-SCATTERING
FROM GROUP 1
4.81316e-01 1.72664e-02
FROM GROUP 2
1.29004e-03 1.23494e+00

FISS SOURCE
1.00001e+00 0.00000e+00

EDIT-B GROUPS

ASSM AVERAGED CROSS SECTIONS
**********

| GROUP | ABSORPTION | FISSION | NU-FISSION | TRANSPORT |
|---|---|---|---|---|
| 1 | 3.50985e-03 | 2.78714e-03 | 7.80007e-03 | 1.46242e-01 |
| 2 | 2.03107e-03 | 2.16296e-04 | 5.28714e-04 | 2.78065e-01 |
| 3 | 1.98385e-02 | 3.14557e-03 | 7.60869e-03 | 4.06718e-01 |
| 4 | 6.18380e-02 | 3.40252e-02 | 8.23001e-02 | 9.50512e-01 |

P0-SCATTERING
FROM GROUP 1
1.25814e-01 6.29696e-02 2.83413e-04 0.00000e+00
FROM GROUP 2
0.00000e+00 4.45681e-01 6.05838e-02 5.83050e-06
FROM GROUP 3
0.00000e+00 0.00000e+00 7.18899e-01 5.41322e-02
FROM GROUP 4
0.00000e+00 0.00000e+00 1.29004e-03 1.23494e+00

FISS SOURCE
7.56010e-01 2.43819e-01 1.80784e-04 0.00000e+00

A2.8 Fuel Composition A00TF

```
* C A S M O -3  3.4 87/07/07 STUDSVIK * EXECUTION 87/10/21   17:34:54

*  BATCH A  : FUEL TEMP. BRANC
*  BURNUP =      0.000 V= 0.0  TF=1500.0  TM= 585.0  BOR= 500.0


*************************************************************************
* K-INF = 1.07979  K-EFF = 1.07979                                      *
*                  B2G =  0.000e+00  B2M =  1.252e-03  M2 =   63.73 *
*************************************************************************
```

MACRO GROUPS

ASSM AVERAGED CROSS SECTIONS

| GROUP | ABSORPTION | FISSION | NU-FISSION | TRANSPORT |
|---|---|---|---|---|
| 1 | 5.03629e-03 | 6.12133e-03 | 2.10938e-02 | 9.25304e-02 |
| 2 | 5.62937e-03 | 3.93690e-03 | 1.19125e-02 | 1.07280e-01 |
| 3 | 4.36849e-03 | 3.96381e-03 | 1.09037e-02 | 1.20877e-01 |
| 4 | 3.56440e-03 | 2.98397e-03 | 7.75976e-03 | 1.40293e-01 |
| 5 | 1.26417e-03 | 3.31985e-04 | 8.38447e-04 | 2.02433e-01 |
| 6 | 1.07773e-03 | 1.59674e-04 | 3.98873e-04 | 2.02182e-01 |
| 7 | 1.16165e-03 | 1.71477e-04 | 4.20645e-04 | 2.77271e-01 |
| 8 | 3.08902e-03 | 2.61008e-04 | 6.32658e-04 | 3.12146e-01 |
| 9 | 5.30062e-03 | 4.56466e-04 | 1.10451e-03 | 3.55266e-01 |
| 10 | 1.23741e-02 | 1.33615e-03 | 3.23227e-03 | 3.87660e-01 |
| 11 | 3.13552e-02 | 4.36828e-03 | 1.05660e-02 | 4.21121e-01 |
| 12 | 1.45375e-02 | 5.57321e-03 | 1.34805e-02 | 3.81068e-01 |
| 13 | 6.11776e-02 | 4.51405e-03 | 1.09186e-02 | 4.24730e-01 |
| 14 | 8.82551e-03 | 2.36743e-03 | 5.72622e-03 | 4.02577e-01 |
| 15 | 1.12885e-02 | 4.01989e-03 | 9.72332e-03 | 4.31006e-01 |
| 16 | 1.90934e-02 | 1.08057e-02 | 2.61367e-02 | 4.52199e-01 |
| 17 | 1.52453e-02 | 7.43925e-03 | 1.79941e-02 | 4.71679e-01 |
| 18 | 2.24429e-02 | 1.18986e-02 | 2.87802e-02 | 5.33817e-01 |
| 19 | 3.75809e-02 | 2.18973e-02 | 5.29644e-02 | 6.05045e-01 |
| 20 | 4.13961e-02 | 2.26182e-02 | 5.47090e-02 | 7.06163e-01 |
| 21 | 5.88707e-02 | 3.16647e-02 | 7.65912e-02 | 9.19226e-01 |
| 22 | 8.69542e-02 | 4.84902e-02 | 1.17287e-01 | 1.26339e+00 |
| 23 | 1.40897e-01 | 7.93460e-02 | 1.91921e-01 | 1.87357e+00 |

P0-SCATTERING

```
FROM GROUP  1
 2.85775e-02  2.11513e-02  9.00310e-03  8.67723e-03  8.30748e-03
 6.61119e-03  8.00899e-03  1.12221e-03  1.73181e-05  2.59745e-05
 3.53455e-07  0.00000e+00  0.00000e+00  0.00000e+00  0.00000e+00
 0.00000e+00  0.00000e+00  0.00000e+00  0.00000e+00  0.00000e+00
 0.00000e+00  0.00000e+00  0.00000e+00
FROM GROUP  2
 0.00000e+00  5.40700e-02  3.08682e-02  1.24965e-02  1.06900e-02
 8.36335e-03  1.04681e-02  1.71653e-03  3.84391e-05  5.74120e-05
 1.07412e-06  0.00000e+00  0.00000e+00  0.00000e+00  0.00000e+00
 0.00000e+00  0.00000e+00  0.00000e+00  0.00000e+00  0.00000e+00
 0.00000e+00  0.00000e+00  0.00000e+00
FROM GROUP  3
 0.00000e+00  0.00000e+00  6.75971e-02  2.79836e-02  1.64133e-02
 1.31736e-02  1.72274e-02  3.23867e-03  8.34388e-05  1.25144e-04
 3.08749e-06  0.00000e+00  0.00000e+00  0.00000e+00  0.00000e+00
 0.00000e+00  0.00000e+00  0.00000e+00  0.00000e+00  0.00000e+00
 0.00000e+00  0.00000e+00  0.00000e+00
FROM GROUP  4
 0.00000e+00  0.00000e+00  0.00000e+00  8.29167e-02  4.35536e-02
 2.06751e-02  2.86394e-02  6.98285e-03  1.90982e-04  2.69172e-04
 6.64074e-06  3.04683e-07  2.93971e-07  0.00000e+00  0.00000e+00
 0.00000e+00  0.00000e+00  0.00000e+00  0.00000e+00  0.00000e+00
 0.00000e+00  0.00000e+00  0.00000e+00
FROM GROUP  5
 0.00000e+00  0.00000e+00  0.00000e+00  0.00000e+00  1.52634e-01
 6.60733e-02  4.77771e-02  1.15604e-02  3.83332e-04  5.74942e-04
 1.41846e-05  6.50776e-07  6.27925e-07  0.00000e+00  0.00000e+00
 0.00000e+00  0.00000e+00  0.00000e+00  0.00000e+00  0.00000e+00
 0.00000e+00  0.00000e+00  0.00000e+00
FROM GROUP  6
 0.00000e+00  0.00000e+00  0.00000e+00  0.00000e+00  0.00000e+00
 1.62909e-01  1.08064e-01  2.35413e-02  8.15017e-04  1.22242e-03
 3.01585e-05  1.38369e-06  1.33507e-06  0.00000e+00  0.00000e+00
 0.00000e+00  0.00000e+00  0.00000e+00  0.00000e+00  0.00000e+00
 0.00000e+00  0.00000e+00  0.00000e+00
FROM GROUP  7
 0.00000e+00  0.00000e+00  0.00000e+00  0.00000e+00  0.00000e+00
 0.00000e+00  3.23852e-01  1.19946e-01  3.96626e-03  5.94874e-03
 1.46762e-04  6.73336e-06  6.49689e-06  2.14048e-06  5.19552e-07
 0.00000e+00  8.68498e-08  0.00000e+00  0.00000e+00  0.00000e+00
 0.00000e+00  0.00000e+00  0.00000e+00
FROM GROUP  8
 0.00000e+00  0.00000e+00  0.00000e+00  0.00000e+00  0.00000e+00
 0.00000e+00  0.00000e+00  4.89974e-01  6.82948e-02  9.57852e-02
 2.36265e-03  1.08398e-04  1.04589e-04  3.81732e-05  1.33419e-05
 1.15569e-06  6.72845e-06  4.84107e-06  1.05063e-06  2.23947e-06
 1.19548e-06  1.72746e-07  0.00000e+00
```

FROM GROUP 9
0.00000e+00 0.00000e+00 0.00000e+00 0.00000e+00 0.00000e+00
0.00000e+00 0.00000e+00 0.00000e+00 3.08340e-01 4.37509e-01
1.01348e-02 4.64974e-04 4.48655e-04 1.63749e-04 5.78655e-05
5.87812e-06 3.01542e-05 2.09935e-05 5.34376e-06 1.06875e-05
6.25986e-06 2.13751e-06 2.28885e-06
FROM GROUP 10
0.00000e+00 0.00000e+00 0.00000e+00 0.00000e+00 0.00000e+00
0.00000e+00 0.00000e+00 0.00000e+00 0.00000e+00 6.28481e-01
1.33950e-01 5.98699e-03 5.77668e-03 2.10837e-03 7.45060e-04
7.56851e-05 3.88260e-04 2.70306e-04 6.88047e-05 1.37611e-04
8.06004e-05 2.75219e-05 2.94865e-05
FROM GROUP 11
0.00000e+00 0.00000e+00 0.00000e+00 0.00000e+00 0.00000e+00
0.00000e+00 0.00000e+00 0.00000e+00 0.00000e+00 0.00000e+00
5.56257e-01 8.97337e-02 8.14648e-02 2.97332e-02 1.05071e-02
1.06734e-03 5.47533e-03 3.81198e-03 9.70309e-04 1.94063e-03
1.13665e-03 3.88125e-04 4.15846e-04
FROM GROUP 12
0.00000e+00 0.00000e+00 0.00000e+00 0.00000e+00 0.00000e+00
0.00000e+00 0.00000e+00 0.00000e+00 0.00000e+00 0.00000e+00
0.00000e+00 2.73744e-01 2.94591e-01 9.75698e-02 3.44783e-02
3.50243e-03 1.79670e-02 1.25086e-02 3.18402e-03 6.36804e-03
3.72983e-03 1.27360e-03 1.36458e-03
FROM GROUP 13
0.00000e+00 0.00000e+00 0.00000e+00 0.00000e+00 0.00000e+00
0.00000e+00 0.00000e+00 0.00000e+00 0.00000e+00 0.00000e+00
0.00000e+00 0.00000e+00 3.66970e-01 2.18694e-01 7.21882e-02
7.33321e-03 3.76186e-02 2.61904e-02 6.66654e-03 1.33328e-02
7.80928e-03 2.66665e-03 2.85713e-03
FROM GROUP 14
0.00000e+00 0.00000e+00 0.00000e+00 0.00000e+00 0.00000e+00
0.00000e+00 0.00000e+00 0.00000e+00 0.00000e+00 0.00000e+00
0.00000e+00 0.00000e+00 5.39860e-04 3.50971e-01 1.82666e-01
1.64619e-02 8.35066e-02 5.75404e-02 1.43888e-02 2.70100e-02
1.31753e-02 3.32259e-03 2.10485e-03
FROM GROUP 15
0.00000e+00 0.00000e+00 0.00000e+00 0.00000e+00 0.00000e+00
0.00000e+00 0.00000e+00 0.00000e+00 0.00000e+00 0.00000e+00
0.00000e+00 0.00000e+00 0.00000e+00 4.08608e-03 2.95451e-01
4.09921e-02 1.63727e-01 1.04476e-01 2.61161e-02 4.97849e-02
2.44376e-02 6.25830e-03 3.92322e-03
FROM GROUP 16
0.00000e+00 0.00000e+00 0.00000e+00 0.00000e+00 0.00000e+00
0.00000e+00 0.00000e+00 0.00000e+00 0.00000e+00 0.00000e+00
0.00000e+00 0.00000e+00 0.00000e+00 2.84400e-06 4.13892e-02
1.37279e-01 2.97661e-01 1.44664e-01 3.61498e-02 6.90414e-02
3.40984e-02 8.72013e-03 5.44999e-03
FROM GROUP 17
0.00000e+00 0.00000e+00 0.00000e+00 0.00000e+00 0.00000e+00
0.00000e+00 0.00000e+00 0.00000e+00 0.00000e+00 0.00000e+00
0.00000e+00 0.00000e+00 0.00000e+00 1.00082e-07 1.56447e-03
6.64965e-03 3.52132e-01 2.26492e-01 4.74985e-02 9.13950e-02
4.54344e-02 1.15878e-02 7.19680e-03
FROM GROUP 18
0.00000e+00 0.00000e+00 0.00000e+00 0.00000e+00 0.00000e+00
0.00000e+00 0.00000e+00 0.00000e+00 0.00000e+00 0.00000e+00
0.00000e+00 0.00000e+00 0.00000e+00 0.00000e+00 6.10981e-07
2.38303e-06 1.63729e-02 4.24866e-01 1.14031e-01 1.75412e-01
7.85797e-02 1.95981e-02 1.19650e-02
FROM GROUP 19
0.00000e+00 0.00000e+00 0.00000e+00 0.00000e+00 0.00000e+00
0.00000e+00 0.00000e+00 0.00000e+00 0.00000e+00 0.00000e+00
0.00000e+00 0.00000e+00 0.00000e+00 0.00000e+00 0.00000e+00
0.00000e+00 2.02922e-04 8.79061e-02 2.96022e-01 3.37546e-01
1.30662e-01 3.13148e-02 1.85863e-02
FROM GROUP 20
0.00000e+00 0.00000e+00 0.00000e+00 0.00000e+00 0.00000e+00
0.00000e+00 0.00000e+00 0.00000e+00 0.00000e+00 0.00000e+00
0.00000e+00 0.00000e+00 0.00000e+00 0.00000e+00 0.00000e+00
0.00000e+00 3.44535e-05 1.00240e-02 3.91804e-02 5.67240e-01
2.88525e-01 6.04736e-02 3.46593e-02
FROM GROUP 21
0.00000e+00 0.00000e+00 0.00000e+00 0.00000e+00 0.00000e+00
0.00000e+00 0.00000e+00 0.00000e+00 0.00000e+00 0.00000e+00
0.00000e+00 0.00000e+00 0.00000e+00 0.00000e+00 0.00000e+00
0.00000e+00 7.67822e-06 1.71731e-03 5.59478e-03 1.56204e-01
7.68983e-01 1.83761e-01 8.40312e-02
FROM GROUP 22
0.00000e+00 0.00000e+00 0.00000e+00 0.00000e+00 0.00000e+00
0.00000e+00 0.00000e+00 0.00000e+00 0.00000e+00 0.00000e+00
0.00000e+00 0.00000e+00 0.00000e+00 0.00000e+00 0.00000e+00
0.00000e+00 4.36259e-06 9.59029e-04 3.03130e-03 6.88930e-02
4.42953e-01 7.31419e-01 2.77480e-01
FROM GROUP 23
0.00000e+00 0.00000e+00 0.00000e+00 0.00000e+00 0.00000e+00
0.00000e+00 0.00000e+00 0.00000e+00 0.00000e+00 0.00000e+00
0.00000e+00 0.00000e+00 0.00000e+00 0.00000e+00 0.00000e+00
0.00000e+00 4.64471e-06 9.92215e-04 3.07169e-03 6.67416e-02
3.32261e-01 4.83014e-01 1.29879e+00

A2.9 Fuel Composition A00TM

```
* C A S M O -3  3.4 87/07/07 STUDSVIK * EXECUTION 87/10/21   17:34:54

*  BATCH A  : MODERATOR BRANCH
*  BURNUP =     0.000 V= 0.0  TF=900.0  TM= 620.0 BOR= 500.0

**********************************************************************
* K-INF = 1.09096  K-EFF = 1.09096                                   *
*                  B2G =  0.000e+00  B2M =  1.141e-03  M2 =   79.76 *
**********************************************************************
```

MACRO GROUPS

ASSM AVERAGED CROSS SECTIONS

| GROUP | ABSORPTION | FISSION | NU-FISSION | TRANSPORT |
|---|---|---|---|---|
| 1 | 4.84674e-03 | 6.12903e-03 | 2.11204e-02 | 8.59084e-02 |
| 2 | 5.52203e-03 | 3.93790e-03 | 1.19155e-02 | 9.86348e-02 |
| 3 | 4.36760e-03 | 3.96457e-03 | 1.09057e-02 | 1.10993e-01 |
| 4 | 3.56245e-03 | 2.98247e-03 | 7.75586e-03 | 1.28767e-01 |
| 5 | 1.26346e-03 | 3.31831e-04 | 8.38057e-04 | 1.86203e-01 |
| 6 | 1.07813e-03 | 1.59778e-04 | 3.99132e-04 | 1.86809e-01 |
| 7 | 1.16382e-03 | 1.71892e-04 | 4.21662e-04 | 2.56331e-01 |
| 8 | 3.10339e-03 | 2.62344e-04 | 6.35898e-04 | 2.87751e-01 |
| 9 | 5.20696e-03 | 4.59019e-04 | 1.11069e-03 | 3.25138e-01 |
| 10 | 1.15183e-02 | 1.34745e-03 | 3.25961e-03 | 3.52457e-01 |
| 11 | 2.87019e-02 | 4.36342e-03 | 1.05542e-02 | 3.80547e-01 |
| 12 | 1.42125e-02 | 5.50015e-03 | 1.33038e-02 | 3.41781e-01 |
| 13 | 5.57101e-02 | 4.48797e-03 | 1.08555e-02 | 3.80436e-01 |
| 14 | 8.56902e-03 | 2.38202e-03 | 5.76151e-03 | 3.58759e-01 |
| 15 | 1.09269e-02 | 4.03262e-03 | 9.75411e-03 | 3.83236e-01 |
| 16 | 1.87141e-02 | 1.08653e-02 | 2.62809e-02 | 4.01094e-01 |
| 17 | 1.47643e-02 | 7.47556e-03 | 1.80820e-02 | 4.17471e-01 |
| 18 | 2.17907e-02 | 1.19324e-02 | 2.88619e-02 | 4.70548e-01 |
| 19 | 3.66832e-02 | 2.18635e-02 | 5.28826e-02 | 5.32136e-01 |
| 20 | 4.03136e-02 | 2.26287e-02 | 5.47343e-02 | 6.16056e-01 |
| 21 | 5.76416e-02 | 3.18741e-02 | 7.70976e-02 | 7.93997e-01 |
| 22 | 8.56817e-02 | 4.91771e-02 | 1.18949e-01 | 1.08283e+00 |
| 23 | 1.38575e-01 | 8.05744e-02 | 1.94892e-01 | 1.59414e+00 |

P0-SCATTERING

FROM GROUP 1

| | | | | |
|---|---|---|---|---|
| 2.64803e-02 | 1.85617e-02 | 7.84093e-03 | 7.92650e-03 | 7.83973e-03 |
| 6.33294e-03 | 7.68588e-03 | 1.04066e-03 | 1.44535e-05 | 2.16780e-05 |
| 2.94990e-07 | 0.00000e+00 | 0.00000e+00 | 0.00000e+00 | 0.00000e+00 |
| 0.00000e+00 | 0.00000e+00 | 0.00000e+00 | 0.00000e+00 | 0.00000e+00 |
| 0.00000e+00 | 0.00000e+00 | 0.00000e+00 | | |

FROM GROUP 2

| | | | | |
|---|---|---|---|---|
| 0.00000e+00 | 4.99789e-02 | 2.72244e-02 | 1.09692e-02 | 9.76018e-03 |
| 7.80101e-03 | 9.78546e-03 | 1.53742e-03 | 3.21267e-05 | 4.79444e-05 |
| 8.96992e-07 | 0.00000e+00 | 0.00000e+00 | 0.00000e+00 | 0.00000e+00 |
| 0.00000e+00 | 0.00000e+00 | 0.00000e+00 | 0.00000e+00 | 0.00000e+00 |
| 0.00000e+00 | 0.00000e+00 | 0.00000e+00 | | |

FROM GROUP 3

| | | | | |
|---|---|---|---|---|
| 0.00000e+00 | 0.00000e+00 | 6.25024e-02 | 2.42293e-02 | 1.43893e-02 |
| 1.19490e-02 | 1.57398e-02 | 2.84833e-03 | 6.96846e-05 | 1.04515e-04 |
| 2.57855e-06 | 0.00000e+00 | 0.00000e+00 | 0.00000e+00 | 0.00000e+00 |
| 0.00000e+00 | 0.00000e+00 | 0.00000e+00 | 0.00000e+00 | 0.00000e+00 |
| 0.00000e+00 | 0.00000e+00 | 0.00000e+00 | | |

FROM GROUP 4

| | | | | |
|---|---|---|---|---|
| 0.00000e+00 | 0.00000e+00 | 0.00000e+00 | 7.67125e-02 | 3.81173e-02 |
| 1.80435e-02 | 2.54399e-02 | 6.14354e-03 | 1.61439e-04 | 2.24871e-04 |
| 5.54778e-06 | 2.54537e-07 | 2.45588e-07 | 0.00000e+00 | 0.00000e+00 |
| 0.00000e+00 | 0.00000e+00 | 0.00000e+00 | 0.00000e+00 | 0.00000e+00 |
| 0.00000e+00 | 0.00000e+00 | 0.00000e+00 | | |

FROM GROUP 5

| | | | | |
|---|---|---|---|---|
| 0.00000e+00 | 0.00000e+00 | 0.00000e+00 | 0.00000e+00 | 1.41728e-01 |
| 5.82226e-02 | 4.09550e-02 | 9.77024e-03 | 3.20271e-04 | 4.80359e-04 |
| 1.18511e-05 | 5.43718e-07 | 5.24627e-07 | 0.00000e+00 | 0.00000e+00 |
| 0.00000e+00 | 0.00000e+00 | 0.00000e+00 | 0.00000e+00 | 0.00000e+00 |
| 0.00000e+00 | 0.00000e+00 | 0.00000e+00 | | |

FROM GROUP 6

| | | | | |
|---|---|---|---|---|
| 0.00000e+00 | 0.00000e+00 | 0.00000e+00 | 0.00000e+00 | 0.00000e+00 |
| 1.52236e-01 | 9.22709e-02 | 1.97251e-02 | 6.80550e-04 | 1.02074e-03 |
| 2.51828e-05 | 1.15540e-06 | 1.11480e-06 | 0.00000e+00 | 0.00000e+00 |
| 0.00000e+00 | 0.00000e+00 | 0.00000e+00 | 0.00000e+00 | 0.00000e+00 |
| 0.00000e+00 | 0.00000e+00 | 0.00000e+00 | | |

FROM GROUP 7

| | | | | |
|---|---|---|---|---|
| 0.00000e+00 | 0.00000e+00 | 0.00000e+00 | 0.00000e+00 | 0.00000e+00 |
| 0.00000e+00 | 2.94805e-01 | 1.00789e-01 | 3.30819e-03 | 4.96174e-03 |
| 1.22412e-04 | 5.61618e-06 | 5.41894e-06 | 1.78534e-06 | 4.33349e-07 |
| 0.00000e+00 | 7.24399e-08 | 0.00000e+00 | 0.00000e+00 | 0.00000e+00 |
| 0.00000e+00 | 0.00000e+00 | 0.00000e+00 | | |

FROM GROUP 8

| | | | | |
|---|---|---|---|---|
| 0.00000e+00 | 0.00000e+00 | 0.00000e+00 | 0.00000e+00 | 0.00000e+00 |
| 0.00000e+00 | 0.00000e+00 | 4.35070e-01 | 5.72841e-02 | 7.97607e-02 |
| 1.96731e-03 | 9.02600e-05 | 8.70884e-05 | 3.17857e-05 | 1.11095e-05 |
| 9.62311e-07 | 5.60259e-06 | 4.03102e-06 | 8.74834e-07 | 1.86474e-06 |
| 9.95445e-07 | 1.43841e-07 | 0.00000e+00 | | |

FROM GROUP 9
0.00000e+00 0.00000e+00 0.00000e+00 0.00000e+00 0.00000e+00
0.00000e+00 0.00000e+00 0.00000e+00 2.83157e-01 3.66653e-01
8.43593e-03 3.87031e-04 3.73447e-04 1.36300e-04 4.81656e-05
4.89276e-06 2.50995e-05 1.74744e-05 4.44799e-06 8.89598e-06
5.21054e-06 1.77921e-06 1.90517e-06
FROM GROUP 10
0.00000e+00 0.00000e+00 0.00000e+00 0.00000e+00 0.00000e+00
0.00000e+00 0.00000e+00 0.00000e+00 0.00000e+00 5.51632e-01
1.11768e-01 4.98131e-03 4.80633e-03 1.75422e-03 6.19907e-04
6.29717e-05 3.23041e-04 2.24901e-04 5.72471e-05 1.14496e-04
6.70614e-05 2.28989e-05 2.45335e-05
FROM GROUP 11
0.00000e+00 0.00000e+00 0.00000e+00 0.00000e+00 0.00000e+00
0.00000e+00 0.00000e+00 0.00000e+00 0.00000e+00 0.00000e+00
4.90665e-01 7.48315e-02 6.75179e-02 2.46428e-02 8.70824e-03
8.84609e-04 4.53794e-03 3.15936e-03 8.04190e-04 1.60839e-03
9.42056e-04 3.21677e-04 3.44653e-04
FROM GROUP 12
0.00000e+00 0.00000e+00 0.00000e+00 0.00000e+00 0.00000e+00
0.00000e+00 0.00000e+00 0.00000e+00 0.00000e+00 0.00000e+00
0.00000e+00 2.48220e-01 2.47599e-01 8.11808e-02 2.86869e-02
2.91412e-03 1.49490e-02 1.04075e-02 2.64919e-03 5.29838e-03
3.10333e-03 1.05967e-03 1.13537e-03
FROM GROUP 13
0.00000e+00 0.00000e+00 0.00000e+00 0.00000e+00 0.00000e+00
0.00000e+00 0.00000e+00 0.00000e+00 0.00000e+00 0.00000e+00
0.00000e+00 0.00000e+00 3.26577e-01 1.82849e-01 5.99174e-02
6.08668e-03 3.12241e-02 2.17385e-02 5.53334e-03 1.10665e-02
6.48184e-03 2.21337e-03 2.37147e-03
FROM GROUP 14
0.00000e+00 0.00000e+00 0.00000e+00 0.00000e+00 0.00000e+00
0.00000e+00 0.00000e+00 0.00000e+00 0.00000e+00 0.00000e+00
0.00000e+00 0.00000e+00 3.87384e-04 3.12583e-01 1.54860e-01
1.36538e-02 6.93835e-02 4.78265e-02 1.19576e-02 2.24406e-02
1.09439e-02 2.75967e-03 1.74828e-03
FROM GROUP 15
0.00000e+00 0.00000e+00 0.00000e+00 0.00000e+00 0.00000e+00
0.00000e+00 0.00000e+00 0.00000e+00 0.00000e+00 0.00000e+00
0.00000e+00 0.00000e+00 0.00000e+00 3.25906e-03 2.64181e-01
3.57445e-02 1.36647e-01 8.68199e-02 2.16977e-02 4.13229e-02
2.02535e-02 5.18268e-03 3.24809e-03
FROM GROUP 16
0.00000e+00 0.00000e+00 0.00000e+00 0.00000e+00 0.00000e+00
0.00000e+00 0.00000e+00 0.00000e+00 0.00000e+00 0.00000e+00
0.00000e+00 0.00000e+00 0.00000e+00 2.69424e-06 3.37707e-02
1.25349e-01 2.60507e-01 1.20008e-01 3.00620e-02 5.73550e-02
2.82831e-02 7.22930e-03 4.51818e-03

FROM GROUP 17
0.00000e+00 0.00000e+00 0.00000e+00 0.00000e+00 0.00000e+00
0.00000e+00 0.00000e+00 0.00000e+00 0.00000e+00 0.00000e+00
0.00000e+00 0.00000e+00 0.00000e+00 1.06007e-07 1.19982e-03
5.40531e-03 3.14751e-01 1.91052e-01 3.94621e-02 7.59835e-02
3.77139e-02 9.61917e-03 5.97857e-03
FROM GROUP 18
0.00000e+00 0.00000e+00 0.00000e+00 0.00000e+00 0.00000e+00
0.00000e+00 0.00000e+00 0.00000e+00 0.00000e+00 0.00000e+00
0.00000e+00 0.00000e+00 0.00000e+00 0.00000e+00 7.11792e-07
2.58374e-06 1.35448e-02 3.76650e-01 9.73217e-02 1.45205e-01
6.52622e-02 1.63040e-02 9.97881e-03
FROM GROUP 19
0.00000e+00 0.00000e+00 0.00000e+00 0.00000e+00 0.00000e+00
0.00000e+00 0.00000e+00 0.00000e+00 0.00000e+00 0.00000e+00
0.00000e+00 0.00000e+00 0.00000e+00 0.00000e+00 0.00000e+00
0.00000e+00 2.15527e-04 7.44782e-02 2.64160e-01 2.87425e-01
1.08123e-01 2.60150e-02 1.54904e-02
FROM GROUP 20
0.00000e+00 0.00000e+00 0.00000e+00 0.00000e+00 0.00000e+00
0.00000e+00 0.00000e+00 0.00000e+00 0.00000e+00 0.00000e+00
0.00000e+00 0.00000e+00 0.00000e+00 0.00000e+00 0.00000e+00
0.00000e+00 3.87112e-05 9.39324e-03 3.43553e-02 4.95519e-01
2.39062e-01 4.97149e-02 2.87232e-02
FROM GROUP 21
0.00000e+00 0.00000e+00 0.00000e+00 0.00000e+00 0.00000e+00
0.00000e+00 0.00000e+00 0.00000e+00 0.00000e+00 0.00000e+00
0.00000e+00 0.00000e+00 0.00000e+00 0.00000e+00 0.00000e+00
0.00000e+00 8.71889e-06 1.80848e-03 5.58275e-03 1.37026e-01
6.56092e-01 1.51540e-01 6.91213e-02
FROM GROUP 22
0.00000e+00 0.00000e+00 0.00000e+00 0.00000e+00 0.00000e+00
0.00000e+00 0.00000e+00 0.00000e+00 0.00000e+00 0.00000e+00
0.00000e+00 0.00000e+00 0.00000e+00 0.00000e+00 0.00000e+00
0.00000e+00 4.94702e-06 1.02653e-03 3.12398e-03 6.49295e-02
3.77338e-01 6.14434e-01 2.30087e-01
FROM GROUP 23
0.00000e+00 0.00000e+00 0.00000e+00 0.00000e+00 0.00000e+00
0.00000e+00 0.00000e+00 0.00000e+00 0.00000e+00 0.00000e+00
0.00000e+00 0.00000e+00 0.00000e+00 0.00000e+00 0.00000e+00
0.00000e+00 5.27309e-06 1.07009e-03 3.20222e-03 6.47205e-02
2.94499e-01 4.06853e-01 1.07784e+00

A2.10 Water Composition REFREF

* C A S M O -3 3.4 87/07/07 STUDSVIK * EXECUTION 88/ 1/ 7

* BATCH WATER : TAVE
* BURNUP = 0.000 V= 0.0 TF= 900.0 TM= 585.0 BOR= 500.0

WATER CROSS SECTIONS
********************

| GROUP | ABSORPTION | FISSION | NU-FISSION | TRANSPORT |
|---|---|---|---|---|
| 1 | 2.21218e-03 | 0.00000e+00 | 0.00000e+00 | 7.35833e-02 |
| 2 | 1.18560e-03 | 0.00000e+00 | 0.00000e+00 | 9.44927e-02 |
| 3 | 7.06108e-05 | 0.00000e+00 | 0.00000e+00 | 1.08284e-01 |
| 4 | 9.51903e-06 | 0.00000e+00 | 0.00000e+00 | 1.26019e-01 |
| 5 | 3.63600e-05 | 0.00000e+00 | 0.00000e+00 | 1.76619e-01 |
| 6 | 6.69019e-05 | 0.00000e+00 | 0.00000e+00 | 1.77547e-01 |
| 7 | 6.62802e-05 | 0.00000e+00 | 0.00000e+00 | 2.29577e-01 |
| 8 | 3.30165e-05 | 0.00000e+00 | 0.00000e+00 | 2.64456e-01 |
| 9 | 1.22328e-04 | 0.00000e+00 | 0.00000e+00 | 3.10721e-01 |
| 10 | 1.22830e-03 | 0.00000e+00 | 0.00000e+00 | 3.49802e-01 |
| 11 | 6.56820e-04 | 0.00000e+00 | 0.00000e+00 | 3.77699e-01 |
| 12 | 1.24973e-03 | 0.00000e+00 | 0.00000e+00 | 3.88023e-01 |
| 13 | 1.78264e-03 | 0.00000e+00 | 0.00000e+00 | 3.79371e-01 |
| 14 | 2.73585e-03 | 0.00000e+00 | 0.00000e+00 | 4.29995e-01 |
| 15 | 3.72562e-03 | 0.00000e+00 | 0.00000e+00 | 4.68948e-01 |
| 16 | 4.32249e-03 | 0.00000e+00 | 0.00000e+00 | 4.95452e-01 |
| 17 | 4.99617e-03 | 0.00000e+00 | 0.00000e+00 | 5.24934e-01 |
| 18 | 6.56548e-03 | 0.00000e+00 | 0.00000e+00 | 6.05543e-01 |
| 19 | 7.98962e-03 | 0.00000e+00 | 0.00000e+00 | 6.91233e-01 |
| 20 | 1.02291e-02 | 0.00000e+00 | 0.00000e+00 | 8.34071e-01 |
| 21 | 1.48143e-02 | 0.00000e+00 | 0.00000e+00 | 1.12072e+00 |
| 22 | 2.14877e-02 | 0.00000e+00 | 0.00000e+00 | 1.57106e+00 |
| 23 | 3.57480e-02 | 0.00000e+00 | 0.00000e+00 | 2.33902e+00 |

P0-SCATTERING
FROM GROUP 1
2.25385e-02 2.49099e-02 1.23407e-02 9.11904e-03 6.16593e-03
3.71133e-03 3.95797e-03 8.25462e-04 2.66130e-05 3.99153e-05
5.43158e-07 0.00000e+00 0.00000e+00 0.00000e+00 0.00000e+00
0.00000e+00 0.00000e+00 0.00000e+00 0.00000e+00 0.00000e+00
0.00000e+00 0.00000e+00 0.00000e+00
FROM GROUP 2
0.00000e+00 4.32066e-02 3.55391e-02 1.63235e-02 1.08031e-02
6.72367e-03 7.73429e-03 1.77366e-03 5.90180e-05 8.85164e-05
1.65605e-06 0.00000e+00 0.00000e+00 0.00000e+00 0.00000e+00
0.00000e+00 0.00000e+00 0.00000e+00 0.00000e+00 0.00000e+00
0.00000e+00 0.00000e+00 0.00000e+00
FROM GROUP 3
0.00000e+00 0.00000e+00 5.67150e-02 3.70877e-02 2.06528e-02
1.28589e-02 1.53820e-02 3.76735e-03 1.28542e-04 1.92791e-04
4.75644e-06 0.00000e+00 0.00000e+00 0.00000e+00 0.00000e+00
0.00000e+00 0.00000e+00 0.00000e+00 0.00000e+00 0.00000e+00
0.00000e+00 0.00000e+00 0.00000e+00
FROM GROUP 4
0.00000e+00 0.00000e+00 0.00000e+00 7.13060e-02 5.29244e-02
2.67196e-02 3.07339e-02 7.87155e-03 2.76681e-04 4.14982e-04
1.02380e-05 4.69730e-07 4.53215e-07 0.00000e+00 0.00000e+00
0.00000e+00 0.00000e+00 0.00000e+00 0.00000e+00 0.00000e+00
0.00000e+00 0.00000e+00 0.00000e+00
FROM GROUP 5
0.00000e+00 0.00000e+00 0.00000e+00 0.00000e+00 1.23796e-01
7.50965e-02 6.52562e-02 1.68061e-02 5.91091e-04 8.86549e-04
2.18724e-05 1.00348e-06 9.68248e-07 0.00000e+00 0.00000e+00
0.00000e+00 0.00000e+00 0.00000e+00 0.00000e+00 0.00000e+00
0.00000e+00 0.00000e+00 0.00000e+00
FROM GROUP 6
0.00000e+00 0.00000e+00 0.00000e+00 0.00000e+00 0.00000e+00
1.32161e-01 1.49149e-01 3.57160e-02 1.25843e-03 1.88748e-03
4.65662e-05 2.13648e-06 2.06141e-06 0.00000e+00 0.00000e+00
0.00000e+00 0.00000e+00 0.00000e+00 0.00000e+00 0.00000e+00
0.00000e+00 0.00000e+00 0.00000e+00
FROM GROUP 7
0.00000e+00 0.00000e+00 0.00000e+00 0.00000e+00 0.00000e+00
0.00000e+00 3.04007e-01 1.77431e-01 6.07929e-03 9.11794e-03
2.24950e-04 1.03206e-05 9.95811e-06 3.28082e-06 7.96344e-07
0.00000e+00 1.33119e-07 0.00000e+00 0.00000e+00 0.00000e+00
0.00000e+00 0.00000e+00 0.00000e+00
FROM GROUP 8
0.00000e+00 0.00000e+00 0.00000e+00 0.00000e+00 0.00000e+00
0.00000e+00 0.00000e+00 5.39411e-01 9.97779e-02 1.44670e-01
3.56910e-03 1.63750e-04 1.57996e-04 5.76656e-05 2.01548e-05
1.74582e-06 1.01642e-05 7.31308e-06 1.58712e-06 3.38302e-06
1.80594e-06 2.60956e-07 0.00000e+00
FROM GROUP 9
0.00000e+00 0.00000e+00 0.00000e+00 0.00000e+00 0.00000e+00
0.00000e+00 0.00000e+00 0.00000e+00 2.65030e-01 6.37561e-01
1.52343e-02 6.98934e-04 6.74403e-04 2.46142e-04 8.69817e-05
8.83580e-06 4.53269e-05 3.15567e-05 8.03258e-06 1.60652e-05
9.40963e-06 3.21304e-06 3.44052e-06
FROM GROUP 10
0.00000e+00 0.00000e+00 0.00000e+00 0.00000e+00 0.00000e+00
0.00000e+00 0.00000e+00 0.00000e+00 0.00000e+00 7.27859e-01
1.98337e-01 8.97875e-03 8.66335e-03 3.16195e-03 1.11737e-03
1.13506e-04 5.82277e-04 4.05381e-04 1.03187e-04 2.06377e-04
1.20877e-04 4.12750e-05 4.42212e-05

FROM GROUP 11
0.00000e+00 0.00000e+00 0.00000e+00 0.00000e+00 0.00000e+00
0.00000e+00 0.00000e+00 0.00000e+00 0.00000e+00 0.00000e+00
6.23043e-01 1.30418e-01 1.21747e-01 4.44355e-02 1.57026e-02
1.59511e-03 8.18274e-03 5.69690e-03 1.45010e-03 2.90022e-03
1.69870e-03 5.80043e-04 6.21472e-04
FROM GROUP 12
0.00000e+00 0.00000e+00 0.00000e+00 0.00000e+00 0.00000e+00
0.00000e+00 0.00000e+00 0.00000e+00 0.00000e+00 0.00000e+00
0.00000e+00 2.64861e-01 4.21012e-01 1.46040e-01 5.16062e-02
5.24235e-03 2.68925e-02 1.87226e-02 4.76576e-03 9.53152e-03
5.58272e-03 1.90629e-03 2.04247e-03
FROM GROUP 13
0.00000e+00 0.00000e+00 0.00000e+00 0.00000e+00 0.00000e+00
0.00000e+00 0.00000e+00 0.00000e+00 0.00000e+00 0.00000e+00
0.00000e+00 0.00000e+00 3.89828e-01 3.10341e-01 1.05740e-01
1.07415e-02 5.51028e-02 3.83631e-02 9.76498e-03 1.95296e-02
1.14389e-02 3.90605e-03 4.18506e-03
FROM GROUP 14
0.00000e+00 0.00000e+00 0.00000e+00 0.00000e+00 0.00000e+00
0.00000e+00 0.00000e+00 0.00000e+00 0.00000e+00 0.00000e+00
0.00000e+00 0.00000e+00 2.02159e-04 3.82416e-01 2.51415e-01
2.44713e-02 1.25034e-01 8.62674e-02 2.15724e-02 4.04951e-02
1.97501e-02 4.98002e-03 3.15462e-03
FROM GROUP 15
0.00000e+00 0.00000e+00 0.00000e+00 0.00000e+00 0.00000e+00
0.00000e+00 0.00000e+00 0.00000e+00 0.00000e+00 0.00000e+00
0.00000e+00 0.00000e+00 0.00000e+00 3.16944e-03 3.19162e-01
5.49917e-02 2.36209e-01 1.57532e-01 3.94098e-02 7.51275e-02
3.68786e-02 9.44452e-03 5.92058e-03
FROM GROUP 16
0.00000e+00 0.00000e+00 0.00000e+00 0.00000e+00 0.00000e+00
0.00000e+00 0.00000e+00 0.00000e+00 0.00000e+00 0.00000e+00
0.00000e+00 0.00000e+00 0.00000e+00 3.21113e-06 3.62602e-02
1.26090e-01 3.92146e-01 2.14500e-01 5.40856e-02 1.03297e-01
5.10165e-02 1.30467e-02 8.15403e-03
FROM GROUP 17
0.00000e+00 0.00000e+00 0.00000e+00 0.00000e+00 0.00000e+00
0.00000e+00 0.00000e+00 0.00000e+00 0.00000e+00 0.00000e+00
0.00000e+00 0.00000e+00 0.00000e+00 1.33418e-07 1.31954e-03
6.05976e-03 3.87657e-01 3.17945e-01 7.08102e-02 1.37055e-01
6.81513e-02 1.73818e-02 1.07954e-02
FROM GROUP 18
0.00000e+00 0.00000e+00 0.00000e+00 0.00000e+00 0.00000e+00
0.00000e+00 0.00000e+00 0.00000e+00 0.00000e+00 0.00000e+00
0.00000e+00 0.00000e+00 0.00000e+00 0.00000e+00 9.00153e-07
3.39957e-06 1.64707e-02 4.94216e-01 1.58311e-01 2.54776e-01
1.17492e-01 2.93289e-02 1.79059e-02

FROM GROUP 19
0.00000e+00 0.00000e+00 0.00000e+00 0.00000e+00 0.00000e+00
0.00000e+00 0.00000e+00 0.00000e+00 0.00000e+00 0.00000e+00
0.00000e+00 0.00000e+00 0.00000e+00 0.00000e+00 0.00000e+00
0.00000e+00 2.94114e-04 1.00024e-01 3.41038e-01 4.69988e-01
1.92809e-01 4.66690e-02 2.77031e-02
FROM GROUP 20
0.00000e+00 0.00000e+00 0.00000e+00 0.00000e+00 0.00000e+00
0.00000e+00 0.00000e+00 0.00000e+00 0.00000e+00 0.00000e+00
0.00000e+00 0.00000e+00 0.00000e+00 0.00000e+00 0.00000e+00
0.00000e+00 5.18489e-05 1.32557e-02 4.86150e-02 7.12260e-01
4.04654e-01 8.84432e-02 5.12554e-02
FROM GROUP 21
0.00000e+00 0.00000e+00 0.00000e+00 0.00000e+00 0.00000e+00
0.00000e+00 0.00000e+00 0.00000e+00 0.00000e+00 0.00000e+00
0.00000e+00 0.00000e+00 0.00000e+00 0.00000e+00 0.00000e+00
0.00000e+00 1.12512e-05 2.51018e-03 8.05987e-03 2.03995e-01
1.00621e+00 2.58653e-01 1.20293e-01
FROM GROUP 22
0.00000e+00 0.00000e+00 0.00000e+00 0.00000e+00 0.00000e+00
0.00000e+00 0.00000e+00 0.00000e+00 0.00000e+00 0.00000e+00
0.00000e+00 0.00000e+00 0.00000e+00 0.00000e+00 0.00000e+00
0.00000e+00 6.29853e-06 1.38456e-03 4.37564e-03 9.77738e-02
5.91125e-01 9.65589e-01 3.84730e-01
FROM GROUP 23
0.00000e+00 0.00000e+00 0.00000e+00 0.00000e+00 0.00000e+00
0.00000e+00 0.00000e+00 0.00000e+00 0.00000e+00 0.00000e+00
0.00000e+00 0.00000e+00 0.00000e+00 0.00000e+00 0.00000e+00
0.00000e+00 6.55121e-06 1.39927e-03 4.33158e-03 9.39422e-02
4.51498e-01 6.39612e-01 1.73578e+00

A2.11 Water Composition REFTF

* C A S M O -3 3.4 87/07/07 STUDSVIK * EXECUTION 88/ 1/ 7

* BATCH WATER : FUEL TEMP. BRANC
* BURNUP = 0.000 V= 0.0 TF=1500.0 TM= 585.0 BOR= 500.0

WATER CROSS SECTIONS
********************

| GROUP | ABSORPTION | FISSION | NU-FISSION | TRANSPORT |
|---|---|---|---|---|
| 1 | 2.21218e-03 | 0.00000e+00 | 0.00000e+00 | 7.35833e-02 |
| 2 | 1.18560e-03 | 0.00000e+00 | 0.00000e+00 | 9.44927e-02 |
| 3 | 7.06307e-05 | 0.00000e+00 | 0.00000e+00 | 1.08284e-01 |
| 4 | 9.51903e-06 | 0.00000e+00 | 0.00000e+00 | 1.26019e-01 |
| 5 | 3.63599e-05 | 0.00000e+00 | 0.00000e+00 | 1.76619e-01 |
| 6 | 6.69006e-05 | 0.00000e+00 | 0.00000e+00 | 1.77547e-01 |
| 7 | 6.62789e-05 | 0.00000e+00 | 0.00000e+00 | 2.29577e-01 |
| 8 | 3.30164e-05 | 0.00000e+00 | 0.00000e+00 | 2.64456e-01 |
| 9 | 1.22328e-04 | 0.00000e+00 | 0.00000e+00 | 3.10721e-01 |
| 10 | 1.22808e-03 | 0.00000e+00 | 0.00000e+00 | 3.49803e-01 |
| 11 | 6.56539e-04 | 0.00000e+00 | 0.00000e+00 | 3.77701e-01 |
| 12 | 1.24979e-03 | 0.00000e+00 | 0.00000e+00 | 3.88026e-01 |
| 13 | 1.78283e-03 | 0.00000e+00 | 0.00000e+00 | 3.79381e-01 |
| 14 | 2.73590e-03 | 0.00000e+00 | 0.00000e+00 | 4.30004e-01 |
| 15 | 3.72577e-03 | 0.00000e+00 | 0.00000e+00 | 4.68958e-01 |
| 16 | 4.32254e-03 | 0.00000e+00 | 0.00000e+00 | 4.95455e-01 |
| 17 | 4.99627e-03 | 0.00000e+00 | 0.00000e+00 | 5.24938e-01 |
| 18 | 6.56517e-03 | 0.00000e+00 | 0.00000e+00 | 6.05522e-01 |
| 19 | 7.98875e-03 | 0.00000e+00 | 0.00000e+00 | 6.91171e-01 |
| 20 | 1.02275e-02 | 0.00000e+00 | 0.00000e+00 | 8.33961e-01 |
| 21 | 1.48119e-02 | 0.00000e+00 | 0.00000e+00 | 1.12058e+00 |
| 22 | 2.14894e-02 | 0.00000e+00 | 0.00000e+00 | 1.57120e+00 |
| 23 | 3.57524e-02 | 0.00000e+00 | 0.00000e+00 | 2.33932e+00 |

P0-SCATTERING
FROM GROUP 1
2.25385e-02 2.49099e-02 1.23407e-02 9.11904e-03 6.16593e-03
3.71133e-03 3.95797e-03 8.25462e-04 2.66130e-05 3.99153e-05
5.43158e-07 0.00000e+00 0.00000e+00 0.00000e+00 0.00000e+00
0.00000e+00 0.00000e+00 0.00000e+00 0.00000e+00 0.00000e+00
0.00000e+00 0.00000e+00 0.00000e+00
FROM GROUP 2
0.00000e+00 4.32066e-02 3.55391e-02 1.63235e-02 1.08031e-02
6.72367e-03 7.73429e-03 1.77366e-03 5.90180e-05 8.85164e-05
1.65605e-06 0.00000e+00 0.00000e+00 0.00000e+00 0.00000e+00
0.00000e+00 0.00000e+00 0.00000e+00 0.00000e+00 0.00000e+00
0.00000e+00 0.00000e+00 0.00000e+00
FROM GROUP 3
0.00000e+00 0.00000e+00 5.67150e-02 3.70877e-02 2.06528e-02
1.28589e-02 1.53820e-02 3.76735e-03 1.28542e-04 1.92791e-04
4.75644e-06 0.00000e+00 0.00000e+00 0.00000e+00 0.00000e+00
0.00000e+00 0.00000e+00 0.00000e+00 0.00000e+00 0.00000e+00
0.00000e+00 0.00000e+00 0.00000e+00
FROM GROUP 4
0.00000e+00 0.00000e+00 0.00000e+00 7.13060e-02 5.29244e-02
2.67196e-02 3.07339e-02 7.87155e-03 2.76681e-04 4.14982e-04
1.02380e-05 4.69730e-07 4.53215e-07 0.00000e+00 0.00000e+00
0.00000e+00 0.00000e+00 0.00000e+00 0.00000e+00 0.00000e+00
0.00000e+00 0.00000e+00 0.00000e+00
FROM GROUP 5
0.00000e+00 0.00000e+00 0.00000e+00 0.00000e+00 1.23796e-01
7.50965e-02 6.52562e-02 1.68061e-02 5.91091e-04 8.86550e-04
2.18724e-05 1.00349e-06 9.68249e-07 0.00000e+00 0.00000e+00
0.00000e+00 0.00000e+00 0.00000e+00 0.00000e+00 0.00000e+00
0.00000e+00 0.00000e+00 0.00000e+00
FROM GROUP 6
0.00000e+00 0.00000e+00 0.00000e+00 0.00000e+00 0.00000e+00
1.32161e-01 1.49149e-01 3.57161e-02 1.25843e-03 1.88749e-03
4.65664e-05 2.13649e-06 2.06142e-06 0.00000e+00 0.00000e+00
0.00000e+00 0.00000e+00 0.00000e+00 0.00000e+00 0.00000e+00
0.00000e+00 0.00000e+00 0.00000e+00
FROM GROUP 7
0.00000e+00 0.00000e+00 0.00000e+00 0.00000e+00 0.00000e+00
0.00000e+00 3.04007e-01 1.77431e-01 6.07930e-03 9.11797e-03
2.24950e-04 1.03206e-05 9.95814e-06 3.28083e-06 7.96346e-07
0.00000e+00 1.33120e-07 0.00000e+00 0.00000e+00 0.00000e+00
0.00000e+00 0.00000e+00 0.00000e+00
FROM GROUP 8
0.00000e+00 0.00000e+00 0.00000e+00 0.00000e+00 0.00000e+00
0.00000e+00 0.00000e+00 5.39411e-01 9.97780e-02 1.44670e-01
3.56910e-03 1.63750e-04 1.57996e-04 5.76657e-05 2.01548e-05
1.74583e-06 1.01642e-05 7.31309e-06 1.58712e-06 3.38302e-06
1.80594e-06 2.60956e-07 0.00000e+00
FROM GROUP 9
0.00000e+00 0.00000e+00 0.00000e+00 0.00000e+00 0.00000e+00
0.00000e+00 0.00000e+00 0.00000e+00 2.65030e-01 6.37562e-01
1.52344e-02 6.98935e-04 6.74405e-04 2.46143e-04 8.69818e-05
8.83582e-06 4.53270e-05 3.15567e-05 8.03259e-06 1.60652e-05
9.40965e-06 3.21305e-06 3.44053e-06
FROM GROUP 10
0.00000e+00 0.00000e+00 0.00000e+00 0.00000e+00 0.00000e+00
0.00000e+00 0.00000e+00 0.00000e+00 0.00000e+00 7.27871e-01
1.98343e-01 8.97900e-03 8.66359e-03 3.16204e-03 1.11741e-03
1.13509e-04 5.82293e-04 4.05392e-04 1.03190e-04 2.06382e-04
1.20881e-04 4.12761e-05 4.42225e-05

FROM GROUP 11
0.00000e+00 0.00000e+00 0.00000e+00 0.00000e+00 0.00000e+00
0.00000e+00 0.00000e+00 0.00000e+00 0.00000e+00 0.00000e+00
6.23381e-01 1.30300e-01 1.21644e-01 4.43979e-02 1.56892e-02
1.59376e-03 8.17581e-03 5.69208e-03 1.44887e-03 2.89776e-03
1.69726e-03 5.79552e-04 6.20945e-04
FROM GROUP 12
0.00000e+00 0.00000e+00 0.00000e+00 0.00000e+00 0.00000e+00
0.00000e+00 0.00000e+00 0.00000e+00 0.00000e+00 0.00000e+00
0.00000e+00 2.64860e-01 4.21036e-01 1.46048e-01 5.16092e-02
5.24265e-03 2.68940e-02 1.87237e-02 4.76603e-03 9.53207e-03
5.58304e-03 1.90640e-03 2.04259e-03
FROM GROUP 13
0.00000e+00 0.00000e+00 0.00000e+00 0.00000e+00 0.00000e+00
0.00000e+00 0.00000e+00 0.00000e+00 0.00000e+00 0.00000e+00
0.00000e+00 0.00000e+00 3.89841e-01 3.10378e-01 1.05752e-01
1.07428e-02 5.51096e-02 3.83678e-02 9.76617e-03 1.95320e-02
1.14402e-02 3.90653e-03 4.18557e-03
FROM GROUP 14
0.00000e+00 0.00000e+00 0.00000e+00 0.00000e+00 0.00000e+00
0.00000e+00 0.00000e+00 0.00000e+00 0.00000e+00 0.00000e+00
0.00000e+00 0.00000e+00 2.02342e-04 3.82426e-01 2.51422e-01
2.44725e-02 1.25040e-01 8.62711e-02 2.15733e-02 4.04962e-02
1.97501e-02 4.97983e-03 3.15449e-03
FROM GROUP 15
0.00000e+00 0.00000e+00 0.00000e+00 0.00000e+00 0.00000e+00
0.00000e+00 0.00000e+00 0.00000e+00 0.00000e+00 0.00000e+00
0.00000e+00 0.00000e+00 0.00000e+00 3.16917e-03 3.19154e-01
5.49972e-02 2.36228e-01 1.57544e-01 3.94128e-02 7.51332e-02
3.68815e-02 9.44525e-03 5.92104e-03
FROM GROUP 16
0.00000e+00 0.00000e+00 0.00000e+00 0.00000e+00 0.00000e+00
0.00000e+00 0.00000e+00 0.00000e+00 0.00000e+00 0.00000e+00
0.00000e+00 0.00000e+00 0.00000e+00 3.21118e-06 3.62602e-02
1.26089e-01 3.92151e-01 2.14504e-01 5.40865e-02 1.03298e-01
5.10174e-02 1.30469e-02 8.15417e-03
FROM GROUP 17
0.00000e+00 0.00000e+00 0.00000e+00 0.00000e+00 0.00000e+00
0.00000e+00 0.00000e+00 0.00000e+00 0.00000e+00 0.00000e+00
0.00000e+00 0.00000e+00 0.00000e+00 1.33328e-07 1.31872e-03
6.05587e-03 3.87625e-01 3.17967e-01 7.08128e-02 1.37060e-01
6.81541e-02 1.73825e-02 1.07958e-02
FROM GROUP 18
0.00000e+00 0.00000e+00 0.00000e+00 0.00000e+00 0.00000e+00
0.00000e+00 0.00000e+00 0.00000e+00 0.00000e+00 0.00000e+00
0.00000e+00 0.00000e+00 0.00000e+00 0.00000e+00 9.00091e-07
3.39933e-06 1.64701e-02 4.94200e-01 1.58301e-01 2.54759e-01
1.17484e-01 2.93269e-02 1.79047e-02
FROM GROUP 19
0.00000e+00 0.00000e+00 0.00000e+00 0.00000e+00 0.00000e+00
0.00000e+00 0.00000e+00 0.00000e+00 0.00000e+00 0.00000e+00
0.00000e+00 0.00000e+00 0.00000e+00 0.00000e+00 0.00000e+00
0.00000e+00 2.94067e-04 1.00013e-01 3.41017e-01 4.69923e-01
1.92779e-01 4.66616e-02 2.76987e-02
FROM GROUP 20
0.00000e+00 0.00000e+00 0.00000e+00 0.00000e+00 0.00000e+00
0.00000e+00 0.00000e+00 0.00000e+00 0.00000e+00 0.00000e+00
0.00000e+00 0.00000e+00 0.00000e+00 0.00000e+00 0.00000e+00
0.00000e+00 5.18623e-05 1.32597e-02 4.86334e-02 7.12229e-01
4.04527e-01 8.84185e-02 5.12417e-02
FROM GROUP 21
0.00000e+00 0.00000e+00 0.00000e+00 0.00000e+00 0.00000e+00
0.00000e+00 0.00000e+00 0.00000e+00 0.00000e+00 0.00000e+00
0.00000e+00 0.00000e+00 0.00000e+00 0.00000e+00 0.00000e+00
0.00000e+00 1.12563e-05 2.51132e-03 8.06353e-03 2.04111e-01
1.00615e+00 2.58502e-01 1.20251e-01
FROM GROUP 22
0.00000e+00 0.00000e+00 0.00000e+00 0.00000e+00 0.00000e+00
0.00000e+00 0.00000e+00 0.00000e+00 0.00000e+00 0.00000e+00
0.00000e+00 0.00000e+00 0.00000e+00 0.00000e+00 0.00000e+00
0.00000e+00 6.29929e-06 1.38473e-03 4.37617e-03 9.77859e-02
5.91197e-01 9.65672e-01 3.84760e-01
FROM GROUP 23
0.00000e+00 0.00000e+00 0.00000e+00 0.00000e+00 0.00000e+00
0.00000e+00 0.00000e+00 0.00000e+00 0.00000e+00 0.00000e+00
0.00000e+00 0.00000e+00 0.00000e+00 0.00000e+00 0.00000e+00
0.00000e+00 6.55211e-06 1.39946e-03 4.33215e-03 9.39546e-02
4.51555e-01 6.39663e-01 1.73604e+00

A2.12 Water Composition REFTM

* C A S M O -3 3.4 87/07/07 STUDSVIK * EXECUTION 88/ 1/ 7

* BATCH WATER : MODERATER BRANCH
* BURNUP = 0.000 V= 0.0 TF= 900.0 TM= 620.0 BOR= 500.0

WATER CROSS SECTIONS
**********

| GROUP | ABSORPTION | FISSION | NU-FISSION | TRANSPORT |
|---|---|---|---|---|
| 1 | 1.90836e-03 | 0.00000e+00 | 0.00000e+00 | 6.31333e-02 |
| 2 | 1.01458e-03 | 0.00000e+00 | 0.00000e+00 | 8.08567e-02 |
| 3 | 6.77989e-05 | 0.00000e+00 | 0.00000e+00 | 9.27041e-02 |
| 4 | 9.22509e-06 | 0.00000e+00 | 0.00000e+00 | 1.07868e-01 |
| 5 | 3.60345e-05 | 0.00000e+00 | 0.00000e+00 | 1.51045e-01 |
| 6 | 6.63274e-05 | 0.00000e+00 | 0.00000e+00 | 1.53208e-01 |
| 7 | 6.53618e-05 | 0.00000e+00 | 0.00000e+00 | 1.96536e-01 |
| 8 | 3.09895e-05 | 0.00000e+00 | 0.00000e+00 | 2.26352e-01 |
| 9 | 1.11749e-04 | 0.00000e+00 | 0.00000e+00 | 2.64187e-01 |
| 10 | 1.19595e-03 | 0.00000e+00 | 0.00000e+00 | 2.96820e-01 |
| 11 | 5.46865e-04 | 0.00000e+00 | 0.00000e+00 | 3.19793e-01 |
| 12 | 1.04294e-03 | 0.00000e+00 | 0.00000e+00 | 3.28392e-01 |
| 13 | 1.48757e-03 | 0.00000e+00 | 0.00000e+00 | 3.21149e-01 |
| 14 | 2.28903e-03 | 0.00000e+00 | 0.00000e+00 | 3.63198e-01 |
| 15 | 3.11759e-03 | 0.00000e+00 | 0.00000e+00 | 3.95646e-01 |
| 16 | 3.61795e-03 | 0.00000e+00 | 0.00000e+00 | 4.17695e-01 |
| 17 | 4.18184e-03 | 0.00000e+00 | 0.00000e+00 | 4.42224e-01 |
| 18 | 5.49855e-03 | 0.00000e+00 | 0.00000e+00 | 5.09253e-01 |
| 19 | 6.69065e-03 | 0.00000e+00 | 0.00000e+00 | 5.80455e-01 |
| 20 | 8.54162e-03 | 0.00000e+00 | 0.00000e+00 | 6.97667e-01 |
| 21 | 1.23631e-02 | 0.00000e+00 | 0.00000e+00 | 9.34951e-01 |
| 22 | 1.79754e-02 | 0.00000e+00 | 0.00000e+00 | 1.31095e+00 |
| 23 | 2.98915e-02 | 0.00000e+00 | 0.00000e+00 | 1.94941e+00 |

P0-SCATTERING
FROM GROUP 1
1.92306e-02 2.08542e-02 1.05211e-02 7.93755e-03 5.42392e-03
3.26666e-03 3.44113e-03 6.96833e-04 2.21390e-05 3.32051e-05
4.51847e-07 0.00000e+00 0.00000e+00 0.00000e+00 0.00000e+00
0.00000e+00 0.00000e+00 0.00000e+00 0.00000e+00 0.00000e+00
0.00000e+00 0.00000e+00 0.00000e+00
FROM GROUP 2
0.00000e+00 3.67559e-02 2.98070e-02 1.39179e-02 9.33554e-03
5.83495e-03 6.65630e-03 1.49178e-03 4.90996e-05 7.36405e-05
1.37774e-06 0.00000e+00 0.00000e+00 0.00000e+00 0.00000e+00
0.00000e+00 0.00000e+00 0.00000e+00 0.00000e+00 0.00000e+00
0.00000e+00 0.00000e+00 0.00000e+00
FROM GROUP 3
0.00000e+00 0.00000e+00 4.86807e-02 3.11850e-02 1.74687e-02
1.09304e-02 1.30397e-02 3.15377e-03 1.06940e-04 1.60392e-04
3.95711e-06 0.00000e+00 0.00000e+00 0.00000e+00 0.00000e+00
0.00000e+00 0.00000e+00 0.00000e+00 0.00000e+00 0.00000e+00
0.00000e+00 0.00000e+00 0.00000e+00
FROM GROUP 4
0.00000e+00 0.00000e+00 0.00000e+00 6.15295e-02 4.43696e-02
2.25742e-02 2.57028e-02 6.55204e-03 2.30195e-04 3.45260e-04
8.51789e-06 3.90809e-07 3.77068e-07 0.00000e+00 0.00000e+00
0.00000e+00 0.00000e+00 0.00000e+00 0.00000e+00 0.00000e+00
0.00000e+00 0.00000e+00 0.00000e+00
FROM GROUP 5
0.00000e+00 0.00000e+00 0.00000e+00 0.00000e+00 1.06604e-01
6.27418e-02 5.45135e-02 1.39877e-02 4.91793e-04 7.37617e-04
1.81980e-05 8.34908e-07 8.05592e-07 0.00000e+00 0.00000e+00
0.00000e+00 0.00000e+00 0.00000e+00 0.00000e+00 0.00000e+00
0.00000e+00 0.00000e+00 0.00000e+00
FROM GROUP 6
0.00000e+00 0.00000e+00 0.00000e+00 0.00000e+00 0.00000e+00
1.15225e-01 1.24301e-01 2.97150e-02 1.04699e-03 1.57035e-03
3.87422e-05 1.77751e-06 1.71506e-06 0.00000e+00 0.00000e+00
0.00000e+00 0.00000e+00 0.00000e+00 0.00000e+00 0.00000e+00
0.00000e+00 0.00000e+00 0.00000e+00
FROM GROUP 7
0.00000e+00 0.00000e+00 0.00000e+00 0.00000e+00 0.00000e+00
0.00000e+00 2.58382e-01 1.47665e-01 5.05733e-03 7.58517e-03
1.87135e-04 8.58563e-06 8.28411e-06 2.72930e-06 6.62475e-07
0.00000e+00 1.10741e-07 0.00000e+00 0.00000e+00 0.00000e+00
0.00000e+00 0.00000e+00 0.00000e+00
FROM GROUP 8
0.00000e+00 0.00000e+00 0.00000e+00 0.00000e+00 0.00000e+00
0.00000e+00 0.00000e+00 4.55004e-01 8.30384e-02 1.20333e-01
2.96869e-03 1.36203e-04 1.31417e-04 4.79650e-05 1.67643e-05
1.45214e-06 8.45437e-06 6.08285e-06 1.32013e-06 2.81391e-06
1.50214e-06 2.17057e-07 0.00000e+00
FROM GROUP 9
0.00000e+00 0.00000e+00 0.00000e+00 0.00000e+00 0.00000e+00
0.00000e+00 0.00000e+00 0.00000e+00 2.25922e-01 5.30544e-01
1.26712e-02 5.81339e-04 5.60936e-04 2.04729e-04 7.23471e-05
7.34916e-06 3.77007e-05 2.62473e-05 6.68109e-06 1.33622e-05
7.82647e-06 2.67245e-06 2.86166e-06
FROM GROUP 10
0.00000e+00 0.00000e+00 0.00000e+00 0.00000e+00 0.00000e+00
0.00000e+00 0.00000e+00 0.00000e+00 0.00000e+00 6.11041e-01
1.64988e-01 7.46757e-03 7.20526e-03 2.62978e-03 9.29314e-04
9.44020e-05 4.84277e-04 3.37153e-04 8.58201e-05 1.71642e-04
1.00533e-04 3.43281e-05 3.67786e-05

FROM GROUP 11
0.00000e+00 0.00000e+00 0.00000e+00 0.00000e+00 0.00000e+00
0.00000e+00 0.00000e+00 0.00000e+00 0.00000e+00 0.00000e+00
5.25228e-01 1.07945e-01 1.00747e-01 3.67708e-02 1.29940e-02
1.31997e-03 6.77129e-03 4.71424e-03 1.19997e-03 2.39996e-03
1.40569e-03 4.79990e-04 5.14274e-04
FROM GROUP 12
0.00000e+00 0.00000e+00 0.00000e+00 0.00000e+00 0.00000e+00
0.00000e+00 0.00000e+00 0.00000e+00 0.00000e+00 0.00000e+00
0.00000e+00 2.25701e-01 3.50390e-01 1.21453e-01 4.29179e-02
4.35976e-03 2.23649e-02 1.55705e-02 3.96341e-03 7.92682e-03
4.64283e-03 1.58535e-03 1.69860e-03
FROM GROUP 13
0.00000e+00 0.00000e+00 0.00000e+00 0.00000e+00 0.00000e+00
0.00000e+00 0.00000e+00 0.00000e+00 0.00000e+00 0.00000e+00
0.00000e+00 0.00000e+00 3 29704e-01 2.58232e-01 8.79382e-02
8 93316e-03 4.58263e-02 3 19047e-02 8.12105e-03 1.62418e-02
9.51312e-03 3 24847e-03 3 48051e-03
FROM GROUP 14
0 00000e+00 0.00000e+00 0 00000e+00 0.00000e+00 0 00000e+00
0.00000e+00 0 00000e+00 0 00000e+00 0.00000e+00 0 00000e+00
0.00000e+00 0.00000e+00 2.03291e-04 3.23759e-01 2 09500e-01
2.03330e-02 1.03873e-01 7 16599e-02 1.79165e-02 3.36225e-02
1.63934e-02 4.13298e-03 2.61807e-03
FROM GROUP 15
0.00000e+00 0.00000e+00 0.00000e+00 0.00000e+00 0.00000e+00
0.00000e+00 0.00000e+00 0.00000e+00 0.00000e+00 0.00000e+00
0.00000e+00 0.00000e+00 0.00000e+00 2.98021e-03 2.70471e-01
4.58351e-02 1.96377e-01 1.30859e-01 3.27189e-02 6.23136e-02
3.05428e-02 7.81577e-03 4.89828e-03
FROM GROUP 16
0.00000e+00 0.00000e+00 0.00000e+00 0.00000e+00 0.00000e+00
0.00000e+00 0.00000e+00 0.00000e+00 0.00000e+00 0.00000e+00
0.00000e+00 0.00000e+00 0.00000e+00 3.54947e-06 3.31637e-02
1.06982e-01 3.27467e-01 1.78388e-01 4.49349e-02 8.57309e-02
4.22759e-02 1.08059e-02 6.75351e-03
FROM GROUP 17
0.00000e+00 0.00000e+00 0.00000e+00 0.00000e+00 0.00000e+00
0.00000e+00 0.00000e+00 0.00000e+00 0.00000e+00 0.00000e+00
0.00000e+00 0.00000e+00 0.00000e+00 1.51892e-07 1.29673e-03
5.55504e-03 3.28092e-01 2.64717e-01 5.88968e-02 1.13810e-01
5.64968e-02 1.44100e-02 8.95628e-03
FROM GROUP 18
0.00000e+00 0.00000e+00 0.00000e+00 0.00000e+00 0.00000e+00
0.00000e+00 0.00000e+00 0.00000e+00 0.00000e+00 0.00000e+00
0.00000e+00 0.00000e+00 0.00000e+00 0.00000e+00 1.05630e-06
3.78180e-06 1.52308e-02 4.16799e-01 1.31678e-01 2.11507e-01
9.73916e-02 2.43431e-02 1.48991e-02
FROM GROUP 19
0.00000e+00 0.00000e+00 0.00000e+00 0.00000e+00 0.00000e+00
0.00000e+00 0.00000e+00 0.00000e+00 0.00000e+00 0.00000e+00
0.00000e+00 0.00000e+00 0.00000e+00 0.00000e+00 0.00000e+00
0.00000e+00 3.16041e-04 9.02590e-02 2.84664e-01 3.90333e-01
1.59450e-01 3.86016e-02 2.29867e-02
FROM GROUP 20
0.00000e+00 0.00000e+00 0.00000e+00 0.00000e+00 0.00000e+00
0.00000e+00 0.00000e+00 0.00000e+00 0.00000e+00 0.00000e+00
0.00000e+00 0.00000e+00 0.00000e+00 0.00000e+00 0.00000e+00
0.00000e+00 5.82659e-05 1.32213e-02 4.49977e-02 5.97187e-01
3.31760e-01 7.27276e-02 4.23192e-02
FROM GROUP 21
0.00000e+00 0.00000e+00 0.00000e+00 0.00000e+00 0.00000e+00
0.00000e+00 0.00000e+00 0.00000e+00 0.00000e+00 0.00000e+00
0.00000e+00 0.00000e+00 0.00000e+00 0.00000e+00 0.00000e+00
0.00000e+00 1.28051e-05 2.65317e-03 8.13369e-03 1.85494e-01
8.30193e-01 2.10778e-01 9.95997e-02
FROM GROUP 22
0.00000e+00 0.00000e+00 0.00000e+00 0.00000e+00 0.00000e+00
0.00000e+00 0.00000e+00 0.00000e+00 0.00000e+00 0.00000e+00
0.00000e+00 0.00000e+00 0.00000e+00 0.00000e+00 0.00000e+00
0.00000e+00 7.16793e-06 1.48735e-03 4.52600e-03 9.32598e-02
5.11871e-01 7.84952e-01 3.17317e-01
FROM GROUP 23
0.00000e+00 0.00000e+00 0.00000e+00 0.00000e+00 0.00000e+00
0.00000e+00 0.00000e+00 0.00000e+00 0.00000e+00 0.00000e+00
0.00000e+00 0.00000e+00 0.00000e+00 0.00000e+00 0.00000e+00
0.00000e+00 7.47460e-06 1.51662e-03 4.53815e-03 9.16372e-02
4.08248e-01 5.43814e-01 1.41787e+00

## Appendix 3

### DERIVATION OF THE CURRENT-FLUX COUPLING RELATIONSHIP

The time difference form of P-1 transport equations is given by Eq.(4.3) and (4.11),

$$\frac{d}{dx}[J(x)]^{n+1} + [A_0(x)]^{n+1}[\phi(x)]^{n+1} + \frac{1}{\Delta_n}[V_0^{-1}(x)][\phi(x)]^{n+1}$$
$$- k_{eff}^{-1}\left\{[1-\beta_{eff}(x)][\chi_p(x)]^{n+1} + \sum_i \beta_i(x)[\chi_{d_i}(x)]^{n+1}\zeta_i\right\}$$
$$\times\left\{[\nu\Sigma_f(x)]^T[\phi(x)]\right\}^{n+1}$$
$$= k_{eff}^{-1}\sum_i \beta_i(x)[\chi_{d_i}(x)]^{n+1}\eta_i\left\{[\nu\Sigma_f(x)]^T[\phi(x)]\right\}^n$$
$$+ \frac{1}{\Delta_n}[V_0^{-1}(x)][\phi(x)]^n + \sum_i [\chi_{d_i}(x)]^{n+1}\lambda_i\,\theta_i\,C_i^n(x) \qquad \text{(A3.1)}$$

$$\frac{d}{dx}[\phi(x)]^n = -[D^{-1}(x)]^n\,[J(x)]^n \qquad \text{(A3.2)}$$

and the flux shape within a node is approximated by Eq.(4.12)

$$[\phi(x)]^n \simeq [\phi(x_i^+)]^n\,Q_i^-(x) + [\bar{\phi}_i]^n\,\tilde{Q}_i(x) + [\phi(x_{i+1}^-)]^n\,Q_i^+(x) \qquad \text{(A3.3)}$$

where

$$Q_i^-(x) = \frac{(x_{i+1}-x_i)}{h_i}\left[\,1 - \frac{3}{h_i}(x - x_i)\,\right]$$

$$\tilde{Q}_i(x) = \frac{6}{h_i^2}(x - x_i)(x_{i+1} - x) \qquad \text{(A3.4)}$$

$$Q_i^+(x) = \frac{(x-x_i)}{h_i}\left[\,1 - \frac{3}{h_i}(x_{i+1} - x)\right]$$

Substitution of this approximation into Eq.(A3.2) yields a general expression for the net current.

$$[J_i(x)]^n \simeq -[D_i]^n \left\{ \frac{1}{h_i}\left[[\phi(x_{i+1}^-)]^n - [\phi(x_i^+)]^n\right] + \frac{3[x_{i+1}-2x+x_i]}{h_i^2}\left[2[\bar{\phi}_i]^n - [\phi(x_i^+)]^n - [\phi(x_{i+1}^-)]^n\right]\right\} \qquad \text{(A3.5)}$$

## A3.1 The Net Current $[J_{i-1}(x_i^-)]^{n+1}$

The surface average current on the two sides of node i-1 is given by Eq.(A3.5) as:

$$[J(x_{i-1}^+)] \simeq -[D_{i-1}]\frac{1}{h_{i-1}}\left\{6[\bar{\phi}_{i-1}] - 2[\phi(x_i^-)] - 4[\phi(x_{i-1}^+)]\right\} \qquad \text{(A3.6)}$$

$$[J(x_i^-)] \simeq -[D_{i-1}]\frac{1}{h_{i-1}}\left\{-6[\bar{\phi}_{i-1}] + 4[\phi(x_i^-)] + 2[\phi(x_{i-1}^+)]\right\} \qquad \text{(A3.7)}$$

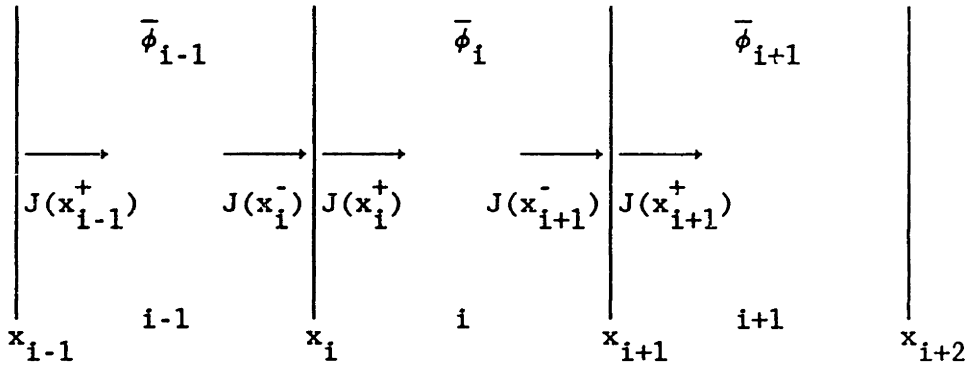


Figure A3.1 Sign Convention of the Net Currents

Equation (A3.7) can be solved for $[\phi(x^+_{i-1})]$, and when that is substituted into Eq.(A3.6), the result is

$$[J(x^+_{i-1})]^n \simeq \frac{6}{h_{i-1}} [D_{i-1}]^n \left\{ [\bar{\phi}_{i-1}]^n - [\phi(x^-_i)]^n \right\} - 2\,[J(x^-_i)]^n \tag{A3.8}$$

Now integration of Eq.(A3.1) over the node length $(x_{i-1}, x_i)$ yields the following equation for node i-1:

$$\begin{aligned} &[J(x^-_i)]^{n+1} - [J(x^+_{i-1})]^{n+1} + h_{i-1}\,[\bar{A}_{o\,i-1}]^{n+1}[\bar{\phi}_{i-1}]^{n+1} \\ &\quad + h_{i-1}\frac{1}{\Delta n}\,[V_o]^{-1}[\bar{\phi}_{i-1}]^{n+1} - h_{i-1}\,[M_{i-1}]^{n+1}[\bar{\phi}_{i-1}]^{n+1} \\ &= h_{i-1}\frac{1}{\Delta n}\,[V_o]^{-1}[\bar{\phi}_{i-1}]^n + h_{i-1}\,[MD_{i-1}]^n[\bar{\phi}_{i-1}]^n \\ &\quad + h_{i-1}\,[SD_{i-1}]^n \end{aligned} \tag{A3.9}$$

where

$$[M_i]^n = k_{eff}^{-1}\left((1-\beta_{eff_i})[\bar{\chi}_{p_i}] + \sum_\iota \beta_{\iota_i}[\bar{\chi}_{d_{\iota,i}}]\,\zeta_{\iota_i}\right)[\nu\bar{\Sigma}_{f_i}]^{T,n}$$

$$[MD_i]^n = k_{eff}^{-1}\sum_\iota \beta_{\iota_i}[\bar{\chi}_{d_{\iota,i}}]\,\eta_{\iota_i}\,[\nu\bar{\Sigma}_{f_i}]^{T,n} \qquad \text{(A3.10)}$$

$$[SD_i]^n = \sum_\iota [\chi_{d_{\iota,i}}]\,\lambda_{\iota_i}\,\theta_{\iota_i}\bar{C}_{\iota_i}^n$$

Substituting Eq.(A3.8) into Eq.(A3.9) yields

$$\begin{aligned}
&3\,[J(x_i^-)]^{n+1} + \frac{6}{h_{i-1}}[D_{i-1}]^{n+1}[\phi(x_i^-)]^{n+1} \\
&\simeq \frac{6}{h_{i-1}}[D_{i-1}]^{n+1}[\bar{\phi}_{i-1}]^{n+1} - h_{i-1}\,[\bar{A}_{o_{i-1}}]^{n+1}[\bar{\phi}_{i-1}]^{n+1} \\
&\quad - h_{i-1}\frac{1}{\Delta n}[V_o]^{-1}[\bar{\phi}_{i-1}]^{n+1} + h_{i-1}\,[M_{i-1}]^{n+1}[\bar{\phi}_{i-1}]^{n+1} \qquad \text{(A3.11)} \\
&\quad + h_{i-1}\frac{1}{\Delta n}[V_o]^{-1}[\bar{\phi}_{i-1}]^{n} + h_{i-1}\,[MD_{i-1}]^{n}[\bar{\phi}_{i-1}]^{n} \\
&\quad + h_{i-1}\,[SD_{i-1}]^{n}
\end{aligned}$$

Because the flux shape within a node is approximated by the quadratic expansion functions, the flux gradient at the node surface is not predicted correctly. As a result, if reference values for all term in (A3.11) except $[J(x_i^-)]^{n+1}$ are inserted, the resultant value of $J(x_i^-)$ will not match the reference and currents will become discontinuous at the interfaces between two adjacent nodes. In order to compensate for the error, Equation (A3.11) is corrected. This is done by dividing the surface average fluxes $[\phi(x_i^-)]^{n+1}$ by "discontinuity factors" defined so that (A3.11) is forced to be valid when reference values are used for all terms. Equation (A3.11) then becomes

$$
\begin{aligned}
&3\,[J(x_i^-)]^{n+1} + \frac{6}{h_{i-1}}\,[D_{i-1}]^{n+1}[f_{i-1}^R]^{-1}\,[\phi(x_i)]^{n+1} \\
&- \frac{6}{h_{i-1}}\,[D_{i-1}]^{n+1}[\bar{\phi}_{i-1}]^{n+1} - h_{i-1}\,[\bar{A}_{o_{i-1}}]^{n+1}[\bar{\phi}_{i-1}]^{n+1} \\
&- h_{i-1}\frac{1}{\Delta n}\,[V_o]^{-1}[\bar{\phi}_{i-1}]^{n+1} + h_{i-1}\,[M_{i-1}]^{n+1}[\bar{\phi}_{i-1}]^{n+1} \\
&+ h_{i-1}\frac{1}{\Delta n}\,[V_o]^{-1}[\bar{\phi}_{i-1}]^{n} + h_{i-1}\,[MD_{i-1}]^{n}[\bar{\phi}_{i-1}]^{n} \\
&+ h_{i-1}\,[SD_{i-1}]^{n}
\end{aligned}
\qquad \text{(A3.12)}
$$

where $[f_i^R]$ is a diagonal G×G matrix containing discontinuity factors for the right (positive x-direction) side of node i. Equation (A3.12) really defines $[f_{i-1}^R]$. (More information on the discontinuity factors can be found in reference [S-1].)

## A3.2 The Net Current $[J_i(x_i^+)]^{n+1}$

The surface currents on the two sides of node i are given by Eq.(A3.5) as:

$$
[J(x_i^+)] \simeq -\,[D_i]\,\frac{1}{h_i}\left\{6[\bar{\phi}_i] - 4[\phi(x_i^+)] - 2[\phi(x_{i+1}^-)]\right\} \qquad \text{(A3.13)}
$$

$$
[J(x_{i+1}^-)] \simeq -\,[D_i]\,\frac{1}{h_i}\left\{-\,6[\bar{\phi}_i] + 2[\phi(x_i^+)] + 4[\phi(x_{i+1}^-)]\right\} \qquad \text{(A3.14)}
$$

Equation (A3.13) can be solved for $[\phi(x_{i+1}^-)]$ and when that is substituted into Eq.(A3.14), the result is

$$[J(x_{i+1}^-)]^n \simeq \frac{-6}{h_i}[D_i]^n\left\{[\bar{\phi}_i]^n - [\phi(x_i^+)]^n\right\} - 2\,[J(x_i^+)]^n \tag{A3.15}$$

Now integration of Eq.(A3.1) over the node length $(x_i, x_{i+1})$ yields the following equation for node i:

$$\begin{aligned}&[J(x_{i+1}^-)]^{n+1} - [J(x_i^+)]^{n+1} + h_i\,[\bar{A}_{0i}]^{n+1}[\bar{\phi}_i]^{n+1}\\ &+ h_i\frac{1}{\Delta n}[V_0]^{-1}[\bar{\phi}_i]^{n+1} - h_i\,[M_i]^{n+1}[\bar{\phi}_i]^{n+1}\\ &= h_i\frac{1}{\Delta n}[V_0]^{-1}[\bar{\phi}_i]^n + h_i\,[MD_i]^n[\bar{\phi}_i]^n + h_i\,[SD_i]^n\end{aligned} \tag{A3.16}$$

Substituting Eq.(A3.15) into Eq.(A3.16) and introducing discontinuity factors as in section A3.1 yields

$$\begin{aligned}&-3\,[J(x_i^+)]^{n+1} + \frac{6}{h_i}[D_i]^{n+1}[f_i^L]^{-1}[\phi(x_i)]^{n+1}\\ &= \frac{6}{h_i}[D_i]^{n+1}[\bar{\phi}_i]^{n+1} - h_i\,[\bar{A}_{0i}]^{n+1}[\bar{\phi}_i]^{n+1}\\ &- h_i\frac{1}{\Delta n}[V_0]^{-1}[\bar{\phi}_i]^{n+1} + h_i\,[M_i]^{n+1}[\bar{\phi}_i]^{n+1}\\ &+ h_i\frac{1}{\Delta n}[V_0]^{-1}[\bar{\phi}_i]^n + h_i\,[MD_i]^n[\bar{\phi}_i]^n\\ &+ h_i\,[SD_i]^n\end{aligned} \tag{A3.17}$$

where $[f_i^L]$ is a diagonal G×G matrix containing discontinuity factors for the left (negative x-direction) side of node i.

## A3.3 Spatial Coupling Equation for $[J(x_i)]$

Equations (A3.12) and (A3.17) are expressions for surface net currents each having two unknown variables, node average flux and surface-average flux. Because we have forced the current at the interface to be continuous by using discontinuity factors,

$$[J(x_i)] = [J(x_i^+)] = [J(x_i^-)] \tag{A3.18}$$

and we can derive one expression for $[J(x_i)]$ by eliminating $[\phi(x_i)]$.

Equations (A3.12) and (A3.17) can be written as:

$$\begin{aligned}
&\tfrac{1}{2}h_{i-1}[f_{i-1}^R][D_{i-1}^{-1}]^{n+1}[J(x_i)]^{n+1} + [\phi(x_i)]^{n+1} \\
&= [f_{i-1}^R]\left([I] - \tfrac{1}{6}h_{i-1}^2[D_{i-1}^{-1}]^{n+1}[\bar{A}_{0_{i-1}}]^{n+1}\right)[\bar{\phi}_{i-1}]^{n+1} \\
&\quad + [f_{i-1}^R]\tfrac{1}{6}h_{i-1}^2[D_{i-1}^{-1}]^{n+1}[M_{i-1}]^{n+1}[\bar{\phi}_{i-1}]^{n+1} \\
&\quad - [f_{i-1}^R]\tfrac{1}{6}h_{i-1}^2[D_{i-1}^{-1}]^{n+1}\frac{1}{\Delta n}[V_0]^{-1}[\bar{\phi}_{i-1}]^{n+1} \\
&\quad + [f_{i-1}^R]\tfrac{1}{6}h_{i-1}^2[D_{i-1}^{-1}]^{n+1}\frac{1}{\Delta n}[V_0]^{-1}[\bar{\phi}_{i-1}]^{n} \\
&\quad + [f_{i-1}^R]\tfrac{1}{6}h_{i-1}^2[D_{i-1}^{-1}]^{n+1}[MD_{i-1}]^{n}[\bar{\phi}_{i-1}]^{n} \\
&\quad + [f_{i-1}^R]\ \tfrac{1}{6}h_{i-1}^2\ [D_{i-1}^{-1}]^{n+1}[SD_{i-1}]^{n}
\end{aligned} \tag{A3.19}$$

$$
\begin{aligned}
&- \frac{1}{2} h_i [f_i^L][D_i^{-1}]^{n+1}[J(x_i)]^{n+1} + [\phi(x_i)]^{n+1} \\
&= [f_i^L]\left([I] - \frac{1}{6} h_i^2 [D_i^{-1}]^{n+1}[\bar{A}_{o_i}]^{n+1}\right)[\bar{\phi}_i]^{n+1} \\
&\quad + [f_i^L]\frac{1}{6} h_i^2 \, [D_i^{-1}]^{n+1}[M_i]^{n+1}[\bar{\phi}_i]^{n+1} \\
&\quad - [f_i^L]\frac{1}{6} h_i^2 \, [D_i^{-1}]^{n+1}\frac{1}{\Delta n}\,[V_o]^{-1}[\bar{\phi}_i]^{n+1} \\
&\quad + [f_i^L]\frac{1}{6} h_i^2 \, [D_i^{-1}]^{n+1}\frac{1}{\Delta n}\,[V_o]^{-1}[\bar{\phi}_i]^{n} \\
&\quad + [f_i^L]\frac{1}{6} h_i^2 \, [D_i^{-1}]^{n+1}[MD_i]^{n}[\bar{\phi}_i]^{n} \\
&\quad + [f_i^L]\frac{1}{6} h_i^2 \, [D_i^{-1}]^{n+1}[SD_i]^{n}
\end{aligned}
\tag{A3.20}
$$

Eliminating the surface-average flux, $[\phi(x_i)]^{n+1}$ from these two equations yields

$$
\begin{aligned}
[K_i]\,[J(x_i)]^{n+1} &= [f_{i-1}^R]\,[TA_{i-1}]\,[\bar{\phi}_{i-1}]^{n+1} - [f_i^L]\,[TA_i]\,[\bar{\phi}_i]^{n+1} \\
&\quad + [f_{i-1}^R]\,[TM_{i-1}]\,[\bar{\phi}_{i-1}]^{n+1} - [f_i^L]\,[TM_i]\,[\bar{\phi}_i]^{n+1} \\
&\quad + [f_{i-1}^R]\,[TD_{i-1}]\,[\bar{\phi}_{i-1}]^{n} - [f_i^L]\,[TD_i]\,[\bar{\phi}_i]^{n} \\
&\quad + [f_{i-1}^R]\,[TC_{i-1}]\,[SD_{i-1}]^{n} - [f_i^L]\,[TC_i]\,[SD_i]^{n}
\end{aligned}
\tag{A3.21}
$$

where

$$
\begin{aligned}
[K_i]^{n+1} &= \frac{1}{2}\left(h_{i-1}\,[f_{i-1}^R]\,[D_{i-1}^{-1}]^{n+1} + h_i\,[f_i^L]\,[D_i^{-1}]^{n+1}\right) \\
[TA_i]^{n+1} &= [I] - \frac{1}{6} h_i^2\,[D_i^{-1}]^{n+1}[\bar{A}_{o_i}]^{n+1} - \frac{1}{6} h_i^2\,[D_i^{-1}]^{n+1}\frac{1}{\Delta_n}[V_o]^{-1} \\
[TM_i]^{n+1} &= \frac{1}{6} h_i^2\,[D_i^{-1}]^{n+1}[M_i]^{n+1} \\
[TD_i]^{n+1} &= \frac{1}{6} h_i^2\,[D_i^{-1}]^{n+1}[MD_i]^{n} + \frac{1}{6} h_i^2\,[D_i^{-1}]^{n+1}\frac{1}{\Delta_n}[V_o]^{-1} \\
[TC_i]^{n+1} &= \frac{1}{6} h_i^2\,[D_i^{-1}]^{n+1}
\end{aligned}
\tag{A3.22}
$$

The superscripts n+1 have been removed from the matrices of Eq.(A3.21).

## Appendix 4

### DERIVATION OF NODAL BALANCE EQUATIONS

The nodal balance equation for the node i can be obtained by an integration of Eq.(A3.1) over the node length $(x_i, x_{i+1})$. The result (already given by Eq. A3.16) is

$$\begin{aligned}
&[J(x_{i+1})]^{n+1} - [J(x_i)]^{n+1} + h_i\,[\bar{A}_{o_i}]^{n+1}[\bar{\phi}_i]^{n+1} \\
&+ h_i \frac{1}{\Delta n}\,[V_o]^{-1}[\bar{\phi}_i]^{n+1} - h_i\,[M_i]^{n+1}[\bar{\phi}_i]^{n+1} \\
&- h_i \frac{1}{\Delta n}\,[V_o]^{-1}[\bar{\phi}_i]^{n} + h_i\,[MD_i]^{n}[\bar{\phi}_i]^{n} + h_i\,[SD_i]^{n}
\end{aligned} \tag{A4.1}$$

In Appendix 3, $[J(x_i)]^{n+1}$ was determined as a function of $[\bar{\phi}_{i-1}]$ and $[\bar{\phi}_i]$ by eliminating the surface fluxes of nodes i-1 and i. Written explicitly for $[J(x_i)]^{n+1}$, Equation (A3.21) is

$$\begin{aligned}
[J(x_i)]^{n+1} = \;& [K_i^{-1}]^{n+1}[f_{i-1}^R][TA_{i-1}]^{n+1}[\bar{\phi}_{i-1}]^{n+1} \\
&- [K_i^{-1}]^{n+1}[f_i^L]\;[TA_i]^{n+1}\;[\bar{\phi}_i]^{n+1} \\
&+ [K_i^{-1}]^{n+1}[f_{i-1}^R][TM_{i-1}]^{n+1}[\bar{\phi}_{i-1}]^{n+1} \\
&- [K_i^{-1}]^{n+1}[f_i^L]\;[TM_i]^{n+1}\;[\bar{\phi}_i]^{n+1} \\
&+ [K_i^{-1}]^{n+1}[f_{i-1}^R][TD_{i-1}]^{n+1}[\bar{\phi}_{i-1}]^{n} \\
&- [K_i^{-1}]^{n+1}[f_i^L]\;[TD_i]^{n+1}\;[\bar{\phi}_i]^{n} \\
&+ [K_i^{-1}]^{n+1}[f_{i-1}^R][TC_{i-1}]^{n+1}[SD_{i-1}]^{n} \\
&- [K_i^{-1}]^{n+1}[f_i^L]\;[TC_i]^{n+1}\;[SD_i]^{n}
\end{aligned} \tag{A4.2}$$

Similarly,

$$
\begin{aligned}
[J(x_{i+1})]^{n+1} = {} & [K_{i+1}^{-1}]^{n+1}[f_i^R] \quad [TA_i]^{n+1} \quad [\bar{\phi}_i]^{n+1} \\
& - [K_{i+1}^{-1}]^{n+1}[f_{i+1}^L][TA_{i+1}]^{n+1}[\bar{\phi}_{i+1}]^{n+1} \\
& + [K_{i+1}^{-1}]^{n+1}[f_i^R] \quad [TM_i]^{n+1} \quad [\bar{\phi}_i]^{n+1} \\
& - [K_{i+1}^{-1}]^{n+1}[f_{i+1}^L][TM_{i+1}]^{n+1}[\bar{\phi}_{i+1}]^{n+1} \\
& + [K_{i+1}^{-1}]^{n+1}[f_i^R] \quad [TD_i]^{n+1} \quad [\bar{\phi}_i]^{n} \\
& - [K_{i+1}^{-1}]^{n+1}[f_{i+1}^L][TD_{i+1}]^{n+1}[\bar{\phi}_{i+1}]^{n} \\
& + [K_{i+1}^{-1}]^{n+1}[f_i^R] \quad [TC_i]^{n+1} \quad [SD_i]^{n} \\
& - [K_{i+1}^{-1}]^{n+1}[f_{i+1}^L][TC_{i+1}]^{n+1}[SD_{i+1}]^{n}
\end{aligned}
\tag{A4.3}
$$

The net currents given by Eq.(A4.2) and (A4.3) can now be substituted into (A4.1). The three-point nodal balance equation which results is given by:

$$
\begin{aligned}
& - [P^{i-1}]^{n+1} [\bar{\phi}_{i-1}]^{n+1} + [Q^i]^{n+1} [\bar{\phi}_i]^{n+1} - [R^{i+1}]^{n+1} [\bar{\phi}_{i+1}]^{n+1} \\
& = [U^{i-1}]^{n+1} [\bar{\phi}_{i-1}]^{n+1} + [V^i]^{n+1} [\bar{\phi}_i]^{n+1} + [W^{i+1}]^{n+1} [\bar{\phi}_{i+1}]^{n+1} \\
& \quad + [S_i]^{n+1}
\end{aligned}
\tag{A4.4}
$$

where

$$
\begin{aligned}
[S_i]^{n+1} = {} & [UD^{i-1}]^{n+1}[\bar{\phi}_{i-1}]^{n} + [VD^i]^{n+1}[\bar{\phi}_i]^{n} + [WD^{i+1}]^{n+1}[\bar{\phi}_{i+1}]^{n} \\
& + [\alpha^{i-1}]^{n+1}[SD_{i-1}]^{n} + [\beta^i]^{n+1}[SD_i]^{n} + [\gamma^{i+1}]^{n+1}[SD_{i+1}]^{n}
\end{aligned}
\tag{A4.5}
$$

and the coefficient matrices are defined as:

$$
\begin{aligned}
[P^i]^{n+1} &= [K_{i+1}^{-1}]^{n+1}[f_i^R][TA_i]^{n+1} \\
[Q^i]^{n+1} &= h_i[\bar{A}_{o_i}]^{n+1} + h_i\frac{1}{\Delta_n}[V_o]^{-1} + \\
&\quad + \left([K_{i+1}^{-1}]^{n+1}[f_i^R] + [K_i^{-1}]^{n+1}[f_i^L]\right)[TA_i]^{n+1} \\
[R^i]^{n+1} &= [K_i^{-1}]^{n+1}[f_i^L][TA_i]^{n+1}
\end{aligned}
$$

$$
\begin{aligned}
[U^i]^{n+1} &= [K_{i+1}^{-1}]^{n+1}[f_i^R][TM_i]^{n+1} \\
[V^i]^{n+1} &= h_i[M_i]^{n+1} - \left([K_{i+1}^{-1}]^{n+1}[f_i^R] + [K_i^{-1}]^{n+1}[f_i^L]\right)[TM_i]^{n+1} \\
[W^i]^{n+1} &= [K_i^{-1}]^{n+1}[f_i^L][TM_i]^{n+1}
\end{aligned}
$$

(A4.6)

$$
\begin{aligned}
[UD^i]^{n+1} &= [K_{i+1}^{-1}]^{n+1}[f_i^R][TD_i]^{n+1} \\
[VD^i]^{n+1} &= h_i[MD_i]^{n+1} + h_i\frac{1}{\Delta_n}[V_o]^{-1} \\
&\quad - \left([K_{i+1}^{-1}]^{n+1}[f_i^R] + [K_i^{-1}]^{n+1}[f_i^L]\right)[TD_i]^{n+1} \\
[WD^i]^{n+1} &= [K_i^{-1}]^{n+1}[f_i^L][TD_i]^{n+1}
\end{aligned}
$$

$$
\begin{aligned}
[\alpha^i]^{n+1} &= [K_{i+1}^{-1}]^{n+1}[f_i^R][TC_i]^{n+1} \\
[\beta^i]^{n+1} &= h_i - \left([K_{i+1}^{-1}]^{n+1}[f_i^R] + [K_i^{-1}]^{n+1}[f_i^L]\right)[TC_i]^{n+1} \\
[\gamma^i]^{n+1} &= [K_i^{-1}]^{n+1}[f_i^L][TC_i]^{n+1}
\end{aligned}
$$

## Appendix 5

DESCRIPTION OF TEST PROBLEMS

## A5.1 The 2-Group Benchmark Problem for the Static Calculation

Geometry

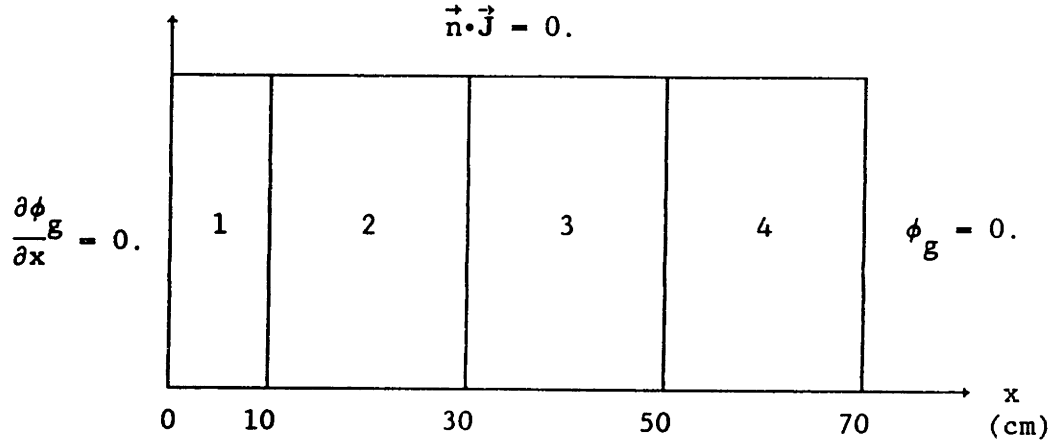


Material Properties

| Composition | Group, g | $D_g$ (cm) | $\Sigma_{a_g}$ ($cm^{-1}$) | $\nu\Sigma_{f_g}$ ($cm^{-1}$) |
|---|---|---|---|---|
| 1 | 1 | 1.44778 | 0.00814315 | 0.00491325 |
| | 2 | 0.390636 | 0.0618380 | 0.0823002 |
| 2 | 1 | 1.44897 | 0.00922036 | 0.00563319 |
| | 2 | 0.386548 | 0.0877775 | 0.103844 |
| 3 | 1 | 1.45915 | 0.00894364 | 0.00662150 |
| | 2 | 0.389813 | 0.0845164 | 0.128657 |
| 4 | 1 | 1.70 | 0.0010 | 0.0 |
| | 2 | 0.350 | 0.050 | 0.0 |

| Composition | Group, g | $\Sigma_{s_{g,1}}$ ($cm^{-1}$) | $\Sigma_{s_{g,2}}$ ($cm^{-1}$) |
|---|---|---|---|
| 1 | 1 | 0.481321 | 0.0 |
| | 2 | 0.0172675 | 1.23494 |
| 2 | 1 | 0.481647 | 0.0 |
| | 2 | 0.0167655 | 1.22821 |
| 3 | 1 | 0.476988 | 0.0 |
| | 2 | 0.0160496 | 1.22432 |
| 4 | 1 | 0.50 | 0.0 |
| | 2 | 0.0350 | 1.30 |

$\chi_1 = 1.0$ , $\chi_2 = 0.0$

$\nu = 2.50$

Discontinuity Factors

1.0 for all groups and nodes

## A5.2 THE HOMOGENEOUS BARE REACTOR PROBLEMS (TWO-GROUP)

Geometry

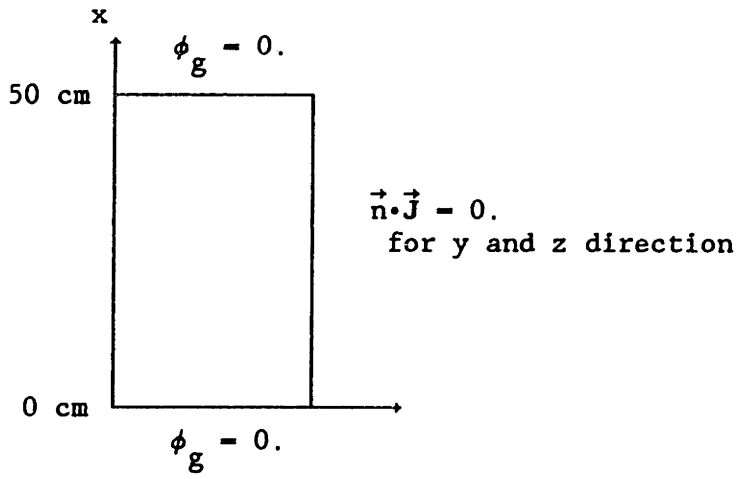


Material Properties

| Group,g | $D_g$ (cm) | $\Sigma_{a_g}$ ($cm^{-1}$) | $\nu\Sigma_{f_g}$ ($cm^{-1}$) | $\Sigma_{s_{g,1}}$ ($cm^{-1}$) | $\Sigma_{s_{g,2}}$ ($cm^{-1}$) |
|---|---|---|---|---|---|
| 1 | 1.4176 | 0.00855 | 0.00536 | 0.50 | 0.0 |
| 2 | 0.37336 | 0.06669 | 0.10433 | 0.01742 | 1.250 |

$\chi_1 = 1.0$ , $\chi_2 = 0.0$ , $\nu = 2.43$

$v_1 = 1.25 \times 10^7$ cm/sec. , $v_2 = 2.50 \times 10^5$ cm/sec.

Initial Reactor Power : 1.0 KWatts

Delayed Neutron Data

| Family,d | $\beta_d$ | $\lambda_d$ ($sec^{-1}$) |
|---|---|---|
| 1 | 0.0075 | 0.080 |

WIGL Thermal Hydraulic Parameters

$C_f$ = 2.46 × $10^6$ ergs/gm/K

$C_c$ = 5.43 × $10^7$ ergs/gm/K

$\rho_f$ = 10.3 gm/$cm^3$

$W_0$ for a fuel channel = 10.0 gm/sec

$h_0$ = 2.71 × $10^7$ ergs/$cm^2$/K/sec

$U_f$ = 2.20 × $10^6$ ergs/$cm^2$/K/sec

$A_h$ = 2.95 $cm^{-1}$

$V_c/(V_c+V_f)$ = 0.559

coolant inlet temperature = 533. K

fraction of fission energy in coolant = 0.0

coolant pressure = 1.53 × $10^7$ Pascals

$\left(\frac{\partial\ \rho_c H}{\partial\ \bar{T}_c}\right)$ = 1.60 × $10^7$ ergs/$cm^3$/K

energy conversion factor = 3.204 × $10^{-11}$ watts-sec/fission

cross-sectional area of fuel cell = 1.0 $cm^2$

Feedback Coefficients

| Parameters $\Sigma$ | $\frac{\partial\ \Sigma}{\partial\ \bar{T}_f}$ | $\frac{\partial\ \Sigma}{\partial\ \bar{T}_m}$ | $\frac{\partial\ \Sigma}{\partial\ \bar{\rho}_c}$ |
|---|---|---|---|
| $\Sigma_{tr_1}$ | -2.200 ×$10^{-6}$ | -2.666 ×$10^{-5}$ | +1.367 ×$10^{-1}$ |
| $\Sigma_{tr_2}$ | -8.666 ×$10^{-7}$ | -4.333 ×$10^{-4}$ | +9.000 ×$10^{-1}$ |
| $\Sigma_{c_1}$ | +3.300 ×$10^{-7}$ | +3.000 ×$10^{-6}$ | +2.830 ×$10^{-3}$ |
| $\Sigma_{c_2}$ | -3.800 ×$10^{-7}$ | -8.200 ×$10^{-6}$ | +1.400 ×$10^{-2}$ |
| $\Sigma_{21}$ | +8.500 ×$10^{-8}$ | -1.500 ×$10^{-6}$ | +2.400 ×$10^{-2}$ |
| $\nu\Sigma_{f_1}$ | 0.0 | 0.0 | 0.0 |
| $\nu\Sigma_{f_2}$ | -2.500 ×$10^{-6}$ | -2.075 ×$10^{-5}$ | +4.250 ×$10^{-2}$ |
| $\Sigma_{f_1}$ | 0.0 | 0.0 | 0.0 |
| $\Sigma_{f_2}$ | -1.000 ×$10^{-6}$ | -8.300 ×$10^{-6}$ | +1.700 ×$10^{-2}$ |

reference fuel temperature = 533 K
reference moderator temperature = 533 K
reference coolant density = 0.796100 gm/cm$^3$

Perturbations

1. step change transient

   Decrease in value of $\Sigma_{a_2}$ to 0.06630 cm$^{-1}$

2. coolant flow rate change transient

   $W_0 = 10 + 2.0 \times \text{time}$ (gm/sec)

3. coolant inlet temperature change transient

   $T_{inlet} = 533 - 5.0 \times \text{time}$ ( $^0$K )

4. control rod bank movement transient

   control rod worth : $\Delta\Sigma_{a_2} = 0.00039$ cm$^{-1}$

   0.0 sec through 2.5 sec : withdrawal from bottom to top
   2.5 sec through 5.0 sec : no movement
   5.0 sec through 7.5 sec : insertion from top to bottom
   7.5 sec through 10.0 sec : no movement
   10.0 sec through 12.5 sec : withdrawal from bottom to top
   12.5 sec through 15.0 sec : no movement

## A5.3 THE HOMOGENEOUS BARE REACTOR PROBLEMS (23-GROUP)

Geometry

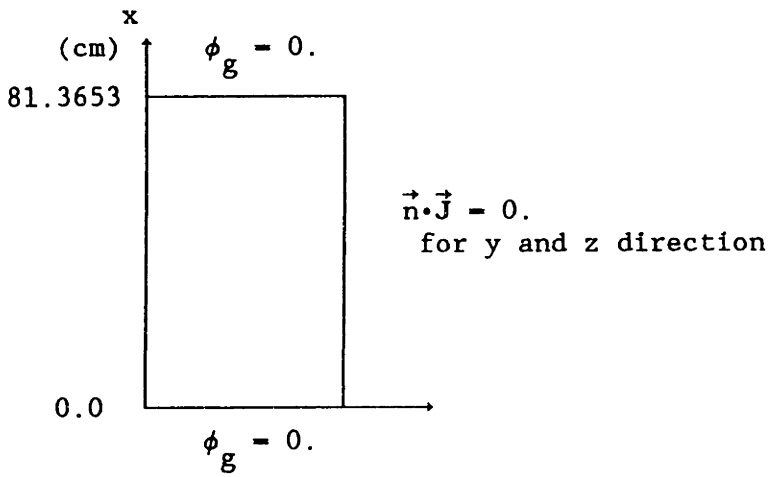


Material Properties

Fuel Assembly Composition A00REF
( See Appendix 2 )

Initial Reactor Power : 1.0 KWatts

WIGL Thermal Hydraulic Parameters

The same with data in Appendix A5.2

Reference Temperatures for the Feedback Calculation

reference fuel temperature = 533 K
reference moderator temperature = 533 K
reference coolant density = 0.796100 gm/cm$^3$

Perturbations

1. Control Rod Drop Transient

   cotrol rod worth : $\Delta\Sigma_{a_g} = 1.0\ cm^{-1}$, $g=1,2,\cdots,23.$

   Cotrol rod starts to drop from the top of the core to the bottom at time zero and reaches the bottom in 10. sec.

   rod traveling speed = 81.3653 cm/sec

2. Inlet-Coolant-Temperature Drop Transient

   $T_{inlet} = 533 - 1.0 \times time \quad (\ ^{o}K\ )$

## A5.4 A TWO-REGION UNREFLECTED REACTOR PROBLEM

Geometry

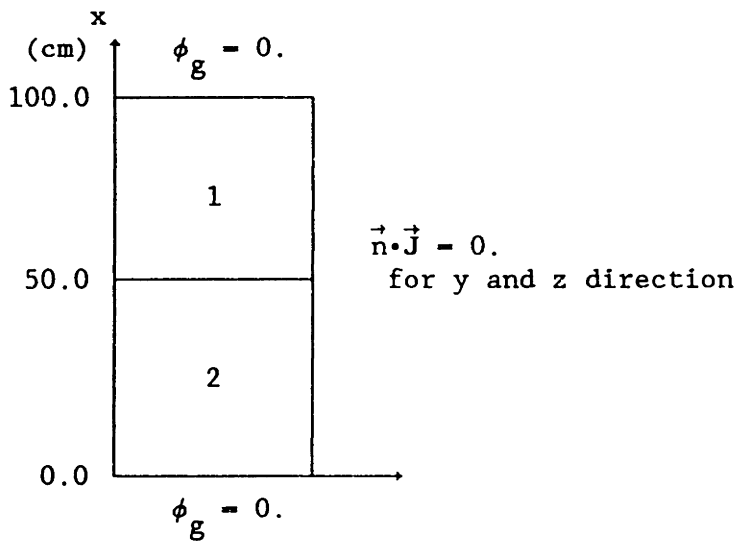


Material Properties

Region 1 : Fuel Assembly Composition CLOREF
Region 2 : Fuel Assembly Composition COOREF
( See Appendix 2 )

Initial Reactor Power : 100.0 MWatts

WIGL Thermal Hydraulic Parameters

The same with data in Appendix A5.2
except

$W_0 = 1.5 \times 10^6$ gm/sec

$h_0 = 2.00 \times 10^7$ ergs/cm$^2$/K/sec

$U_f = 1.50 \times 10^6$ ergs/cm$^2$/K/sec

cross-sectional area of a fuel cell = 4.0 cm$^2$
total number of fuel cells in a reactor = 5000.

Reference Temperatures for the Feedback Calculation

reference fuel temperature = 759 K
reference moderator temperature = 539 K
no moderator density feedback

Perturbations

Inlet-Coolant-Temperature Change Transient

$$T_{inlet} = 533 - 16.0 \times time + 10.0 \times (time)^2 \quad (\ ^{o}K\ )$$

## A5.5 FOUR-REGION REACTOR PROBLEMS

Geometry

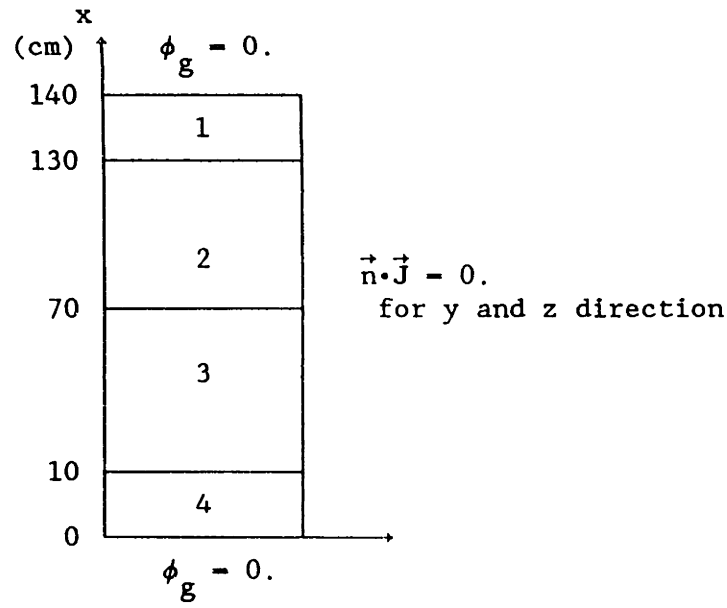


Material Properties

Region 1 : Water Reflector REFREF
Region 2 : Fuel Assembly Composition CLOREF
Region 3 : Fuel Assembly Composition COOREF
Region 4 : Water Reflector REFREF
( See Appendix 2 )

Initial Reactor Power : 100.0 MWatts

WIGL Thermal Hydraulic Parameters

The same with data in Appendix A5.2
except
$W_0 = 1.5 \times 10^6$ gm/sec
$h_0 = 2.00 \times 10^7$ ergs/cm$^2$/K/sec
$U_f = 1.50 \times 10^6$ ergs/cm$^2$/K/sec
cross-sectional area of a fuel cell = 3.0 cm$^2$
total number of fuel cells in a reactor = 4000.

Reference Temperatures for the Feedback Calculation

reference fuel temperature = 800 K
reference moderator temperature = 540 K
no moderator density feedback

Perturbations

1. Control Rod Banks Removal Transient

   initial rod position : inserted to the center of the core from the top

   rod removal speed = 1 cm/sec.

   As a fictitious control rod tip passes, a rodded composition (region 2) is replaced by an unrodded composition (region 3).

2. Inlet-Coolant-Temperature Drop Transient

   $T_{inlet} = 533 - 1.0 \times time \quad (\ ^{0}K\ )$

## Appendix 6

### ANALYTICAL SOLUTIONS FOR THE TWO GROUP HOMOGENEOUS REACTOR PROBLEM

All results provided in this Appendix are based on the 3-D analytical solutions of Antonio F. V. Dias [D-2]. Here, however, one-dimensional solutions are found. Detailed data for the reactor compositions and perturbations are given in Section A5.2 of Appendix 5. What is described there, is a homogeneous slab reactor with zero-flux boundary conditions. The analytical solutions are derived only for the step change of thermal absorption cross sections without thermal hydraulic feedbacks.

The two-group diffusion equations for the steady state are:

$$-D_1 \frac{d^2}{dx^2}\phi_1(x) + \Sigma_1 \phi_1(x) = \frac{1}{k_{eff}} [\nu\Sigma_{f_1}\phi_1(x) + \nu\Sigma_{f_2}\phi_2(x)]$$

$$-D_2 \frac{d^2}{dx^2}\phi_2(x) + \Sigma_2 \phi_2(x) = \Sigma_{21} \phi_1(x). \qquad \text{(A6.1)}$$

We can assume the solutions for the slab reactor as

$$\phi_g(x) = A_g \sin\left(\frac{\pi x}{L}\right) ; \qquad g = 1,2 \qquad \text{(A6.2)}$$

where L is the thickness of the reactor.

Substituting this into Eq. (A6.1) we have:

$$D_1 B^2 + \Sigma_1 = k_{eff}^{-1} [ \nu\Sigma_{f_1} + r_0 \nu\Sigma_{f_2} ] \quad (A6.3)$$

$$D_2 B^2 + \Sigma_2 = \Sigma_{21} \frac{1}{r_0} \quad (A6.4)$$

where $B^2 = (\frac{\pi}{L})^2$ and $r_0 = \phi_2 / \phi_1 = A_2 / A_1$ . From Eq. (A6.4) we have

$$r_0 = \frac{\Sigma_{21}}{D_2 B^2 + \Sigma_2} . \quad (A6.5)$$

Substituting this into Eq. (A6.3) we also have

$$\frac{1}{k_{eff}} = \frac{D_1 B^2 + \Sigma_1}{\nu\Sigma_{f_1} + \frac{\Sigma_{21} \nu\Sigma_{f_2}}{D_2 B^2 + \Sigma_2}} . \quad (A6.6)$$

Using the values for cross sections and dimensions given in Appendix 5, we have

$$r_0 = 0.2555602 , \quad k_{eff} = 1.014450 .$$

For a transient situation, the time dependent diffusion equations for the problem are :

$$\frac{1}{v_1}\frac{\partial}{\partial t}\phi_1(x,t) = (1-\beta)k_{eff}^{-1}\left[\nu\Sigma_{f_1}\phi_1(x,t) + \nu\Sigma_{f_2}\phi_2(x,t)\right] + D_1\frac{\partial^2}{\partial x^2}\phi_1(x,t) - \Sigma_1\phi_1(x,t) + \lambda\, C(x,t)$$

$$\frac{1}{v_2}\frac{\partial}{\partial t}\phi_2(x,t) = \Sigma_{21}\phi_1(x,t) + D_2\frac{\partial^2}{\partial x^2}\phi_2(x,t) - \Sigma_2\phi_2(x,t) \qquad \text{(A6.7)}$$

$$\frac{\partial}{\partial t}C(x,t) = \beta\, k_{eff}^{-1}\left[\nu\Sigma_{f_1}\phi_1(x,t) + \nu\Sigma_{f_2}\phi_2(x,t)\right] - \lambda\, C(x,t)$$

In the steady state, we have the relation

$$C(x,0) = S_0\,\phi_1(x,0) \qquad \text{(A6.8)}$$

where $S_0 = \frac{\beta}{\lambda}\, k_{eff}^{-1}[\nu\Sigma_{f_1} + r_0\,\nu\Sigma_{f_2}] = 3.045499 \times 10^{-3}$.

In order to solve Eqs. (A6.7) for a spatially uniform step transient, we assume that

$$\frac{\partial}{\partial t}\phi_g = \omega\phi_g\ , \qquad \frac{\partial}{\partial t}C = \omega C\ , \qquad \frac{\partial^2}{\partial x^2}\phi_g = -B^2\phi_g \qquad \text{(A6.9)}$$

If Eqs. (A6.9) are substituted into Eqs. (A6.7), we obtain

$$\frac{\omega}{v_1}\phi_1 = k_{eff}^{-1}(1-\beta)[\nu\Sigma_{f_1}\phi_1 + \nu\Sigma_{f_2}\phi_2] + \lambda C - D_1B^2\phi_1 - \Sigma_1\phi_1 \qquad \text{(A6.10)}$$

$$\frac{\omega}{v_2}\phi_2 = \Sigma_{21}\phi_1 - D_2B^2\phi_2 - \Sigma_2\phi_2 \qquad \text{(A6.11)}$$

$$\omega\, C = k_{eff}^{-1}\,\beta\,[\nu\Sigma_{f_1}\phi_1 + \nu\Sigma_{f_2}\phi_2] - \lambda C \qquad \text{(A6.12)}$$

From Eq. (A6.11), we have the expression

$$\phi_2 = \frac{\Sigma_{21}}{D_2B^2 + \Sigma_2 + \frac{\omega}{v_2}} \phi_1 \cdot \tag{A6.13}$$

From Eqs. (A6.12) and (A6.13), we have

$$\nu' = \frac{\beta}{(\omega + \lambda)} k_{eff}^{-1} \left[\nu\Sigma_{f_1} + \frac{\nu\Sigma_{f_2} \Sigma_{21}}{D_2B^2 + \Sigma_2 + \frac{\omega}{v_2}}\right] \phi_1 \tag{A6.14}$$

If Eqs. (A6.13) and (A6.14) are substituted into Eq. (A6.10), we obtain an expression containing terms multiplied by only $\phi_1$. After a long algebraic manipulation, a third-order equation of $\omega$'s is obtained :

$$\omega^3 + C_1\omega^2 + C_2\omega + C_3 = 0. \tag{A6.15}$$

where
$$C_1 = \lambda + v_1 [\Sigma_1 + D_1B^2 - (1-\beta)k_{eff}^{-1}\nu\Sigma_{f_1}] + v_2 (\Sigma_2 + D_2B^2)$$

$$C_2 = \lambda v_1 (\Sigma_1 + D_1B^2 - k_{eff}^{-1}\nu\Sigma_{f_1}) + \lambda v_2 (\Sigma_2 + D_2B^2)$$
$$- v_1v_2 (1-\beta)k_{eff}^{-1}\nu\Sigma_{f_2}\Sigma_{21}$$
$$+ v_1v_2 (\Sigma_2 + D_2B^2) [\Sigma_1 + D_1B^2 - (1-\beta)k_{eff}^{-1}\nu\Sigma_{f_1}]$$

$$C_3 = -\lambda v_1v_2 \left[k_{eff}^{-1}\nu\Sigma_{f_2}\Sigma_{21} - (\Sigma_2 + D_2B^2) (\Sigma_1 + D_1B^2 - k_{eff}^{-1}\nu\Sigma_{f_1})\right]$$

If the values for all cross sections are substituted, Eq. (A6.15) can be

solved for the three values of $\omega$ : $\omega_1$, $\omega_2$ and $\omega_3$.

As a result the solution of Eq. (A6.7) can be written as:

$$\phi_1(x,t) = \left( B_1 e^{\omega_1 t} + B_2 e^{\omega_2 t} + B_3 e^{\omega_3 t} \right) \sin \frac{\pi x}{L}$$

$$\phi_2(x,t) = \left( B_1 r_1 e^{\omega_1 t} + B_2 r_2 e^{\omega_2 t} + B_3 r_3 e^{\omega_3 t} \right) \sin \frac{\pi x}{L} \qquad \text{(A6.1o,}$$

$$C(x,t) = \left( B_1 S_1 e^{\omega_1 t} + B_2 S_2 e^{\omega_2 t} + B_3 S_3 e^{\omega_3 t} \right) \sin \frac{\pi x}{L}$$

where :

$$r_i = \frac{\Sigma_{21}}{D_2 B^2 + \Sigma_2 + \frac{\omega_i}{v_2}}$$

$$S_i = \frac{\beta}{\omega_i + \lambda} k_{eff}^{-1} (\nu\Sigma_{f_1} + r_i \nu\Sigma_{f_2})$$

The expressions for $r_i$ and $S_i$ are obtained from Eqs. (A6.13) and (A6.14) and the coefficients $B_1$, $B_2$ and $B_3$ are to be found from the initial conditions

From the results previously discussed, the initial conditions for the problems are :

$$\phi_1(x,0) = A \sin \frac{\pi x}{L} \qquad \text{(A6.17)}$$

$$\phi_2(x,0) = r_o \phi_1(x,0) \qquad \text{(A6.18)}$$

$$C(x,0) = S_o \phi_1(x,0) \qquad \text{(A6.19)}$$

$P_o$ = steady-state power

$$= C_f A_c \int_0^L [\Sigma_{f_1} \phi_1(x,0) + \Sigma_{f_1} \phi_1(x,0)] \, dx \qquad \text{(A6.20)}$$

where $C_f$ is a fission energy conversion factor and $A_c$ is a cross sectional area of reactor.

Substituting Eqs. (A6.17) and (A6.18) into Eq. (A6.20), we have

$$A = \left(\frac{P}{C_f A_c}\right)\left(\frac{\pi}{2L}\right)\left(\frac{1}{\Sigma_{f_1} + r_0\Sigma_{f_2}}\right) \tag{A6.21}$$

Substituting the initial conditions (A6.17), (A6.18) and (A6.19) into Eqs. (A6.16), we find :

$$\begin{aligned} B_1 + B_2 + B_3 &= A \\ r_1B_1 + r_2B_2 + r_3B_3 &= r_0A \\ S_1B_1 + S_2B_2 + S_3B_3 &= S_0A \end{aligned} \tag{A6.22}$$

Therefore, we can obtain the solution of this linear system as follows :

$$B_1 = f_1A\ , \qquad B_2 = f_2A\ , \qquad B_3 = f_3A \tag{A6.23}$$

where :

$$f_1 = \frac{(r_2S_3 - r_3S_2) - r_0(S_3 - S_2) + S_0(r_3 - r_2)}{r_2S_3 - r_3S_2 + r_3S_1 - r_1S_3 + r_1S_2 - r_2S_1}$$

$$f_2 = \frac{-(r_1S_3 - r_3S_1) + r_0(S_3 - S_1) - S_0(r_3 - r_1)}{r_2S_3 - r_3S_2 + r_3S_1 - r_1S_3 + r_1S_2 - r_2S_1}$$

$$f_3 = \frac{(r_1S_2 - r_2S_1) - r_0(S_2 - S_1) + S_0(r_2 - r_1)}{r_2S_3 - r_3S_2 + r_3S_1 - r_1S_3 + r_1S_2 - r_2S_1}$$

The expression for the power evolution with time is given by :

$$P(t) = C_f A_c \int_0^L [\Sigma_{f_1} \phi_1(x,t) + \Sigma_{f_2} \phi_2(x,t)]\, dx \qquad (A6.24)$$

Using Eqs. (A6.16), (A6.21) and (A6.23), the expression above can be written as :

$$P(t) = P_0 \times \left[ p_1 e^{\omega_1 t} + p_2 e^{\omega_2 t} + p_3 e^{\omega_3 t} \right] \qquad (A6.25)$$

where :

$$p_1 = f_1 \frac{\Sigma_{f_1} + r_1 \Sigma_{f_2}}{\Sigma_{f_1} + r_0 \Sigma_{f_2}}$$

$$p_2 = f_2 \frac{\Sigma_{f_1} + r_2 \Sigma_{f_2}}{\Sigma_{f_1} + r_0 \Sigma_{f_2}}$$

$$p_3 = f_3 \frac{\Sigma_{f_1} + r_3 \Sigma_{f_2}}{\Sigma_{f_1} + r_0 \Sigma_{f_2}}$$

For the step transient described in Appendix A5.2, we find the following values :

| | | |
|---|---|---|
| $\omega_1 = 0.1390774$ | $r_1 = 0.2570287$ | $S_1 = 1.085831 \times 10^{-3}$ |
| $\omega_2 = -53.26490$ | $r_2 = 0.2578414$ | $S_2 = -4.484506 \times 10^{-6}$ |
| $\omega_3 = -345921.0$ | $r_3 = -0.01323799$ | $S_3 = -8.503833 \times 10^{-11}$ |

$$f_1 = 2.718331 \qquad p_1 = 2.731336$$
$$f_2 = -1.718596 \qquad p_2 = -1.731369$$
$$f_3 = 2.657283 \times 10^{-4} \qquad p_3 = 3.301735 \times 10^{-5}$$

The final expression for the power can be written as :

$$P(t) = P_0 \left[ 2.718331\, e^{0.1390774\, t} - 1.718596\, e^{-53.26490\, t} + 0.000025\, e^{-345921.0\, t} \right] \qquad \text{(A6.26)}$$

The two-group adjoint diffusion equations for the steady state are:

$$-D_1 \frac{d^2}{dx^2}\phi_1^*(x) + \Sigma_1\, \phi_1^*(x) = \frac{1}{k_{eff}}\, \nu\Sigma_{f_1} \phi_1^*(x) + \Sigma_{21}\, \phi_2^*(x)$$
$$-D_2 \frac{d^2}{dx^2}\phi_2^*(x) + \Sigma_2\, \phi_2^*(x) = \frac{1}{k_{eff}}\, \nu\Sigma_{f_2} \phi_2^*(x). \qquad \text{(A6.27)}$$

We can assume the solutions as

$$\phi_g^*(x) = A_g^* \sin\left(\frac{\pi x}{L}\right) ; \qquad g = 1,2 \qquad \text{(A6.28)}$$

Substituting this into Eq. (A6.27) we have:

$$D_1 B^2 + \Sigma_1 = k_{eff}^{-1}\, \nu\Sigma_{f_1} + R_0\, \Sigma_{21} \qquad \text{(A6.29)}$$
$$D_2 B^2 + \Sigma_2 = k_{eff}^{-1}\, \nu\Sigma_{f_2}\, \frac{1}{R_0} \qquad \text{(A6.30)}$$

where $R_o = \phi_2^* / \phi_1^* = A_2^* / A_1^*$ . From Eq. (A6.30) we have

$$R_o = \frac{k_{eff}^{-1} \nu\Sigma_{f_2}}{D_2 B^2 + \Sigma_2} . \qquad \text{(A6.31)}$$

Substituting this into Eq. (A6.29) we also have

$$\frac{1}{k_{eff}} = \frac{D_1 B^2 + \Sigma_1}{\nu\Sigma_{f_1} + \frac{\Sigma_{21} \nu\Sigma_{f_2}}{D_2 B^2 + \Sigma_2}} \qquad \text{(A6.32)}$$

which is identical with Eq. (A6.6).

Using the data for cross sections in Appendix 5, we have

$$R_o = 1.5087722 , \quad k_{eff} = 1.014450 .$$

## Appendix 7

CALCULATED TWO GROUP P-1 PARAMETERS

A7.1 Two-Group Cross Sections of Fuel CLOREF

A7.2 Two-Group Cross Sections of Fuel COOREF

A7.3 Two-Group Cross Sections of Fuel AOOREF

A7.4 Two-Group Cross Sections of Reflector REFREF

A7.5 Two-Group Temperature Feedback Coefficients of Fuel CLOREF

A7.6 Two-Group Temperature Feedback Coefficients of Fuel COOREF

A7.7 Two-Group Temperature Feedback Coefficients of Fuel AOOREF

A7.8 Two-Group Temperature Feedback Coefficients of Reflector REFREF

## A7.1 Two-Group Cross Sections of Fuel CLOREF

Bm^2 = 1.548157E-03

REGULARLY WEIGHTED FEW GROUP CROSS-SECTIONS

| GROUP | TOTAL | ABSORPTION | SCATTERING | DIFF(1/3TR) |
|---|---|---|---|---|
| 1 | 5.043080E-01 | 9.026068E-03 | 4.952820E-01 | 1.455884E+00 |
| 2 | 1.316215E+00 | 9.112466E-02 | 1.225090E+00 | 3.883716E-01 |

| GROUP | TRANSPORT | FISS FRAC. | NU-FISSION | FISSION |
|---|---|---|---|---|
| 1 | 2.289560E-01 | 1.000000E+00 | 6.255331E-03 | 2.460834E-03 |
| 2 | 8.582846E-01 | 0.000000E+00 | 1.203259E-01 | 4.974615E-02 |

Po-SCATTERING

FROM GROUP 1

4.788635E-01 1.641843E-02

FROM GROUP 2

1.731151E-03 1.223359E+00

| GROUP | 1/V (sec/cm) | SPEED (cm/s) |
|---|---|---|
| 1 | 6.016989E-08 | 1.661961E+07 |
| 2 | 2.330693E-06 | 4.290569E+05 |

CHI-D

DELAYED-NEUTRON PRECURSOR GROUP \ ENERGY-GROUP

| | 1 | 2 |
|---|---|---|
| 1 | 1.000000E+00 | 0.000000E+00 |
| 2 | 1.000000E+00 | 0.000000E+00 |
| 3 | 1.000000E+00 | 0.000000E+00 |
| 4 | 1.000000E+00 | 0.000000E+00 |
| 5 | 1.000000E+00 | 0.000000E+00 |
| 6 | 1.000000E+00 | 0.000000E+00 |

BI-LINEARLY WEIGHTED FEW GROUP CROSS-SECTIONS
**********

| GROUP | TOTAL | ABSORPTION | SCATTERING | DIFF(1/3TR) |
|---|---|---|---|---|
| 1 | 4.840064E-01 | 6.768483E-03 | 4.772379E-01 | 1.349671E+00 |
| 2 | 1.316693E+00 | 9.020130E-02 | 1.226491E+00 | 3.871256E-01 |

| GROUP | TRANSPORT | FISS FRAC. | NU-FISSION | FISSION |
|---|---|---|---|---|
| 1 | 2.469737E-01 | 9.056618E-01 | 6.255331E-03 | 2.460834E-03 |
| 2 | 8.610471E-01 | 0.000000E+00 | 1.203259E-01 | 4.974615E-02 |

Po-SCATTERING
FROM GROUP 1
4.609289E-01 1.630902E-02
FROM GROUP 2
2.033660E-03 1.224458E+00

| GROUP | 1/V (sec/cm) | SPEED (cm/s) |
|---|---|---|
| 1 | 6.582506E-08 | 1.519178E+07 |
| 2 | 2.333363E-06 | 4.285660E+05 |

CHI-D
DELAYED-NEUTRON PRECURSOR GROUP \ ENERGY-GROUP

| | 1 | 2 |
|---|---|---|
| 1 | 9.080778E-01 | 0.000000E+00 |
| 2 | 9.011283E-01 | 0.000000E+00 |
| 3 | 9.031184E-01 | 0.000000E+00 |
| 4 | 9.025198E-01 | 0.000000E+00 |
| 5 | 9.025198E-01 | 0.000000E+00 |
| 6 | 9.025198E-01 | 0.000000E+00 |

## A7.2 Two-Group Cross Sections of Fuel COOREF

Bm^2 = 3.763949E-03

REGULARLY WEIGHTED FEW GROUP CROSS-SECTIONS

| GROUP | TOTAL | ABSORPTION | SCATTERING | DIFF(1/3TR) |
|---|---|---|---|---|
| 1 | 5.019716E-01 | 8.943164E-03 | 4.930284E-01 | 1.459171E+00 |
| 2 | 1.310501E+00 | 8.451644E-02 | 1.225984E+00 | 3.898135E-01 |

| GROUP | TRANSPORT | FISS FRAC. | NU-FISSION | FISSION |
|---|---|---|---|---|
| 1 | 2.284403E-01 | 1.000000E+00 | 6.621293E-03 | 2.602991E-03 |
| 2 | 8.551097E-01 | 0.000000E+00 | 1.286577E-01 | 5.319076E-02 |

Po-SCATTERING
FROM GROUP 1
4.769800E-01 1.604848E-02
FROM GROUP 2
1.662916E-03 1.224321E+00

| GROUP | 1/V (sec/cm) | SPEED (cm/s) |
|---|---|---|
| 1 | 5.884556E-08 | 1.699364E+07 |
| 2 | 2.345031E-06 | 4.264336E+05 |

CHI-D
DELAYED-NEUTRON PRECURSOR GROUP \ ENERGY-GROUP

| | 1 | 2 |
|---|---|---|
| 1 | 1.000000E+00 | 0.000000E+00 |
| 2 | 1.000000E+00 | 0.000000E+00 |
| 3 | 1.000000E+00 | 0.000000E+00 |
| 4 | 1.000000E+00 | 0.000000E+00 |
| 5 | 1.000000E+00 | 0.000000E+00 |
| 6 | 1.000000E+00 | 0.000000E+00 |

BI-LINEARLY WEIGHTED FEW GROUP CROSS-SECTIONS
**********

| GROUP | TOTAL | ABSORPTION | SCATTERING | DIFF(1/3TR) |
|---|---|---|---|---|
| 1 | 4.877312E-01 | 4.902341E-03 | 4.828289E-01 | 1.298373E+00 |
| 2 | 1.310286E+00 | 8.384783E-02 | 1.226438E+00 | 3.891526E-01 |

| GROUP | TRANSPORT | FISS FRAC. | NU-FISSION | FISSION |
|---|---|---|---|---|
| 1 | 2.567316E-01 | 8.419885E-01 | 6.621293E-03 | 2.602991E-03 |
| 2 | 8.565620E-01 | 0.000000E+00 | 1.286577E-01 | 5.319076E-02 |

Po-SCATTERING
FROM GROUP 1
4.668269E-01 1.600196E-02
FROM GROUP 2
2.079931E-03 1.224358E+00

| GROUP | 1/V (sec/cm) | SPEED (cm/s) |
|---|---|---|
| 1 | 6.799895E-08 | 1.470611E+07 |
| 2 | 2.345384E-06 | 4.263693E+05 |

CHI-D

| DELAYED-NEUTRON PRECURSOR GROUP \ ENERGY-GROUP | 1 | 2 |
|---|---|---|
| 1 | 9.003920E-01 | 0.000000E+00 |
| 2 | 8.852849E-01 | 0.000000E+00 |
| 3 | 8.895579E-01 | 0.000000E+00 |
| 4 | 8.882920E-01 | 0.000000E+00 |
| 5 | 8.882920E-01 | 0.000000E+00 |
| 6 | 8.882920E-01 | 0.000000E+00 |

## A7.3 **Two-Group Cross Sections of Fuel A00REF**

Bm^2 = 1.490807E-03

REGULARLY WEIGHTED FEW GROUP CROSS-SECTIONS

| GROUP | TOTAL | ABSORPTION | SCATTERING | DIFF(1/3TR) |
|---|---|---|---|---|
| 1 | 5.067250E-01 | 8.142784E-03 | 4.985822E-01 | 1.447774E+00 |
| 2 | 1.298070E+00 | 6.183800E-02 | 1.236232E+00 | 3.906361E-01 |

| GROUP | TRANSPORT | FISS FRAC. | NU-FISSION | FISSION |
|---|---|---|---|---|
| 1 | 2.302385E-01 | 1.000000E+00 | 4.913179E-03 | 1.902351E-03 |
| 2 | 8.533092E-01 | 0.000000E+00 | 8.230017E-02 | 3.402521E-02 |

Po-SCATTERING
FROM GROUP 1
4.813158E-01 1.726641E-02
FROM GROUP 2
1.290040E-03 1.234942E+00

| GROUP | 1/V (sec/cm) | SPEED (cm/s) |
|---|---|---|
| 1 | 6.263706E-08 | 1.596499E+07 |
| 2 | 2.419570E-06 | 4.132966E+05 |

CHI-D
DELAYED-NEUTRON PRECURSOR GROUP \ ENERGY-GROUP

| | 1 | 2 |
|---|---|---|
| 1 | 1.000000E+00 | 0.000000E+00 |
| 2 | 1.000000E+00 | 0.000000E+00 |
| 3 | 1.000000E+00 | 0.000000E+00 |
| 4 | 1.000000E+00 | 0.000000E+00 |
| 5 | 1.000000E+00 | 0.000000E+00 |
| 6 | 1.000000E+00 | 0.000000E+00 |

BI-LINEARLY WEIGHTED FEW GROUP CROSS-SECTIONS
**********

| GROUP | TOTAL | ABSORPTION | SCATTERING | DIFF(1/3TR) |
|---|---|---|---|---|
| 1 | 4.848082E-01 | 5.702407E-03 | 4.791058E-01 | 1.336468E+00 |
| 2 | 1.297975E+00 | 6.144209E-02 | 1.236533E+00 | 3.901155E-01 |

| GROUP | TRANSPORT | FISS FRAC. | NU-FISSION | FISSION |
|---|---|---|---|---|
| 1 | 2.494136E-01 | 9.003017E-01 | 4.913179E-03 | 1.902351E-03 |
| 2 | 8.544478E-01 | 0.000000E+00 | 8.230017E-02 | 3.402521E-02 |

Po-SCATTERING
FROM GROUP 1
4.618841E-01 1.722173E-02
FROM GROUP 2
1.521841E-03 1.235011E+00

| GROUP | 1/V (sec/cm) | SPEED (cm/s) |
|---|---|---|
| 1 | 6.897009E-08 | 1.449904E+07 |
| 2 | 2.419962E-06 | 4.132296E+05 |

CHI-D
DELAYED-NEUTRON PRECURSOR GROUP \ ENERGY-GROUP

| | 1 | 2 |
|---|---|---|
| 1 | 8.995329E-01 | 0.000000E+00 |
| 2 | 8.924026E-01 | 0.000000E+00 |
| 3 | 8.944561E-01 | 0.000000E+00 |
| 4 | 8.938281E-01 | 0.000000E+00 |
| 5 | 8.938281E-01 | 0.000000E+00 |
| 6 | 8.938281E-01 | 0.000000E+00 |

## A7.4 **Two-Group Cross Sections of Reflector REFREF**

REGULARLY WEIGHTED FEW GROUP CROSS-SECTIONS

| GROUP | TOTAL | ABSORPTION | SCATTERING | DIFF(1/3TR) |
|---|---|---|---|---|
| 1 | 5.789566E-01 | 6.830601E-04 | 5.782736E-01 | 1.695781E+00 |
| 2 | 1.757191E+00 | 1.692357E-02 | 1.740268E+00 | 2.993161E-01 |

| GROUP | TRANSPORT | FISS FRAC. | NU-FISSION | FISSION |
|---|---|---|---|---|
| 1 | 1.965663E-01 | 1.000000E+00 | 0.000000E+00 | 0.000000E+00 |
| 2 | 1.113650E+00 | 0.000000E+00 | 0.000000E+00 | 0.000000E+00 |

Po-SCATTERING
FROM GROUP 1
5.474059E-01 3.086765E-02
FROM GROUP 2
4.771069E-04 1.739791E+00

| GROUP | 1/V (sec/cm) | SPEED (cm/s) |
|---|---|---|
| 1 | 7.283996E-08 | 1.372873E+07 |
| 2 | 2.653838E-06 | 3.768127E+05 |

CHI-D
DELAYED-NEUTRON PRECURSOR GROUP \ ENERGY-GROUP

| | 1 | 2 |
|---|---|---|
| 1 | 1.000000E+00 | 0.000000E+00 |
| 2 | 1.000000E+00 | 0.000000E+00 |
| 3 | 1.000000E+00 | 0.000000E+00 |
| 4 | 1.000000E+00 | 0.000000E+00 |
| 5 | 1.000000E+00 | 0.000000E+00 |
| 6 | 1.000000E+00 | 0.000000E+00 |

BI-LINEARLY WEIGHTED FEW GROUP CROSS-SECTIONS
**********

| GROUP | TOTAL | ABSORPTION | SCATTERING | DIFF(1/3TR) |
|---|---|---|---|---|
| 1 | 5.776130E-01 | 8.250249E-04 | 5.767880E-01 | 1.701995E+00 |
| 2 | 1.755749E+00 | 1.693935E-02 | 1.738810E+00 | 2.993131E-01 |

| GROUP | TRANSPORT | FISS FRAC. | NU-FISSION | FISSION |
|---|---|---|---|---|
| 1 | 1.958486E-01 | 1.005451E+00 | 0.000000E+00 | 0.000000E+00 |
| 2 | 1.113661E+00 | 0.000000E+00 | 0.000000E+00 | 0.000000E+00 |

Po-SCATTERING
FROM GROUP 1
5.458987E-01 3.088926E-02
FROM GROUP 2
4.746473E-04 1.738335E+00

| GROUP | 1/V (sec/cm) | SPEED (cm/s) |
|---|---|---|
| 1 | 7.247160E-08 | 1.379851E+07 |
| 2 | 2.651267E-06 | 3.771782E+05 |

CHI-D
DELAYED-NEUTRON PRECURSOR GROUP \ ENERGY-GROUP

| | 1 | 2 |
|---|---|---|
| 1 | 9.972990E-01 | 0.000000E+00 |
| 2 | 9.973611E-01 | 0.000000E+00 |
| 3 | 9.973623E-01 | 0.000000E+00 |
| 4 | 9.973572E-01 | 0.000000E+00 |
| 5 | 9.973572E-01 | 0.000000E+00 |
| 6 | 9.973572E-01 | 0.000000E+00 |

## A7.5 Two-Group Temperature Feedback Coefficients of Fuel CLOREF

Fuel Temperature Coefficients

| group | transport | capture | xx | nu-fission | fission |
|---|---|---|---|---|---|
| Method 1 | | | | | |
| 1 | -1.264277E-06 | 4.158222E-07 | 0.0 | -5.766889E-08 | -2.296977E-08 |
| 2 | -5.223904E-06 | -3.815948E-07 | 0.0 | -2.025361E-06 | -8.374196E-07 |
| Method 2 | | | | | |
| 1 | -9.268582E-07 | 4.703645E-07 | 0.0 | -3.637116E-08 | -1.354868E-08 |
| 2 | -2.598329E-06 | -2.131779E-07 | 0.0 | -1.460226E-06 | -6.037762E-07 |
| Method 3 | | | | | |
| 1 | -1.308583E-06 | 4.235514E-07 | 0.0 | -5.766889E-08 | -2.296977E-08 |
| 2 | -5.206528E-06 | -4.407406E-07 | 0.0 | -2.025361E-06 | -8.374196E-07 |
| Method 4 | | | | | |
| 1 | -9.830272E-07 | 4.697884E-07 | 0.0 | -3.637116E-08 | -1.354868E-08 |
| 2 | -2.601171E-06 | -2.405227E-07 | 0.0 | -1.460226E-06 | -6.037762E-07 |

| | $\Sigma_{s_{11}}$ | $\Sigma_{s_{12}}$ | $\Sigma_{s_{21}}$ | $\Sigma_{s_{22}}$ |
|---|---|---|---|---|
| Method 1 | -1.946331E-06 | 3.723788E-07 | -1.670704E-07 | -4.138146E-06 |
| Method 2 | -1.347782E-06 | 3.661127E-07 | -7.887780E-09 | -6.023565E-07 |
| Method 3 | -2.026820E-06 | 4.374530E-07 | -1.660001E-07 | -4.213954E-06 |
| Method 4 | -1.275592E-06 | 4.300919E-07 | -7.852990E-09 | -6.185276E-07 |

Moderator Temperature Coefficients

| group | transport | capture | xx | nu-fission | fission |
|---|---|---|---|---|---|
| Method 1 | | | | | |
| 1 | -5.093766E-04 | -6.045575E-06 | 0.0 | -3.813405E-06 | -1.421511E-06 |
| 2 | -3.677624E-03 | -7.511162E-05 | 0.0 | -1.198305E-04 | -4.953972E-05 |
| Method 2 | | | | | |
| 1 | -5.557798E-04 | -5.038512E-06 | 0.0 | -7.727147E-07 | -2.941462E-07 |
| 2 | -3.159038E-03 | -3.990732E-05 | 0.0 | 3.445546E-06 | 1.426204E-06 |
| Method 3 | | | | | |
| 1 | -5.501856E-04 | 2.641565E-06 | 0.0 | -3.813405E-06 | -1.421511E-06 |
| 2 | -3.682409E-03 | -7.496474E-05 | 0.0 | -1.198305E-04 | -4.953972E-05 |
| Method 4 | | | | | |
| 1 | -6.013852E-04 | 5.908101E-06 | 0.0 | -7.727147E-07 | -2.941462E-07 |
| 2 | -3.168511E-03 | -3.292952E-05 | 0.0 | 3.445546E-06 | 1.426204E-06 |

| | $\Sigma_{s_{11}}$ | $\Sigma_{s_{12}}$ | $\Sigma_{s_{21}}$ | $\Sigma_{s_{22}}$ |
|---|---|---|---|---|
| Method 1 | -1.609370E-03 | 3.629874E-06 | -8.929297E-05 | -5.837495E-03 |
| Method 2 | -1.689375E-03 | -2.737309E-06 | -7.832785E-05 | -5.229427E-03 |
| Method 3 | -1.570328E-03 | 4.264222E-06 | -8.870411E-05 | -5.856601E-03 |
| Method 4 | -1.637943E-03 | -3.215597E-06 | -7.781324E-05 | -5.238137E-03 |

## A7.6 Two-Group Temperature Feedback Coefficients of Fuel COOREF

Fuel Temperature Coefficients

| group | transport | capture | xx | nu-fission | fission |
|---|---|---|---|---|---|
| Method 1 | | | | | |
| 1 | -1.341963E-06 | 4.306175E-07 | 0.0 | -6.190070E-08 | -2.463762E-08 |
| 2 | -5.588617E-06 | -3.917352E-07 | 0.0 | -2.201906E-06 | -9.104475E-07 |
| Method 2 | | | | | |
| 1 | -1.002319E-06 | 4.848427E-07 | 0.0 | -3.829706E-08 | -1.424170E-08 |
| 2 | -2.755594E-06 | -2.363076E-07 | 0.0 | -1.555924E-06 | -6.433791E-07 |
| Method 3 | | | | | |
| 1 | -1.375485E-06 | 4.518468E-07 | 0.0 | -6.190070E-08 | -2.463762E-08 |
| 2 | -5.583186E-06 | -4.847992E-07 | 0.0 | -2.201906E-06 | -9.104475E-07 |
| Method 4 | | | | | |
| 1 | -1.086917E-06 | 5.114429E-07 | 0.0 | -3.829706E-08 | -1.424170E-08 |
| 2 | -2.757335E-06 | -3.131408E-07 | 0.0 | -1.555924E-06 | -6.433791E-07 |

| | $\Sigma_{s_{11}}$ | $\Sigma_{s_{12}}$ | $\Sigma_{s_{21}}$ | $\Sigma_{s_{22}}$ |
|---|---|---|---|---|
| Method 1 | -2.070525E-06 | 3.821432E-07 | -1.672006E-07 | -4.374542E-06 |
| Method 2 | -1.446923E-06 | 3.756733E-07 | -8.630757E-09 | -5.853272E-07 |
| Method 3 | -2.239691E-06 | 4.779763E-07 | -1.667423E-07 | -4.409534E-06 |
| Method 4 | -1.376913E-06 | 4.698840E-07 | -8.621194E-09 | -5.925766E-07 |

Moderator Temperature Coefficients

| group | transport | capture | xx | nu-fission | fission |
|---|---|---|---|---|---|
| Method 1 | | | | | |
| 1 | -5.090631E-04 | -6.292087E-06 | 0.0 | -4.091849E-06 | -1.534108E-06 |
| 2 | -3.674251E-03 | -7.329990E-05 | 0.0 | -1.239498E-04 | -5.124433E-05 |
| Method 2 | | | | | |
| 1 | -5.527933E-04 | -5.316244E-06 | 0.0 | -8.177290E-07 | -3.122618E-07 |
| 2 | -3.165817E-03 | -4.382458E-05 | 0.0 | 4.792100E-06 | 1.981128E-06 |
| Method 3 | | | | | |
| 1 | -5.814248E-04 | 9.388005E-06 | 0.0 | -4.091849E-06 | -1.534108E-06 |
| 2 | -3.677923E-03 | -7.382091E-05 | 0.0 | -1.239498E-04 | -5.124433E-05 |
| Method 4 | | | | | |
| 1 | -6.247224E-04 | 1.284787E-05 | 0.0 | -8.177290E-07 | -3.122618E-07 |
| 2 | -3.169967E-03 | -4.045441E-05 | 0.0 | 4.792100E-06 | 1.981128E-06 |

| | $\Sigma_{s_{11}}$ | $\Sigma_{s_{12}}$ | $\Sigma_{s_{21}}$ | $\Sigma_{s_{22}}$ |
|---|---|---|---|---|
| Method 1 | -1.602581E-03 | 3.455374E-06 | -8.731880E-05 | -5.815618E-03 |
| Method 2 | -1.677149E-03 | -2.635527E-06 | -7.657135E-05 | -5.219482E-03 |
| Method 3 | -1.598159E-03 | 4.321912E-06 | -8.706822E-05 | -5.821778E-03 |
| Method 4 | -1.660718E-03 | -3.296428E-06 | -7.635231E-05 | -5.221433E-03 |

## A7.7 Two-Group Temperature Feedback Coefficients of Fuel A00REF

Fuel Temperature Coefficients

| group | transport | capture | xx | nu-fission | fission |
|---|---|---|---|---|---|
| Method 1 | | | | | |
| 1 | -1.362759E-06 | 4.420313E-07 | 0.0 | -5.140515E-08 | -2.041342E-08 |
| 2 | -6.560828E-06 | -4.013887E-07 | 0.0 | -1.696416E-06 | -7.013235E-07 |
| Method 2 | | | | | |
| 1 | -9.977008E-07 | 4.957711E-07 | 0.0 | -4.080956E-08 | -1.535380E-08 |
| 2 | -2.752313E-06 | -2.173893E-07 | 0.0 | -1.130659E-06 | -4.674219E-07 |
| Method 3 | | | | | |
| 1 | -1.412124E-06 | 4.534287E-07 | 0.0 | -5.140515E-08 | -2.041342E-08 |
| 2 | -6.553122E-06 | -4.538214E-07 | 0.0 | -1.696416E-06 | -7.013235E-07 |
| Method 4 | | | | | |
| 1 | -1.061765E-06 | 4.940605E-07 | 0.0 | -4.080956E-08 | -1.535380E-08 |
| 2 | -2.752113E-06 | -2.528560E-07 | 0.0 | -1.130659E-06 | -4.674219E-07 |

| | $\Sigma_{s_{11}}$ | $\Sigma_{s_{12}}$ | $\Sigma_{s_{21}}$ | $\Sigma_{s_{22}}$ |
|---|---|---|---|---|
| Method 1 | -2.131220E-06 | 3.040614E-07 | -1.696670E-07 | -5.087977E-06 |
| Method 2 | -1.456530E-06 | 2.943360E-07 | -9.488681E-09 | -1.508000E-07 |
| Method 3 | -2.221727E-06 | 3.586941E-07 | -1.692562E-07 | -5.124808E-06 |
| Method 4 | -1.372721E-06 | 3.472213E-07 | -9.480795E-09 | -1.575891E-07 |

Moderator Temperature Coefficients

| group | transport | capture | xx | nu-fission | fission |
|---|---|---|---|---|---|
| Method 1 | | | | | |
| 1 | -5.102508E-04 | -6.139425E-06 | 0.0 | -3.317802E-06 | -1.206602E-06 |
| 2 | -3.715197E-03 | -7.128572E-05 | 0.0 | -7.879135E-05 | -3.257410E-05 |
| Method 2 | | | | | |
| 1 | -5.590237E-04 | -5.652304E-06 | 0.0 | -6.218241E-07 | -2.321201E-07 |
| 2 | -3.243750E-03 | -4.718641E-05 | 0.0 | 6.824226E-07 | 2.826739E-07 |
| Method 3 | | | | | |
| 1 | -5.536883E-04 | 3.448631E-06 | 0.0 | -3.317802E-06 | -1.206602E-06 |
| 2 | -3.718152E-03 | -7.153664E-05 | 0.0 | -7.879135E-05 | -3.257410E-05 |
| Method 4 | | | | | |
| 1 | -6.078059E-04 | 5.946118E-06 | 0.0 | -6.218241E-07 | -2.321201E-07 |
| 2 | -3.246760E-03 | -4.473996E-05 | 0.0 | 6.824226E-07 | 2.826739E-07 |

| | $\Sigma_{s_{11}}$ | $\Sigma_{s_{12}}$ | $\Sigma_{s_{21}}$ | $\Sigma_{s_{22}}$ |
|---|---|---|---|---|
| Method 1 | -1.614124E-03 | 2.805927E-06 | -9.074286E-05 | -5.799003E-03 |
| Method 2 | -1.695421E-03 | -2.019695E-06 | -8.231048E-05 | -5.243500E-03 |
| Method 3 | -1.570473E-03 | 3.310066E-06 | -9.051094E-05 | -5.804091E-03 |
| Method 4 | -1.639528E-03 | -2.382642E-06 | -8.210061E-05 | -5.245280E-03 |

## A7.8 Two-Group Temperature Feedback Coefficients of Reflector REFREF

Fuel Temperature Coefficients

| group | transport | capture | xx | nu-fission | fission |
|---|---|---|---|---|---|
| Method 1 | | | | | |
| 1 | 9.554511E-09 | -9.567551E-11 | 0.0 | 0.000000E+00 | 0.000000E+00 |
| 2 | -3.596498E-07 | -5.069541E-09 | 0.0 | 0.000000E+00 | 0.000000E+00 |
| Method 2 | | | | | |
| 1 | 5.620241E-10 | -6.380165E-11 | 0.0 | 0.000000E+00 | 0.000000E+00 |
| 2 | -1.506743E-07 | -1.021982E-09 | 0.0 | 0.000000E+00 | 0.000000E+00 |
| Method 3 | | | | | |
| 1 | 9.561807E-09 | -1.199354E-10 | 0.0 | 0.000000E+00 | 0.000000E+00 |
| 2 | -3.599842E-07 | -5.071219E-09 | 0.0 | 0.000000E+00 | 0.000000E+00 |
| Method 4 | | | | | |
| 1 | 5.715733E-10 | -2.691661E-10 | 0.0 | 0.000000E+00 | 0.000000E+00 |
| 2 | -1.500662E-07 | -1.606743E-09 | 0.0 | 0.000000E+00 | 0.000000E+00 |

| | $\Sigma_{s_{11}}$ | $\Sigma_{s_{12}}$ | $\Sigma_{s_{21}}$ | $\Sigma_{s_{22}}$ |
|---|---|---|---|---|
| Method 1 | 5.817305E-08 | 1.840550E-10 | -2.458042E-09 | -2.950782E-07 |
| Method 2 | 1.733872E-08 | -2.154806E-11 | 1.624055E-09 | -3.713359E-08 |
| Method 3 | 5.822995E-08 | 1.826389E-10 | -2.453270E-09 | -2.933668E-07 |
| Method 4 | 1.739687E-08 | -2.190414E-11 | 1.631876E-09 | -3.661287E-08 |

Moderator Temperature Coefficients

| group | transport | capture | xx | nu-fission | fission |
|---|---|---|---|---|---|
| Method 1 | | | | | |
| 1 | -7.961444E-04 | -2.338067E-06 | 0.0 | 0.000000E+00 | 0.000000E+00 |
| 2 | -5.749115E-03 | -8.958240E-05 | 0.0 | 0.000000E+00 | 0.000000E+00 |
| Method 2 | | | | | |
| 1 | -8.150542E-04 | -2.389411E-06 | 0.0 | 0.000000E+00 | 0.000000E+00 |
| 2 | -5.235553E-03 | -7.952934E-05 | 0.0 | 0.000000E+00 | 0.000000E+00 |
| Method 3 | | | | | |
| 1 | -7.928560E-04 | -3.034190E-06 | 0.0 | 0.000000E+00 | 0.000000E+00 |
| 2 | -5.751295E-03 | -8.964888E-05 | 0.0 | 0.000000E+00 | 0.000000E+00 |
| Method 4 | | | | | |
| 1 | -8.119058E-04 | -2.992392E-06 | 0.0 | 0.000000E+00 | 0.000000E+00 |
| 2 | -5.235398E-03 | -8.109913E-05 | 0.0 | 0.000000E+00 | 0.000000E+00 |

| | $\Sigma_{s_{11}}$ | $\Sigma_{s_{12}}$ | $\Sigma_{s_{21}}$ | $\Sigma_{s_{22}}$ |
|---|---|---|---|---|
| Method 1 | -2.450667E-03 | 5.128609E-07 | -1.415821E-04 | -8.716034E-03 |
| Method 2 | -2.491807E-03 | -8.854539E-07 | -1.492103E-04 | -8.070987E-03 |
| Method 3 | -2.443896E-03 | 5.102095E-07 | -1.416808E-04 | -8.705061E-03 |
| Method 4 | -2.484805E-03 | -8.808959E-07 | -1.493144E-04 | -8.062893E-03 |

## Appendix 8

### NOMENCLATURE

Most of variables and symbols shown in this thesis were defined within the text in an order of their appearance. However, since lots of symbols were commonly used in reactor physics field, some variables were not defined within the text. In some symbols, the same character was used for more than two different variables. This nomenclature is given to avoid confusions from these reasons.

| SYMBOLS | DEFINITIONS |
|---|---|
| $A$ | a linear integral operator for neutron removal defined in Eq. (2.2) |
| $A^*$ | adjoint operator of A |
| $A^k_{nn'}$ | homogenized $A_{0_{nn'}}(r)$ for region k |
| $[A_0(r)]$ | N×N full matrix containing $A_{0_{nn'}}(r)$ |
| $A_{0_{nn'}}(r)$ | P-1 scattering removal parameter defined by $\Sigma_{t_n}\delta_{nn'} - \Sigma_{s_{0_{nn'}}}$ |
| $[A_{1_u}(r)]$ | N×N full matrix containing $A_{1_{u_{nn'}}}(r)$ |
| $A_{1_{nn'}}(r)$ | P-1 scattering removal parameter defined by $\Sigma_{t_n}\delta_{nn'} - \Sigma_{s_{1_{nn'}}}$ |
| $B^k_m$ | material buckling of material composition k |

| | |
|---|---|
| $C_\iota(r,t)$ | delayed neutron precursor density at space (r,t) |
| $C^*_\iota(r,t)$ | adjoint delayed neutron precursor density at space (r,t) |
| $D^{-1}$ | a linear integral operator for neutron transport defined in Eq. (2.2) |
| $D^{*-1}$ | adjoint operator of $D^{-1}$ |
| $D_g^k(r)$ | diffusion coefficient of group g for material region k |
| $D_{nn'}^{-1\,k}$ | homogenized multi-group operator of $D^{-1}$ for region k |
| $F_{0g}^k(E)$ | continuous flux energy spectra of few-group g in material region k |
| $F_{0n}^k$ | flux energy spectrum of multi-group n in material region k |
| $F_{1g}^k(E)$ | continuous current energy spectra of few-group g in material region k |
| $F_{1n}^k$ | current energy spectrum of multi-group n in material region k |
| $F_{0g}^{*k}(E)$ | adjoint flux spectra of few-group g in material region k |
| $F_{0n}^{*k}$ | adjoint flux spectrum of multi-group n in material region k |
| $F_{1g}^{*k}(E)$ | adjoint current spectra of few-group g in material region k |
| $F_{1n}^{*k}$ | adjoint current spectrum of multi-group n in material region k |
| $[f_i^L]$ | diagonal matrix of group discontinuity factors at the left side of node i, i.e. at $x_i^+$ |
| $[f_i^R]$ | diagonal matrix of group discontinuity factors at the right side of node i, i.e. at $x_{i+1}^-$ |

| | |
|---|---|
| G | number of energy groups for few-group index |
| $g_n(t)$ | multi-group spectra for g-th group Lagrange multiplier $\alpha$ |
| $h_i$ | node mesh spacing for node i |
| $h_n(t)$ | multi-group spectra for g-th group Lagrange multiplier $\beta$ |
| I | number of delayed neutron precursor groups |
| I | number of node mesh numbers in reactor |
| $\tilde{I}$ | unit diagonal dyadic |
| [J(r)] | column matrix containing $J_{n,u}(r)$ |
| $J_{n,u}(r)$ | net neutron current in direction u and group n |
| $k_{eff}$ | reactor eigenvalue or criticality |
| M | a linear integral operator for total neutron production defined in Eq. (2.2) |
| $M^*$ | adjoint operator of M |
| $M_{nn'}^k$ | homogenized $M_{nn'}^k(r)$ for region k |
| [M(r)] | N×N full matrix containing $M_{nn'}(r)$ |
| $[M_i]^n$ | full matrix for node i at time step n, as defined in Section 4.2.2 |
| $M_{nn'}(r)$ | total fission neutron production parameter defined by $k_{eff}^{-1} \chi_n \nu\Sigma_{f_{n'}}$ |
| $[MD_i]^n$ | full matrix for node i at time step n, as defined in Section 4.2.2 |
| $M_{d_\iota}$ | a linear integral operator for delayed neutron production from precursor group $\iota$, as defined in Eq. (2.2) |

| | |
|---|---|
| $M^{*}_{d_\iota}$ | adjoint operator of $M_{d_\iota}$ |
| $M^{k}_{d_{\iota,n}}$ | homogenized multi-group operator of $M_{d_\iota}$ for region k |
| N | number of energy groups for multi-group index |
| $N_g$ | number of multi groups contained in few-group g |
| T | temperature |
| u(r,E,t) | scalar function used in variational functional, used in Eq. (2.6) |
| $u^{*}(r,E,t)$ | adjoint scalar function used in variational functional, used in Eq. (2.6) |
| $V_g$ | average neutron speed in few-group g |
| $V_n$ | average neutron speed in multi-group n |
| $\vec{v}(r,E,t)$ | vector function used in variational functional, used in Eq. (2.6) |
| $\vec{v}^{*}(r,E,t)$ | adjoint vector function used in variational functional, used in Eq. (2.6) |
| $\alpha(r,E)$ | Lagrange multiplier for internal boundary flux as defined in Eq. (2.9) |
| $[\alpha^{i}]^{n}$ | full matrix for node i at time step n, as defined in Eq. (A4.6) |
| $\beta(r,E)$ | Lagrange multiplier for internal boundary adjoint flux as defined in Eq. (2.9) |
| $[\beta^{i}]^{n}$ | full matrix for node i at time step n, as defined in Eq. (A4.6) |
| $\beta^{j}_{eff}$ | total yield of delayed precursors from isotope j, the same as $\sum_{\iota=1}^{I} \beta^{j}_{\iota}$ |
| $\beta^{j}_{\iota}$ | fraction of delayed neutrons appearing by the decay of $\iota$-th group precursors produced from fission of isotope j |

| | |
|---|---|
| $[\Gamma]$ | full matrix for the general boundary condition defined in Eq. (4.20) |
| $[\gamma^i]^n$ | full matrix for node i at time step n, as defined in Eq. (A4.6) |
| $\zeta_\iota^n$ | an integral constant for time step n and precursor group $\iota$ as defined in Eq. (4.9) |
| $\eta_\iota^n$ | an integral constant for time step n and precursor group $\iota$ as defined in Eq. (4.9) |
| $\theta_\iota^n$ | an integral constant for time step n and precursor group $\iota$ as defined in Eq. (4.9) |
| $\lambda_\iota$ | decay constant of precursor group $\iota$ |
| $\nu$ | average number of neutrons emitted per fission |
| $\rho$ | density |
| $\Sigma_{a_g}^k(r)$ | macroscopic absorption cross section for energy group g and material region k |
| $\Sigma_{f_n}^k(r)$ | macroscopic fission cross section for energy group n and material region k |
| $\Sigma_{s_{0_{nn'}}}^k(r)$ | macroscopic P-0 scattering transfer cross section from group n' to group n for material region k |
| $\Sigma_{s_{1_{nn'}}}^k(r)$ | macroscopic P-1 scattering transfer cross section from group n' to group n for material region k |
| $\Sigma_{t_n}^k(r)$ | macroscopic total cross section for energy group n and material region k |
| $\Sigma_{\alpha_n}$ | general expression for the macroscopic cross sections for energy group n in an unperturbed condition |
| $\hat{\Sigma}_{\alpha_n}$ | general expression for the macroscopic cross sections for energy group n in a perturbed condition |
| $[\Phi(r)]$ | column matrix containing $\phi_n(r)$ |
| $\phi_n(r)$ | neutron flux of group n |

| | |
|---|---|
| $\chi_n$ | fission neutron yield fraction to group n |
| $\chi_{p_n}$ | prompt neutron fission spectrum for energy group n |
| $\chi_{d_{\iota,n}}$ | delayed neutron fission spectrum for precursor group $\iota$ and energy group n |
| $\Psi_0(\mathbf{r},E,t)$ | P-0 component of neutron density $\Psi(\mathbf{r},E,\Omega,t)$ |
| $\Psi_0^*(\mathbf{r},E,t)$ | adjoint neutron flux density |
| $\vec{\Psi}_1(\mathbf{r},E,t)$ | P-1 component vector of neutron density $\Psi(\mathbf{r},E,\Omega,t)$ |
| $\vec{\Psi}_1^*(\mathbf{r},E,t)$ | adjoint neutron current density |
| $\omega_{0_n}^k$ | frequency parameter for multi-group flux for region k |
| $\omega_{1_n}^k$ | frequency parameter for multi-group current for region k |
| $\Delta_n$ | time step spacing at time step n |

| Superscripts | DEFINITIONS |
|---|---|
| i | an index for node mesh |
| j | an index for fissile isotope |
| k | an index for material region |
| n | an index for time step |

| Subscripts | DEFINITIONS |
|---|---|
| f | fuel |
| g | an index for few-group |
| i | an index for node mesh |
| m | moderator |
| n | an index for multi-group |
| $\alpha$ | an index for the kind of cross sections (a,t,f,tr, etc.) |
| $\iota$ | an index for delayed neutron precursor group |